Evolutionary Consequences of Seasonal Migration in North American Birds

by

Teresa M. Pegan

A dissertation submitted in partial fulfillment
of the requirements for the degree of
Doctor of Philosophy
(Ecology and Evolutionary Biology)
in the University of Michigan
2023

Doctoral Committee:

Assistant Professor Benjamin M. Winger, Chair
Professor L. Lacey Knowles
Professor Andrew J. Marshall
Professor Daniel L. Rabosky

Teresa M. Pegan

tmpegan@umich.edu

ORCID iD: 0000-0002-0990-815X

Dedication

To the boreal forest, home to some of my favorite lakes, bogs, orchids, and migratory birds.

Acknowledgements

Many thanks to my advisor, Ben Winger. Ben is a supportive mentor, a trenchant editor, and a frequent dispenser of wisdom. His thoughtful guidance is equally valuable in the halls of the BSB, where he encourages science that gets at the heart of the most interesting ornithological questions, as in the bogs of Manitoba, where we survived a camping situation immortalized by the verse —

It said there was a 50% chance of a storm
We felt pretty safe despite the wind that was warm
As we drifted to sleep, we weren't aware
The other 50% was electric nightmare

In addition to being a great scientist, Ben is also a role model of professionalism and of having a life outside of one's work. Students frequently discuss their experiences with PhD mentorship, and I rarely had such a discussion with peers from my department or other institutions without feeling grateful to have Ben as an advisor. It is an honor to be an inaugural graduate advisee in what I am sure will be a prolific career of great mentorship and science.

Thanks also to my committee, Lacey Knowles, Dan Rabosky, and Andy Marshall. I learned and grew tremendously as a scientist thanks to the rigorous discussions we had about

evolutionary biology, biodiversity, and life history. I appreciate their support over the years and their helpful advice throughout my dissertation.

Beyond my committee, I appreciate the mentorship I received from postdocs associated with my lab, especially Brian Weeks, Shane DuBay, Abby Kimmitt, Jacob Berv, and Valentina Gómez-Bahamón. In the final year of my PhD, I was glad to have the opportunity to interact with Gideon Bradburd and his lab, particularly Zach Hancock and Leonard Jones, which helped me develop intuition for population genetics and gave me another set of mentors in my department.

I benefitted from having a great community at the University of Michigan, including my lab mates Brian Weeks, Susanna Campbell, Eric Gulson-Castillo, Vera Ting, Marketa Zimova, Kristen Wacker, Matt Hack, Abby Kimmitt, and Andrea Benavides; my PhD cohort, especially Rachel Wadleigh and Rumaan Malhotra; and the broader "flappy hour" circle, including Giorgia Auteri, Shane DuBay, Jacob Berv, Natalie Hofmeister, and Valentina Gómez-Bahamón. Abby, Kristen, Rachel, Eric, and Matt were excellent company in the office and the lab, where having their company was a bright spot during tough times. I am so grateful that our friendship also extends beyond the office, from Wingspan and book club to adventures around Michigan and beyond. Finally, I couldn't have asked for better pandemic birding pals than John David Curlis and Molly Hirst, who were always up for a twitch.

Much of my work revolves around natural history collections. At the University of Michigan Museum of Zoology, I thank Janet Hinshaw and especially Brett Benz for assistance with access to specimens and genomic resources. Brett also helped facilitate work that I developed with Vera Ting, who started out measuring museum specimens with me as a freshman at UM and stuck by the UMMZ and our wing shape measurements through the pandemic and

beyond. UMMZ field work would not have been the same without the participation of Andy Jones and Courtney Brennan from the Cleveland Museum of Natural History and Mary Margaret Ferraro from the Cornell University Museum of Vertebrates. The acknowledgments sections of my third chapter includes a long list of the museum curators and collection managers who steward the valuable natural history collections across the US and Canada that provided materials for my dissertation. I am deeply grateful for the work they do that allows me, and countless others, to conduct science on biodiversity.

I also appreciate my broader networks beyond the University of Michigan, especially fellow graduate students Benjamin Van Doren, Jenny Uehling, Maina Handmaker, Amelia-Juliette Demery, Jenn Houtz, Shailee Shah, Jack Hruska, Jacob Drucker, and Jessie Williamson. I found that interacting with other PhD students across different institutions was a valuable form of peer-mentorship. Many of these connections were facilitated through the American Ornithology Society, for which I was a member of the student affairs committee and a student member of council. Interactions with fellow council members and AOS leaders, especially Judith Scarl, gave me great role models for leadership.

I thank my parents for supporting and encouraging my career in science. My interest in nature began through our family hikes and camping trips, including occasions when my Mom took me to see owls and rare pelicans and when my Dad offered quarters to kids who spotted juncos or titmice on a hike. My Uncle John was there for a lot of our earliest birding excursions to Montezuma National Wildlife Refuge. My brothers Matt, Emmett, Jake, and Quentin have tolerated a lot of birdwatching outings over the years—and I think they sometimes even appreciate birds themselves! My family's support of my career goals, from my early childhood plan to study bats through my career as a student of ornithology in college and graduate school,

helped get me to where I am today. I am also grateful for the support of my new family-in-law, Pilar, Rex, and Natalie.

Deepest thanks to my partner in science, adventure, and life, Eric Gulson-Castillo. We have come a long way together, from chasing pittas and broadbills around in Borneo to wrapping up our PhDs. I'm looking forward to wherever life takes us next!

Lastly, thanks to Scribbles and Caramelo. They didn't really help with my dissertation, but it's nice to have a pair of cute guinea pig faces to greet us whenever we come home.

Table of Contents

List of Tables

List of Figures

List of Appendices

Abstract

Seasonally migratory animals breeding at high latitudes escape winter conditions by temporarily moving to warmer climates. Migration requires substantial time and energy, and its influence pervades migratory animals' biology, from their morphology to their annual time budgets. Through adaptation to long-distance travel, migratory animals have few constraints on movement, even as they experience other constraints (e.g., time constraints) that nonmigratory animals do not. In light of their high mobility and constrained annual schedules, I investigated how seasonal migration influences evolutionary processes in a comparative context. My research focuses on small bird species in North America, with a particular focus in two chapters on the migratory avifauna of the boreal forest. The boreal avifauna comprises species with broadly co-distributed breeding ranges that spend the winter in disparate locations, making it a natural system for assessing consequences of variation in migratory strategy. I focus on how migration distance affects the evolutionarily consequential processes of geographic range expansion, gene flow, and life history evolution.

Studies show that high mobility promotes dispersal and range size, yet some have suggested that migratory behavior restricts dispersal and range expansion because innate, spatially precise migratory behaviors do not transfer well into new spatial contexts. To test whether migration distance promotes or constrains range expansion, I conducted multivariate model comparison using songbirds breeding in North America (306 species). I measured a morphological proxy of mobility (wing shape) on over 1000 museum specimens and quantified range expansion using species distribution models based on climate information and millions of citizen science records. My results revealed that migration distance does not promote range size in North American birds. I suggest that these species are all sufficiently mobile that their geographic ranges are not meaningfully constrained by dispersal ability.

Next, to analyze the relationship between migration distance and gene flow, I generated a massive multi-species population genetic dataset (~1780 genome sequences from 34 boreal-breeding species). I quantified and compared continuous spatial genetic variation across species, finding that many long-distance migrants display patterns of geographic structure that reflect reduced dispersal. These two chapters demonstrate that the relationship between mobility and spatial evolution, apparent in many taxa across the globe, breaks down in the North American avifauna.

Finally, I analyzed migration from a novel perspective as a life history strategy—i.e., a strategy correlated with the life history continuum of investment in survival vs reproduction. Species that invest more in survival and less in reproduction have slower rates of molecular evolution than species at the opposite end of the continuum. In the North American boreal avifauna, my work has shown that migration is a life history axis whereby long-distance migrants invest more in survival by spending less time on breeding grounds, and short-distance migrants spend more time breeding at cost to survival. Using mitochondrial genomes from 39 species, I applied a Bayesian modeling framework to co-estimate rates of molecular evolution and their correlation with migration distance. I also used population genomic data from 27 of these species (~950 samples total) to test whether migration distance influenced the dynamics of mitochondrial selection. My results support the hypothesis that long-distance migrants have slower mitochondrial molecular evolution. Overall, my dissertation uses comparative methods to highlight the role played by time and life history constraints, rather than movement constraints, in the evolution of migratory animals.

Chapter 1 Introduction

Organisms that breed at high latitudes require adaptations to persist despite seasonal freezing temperatures and limited resources (Varpe 2017; Auteri 2022). Adaptations to seasonality can influence the evolutionary trajectory of high latitude populations through effects on important processes such as gene flow, breeding phenology, and life history strategy. In this dissertation, I examine how an adaptation to winter—seasonal migration—influences evolution in North American bird species. Migratory animals move long distances to milder climates after breeding, which allows them to avoid harsh winter conditions (Winger et al. 2019). I focus on links between seasonal migration and evolutionary processes associated with movement behavior and life history strategy. Movement behavior influences gene flow, or the rate of mixing between populations, which determines whether populations remain homogenous or undergo evolutionary divergence. Movements also determine where individuals live, thus influencing a species' geographic range. Chapters 2 and 3 examine geographic range patterns and spatial population genetics among bird species with varying migratory strategy. I also investigate whether migration influences evolution through its effect on life history. Species with life history strategies that prioritize survival over reproduction tend to have slower rates of molecular evolution. Chapter 4 tests whether the life history strategy of long-distance migrants, which prioritize survival, influences molecular evolutionary rates in these species.

Each chapter in this dissertation is inspired by a question about how migratory species balance tradeoffs associated with migration and breeding. Evolutionary patterns emerge from the

transmission of genes through space across generations, so tradeoffs that affect where and when animals reproduce have evolutionary consequences. At the individual level, a migratory animal's decision about where to breed is entwined with its decision about where to cease migration (Studds et al. 2008; Wynn et al. 2022). Similarly, the beginning and end of a breeding attempt are linked with the timing of spring and fall migrations (Norris et al. 2004; Heckscher 2018). Migratory strategy differs broadly across migratory species, potentially leading to differences in spatial evolution and life history. I compare species with differing migratory strategies and asking whether these differences are correlated with evolutionary outcomes, while accounting for relatedness between species (Felsenstein 1985).

Migratory species provide a window into how evolutionary processes play out when intrinsic limits to movement ability are not relevant. Models of spatial ecological and evolutionary processes in the natural world generally assume some form of "dispersal limitation," or restriction on where and how far organisms tend to move during their lives (e.g. Wright 1943; MacArthur and Wilson 1967; Hubbell 1997; Hanski 1998; Soberón and Peterson 2005; Cavender-Bares et al. 2009). This assumption is realistic — even highly mobile organisms are distributed non-randomly across the earth. Dispersal limitation is universal, yet the reasons for it are complex and vary across species. Limits to movement arise from tradeoffs influenced by physical and energetic restrictions, temporal restrictions, behavioral syndromes, and niche preferences (Bonte et al. 2012). Comparative studies of dispersal often focus on variation in physical dispersal limitation (e.g. Moore et al. 2008; Weeks and Claramunt 2014; Medina et al. 2018). But what happens in populations that regularly engage in long-distance movement? Long-distance seasonal migrants travel thousands of kilometers twice each year. In doing so, they cross major environmental, physical, and oceanic barriers that structure the biogeography and spatial

evolution of nearly all other species of plants and animals occupying those regions. Like all species, migratory animals face other tradeoffs that constrain their movements and annual cycle, even in the absence of significant physical limitation. Therefore, comparative studies of migratory species are especially suited to shed light on what factors other than physical limitation shape spatial evolution, and, more generally, to highlight evolutionary consequences of tradeoffs in the annual cycle.

1.1 Seasonal migration in birds: an overview

"Seasonal migration" refers to movement behaviors that animals use to avoid harsh seasonal conditions, such as the high latitude winter. Migratory animals demonstrate site fidelity, meaning that they return repeatedly to breed in a particular region during favorable conditions (Huntington 1951; Pearce 2007; Winger et al. 2019). In contrast to other movement behaviors such as dispersal (the movement from one site to another with potential for gene flow; Ronce 2007), seasonal migration is a round-trip, cyclical journey. Seasonal migration is therefore categorically different from other phenomena frequently associated with the word "migration," such as genetic migration (the movement of genes through space) and human migration (typically a large-scale and permanent movement of humans from one place to another).

Migration can be thought of as an adaptation for seasonal persistence that allows individuals to continue breeding in regions where they would not be able to survive year-round (Winger et al. 2019). Within the community of land animals that breed at high latitudes during the summer, species show a variety of seasonal persistence strategies (Auteri 2022). Many species of birds and other flying animals (bats, insects) use migration to survive during the winter (Krauel and McCracken 2013; May 2013; Somveille et al. 2013), while other species in the same region have alternative adaptations including hibernation, behavioral shifts such as

winter food caching, or physical changes such as thicker fur growth (Winger et al. 2019; Auteri 2022). All of these species have evolved to breed successfully during the brief pulse of resource abundance during the high latitude summer.

Species migrate at different times, to different places, and through different routes (reviewed in Newton 2007; Jahn and Cueto 2012; McKinnon and Love 2018; Somveille et al. 2019). Migration distance is an axis of migratory strategy variation that captures some of the most important differences in migratory strategy. Species exhibit a spectrum of migratory distances, ranging from very short-distance movements within a region to hemisphere-crossing journeys between the north and south poles. Species migrating different distances vary in how long they spend on the breeding grounds (Catchpole 1980; Greenberg 1980; Benson and Winker 2001). In comparisons of species with co-distributed breeding habitat, migration distance also corresponds to differences in the non-breeding environments experienced by each species (Winger and Pegan 2021). Short-distance migrants that breed at high latitudes stay close to their breeding grounds and avoid having to shift into a different habitat, but they also must face cold temperatures and limited resources during the winter. For example, many Dark-eyed Juncos (*Junco hyemalis*) depart their Canadian breeding grounds to spend the winter in Michigan, a region where winters are milder than they are further north, but where these birds still face significant challenges in surviving cold temperatures and scarce resources. By contrast, the Swainson's Thrush (*Catharus ustulatus*), a long-distance migrant with a similar breeding range as the junco, trades the boreal forest for the tropical mountain cloud forests of South America in the winter. Migration distance thus reflects consequential differences between species that influence many other aspects of their biology and evolution. In this thesis, I explore associations

between seasonal migration distance and spatial evolution (section 1.2, chapters 2 and 3) and between seasonal migration distance and life history (section 1.3, chapter 4).

1.2 The relationship between seasonal migration and spatial evolution

The biogeography of migratory animals' breeding ranges has attracted continued interest (Blackburn and Gaston 1996; Böhning-Gaese et al. 1998; Hawkins and Felizola Diniz-Filho 2006; Winger et al. 2012, 2014; Outomuro and Johansson 2019). Migratory species' breeding ranges are uniquely ephemeral, scattering and re-forming every year as migrants depart from and return to their breeding grounds. Migratory animals frequently cross major physical barriers (e.g. mountains, oceans) during migration (Williams et al. 2001; Adamík et al. 2016). As a result, researchers often hypothesize that migratory animals should show larger geographic ranges than species with lower mobility (reviewed in Table 2-1). Mobility can also promote range size through its effect on the dynamics of geographic range expansions (Kubisch et al. 2014), leading to a positive relationship between mobility and range expansion rate (Svenning and Skov 2004; Normand et al. 2011; White 2016). The hypothesized positive effect of migration on geographic range size has been supported by several studies at large biogeographic scales (Blackburn and Gaston 1996; Gaston and Blackburn 1996; Lees and Gilroy 2014; Pigot and Tobias 2015).

By contrast, other studies suggest that seasonal migration can actually inhibit range expansion and gene flow in certain conditions (Böhning-Gaese et al. 1998; Engler et al. 2014; Toews 2017; Turbek et al. 2018). These effects may be related to the consequences of spatial mismatch between the location of an individual and its innate migratory program. Migrants rely on successful and repeated migratory journeys for their survival and lifetime fitness (Norris et al. 2004; Reudink et al. 2009; Conklin et al. 2017), so deviations from an optimal migratory route may have severe consequences. The distance and direction of seasonal migration are known to

have a heritable component (Merlin and Liedvogel 2019), which means that individuals may not be able to adapt their migratory strategy to fit a new location after dispersal. As such, migration does not universally enhance range size and gene flow, despite its association with high mobility and ability to cross barriers.

The biogeographic patterns associated with seasonal migration suggest that migration interacts with dispersal, or the process through which individuals move from one breeding site to another (Winkler 2005). This hypothesis is plausible for two reasons. First, seasonal migration is associated with high "dispersal ability" (Bowlin and Wikelski 2008; Weber 2009; Phillips et al. 2018; Sheard et al. 2020), which reduces costs of movement associated with dispersal (Bonte et al. 2012). This means that migratory species potentially face fewer constraints on the evolution of adaptive long-distance dispersal than those with high movement costs. Second, the process of dispersal in migratory animals is spatially and temporally linked to migratory behavior (Norris et al. 2004; Studds et al. 2008; Wynn et al. 2022). Dispersal is most often studied in sedentary species, where the onset of dispersal is defined by departure from the breeding site and the end of dispersal is defined by the establishment of a new breeding location (Bowler and Benton 2005; Ronce 2007). By contrast, migratory species depart their breeding sites each fall and do not arrive on their subsequent breeding locations until the spring. The process of dispersal in migratory species is thus interrupted by the process of migration. Yet, migration behavior itself is not synonymous with dispersal (Winkler 2005; Winger et al. 2019). Many migratory animals migrate without undergoing dispersal, instead returning to the same breeding site year after year (Huntington 1951; Pearce 2007; Cava et al. 2016; Christie et al. 2023). The difficulty of tracking animals over large spatial and temporal scales has prevented a clear understanding of how migration interacts with dispersal when dispersal does occur, and the relationship between these

two behaviors remains poorly understood (Winkler 2005; Winger et al. 2019; Weeks et al. 2022; Vickers et al. 2023).

As in other species, dispersal evolution in migratory birds is likely influenced by tradeoffs associated with time and risk in addition to costs of movement (Ronce 2007; Bonte et al. 2012). Seasonal migration influences time-related tradeoffs that may be relevant to dispersal evolution. Migration distance correlates negatively with time spent on the breeding grounds (Catchpole 1980; Greenberg 1980; Benson and Winker 2001; Winger and Pegan 2021). Dispersers benefit from time spent exploring and assessing potential breeding sites (Reed et al. 1999), and limited time for dispersal can result in selection for natal philopatry. Animals deciding where to breed always have access to the information that their natal area was high enough in quality to produce themselves, making it a safe bet when there is not enough time to assess other possibilities (McNamara and Dall 2011). As such, long-distance migrants with limited time on their breeding grounds may experience strong selection for philopatry even though they also have high dispersal ability. The evolutionary consequences of tradeoffs between dispersal and philopatry in migratory organisms are poorly known.

In chapters 2 and 3, I leverage large comparative datasets to test hypotheses about how seasonal migration distance influences geographic range size and genetic connectivity in birds. I draw on citizen science data, measurements of museum specimens, geospatial datasets, and a massive population genetic dataset (comprising ~1780 low coverage whole genomes) that I generated to test my hypotheses. My study system allows me to move beyond the migratory/nonmigratory binary and examine effects of variation in seasonal migration distance. I address my research questions within a common biogeographic context rather than across latitudes and biomes. Biogeographic patterns such as range size and spatial connectivity vary

strongly across the earth for many reasons (Gaston et al. 1998; Smith et al. 2017). The focused geographic scope of my analyses enhances my ability to isolate apparent effects of seasonal migration from other potential factors in a common avian community.

1.3 The relationship between seasonal migration and life history

Across the tree of life, organisms show strong correlations in trait axes associated with growth, metabolism, reproduction, and longevity (Bromham 2011; White et al. 2022). These trait axes represent a continuum of fitness strategies, often called the "slow-fast" life history continuum, that fundamentally reflects the tradeoff between survival and reproduction (Stearns 1983). At the extreme ends of the continuum, "slow" organisms tend to invest their limited energy in preserving their own lives over the long term and producing few, high-investment offspring, whereas "fast" organisms prioritize maximizing their reproductive output at the expense of survival. The slow-fast life history continuum is among the most prevalent and consistent patterns in biodiversity (Bromham 2011).

A species' position on the life history continuum can evolve in response to natural selection. Many studies suggest that life history strategy is influenced by environmental conditions that affect the balance between investment and risk in reproduction and survival, such as food availability, predation risk, and the amount of time available for breeding (Martin 2004; McNamara et al. 2008; Bears et al. 2009). The distribution of mortality risk across age classes plays an important role in life history evolution (Promislow and Harvey 1990) such that slow life history is associated with low adult mortality compared with juvenile mortality, whereas fast life history increases fitness when adult survival is uncertain. Life history strategies tend to vary along latitudinal and environmental gradients, sometimes in complex ways (Blanck and Lamouroux 2007; Bears et al. 2009; Londoño et al. 2015; Boyce and Martin 2017; Heldstab

2021). For example, classic life history studies characterize tropical birds as slow and temperate birds as fast because of differences in the typical clutch size of species across latitudes (Lack 1948).

Seasonal migration has sometimes been associated with the fast end of the slow-fast continuum because of its association with high latitudes and perceived influence on risk of mortality (Clark and Martin 2007; Sibly et al. 2012; Londoño et al. 2015; Jahn et al. 2020). Classic literature on the evolution of seasonal migration framed this behavior as a risky strategy by species that depart mild tropical regions to take advantage of pulsed resources and reproduce prolifically in the temperate zone (Cox 1968, 1985; Levey and Stiles 1992). However, my co-authors and I argued that seasonal migration is better understood as a winter survival strategy (Winger et al. 2019), in contrast to alternative strategies that involve overwinter persistence at high latitudes. From this perspective, adult migratory organisms invest a large amount of time and energy into preserving their survival between breeding seasons. Life history strategies vary within communities as well as across environments (Varpe 2017), and seasonal migration is not necessarily a fast life history strategy in the context of the high latitude community.

The association between seasonal migration and fast life history is challenged by the observation that long-distance seasonal migrants tend to be long-lived organisms (Møller 2007; Conklin et al. 2017) that show limited annual fecundity (Böhning-Gaese et al. 2000; Bruderer and Salewski 2009). Further, long-distance migrants tend to depart their breeding grounds well in advance of deteriorating climatic conditions, even at the cost of breeding opportunities (Benson and Winker 2001; Heckscher 2018). In Winger and Pegan (2021), I investigated the hypothesis that seasonal migration distance correlates with life history strategy using a long-term dataset of population vital rates in the North American boreal avifauna. We found support for the

hypothesis that long-distance migrants have lower annual fecundity and higher annual survival—in other words, slower life history—than short distance migrants. Long-distance boreal migrants spend the winter in habitats that are warmer and greener than short-distance migrants, which may help enhance their overwinter survival. Additionally, long-distance migrants spend less time on the breeding grounds than short-distance migrants, which results in restricted breeding opportunities and lower annual fecundity. We concluded that the life history strategy of long-distance migrants entails a sacrifice of time on the breeding grounds in favor of spending the winter in distant environments where survival is favored.

In my fourth chapter, I build on work linking seasonal migration and life history (Winger and Pegan 2021) to test whether seasonal migration distance covaries with molecular evolutionary rate. Many studies across vertebrates, invertebrates, plants, and even microbes have demonstrated a strong correlation between the molecular evolutionary rate of a lineage and its position on the slow-fast life history continuum (reviewed in Bromham 2020). My fourth chapter introduces this topic by reviewing theoretical links between life history and molecular evolution, then leverages a large dataset of mitochondrial coding sequences I isolated from my whole genome population genetic data to test whether seasonal migration correlates with mitochondrial molecular evolutionary rate across North American boreal birds in a phylogenetic framework. I also discuss the role of mitochondria in the metabolic demands faced by migratory boreal birds and how these demands may interact with life history to shape the evolutionary rate of the mitochondrial genome. The results of this chapter have implications for how we understand and model the evolutionary history of organisms in seasonal environments. My work adds to the growing body of literature demonstrating that correlation between traits and molecular

evolutionary rates has the potential to bias analyses that link traits with events in evolutionary history (Shafir et al. 2020; Ritchie et al. 2022).

1.4 Spatial and molecular evolution in glaciated North America

The effects of Pleistocene glacial cycles are evident in the present-day spatial patterns of high latitude species (Hewitt 2000; Weir and Schluter 2004), including North American migratory birds. Pleistocene glacial cycles had dynamic effects on climate, environment, and the geographic ranges and population sizes of species inhabiting northern latitudes (Clark et al. 2009; Hofreiter and Stewart 2009; Stralberg et al. 2017; Miller et al. 2021). The most recent major shift involved the retreat of glaciers following the Last Glacial Maximum (LGM; ~20,000 years before present), when a large glacier covered much of northern North America, including the entire landscape currently occupied by the boreal forest (Dyke and Prest 1987; Brandt 2009). Geographic ranges of some species show evidence of "demographic lag," which means that they are still in the process of expanding into suitable habitat following glacial retreat (Svenning and Skov 2004; White 2016). Similarly, spatial genetic patterns that reflect equilibrium conditions on the present-day landscape may not have fully developed yet (Slatkin 1993; Hutchison and Templeton 1999; Castric and Bernatchez 2003; Crispo and Hendry 2005). Ranges of many species were fragmented into different glacial refugia, allowing population genetic divergence to occur in allopatry (Hewitt 2000; Weir and Schluter 2004). Changes in population size such as bottlenecks or recent expansions influence the distribution of genetic diversity through time, leaving an imprint in present-day genetic patterns (reviewed in Knowles 2009). Each of these consequences of Pleistocene glaciation influences and complicates present-day spatial patterns shown by species at high latitudes.

North American glacial cycles present both challenges and opportunities for understanding evolutionary history of high latitude species. One challenge is that species in these regions may not be at geographic or demographic equilibrium. Spatial and population genetic patterns that result from intrinsic species traits arise slowly over time (Slatkin 1993; Hardy and Vekemans 1999; Hutchison and Templeton 1999; Crispo and Hendry 2005). As such, recent dynamic population changes may swamp out or obscure subtler patterns driven by species traits (Hutchison and Templeton 1999; Castric and Bernatchez 2003; De Lafontaine et al. 2013; Jangjoo et al. 2020), including traits associated with movement behavior and seasonal migration. Whereas the presence spatial genetic structure provides information about variation in gene flow, it is not always possible to identify the processes responsible for lack of spatial structure, which can be due to either high gene flow or deviation from equilibrium (Slatkin 1993). However, this challenge is also an opportunity to explicitly test whether species' traits influence the extent to which equilibrium has been achieved. In chapter 2, I address this issue by testing whether traits associated with movement influence "range filling," or the proportion of suitable habitat occupied by each species' geographic range. In chapter 3, I also test whether variation in spatial genetic structure across species is influenced by effective population size, which is expected to play a role in the rate at which equilibrium patterns arise (Maruyama 1971; Hardy and Vekemans 1999; Irwin 2002).

Another advantage of North American glacial history is that we can make a reasonable assumption that all species in a given habitat have been subjected to the same strong environmental pressures. Co-distributed species in high latitude regions typically show broadly concordant demographic histories (Lessa et al. 2003; Miller et al. 2021; Ralston et al. 2021; Kimmitt et al. 2023). Comparison of co-distributed species at high latitudes provides an

opportunity to test hypotheses about how species' traits influence variation in their response to a common environmental shift. In Kimmitt et al. 2023, I used the mitochondrial component of my large population genomic dataset to demonstrate that North American boreal birds show histories of expansion dating to deglaciation during the Wisconsonian period (~57,000 years before present). Thus, the comparisons of spatial genetic patterns I present in chapter 3 are not likely to be biased by categorical differences in demographic history (i.e. recent bottleneck in some species vs expansion in others).

One reason why demographic fluctuations affect genetic patterns is that the strength of genetic drift varies with population size. Variation in effective population size (N_e), a population genetic parameter that is inversely correlated with strength of genetic drift (Waples 2022), has consequences for both spatial population genetic patterns (chapter 3) and molecular evolutionary rates (chapter 4). In populations with large N_e and low drift, neutral alleles persist in populations for longer amounts of time, while deleterious alleles are more likely to be removed by selection, even if they have weak effects (Ohta 1992). Conversely, in populations with small N_e and higher genetic drift, neutral alleles are fixed or lost more rapidly. Deleterious alleles with small effects on fitness are not subject to efficient natural selection in populations with small N_e, so they may behave as neutral alleles, persisting in populations instead of being rapidly removed by selection (Ohta 1992). In spatial population genetics, the influence of N_e on time to coalescence implies that spatial genetic structure should arise more rapidly in populations with small N_e (Maruyama 1971; Hardy and Vekemans 1999; Irwin 2002). In other words, populations with small N_e are expected to reach spatial genetic equilibrium faster than populations with large N_e. In analyses of molecular evolutionary rate, the influence of N_e on strength of selection means that non-neutral alleles are expected to become substitutions more often in species with small N_e. As such, it is

important to account for effects of N_e when analyzing traits that potentially influence spatial or molecular evolution. Correlation between traits and N_e, which are known to exist (Eo et al. 2011; Waples et al. 2013; Chen et al. 2017; Kutschera et al. 2020), have the potential to introduce bias by making it appear that a pattern is directly influenced by a trait when it is actually more strongly influenced by N_e.

In chapters 3 and 4, I combine inferences across and within species to test hypotheses while accounting for effects of demography on population genetic processes. By analyzing genetic patterns within species as well as across species, my work explicitly acknowledges the influence population demographic processes on population genetic patterns and tests for confounding effects of demographic history vs species traits. My analysis framework is facilitated by my large population genetic dataset, which comprises population genetic data from many species co-distributed in the same landscape. My dissertation demonstrates the utility of multi-species population genomic systems for testing evolutionary hypotheses in a robust framework.

Chapter 2 The Influence of Seasonal Migration on Range Size in Temperate North American Passerines

Published as: The Influence of Seasonal Migration on Range Size in Temperate North American Passerines/TM Pegan and BM Winger/Ecography 43(8) https://doi.org/10.1111/ecog.05070.

2.1 Abstract

Seasonal migration has been alternately proposed to promote geographic range size in some contexts and to constrain it in others, but it remains unclear if migratory behavior has a general effect on range size. Because migration involves movement, most hypotheses about the relationship between migration and range size invoke an influence of migration on the process of dispersal-mediated range expansion. Intuitively, a positive relationship between migratory behavior and dispersal ability could bolster range expansion among migratory species, yet some biogeographic patterns suggest that long-distance migration may instead impede range expansion, especially in the temperate zone. We conducted a comparative analysis of the relationship between migratory behavior and range size by testing the effect of migratory status, migration distance, and morphological dispersal ability on breeding range size among all temperate North American passerines. Further, we assessed whether these traits affect range expansion into suitable habitat by analyzing their relationship with range filling (the proportion of climatically-suitable area occupied, or "filled" by a species). Contrary to previous studies, we

found migration and dispersal ability to be poor predictors of range size and range filling in North America. Rather, most variation in range size is explained by latitude. Our results suggest that migratory behavior does not affect range size within the scale of a continent, and furthermore, that temperate North American passerines' breeding ranges are not influenced by their dispersal abilities. To better understand why migratory behavior appears to promote range size in some contexts and constrain it in others, future studies should investigate how migratory behavior affects dispersal at the individual level, as well as the relationship between the evolution of migratory behavior and the breadth of species' climatic niches.

2.2 Introduction

The geographic range boundaries of species are determined by numerous biotic, abiotic and historical factors (Angert 2009; Price and Kirkpatrick 2009; Sexton et al. 2009). Among species occupying seasonal temperate latitudes, specialized adaptations for severe fluctuations in climate and resources are necessary for the persistence or expansion of geographic range. Some species have adaptations to survive seasonality in situ (e.g. hibernation), but a wide variety of animals, including birds, fish, mammals and insects, have independently evolved an alternative strategy: seasonal migration. This annual round-trip journey facilitates persistence by letting animals temporarily escape their breeding locations when climate becomes harsh and resources scarce. Migration therefore carries an important consequence for biogeography: the breeding ranges of migratory species are seasonally ephemeral, arising annually as the result of the site fidelity that drives them to return after traveling sometimes thousands of kilometers away (Winger et al. 2019). Here, we aim to understand how seasonal migration, a common life history

adaptation among birds breeding at high latitudes, influences the size and extent of birds' breeding ranges at a continental scale.

Previous studies have shown conflicting evidence as to whether migratory behavior generally promotes or constrains range size (Table 2-1). Some studies have found migratory behavior to be associated with increased range size (Blackburn and Gaston 1996; Gaston and Blackburn 1996; Böhning-Gaese et al. 2006; Laube et al. 2013b; Pigot and Tobias 2015; Outomuro and Johansson 2019) or increased likelihood of colonizing islands (Lees and Gilroy 2014) or continents (Thorup 2006). These studies have typically interpreted the elevated range size of migratory species to reflect a positive effect of migratory movements on the dispersal-mediated process of range expansion. Dispersal, the one-way movement of an individual from a natal location to a breeding location or from one breeding site to another (in contrast to the round trip of seasonal migration), may occur at higher rates or over longer distances in species with high morphological and physical capacities for movement (dispersal ability), potentially facilitating range expansion in these species (e.g. Cain et al. 2000; Dytham 2009; Kubisch et al. 2014). Indeed, dispersal ability has been shown to be positively associated with range size in a variety of volant animals including birds, dragonflies, and bats (Böhning-Gaese et al. 2006; Rundle et al. 2007; Laube et al. 2013b; White 2016; Luo et al. 2019). Owing to their capacity for long distance flights, migratory birds have inherently high dispersal ability (Bowlin and Wikelski 2008; Phillips et al. 2018). Migratory behavior could also promote range expansion through a tendency of migratory animals to become "lost" and subsequently breed far from where they were born (Lees and Gilroy 2014) as a direct consequence of the migratory journey.

However, other studies have revealed biogeographic patterns suggesting that migratory behavior, particularly long-distance migration, constrains breeding range expansion. These

studies have focused on temperate bird communities whose constituent species are predominately migratory. For example, Böhning-Gaese et al (1998) demonstrated that long-distance migratory birds in the Northern Hemisphere are less likely than short-distance or non-migratory taxa to have colonized multiple continents to become Holarctic in distribution. At a smaller geographic scale, Bensch (1999) and Henningsson and Alerstam (2008) found that long-distance migrants were less likely than short-distance migrants or non-migrants to occupy a large breeding range in the Eurasian boreal forest and in terrestrial arctic regions, respectively. More recently, species distribution modeling (SDM) studies of migratory species have interpreted the presence of apparently suitable habitat outside of the occupied breeding range to reflect a constraint of migratory behavior on range expansion (Engler et al. 2014, Toews 2017). Authors of these studies note that migratory taxa may experience strong selection against dispersal into novel regions if such range expansions are incongruous with their finely tuned migratory routes or timing (Böhning-Gaese et al. 1998; Bensch 1999; Engler et al. 2014; Toews 2017). Migratory routes are thought to have a strong genetic component (Berthold and Querner 1981; Helbig 1991; Delmore and Irwin 2014), such that individuals dispersing to locations outside their normal range may fail to establish a persistent population if their innate migration route leads to unsuitable areas when undertaken from the novel region. That is, failure to adapt migratory routes to new geographic settings could limit range expansion.

As diverse as these hypothesized processes are, all of them suggest migration influences range size through an effect on range expansion — either by promoting or constraining it. These hypotheses assume that unoccupied suitable habitat exists outside of many species' breeding ranges (i.e., that they show range boundary disequilibrium: Sexton et al. 2009; Peterson et al. 2011). However, the relationship between migratory behavior and the extent to which species

occupy suitable habitat has not been investigated at a broad taxonomic scale in a phylogenetic comparative framework.

Here we use the entire passerine fauna of temperate North America to investigate the relationship between seasonal migration and range size. Further, to understand whether seasonal migration influences range size through an effect on the process of range expansion, we test whether migratory behavior is correlated with the amount of climatically suitable habitat each species occupies (a metric called "range filling", assessed with Species Distribution Modeling, e.g. Laube et al. 2013a; Boucher-Lalonde and Currie 2016; Estrada et al. 2018). Previous studies have not produced a clear general prediction for how migration affects range size (Table 2-1), but studies focusing on terrestrial temperate species have tended to find evidence that long-distance migration constrains range expansion, perhaps reflecting the difficulty of adapting the precise timing and direction of long-distance migratory movements to new locations (Böhning-Gaese et al. 1998; Bensch 1999; Henningsson and Alerstam 2008; Toews 2017). As such, we predict that after controlling for latitudinal effects on range size (Stevens 1989; Blackburn and Gaston 1996; Gaston et al. 1998; Hawkins and Felizola Diniz-Filho 2006; Orme et al. 2006), migratory species in temperate North America should have smaller ranges than sedentary species, and migration distance should correlate negatively with range size.

Likewise, we further predict that long-distance migration constrains range filling in temperate North American species, which would be evidence that migration constrains these species' range size specifically through its influence on the process of range expansion (Engler 2014, Toews 2017). Analyzing range filling allows us to assess whether a relationship between migration and range size is mediated by the tendency of species to occupy all area available to them within their climatic niche (sensu Hutchinson 1957). If migratory behavior constrains

range expansion, we predict that migratory species should show more unoccupied suitable habitat (i.e. lower range filling) than nonmigrants and that migration distance should correlate negatively with range filling.

Given the positive relationship between migratory behavior and movement capacity, we also analyze whether dispersal ability (as measured by wing shape) predicts range size and range filling in temperate North America. However, we predict that morphological dispersal ability is not an important determinant of passerine breeding range size in a temperate continental context. Although the high dispersal ability associated with migration may generally promote range expansion when taxa are compared at a global scale (e.g. Pigot and Tobias 2015), temperate bird species tend to show high dispersal ability relative to tropical species regardless of whether they migrate (Moore et al. 2008; Salisbury et al. 2012). That is, we expect that all North American birds are sufficiently vagile that their dispersal ability should not impose a constraint on range size.

Clarifying the relationship between migration, dispersal and range size is an important step for understanding the evolution and biogeography of birds in temperate latitudes where migration is prevalent. The life history and ecology of migratory species are strongly shaped by their migrations (Berthold et al. 2003). If the effects of migratory behavior extend to geographic range size, then migration could also influence range-mediated macroevolutionary and macroecological processes such as extinction (Lawton 1993; Jablonski 2005), speciation (Mayr 1942; Kisel and Barraclough 2010) and community assembly (Arita and Rodríguez 2002; Graves and Rahbek 2005). Yet seasonal migration is only one of numerous factors that can influence range size and it is unclear whether its hypothesized effects should produce a general trend in range size among migratory birds with diverse biogeographic and life histories. Our study, using

the entire passerine avifauna of North America, represents the most comprehensive analysis to date of whether migration shows an emergent effect on range size and range filling in temperate birds.

2.3 Methods

2.3.1 Species and geographic area covered by analyses

For the purposes of our analyses, we defined the southern edge of temperate North America as 23º latitude, which coincides with a recognized transition zone between a primarily sedentary and a primarily migratory avifauna (Cox 1985) and a major biogeographic transition zone more generally (Morrone 2015; White et al. 2019). We included all passerine species whose breeding ranges exist entirely or partially above 23º latitude in continental North America, except 4 species of Eurasian passerines with small portions of breeding range at the margins of arctic North America (*Phylloscopus borealis, Motacilla tschutschensis, Oenanthe oenanthe, Cyanecula svecica*), and two species for which we did not have access to specimens to measure wing morphology (*Melozone aberti, Polioptila nigriceps*). Our study includes 306 species, of which 228 are migratory and 78 are nonmigratory. A list of species used in our analyses can be found in Appendix Table A.1-1.

Some species in our study have breeding ranges extending south of 23º or to the eastern hemisphere, but we include only the portion of the range that exists within North America above 23º. Although limiting the geographic scope of our analyses requires us to draw an artificial boundary to the continent and to species' ranges, it allows us to test our hypotheses within a specific, highly seasonal geographic context with a high proportion of migratory species. Furthermore, bird species in tropical regions show different range size patterns than temperate species (Hawkins and Felizola Diniz-Filho 2006; Orme et al. 2006), and including tropical

species or tropical portions of species' ranges would complicate our ability to interpret results. To test whether using 23° latitude as a boundary for the study biases our results, we also repeated our analyses using only species endemic to higher latitudes (i.e., those whose ranges did not have an artificial boundary at 23º latitude) and report the results of these analyses in Appendix Table A.6-1.

2.3.2 Calculating response variables: range size and range filling.

We calculated range size using BirdLife International polygons (BirdLife International 2015) with Lambert azimuthal equal area projection using the R package *rgeos* (Bivand and Rundel 2019). We calculated range filling using species distribution models (see Supplemental Material for Chapter 2). Briefly, we calculated species distribution models (SDMs) using Maxent as implemented in the R package *maxnet* (Phillips 2017). Presence points came from the citizen science database eBird (Sullivan et al. 2009). We spatially thinned the presence points to reduce sampling bias (Kramer-Schadt et al. 2013; Boria et al. 2014). We sampled 100,000 background points from across North America. Points were sampled randomly but the probability that a background point existed on a particular raster cell was proportional to the number of eBird checklists within that cell (this subjects background points to the same effort biases as the presence points). Our model predictors were all 19 WorldClim bioclimatic variables (Fick and Hijmans 2017); elevation data; and NDVI data from 2010-2012 and 2014-2015 obtained with the R package *gimms* (Pinzon and Tucker 2014; Detsch 2018). After running an SDM, we made a raster of climatically suitable habitat using the function "threshold" (from the R package *dismo;* Hijmans et al. 2017). This function counts a cell as suitable if its predicted suitability value is as high or higher than the suitability value with the highest sum of sensitivity (proportion of correctly-predicted presences) and specificity (proportion of correctly-predicted absences) for

that model. Then, using Lambert azimuthal equal area projection, we calculated the total area predicted to be suitable and compared it to the suitable area within the BirdLife International polygon to calculate range filling (**Error! Reference source not found.**).

2.3.3 Calculating predictors: migratory status and distance, wing shape, mass, and breeding range latitude

We characterized variation in migratory behavior using two metrics: a binary variable indicating whether or not a species is migratory (hereafter, "migratory status"), and a continuous estimate of migration distance. We measured migration distance as the distance between the centroid of a species' breeding range and the centroid of its wintering range. Similarly, we defined migratory status based on whether the distance between the centroid of species' breeding and wintering ranges was greater than 10 kilometers (migratory) or not (nonmigratory). Distances were calculated in a latitude/longitude projection using the function "distGeo," which accounts for the curvature of the earth, from the R package *geosphere* (Hijmans 2019a). Species range shapefiles, including breeding, resident (year-round), and nonbreeding ranges, were downloaded from BirdLife International (2015). For partially migratory species (i.e. species in which some populations migrate and others do not), the resident range where individuals are present year-round was included as part of both the breeding and wintering range when range centroids were calculated.

Variation in morphological dispersal ability in birds is best captured by wing shape (Claramunt and Wright 2017), which is related to flight efficiency (Bowlin and Wikelski 2008). We measured wing shape using a metric of wingtip pointedness called hand-wing index (HWI; Claramunt and Wright 2017). High HWI indicates a pointed wingtip suited for long-distance flight while low HWI indicates a rounded, less-efficient wingtip. We used calipers to measure

two museum specimens for each species from the University of Michigan Museum of Zoology. We use mass as a covariate in all models with wing shape. Mass data were obtained from the CRC Handbook of Avian Body Masses (Dunning 1992). For species not included in the CRC Handbook, we obtained mass data from Birds of North America Online (Rodewald 2015).

In all of our analyses, we include latitude as a covariate. With increasing latitude, migratory behavior becomes increasingly prevalent and migration distances increase (Newton and Dale 1996, Somveille et al. 2015; Appendix Figure A.2-1). Latitudinal gradients in other factors that affect range — such as climatic tolerance, habitat size, biogeographic history, or species richness — may lead to a positive relationship between range size and latitude (Stevens 1989; Hawkins and Felizola Diniz-Filho 2006; Orme et al. 2006). In addition to the possible biotic effects of latitude on range size, the geographically bounded nature of our study results in a strong hump-shaped relationship between latitude and the maximum possible range size at that latitude (Appendix Figure A.2-2). We measured the latitudinal midpoint of each species' North American breeding range in maps with a latitude/longitude projection. For species whose ranges extend south of 23º latitude, we used 23º latitude as the southern range limit in these calculations. We use latitudinal midpoint as a quadratic term in our models of range size because of the relationship between latitude and maximum range size. The maximum possible range filling for every species is 1.0, regardless of range size, so this metric is not affected by continental bounds and we include latitude as a linear predictor in models with range filling as the response variable. We hereafter refer to this predictor simply as "latitude."

2.3.4 Hypothesis testing

We used R (version 3.5.2, R Core Team 2018) to explore our data (following recommendations of Zuur et al. 2010) and to fit generalized linear models assessing the influence

of migratory status, migration distance, and morphological dispersal ability on range size and range filling. Range size shows a positive skewed distribution, so we used Gamma regression with a log link for models with these response variables. Range filling is a proportion, so for models of range filling we used beta regression (Cribari-Neto and Zeileis 2010b). Our predictors span several orders of magnitude, so we centered and standardized all predictors such that the mean was 0 and the standard deviation was 1. We rescaled range size to between 1 and 10 to improve model fitting.

Species with shared evolutionary history are not independent of each other, so it is necessary to consider phylogenetic relationships when comparing traits among many species (Felsenstein 1985). However, unlike methods such as phylogenetic generalized least squares that incorporate phylogenetic relatedness into regression frameworks directly, few methods are available to control for phylogenetic relatedness with gamma and beta regression. Therefore, we tested whether phylogenetic relatedness had an influence on our model results by fitting a full model (i.e. with all predictors) with a phylogenetic covariance matrix and a full model without the matrix using the Bayesian R package *brms* (Bürkner 2017) and comparing the results. We downloaded phylogenetic data for all of our species from birdtree.org (Jetz et al. 2012, "Hackett all species" dataset) as a sample of 2000 phylogenetic trees. We calculated a consensus tree from these data using the SumTrees program in the *DendroPy* python package (Sukumaran and Holder 2010) and used the R packages *ape* (Paradis and Schleip 2019) and *phytools* (Revell 2012) to manipulate phylogenetic data in R.

Our results indicated that the phylogenetic covariance matrix did not influence model results (Appendix Table A.4-1, Appendix Table A.4-2). Therefore, we carried out the remainder

of our analyses using functions from R's default *stats* package and from *betareg* (Cribari-Neto and Zeileis 2010a).

After fitting a full model for each response variable, we used the package *MuMIn* (Bartón 2019) to compare the AICc of the full model with that of three reduced models (one model using only migration predictors, one using only wing shape and mass, and one using only breeding latitude) to test for overfitting of the full model.

Finally, we repeated our analyses on two subset datasets (Appendix Table A.6-1, Appendix Table A.6-2). First, to test whether cropping ranges at 23° latitude influenced our results, we fit models using only the 161 species whose entire range is north of 23° latitude. Second, to test whether wing shape shows a relationship with range size among less-mobile species, we next repeated our analyses on a dataset including only 78 non-migratory species. Models including non-migrants did not include migration-related predictors.

2.4 Results

2.4.1 Species distribution models

The average AUC (a measure of model fit) for our species distribution models was 0.91 (range 0.61 to 1), indicating that our models generally performed much better than a random null model (which would produce AUC = 0.5; Phillips 2010). AUC values are expected to correlate with species range size (Phillips 2010), which we observed in our data: models with low AUC tend to come from species with large ranges (Table A1).

2.4.2 Do migration and wing shape influence range size in North American passerines?

Migration and wing shape are significant predictors of range size in a model with no other predictors, but in our best-fit model predicting range size, which included latitude as a quadratic predictor, no predictors were significant other than latitude (latitude β=7.18, SE=0.51, $p < 0.0001$; latitude^2 β=-3.90, SE=0.43, $p < 0.0001$; migratory status β=0.017; SE=0.070; p=0.81; migration distance β=0.0068; SE=0.033; p=0.83; wing shape β=0.051; SE=0.03; p=0.076; mass β=0.046; SE=0.026; p=0.079). When latitude is included in the model, migratory status, migration distance, and wing shape do not significantly contribute to explaining variation in range size (Figure 2-2; Appendix Table A.5-1).

2.4.3 Do migration and wing shape influence range filling in North American passerines?

The best-fit model for range filling included only migratory status and migration distance as predictors, but these predictors were not significant (migratory status β=0.12, SE=0.14, p=0.36; migration distance β=0.059, SE=0.060, p=0.33) and the pseudo-R^2 of this model was low (0.013). None of the predictor variables were significant in any of the models of range filling (Figure 2-2; Appendix Table A.5-2)

2.4.4 Results of analyses on subset datasets

Models fit with species whose ranges are entirely north of 23° latitude and models fit with only non-migrants produced results that are qualitatively similar to models fit with all species in our dataset: latitude is the strongest predictor of range size and filling, and the addition of other predictors (migratory status and distance, wing shape, mass) does not improve model fit (Appendix Table A.6-1, Appendix Table A.6-2).

2.5 Discussion

Although the geographic location and interannual reappearance of migratory species' breeding ranges depend on their migratory behavior, we found no evidence of an emergent effect of migration or dispersal ability (wing shape) on range size. Our analyses failed to reject the null hypotheses that range size is unrelated to migratory behavior or wing shape. Other possible causes of range size variation, such as latitudinal effects, climatic niche breadth, or biotic factors may have stronger influence on range size in this avifauna. Indeed, we found evidence that latitude shows a strong relationship with range size (Table 2-2; Appendix Figure A.2-3), and migratory behavior and wing shape were not significant predictors of range size or range filling after controlling for latitude. However, our analyses were designed specifically to test the emergent influence of migration and wing shape on range size, rather than to parse which of many other biotic or abiotic factors most strongly influences range size, so we refrain from drawing conclusions about the dynamics that contribute most to range size variation among North American birds.

We also tested whether migration or wing shape influence range filling. Range filling represents the extent to which species occupy climatically-suitable area (as determined by their present distributions), so it allows us to test for an effect of migratory behavior or wing shape on range expansion even in circumstances where raw range size variation is more strongly influenced by climatic niche or other factors. Here, too, we did not reject the null hypotheses that there is neither a relationship between migration nor wing shape and range filling.

Our calculation of range filling comes with two caveats. First, our SDMs assessed only climatic suitability. Biotic interactions (such as the presence of competitors, important resource species, or predators and pathogens) also limit species' capacity to exist in climatically suitable

areas (Peterson et al. 2011; Laube et al. 2013a; Sanín and Anderson 2018). Second, it is also possible that unoccupied "climatically suitable" regions are not actually climatically suitable for the species, but instead represent a mismatch between the predictors we used to build our species distribution models and the factors that determine our species' range boundaries. Without knowledge of the proximate causes of a species' range boundary, it is difficult to assess whether a model is capturing information about what *determines* climatic suitability for that species (Boucher-Lalonde and Currie 2016; Moore et al. 2018). Nonetheless, the hypothesis that long-distance seasonal migration generally limits range filling in temperate birds (Engler et al. 2014; Toews 2017) is not supported by our results.

Our results add to a body of correlative studies that, when considered together, suggest that the apparent effects of migration and wing shape on biogeographic patterns depend on the geographic context and taxonomic scale of the analysis. Past work on smaller groups of taxa has suggested that migration constrains breeding range expansion within the scale of a continent (Bensch 1999, Engler et al 2014, Toews 2017), but we find that this is not a general pattern when considering the full set of North American passerines. However, it is worth noting that our data replicate the pattern described by Toews (2017): among the 17 parulid warbler species considered in that study, longer-distance migrants tend to have smaller ranges and lower range filling values (Appendix Table A.1-1). Further, migration may still constrain colonization between continents (Böhning-Gaese et al 1998), which could require a more abrupt and longer-distance geographic shift that species with inflexible migratory behavior may be unable to accommodate. The processes producing these varying patterns remain elusive.

Our results also contrast with those of other authors who found positive relationships between migration or wing shape and range size even among highly volant taxa (Blackburn and

Gaston 1996, Gaston and Blackburn 1996, Böhning-Gaese et al 2006, Laube et al 2013a, b, White 2016, Pigot and Tobias 2015, Luo et al 2019, Outomuro and Johansson 2019). Unlike our study, most of these other studies include both temperate and tropical fauna. Tropical organisms, including birds and flying insects, are known to be poorer dispersers than their temperate counterparts (Moore et al. 2008; Salisbury et al. 2012; Polato et al. 2018). Our results suggest that temperate passerines are generally mobile enough that dispersal limitation does not affect their ability to expand their ranges. Even nonmigratory members of this avifauna show no relationship between wing shape and range size (Appendix Table A.6-2). As such, relationships between dispersal ability and range size in volant organisms that are apparent at a global scale, such as those found by Blackburn and Gaston (1996), Gaston and Blackburn (1996), Pigot and Tobias (2015), and Luo et al (2019), are likely not maintained when poorly-dispersing tropical species are excluded. Although Laube et al (2013a) found a positive effect of dispersal ability on range size in temperate European passerines (including migratory species), this analysis did not control for breeding latitude and thus is difficult to compare with our results.

Migratory behavior could also affect range size if it is correlated with other determinants of range size that are not directly related to movement (Stevens 1989, Blackburn and Gaston 1996, Gaston and Blackburn 1996). For example, migratory birds may be less ecologically specialized than sedentary birds (Gómez et al. 2016; but see Martin and Fahrig 2018) and as such their suitable habitat area may be larger. Migration also allows birds to breed at high latitudes, where range sizes tend to be larger than they are in the tropics (Blackburn and Gaston 1996; Hawkins and Felizola Diniz-Filho 2006; Orme et al. 2006), while avoiding the harshest climatic conditions associated with these latitudes (Winger et al. 2019). The ability to discern the processes underlying variation in the relationship between migratory behavior and range size

across studies is limited because traits and biogeographic patterns can be spatially autocorrelated: an apparent relationship between a trait and a biogeographic pattern does not necessarily imply that the pattern is caused by the trait, even when there is a putative biological mechanism (Gove et al. 2009; Warren et al. 2014).

To better understand what factors constrain or promote range size in migratory animals, it will be useful to investigate how range boundaries are formed in these species. For example, the processes affecting range size in species whose range boundaries reflect the limits of their climatic niche are different from those of species showing range boundary disequilibrium (Sexton et al. 2009; Hargreaves et al. 2014). In cases when range boundaries are proximately determined by climatic niche (**Error! Reference source not found.**c,d) and the species has nowhere to expand without broadening its niche, traits such as migratory behavior may be less likely to influence range expansion. The relationship between species' migratory behavior and the breadth of their climatic niches has been a topic of increasing interest in recent years (e.g. Gómez et al. 2016; Reif et al. 2016; Martin and Fahrig 2018b; Ponti et al. 2019) and results of further such studies will contribute to our understanding of the biogeography of migratory taxa.

We will also gain insight into the processes affecting range boundaries in migratory animals by tracking the fate of individual dispersers, especially near range edges. For example, recent studies tracking migratory godwits (*Limosa limosa*) have demonstrated that shifts in geographic range and migratory routes are driven by dispersal of young individuals, while adults remain site faithful throughout their lives (Verhoeven et al. 2018; Gill et al. 2019). However, more generally, the relationship between migratory behavior and dispersal is poorly understood. The extent to which dispersal patterns in migratory birds are dictated by exploration of and settlement in novel environments versus site fidelity and natal philopatry— attempting to return

to a previous territory or a habitat similar to where an individual was born—has implications for how the breeding ranges of these species have evolved and how they respond to environmental change (Davis and Stamps 2004; Canestrelli et al. 2016; Jønsson et al. 2016).

2.6 Acknowledgements

We thank Brian Weeks, Eric Gulson-Castillo, Susanna Campbell, Shane DuBay, Marketa Zimova, Kristen Wacker, and Rachel Wadleigh for helpful discussion. Janet Hinshaw and Brett Benz facilitated access to specimens at the University of Michigan Museum of Zoology. Vera Ting, Charles Kotila, and Kaia Newman assisted with wing shape measurements. Vera Ting and Charles Kotila were supported by the University of Michigan Undergraduate Research Opportunity Program. This research was supported in part through computational resources and services provided by Advanced Research Computing at the University of Michigan, Ann Arbor. Teresa Pegan was supported by a National Science Foundation Graduate Research Fellowship.

2.7 Figures and Tables

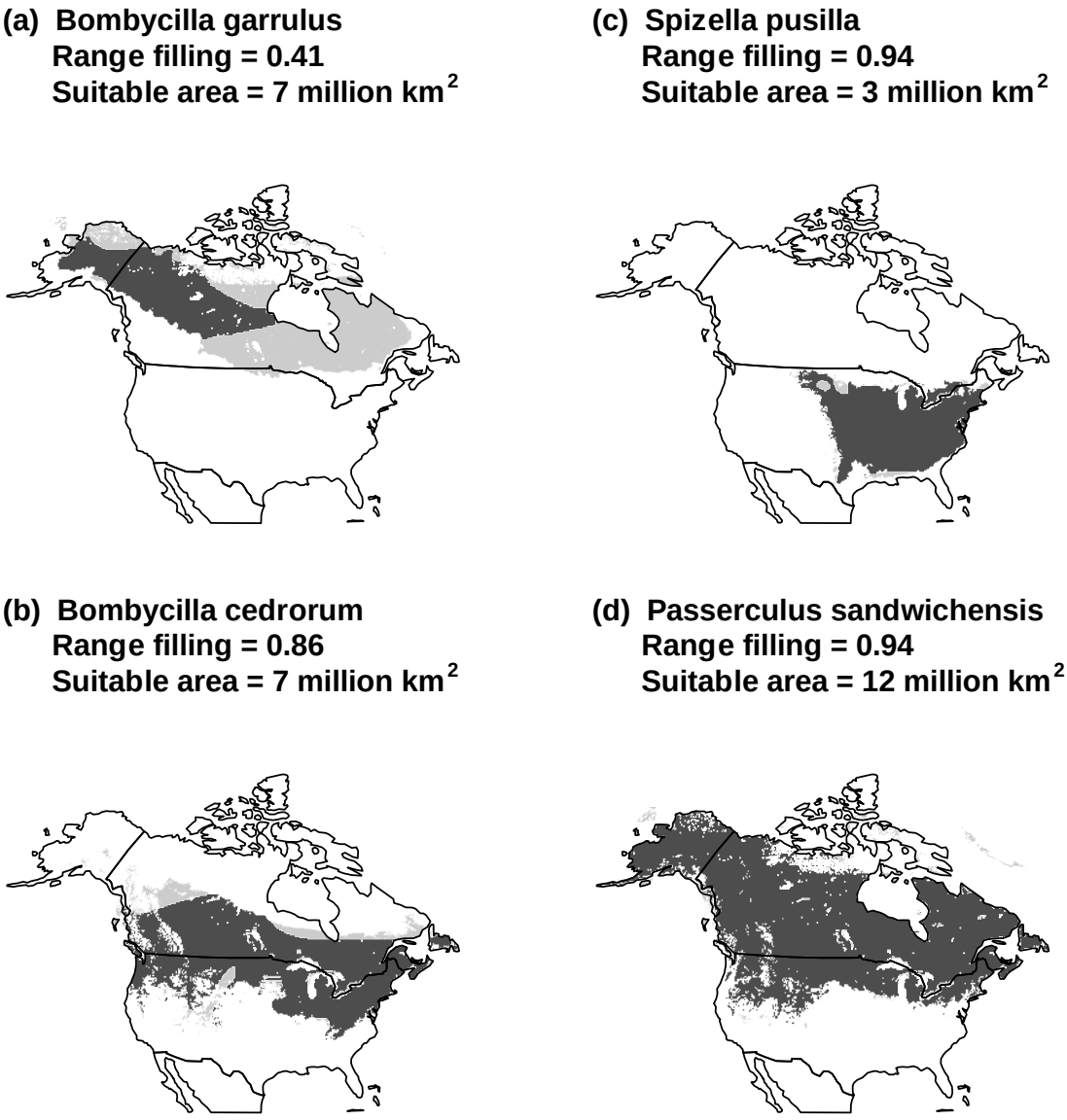

Figure 2-1 Example maps of range filling demonstrate that range size (dark gray) is affected by both suitable habitat area (light gray) and range filling (proportion of suitable habitat covered by range). On the left side of the figure are maps for two species of waxwings which have a similar amount of climatically suitable habitat but different range filling values. *Bombycilla garrulus* (a) has lower range filling than *Bombycilla cedrorum* (b), so it has a smaller range. The substantial range boundary disequilibrium demonstrated by *Bombycilla garrulus* suggests that this species could be constrained from expanding its range by a dispersal limitation or by a biotic factor such as the presence of a competitor. On the right sight of the figure are maps for two species of sparrows that show little range boundary disequilibrium: both species occupy almost the entirety of their suitable habitat. However, their ranges are different in size because *Spizella pusilla* (c) has less suitable habitat than *Passerculus sandwichensis* (d). Because little climatically suitable habitat exists outside of the range of either of these species, the difference in range size between them is not likely attributable to dispersal or migration-related constraints on range expansion.

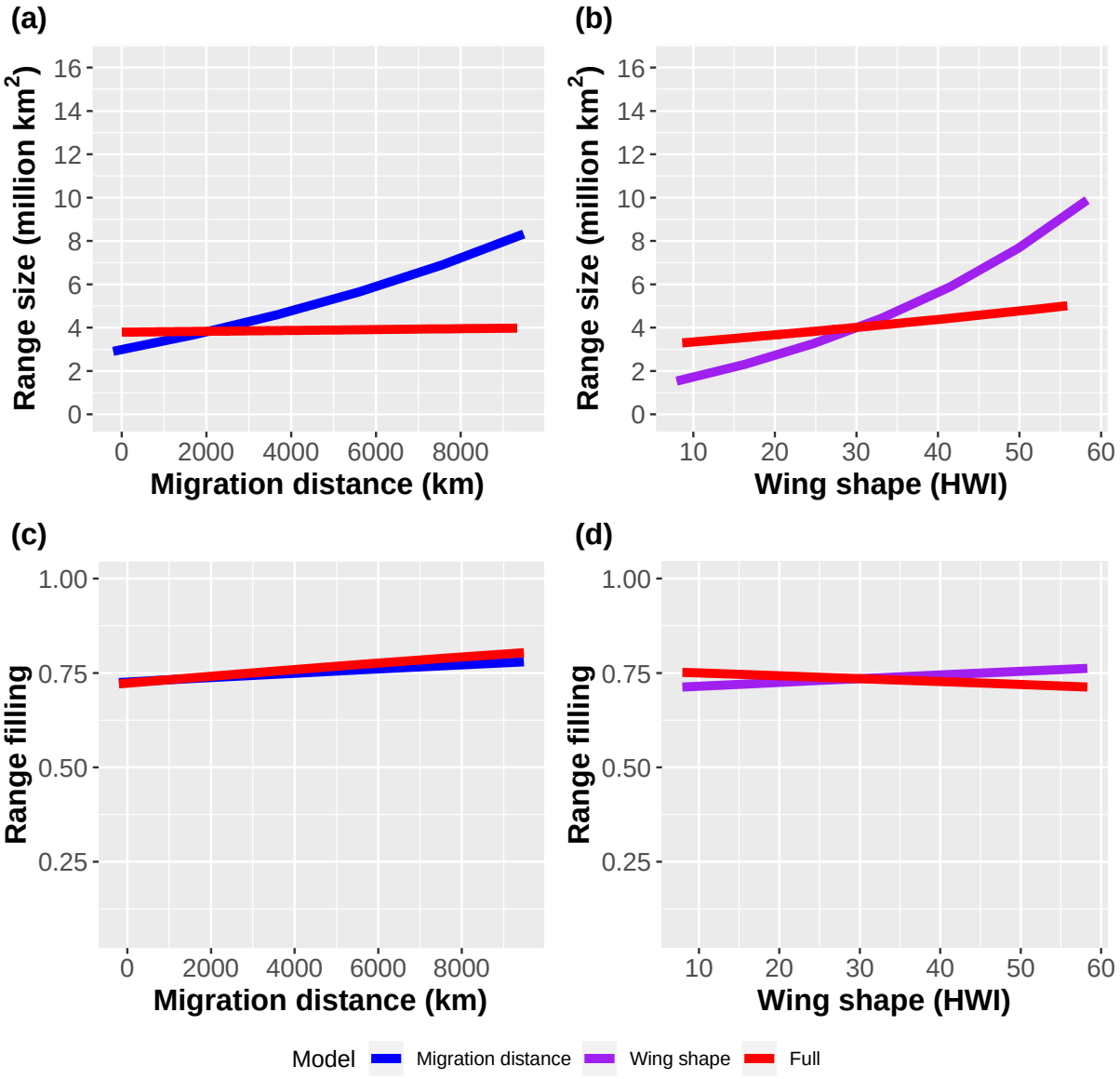

Figure 2-2. Scatter plots of geographic range vs migration distance and wing shape. Range size increases slightly with migration distance and wing shape (a, b; blue and purple line, respectively), but these effects are not significant in models that include latitude as a predictor (a, b; red lines). Migration distance and wing shape show no significant relationship with range filling (c, d). Each point represents one species. Species with wing shape HWI values greater than 50 belong to the family Hirundinidae (swallows). Lines on plots show marginal effects (with confidence intervals) of migration distance on range size or range filling. Line color indicates which model (*Table 2-2*) the plotted migration distance marginal effect estimate comes from: blue lines are from a model with only migratory status and migration distance predictors; purple lines are from a model with only wing shape and mass predictors; and red lines are from a full model which includes all predictors, including latitude.

Table 2-1. A summary of 20 studies assessing the effect of migration on a property of geographic range. For each study, "Migration" column indicates how migration behavior was classified; "Range" column indicates what type of range variable was analyzed; "Phylogeny" column indicates whether the study tested for or accounted for phylogenetic relatedness; "Latitude" column indicates whether the study tested for or accounted for an effect of

latitude on range; and "Effect" column indicates how migration affected range in the study. These studies analyze breeding range and/or resident range, not wintering range, unless otherwise noted. These studies show no consistent relationship between migration and geographic range, but they also vary widely in purpose, method of analysis, and geographic and taxonomic scope. Most of these studies focus on a variety of traits, including migration, to identify traits related to the geographic range variable in question, but some specifically focus on migration (Böhning-Gaese et al. 1998; Bensch 1999; Thorup 2006; Henningsson and Alerstam 2008; Toews 2017).

Ref	**Main question**	**Range**	**Migration**	**Geographic scale**	**Species**	**Phylo-geny**	**Lati-tude**	**Effect**
Gaston and Blackburn 1996	What affects range size?	Range size	Non/short /long	Worldwide	158 Anseriformes (Aves)	Yes	Yes	+
Blackburn and Gaston 1996	What affects range size?	Range size	Nonmigratory /Migratory	Western hemisphere	3906 birds	Yes	Yes	+
Böhning-Gaese et al. 1998	Does migration affect colonization ?	Longitudinal colonization between continents	Non/short /long	North America and Europe	526 land birds, 460 nonvolant mammals	Yes	No	−
Bensch 1999	Testing hypotheses of Böhning-Gaese et al. 1998	Longitudinal colonization within continent	Nonmigratory /Migratory	Scandinavia and Siberia	Land birds: 153 Scandinavian, 187 Siberian	No	Yes	−
Forsyth et al. 2004	What affects invasion success?	Invasion success within continent	Nonmigratory /Migratory	Australia	40 introduced mammals	Yes	No	−
Böhning-Gaese et al. 2006	What affects range size?	Range size	Migration distance	Eastern Hemisphere	26 *Sylvia* (Aves: Sylviidae)	Yes	Yes	+
Thorup 2006	Testing hypotheses of Böhning-Gaese et al. 1998, Bensch 1999	Number of continents comprising wintering range	Non/short /long	South America, India, Africa	5662 Non-pelagic birds	No	No	+
Henningsson and Alerstam 2008	Testing hypotheses of Böhning-Gaese et al. 1998, Bensch 1999	Range size	Non/short /long	Arctic region	208 birds	Yes	No	− in terrestrial birds; + in pelagic birds
Brommer 2008	What affects range shifts?	Range shift in recent time	Non/short /long /irruptive /partial	Finland	116 birds	No	No	No effect
Zuckerberg et al. 2009	What affects range shifts?	Range shift in recent time	Non/short /long	New York	129 birds whose ranges shifted	No	No	− for elevation shifts; no effect on

								latitude shifts
Brommer and Møller 2010	Extension of Brommer 2008	Range shift in recent time	Non/short /long /irruptive /partial	Finland and Britain	138 birds	No	No	+, but partial migrants shifted more than obligate migrants
Angert et al. 2011	What affects range shifts?	Range shift in recent time	Nonmigratory /Migratory	North America and Britain	245 North American birds, 24 British odonates	Yes	Yes	No effect
Tingley et al. 2012	What affects range shifts?	Elevational range shift in recent time	Non/short /long	Sierra Nevada Mountains	99 birds	No	No	− Long distance migrants less likely to shift in elevation
Laube et al. 2013a	What affects range size?	Range size	Non/short /long /facultative /obligate	Europe	165 passerines	Yes	No	+
Lees and Gilroy 2014	What affects island colonization ?	Colonization of islands	Nonmigratory /Migratory	Worldwide	544 birds breeding on or near 66 islands	Yes	Yes	+ in temperat e zone only
Engler et al. 2014	What affects range limits in Citril Finch?	Range filling	NA: not comparative	Europe	*Carduelis citronella* (Aves: Fringillidae)	NA	NA	No statistica l comparis on; negative effect suggeste d
Pigot and Tobias 2015	What affects whether sister species are sympatric?	Whether sister species are sympatric	Non/short /long	Worldwide	533 vertebrate sister species pairs (275 bird pairs)	Yes	Yes	+
Toews 2017	Do migratory warblers have unoccupied suitable habitat in the western boreal forest?	Range filling	NA: not comparative	Boreal forest of North America	17 Parulidae (Aves)	No	No	No statistica l comparis on; negative effect suggeste d

Estrada et al. 2018	What affects range filling?	Range filling	Nonmigratory /Migratory	Europe	335 birds, 125 mammals	Yes	Yes	No effect
Outomuro and Johansson 2019	What affects range size?	Range size	Nonmigratory /Migratory	North America	81 Libellulidae (Odonata)	Yes	Yes	+

Table 2-2 Models predicting range size and range filling. Migratory status and migratory distance are not significant predictors of range size in the best-fit model (see also Appendix Table A.*5-1*). None of our predictors showed a significant relationship with range filling (see also Appendix Table A.*5-2*). Model coefficients were calculated with centered/standardized predictors with mean=0 and sd=1. Range size is rescaled to be between 1 and 10 and range filling is a proportion. R^2 shown for models of range size are trigamma estimates calculated using the R package MuMIn. For models of range filling, we show pseudo R^2 calculated by the R package betareg.

Response	**Migrat-ory status**	**Migrat-ion distance**	**Wing shape**	**Mass**	**Latitude**	**Latitude^2**	**logLik**	**AICc**	**Delta**	**Weight**	**R^2**
Range size	0.017	0.0068	0.051	0.046	7.18	-3.90	-431.1	878.8	0	0.78	0.58
Range size	-	-	-	-	7.67	-3.97	-436.6	881.3	2.58	0.22	0.58
Range size	0.37	0.15	-	-	-	-	-530.4	1069.0	190.2	0	0.19
Range size	-	-	0.21	0.017	-	-	-544.3	1096.7	217.9	0	0.11
Range filling	0.12	0.059	-	-	-	-	122.7	-237.3	0	0.49	0.013
Range filling	-	-	-	-	0.05	-	121.2	-236.3	0.93	0.31	0.002
Range filling	-	-	0.042	0.031	-	-	121.5	-234.8	2.49	0.14	0.004
Range filling	0.18	0.092	-0.033	0.078	-0.028	-	123.7	-233.1	4.18	0.06	0.02

Chapter 3 Spatial Population Genetics of the North American Boreal Avifauna

3.1 Abstract

The consequences of seasonal migratory behavior for long-term spatial evolution are poorly understood. Many seasonal migrants undergo extremely long-distance movements, which potentially promotes gene flow. However, despite their long-distance seasonal movements, adult migrants often have high breeding site fidelity, which could limit gene flow. The extent of natal dispersal in migratory birds is poorly understood due to the difficulties of tracking small volant animals. The influence of seasonal migration on dispersal and gene flow is therefore unclear. To address this question, we take a comparative phylogeographic approach to describe spatial genetic variation in 34 species of seasonally migratory birds co-distributed across the North American boreal forest belt east of the Rocky Mountains. We leverage the lack of major extrinsic barriers in this region, coupled with a high diversity of migratory strategies among sympatrically breeding species, to assess the relationship between seasonal migration and continuous spatial patterns of genetic divergence. To characterize continuous spatial genetic divergence (isolation by distance) across species, we generated low-coverage whole genome sequences from 1778 individuals (n = 17-80 per species). We find that although migratory species tend to have weaker structure than nonmigratory species, long-distance seasonal migration does not appear to promote gene flow. Rather, several long-distance migrants show relatively strong isolation by distance, likely reflecting the role of philopatry in restricting gene flow in these species. Our study takes advantage of massive genome-wide datasets and PCA methods to identify subtle,

continuous spatial patterns that are difficult to detect in summary statistics such as F_{st} and pairwise genetic distance, while controlling for variation in effective population size.

3.2 Introduction

Spatial genetic patterns can be described both in terms of continuous and discrete variation (Wright 1969; Serre and Pääbo 2004; Patterson et al. 2006; Guillot et al. 2009; Bradburd et al. 2018). The observation that discrete population splitting often corresponds to geographic barriers inspired the field of phylogeography (Avise 1987), which has illuminated patterns of spatial genetic variation across numerous landscapes and taxa (Knowles 2009; Rissler 2016; Edwards et al. 2022). Early phylogeographic studies examined splits in lineages using single genes, while more recent advances allow model-based inference of population splitting based on data from many genes (reviewed in Knowles 2009). However, some species and geographic regions are less prone to the buildup of discrete phylogeographic splitting than others (Smith et al. 2017). Genetic differentiation forms as a result of sustained reduction in gene flow between regions, which is less likely to occur in systems that lack stable geographic barriers (Johnson et al. 2023) or in species with high dispersal ability (Burney and Brumfield 2009; Weeks and Claramunt 2014; Singhal et al. 2018). However, populations that lack discrete phylogeographic structure may show continuous spatial genetic variation, which is expected to be ubiquitous in natural populations (Meirmans 2012). The same fundamental processes of nonrandom gene flow that create phylogeographic splits also produce continuous spatial genetic patterns (Rissler 2016; Gagnaire 2020), but in the absence of major extrinsic barriers to gene flow, continuous spatial genetic patterns may reflect subtler effects of ecology and intrinsic species properties (Irwin 2002). Investigating patterns of spatial genetic variation across

continuous landscapes offers a valuable opportunity to investigate how species' traits influence patterns of population genetic differentiation.

The eastern boreal belt of North America is an example of a system where inference about the spatial evolutionary history of populations has been limited by low phylogeographic structure. This region extends over 3700 km from the eastern edge of the Rocky Mountains to the Canadian maritime provinces (Brandt 2009; Figure 3-1). At the edges of the continent, phylogeographic structure is strongly influenced by the Rocky Mountains (Milot et al. 2000; Weir and Schluter 2004; Graham and Burg 2012; van Els et al. 2012; Burg et al. 2014; Ruegg et al. 2014) and a hypothesized glacial refugium in Newfoundland (Colbeck et al. 2008; Hindley et al. 2018; Wilson et al. 2021), but the vast boreal belt in between lacks significant geographic or environmental barriers. Smaller-scale landscape features that potentially shape gene flow are unstable because boreal habitat is prone to natural disturbance (Engelmark 1999) and the region has experienced a dynamic history of glaciation (Dyke and Prest 1987; Brandt 2009; Clark et al. 2009). Populations of the eastern boreal belt consequently tend not to show discrete population structure within this region (Ruegg and Smith 2002; Davis et al. 2006; Milá et al. 2007a,b; Colbeck et al. 2008; Graham and Burg 2012; Ralston and Kirchman 2012; van Els et al. 2014; Haché et al. 2017; Hindley et al. 2018). Yet, continuous genetic variation may differ among boreal species, especially if these species differ in movement-related traits that influence dispersal (Peterson and Denno 1998; Meyer et al. 2009; Singhal et al. 2018).

Spatial genetic patterns arise from non-random gene flow, so species with traits that promote movement between breeding sites tend to show reduced genetic structure compared to species with lower dispersal (Burney and Brumfield 2009; Papadopoulou et al. 2009; Weeks and Claramunt 2014; Medina et al. 2018). Comparative phylogeography—a field comprising

analyses that consider many species across a common landscape—provides a valuable framework to test hypotheses about how traits influence spatial evolutionary patterns (Papadopoulou and Knowles 2016). Here, we apply a comparative phylogeographic framework to many co-distributed species across the continuous landscape of the eastern boreal belt. This system allows us to investigate intrinsic drivers of variation in spatial evolution without strong geographic barriers to dispersal, which can confound the relationship between traits mediating dispersal and phylogeographic patterns (Winger and Bates 2015; Freeman et al. 2023). Specifically, we test whether the strength of continuous genetic variation (isolation by distance) in boreal birds is influenced by seasonal migration, a trait that varies greatly among boreal bird species and is thought to influence spatial population dynamics and possibly gene flow.

Seasonal migration influences spatial population dynamics in complex ways. Migration involves the seasonal movement of individuals, and sometimes entire populations, from one region to another across hundreds to thousands of kilometers. These movements do not influence gene flow *per se* because seasonal migration is a round-trip journey that occurs separately from breeding, but seasonal migration may influence spatial genetic patterns through an effect on dispersal. In comparative studies involving migratory and non-migratory bird species, seasonal migration is often associated with traits thought to promote high dispersal (Phillips et al. 2018; Sheard et al. 2020) and there is evidence that migration promotes dispersal distance (Paradis et al. 1998; Dawideit et al. 2009; Arguedas and Parker 2012; Hung et al. 2017). At the same time, other studies have noted surprisingly low rates or distances of dispersal in long-distance migrants, given their mobility (Hansson et al. 2002; Förschler et al. 2010; Christie et al. 2023). Migration appears to restrict geographic range expansion in some contexts (Böhning-Gaese et al. 1998; Bensch 1999; Henningsson and Alerstam 2006; Engler et al. 2014; Toews 2017) and to

promote population divergence and speciation (Irwin 2009; Winker 2010; Arguedas and Parker 2012; Turbek et al. 2018; Uy et al. 2018; Gómez-Bahamón et al. 2020), reflecting constraints on dispersal and gene flow imposed by migration. More broadly, seasonal migration is distinguished from other movement behaviors by the breeding site fidelity that drives birds to return to their former breeding regions—and often to the same territories—even after moving far away (Winger et al. 2019). Migratory birds are thus characterized by traits that both promote and suppress dispersal, and it is unclear how these conflicting effects of migration influence gene flow over evolutionary time.

Here, we characterize spatial genetic patterns in 34 small-bodied species of sympatrically breeding North American boreal birds and we test whether variation across species can be explained by migration distance. The North American boreal avifauna is a promising system for using comparative phylogeography to develop new understanding of seasonal migration's impact on long-term spatial genetic processes. Boreal bird species are broadly co-distributed in their breeding habitats, but they vary widely in migratory strategy (Winger and Pegan 2021; Figure 3-2). Some species are non-migratory, while others migrate various distances for the winter, ranging from short-distance movements within the north temperate region to long-distance movements to tropical South America. Boreal species also share broadly congruent demographic histories (Kimmitt et al. 2023), which helps to minimize the effects of confounding historical processes on their spatial genetic patterns.

Spatial genetic patterns are influenced by demographic history in addition to gene flow. Weak or absent spatial structure can be explained by high gene flow, lack of demographic equilibrium (i.e. recent disruption of a longer-term pattern by changes in population size or range), or both (Slatkin 1993; Hutchison and Templeton 1999; Whitlock and McCauley 1999).

In the boreal ecoregion, there is a particularly strong possibility that species may not have reached demographic equilibrium following range shifts induced by the last glacial maximum (LGM), which occurred only ~20 thousand years ago. The comparative nature of our study allows us to consider the potential effects of both movement behavior and demographic information on current spatial genetic patterns in an explicit hypothesis-testing framework. Species with high effective population size (N_e) are expected to take longer to reach demographic equilibrium because the low genetic drift associated with high N_e maintains neutral alleles within the population for extended periods (Maruyama 1971; Hardy and Vekemans 1999; Irwin 2002; Piertney et al. 2023). That is, populations with high N_e should show a greater degree of incomplete lineage sorting with respect to geography than populations with low N_e, all else being equal. We characterize genetic diversity in each species as a proxy for N_e and we consider potential effects of N_e when analyzing spatial genetic structure across species.

To test whether seasonal migration distance or effective population size (as reflected by genetic diversity) explains variation in the strength of continuous genetic structure across species, we generated low-coverage whole genome sequences from 17-80 samples for each of the 34 species in our study (1778 genomes in total), representing the efforts of over a decade of field work by ourselves and our colleagues. Analyzing large numbers of loci enhances our ability to infer subtle spatial patterns (Patterson et al. 2006; Novembre et al. 2008), especially when the number of samples available is limited (Gaughran et al. 2018; Iannucci et al. 2021; Lou et al. 2021). We used a genotype likelihood framework to quantify genetic diversity and continuous spatial genetic variation across species in the region.

3.3 Methods

3.3.1 Species and sampling regions

Our study system includes 34 co-distributed boreal forest bird species. These species vary somewhat in microhabitat preference and the extent of their geographic range beyond the boreal forest ecoregion, but they represent a core subset of the small-bodied species breeding in the boreal forest habitat of our sampling area (Cumming et al. 2014; Stralberg et al. 2017). Three species are woodpeckers (Piciformes), and the remaining 31 are from 16 genera and 9 families of songbirds (Passeriformes) (Table 3-1). We did not include species with nomadic tendencies (those in Fringillidae, Sittidae, Bombycillidae) in our analyses to focus on migratory species and non-migratory species. Our study species vary in migration distance (Table 3-1, Figure 3-2) but otherwise have similar life histories (e.g. mating system, age at first breeding season; Winger and Pegan 2021) and are distributed widely across forested habitats of the boreal and the temperate-boreal transition (hemiboreal) region (Weir and Schluter 2004; Omernik and Griffith 2014; Stralberg et al. 2017). We sampled species broadly and evenly across their boreal breeding ranges. Our sampling locations can be roughly grouped into 5 major regions (Figure 3-1) along the longitudinal axis of the boreal forest ecoregion. We refer to these sampling regions for convenience and we distinguish them by color on PCA plots to aid visualization, but we do not specifically expect these sampling regions to correspond to discrete genetic populations.

We sequenced DNA from 1778 samples (mean = 52±15 samples per species, range = 17-80 samples). Excluding regions with 0 samples for a given species (typically species with breeding ranges that do not cover the entire sampling region), the mean number of samples per sampling region was 11 (sd 7, range 1-28) and the mean number of regions sampled per species was 4.4 (sd 0.7, range 3-5). 86.5% of the samples came from ethanol-preserved or flash-frozen

specimen-vouched tissues deposited in the University of Michigan Museum of Zoology or obtained from other museum tissue collections, while the remaining 13.5% came from un-vouchered blood samples collected in the field by our collaborators and stored in ethanol, lysis buffer, or filter paper. All samples were collected during the breeding season. Fieldwork was approved by the University of Michigan Institutional Animal Care and Use Committee and all relevant permitting authorities (*see Acknowledgements*).

3.3.2 Sequencing

We extracted DNA using DNeasy Blood and Tissue Kits (Qiagen Sciences, Germantown, MD, USA) or phenol-chloroform extraction. Libraries were prepared using a modified Illumina Nextera library preparation protocol (Therkildsen and Palumbi 2017; Schweizer et al. 2021) and then sequenced on either an Illumina HiSeq or Illumina NovaSeq 6000 platform using paired-end sequencing of 150 bp reads. Libraries used in analyses produced an average of 32 million reads per sample (sd 9.9 million, range 7.1 million to 155.8 million.

3.3.3 Sequence data processing and alignment

We trimmed remaining adaptors and low-quality bases from demultiplexed data with AdapterRemoval v2.3.1 using the –trimns and –trimqualities options (Schubert et al. 2016). We used fastp v0.23.2 (Chen et al. 2018b) with the --cut_right option to remove low-quality read ends. This filter mitigates batch effects associated with differences between the NovaSeq and HiSeq platforms (Lou and Therkildsen 2021). After trimming and processing by fastp, the mean number of bases per individual at a base quality of at least 30 was 4.3 billion (sd 1.3 billion,

range 0.46 billion to 21.2 billion. The genomes of flighted birds tend to be between 1 and 1.5 billion base pairs in length (Kapusta et al. 2017) and the assembly lengths of our reference genomes range from 1.03 to 1.20 billion, so these numbers approximately reflect average depth of sequencing across the genome.

We confirmed species identity and checked for evidence of cross-contamination and hybridization by examining mitochondrial genes. Mitochondrial genomes were assembled using NOVOplasty v4.3.1 (Dierckxsens et al. 2016) and analysed as described in Kimmitt et al. 2023. At least one mitochondrial gene from each successful assembly was run through BLAST (https://blast.ncbi.nlm.nih.gov/Blast.cgi) to check species identity. We also visually inspected alignments of mitochondrial genes for each species. Based on these assessments, we removed 14 samples that matched an unexpected species on BLAST due to specimen misidentification, sample mix-up, or in some cases potential hybridization. We also removed 5 samples with evidence of mitochondrial chimerism, which suggests sample cross-contamination.

We aligned samples to a reference genome from a related species (Appendix Table B.1-1; Zhang et al. 2014; Laine et al. 2016; Toews et al. 2016; Ruegg et al. 2018; Feng et al. 2020; Manthey et al. 2021; Friis et al. 2022; Sly et al. 2022) using bwa mem (Li 2013) and then sorted them using SAMtools (Danecek et al. 2021). We removed overlapping reads using clipOverlap in bamUtil (Jun et al. 2015), then marked duplicate reads with MarkDuplicates and assigned all reads to a new read-group with AddOrReplaceReadGroups using picard (http://broadinstitute.github.io/picard/). All bam alignment files were then indexed using SAMtools. We discarded 12 samples due to low mapping rates (<50%). The mean raw mapping rate across all samples used in analyses was 94% (sd 4%, range 72%-99%) and varied consistently by species (Appendix Table B.1-1). Samples had an average duplication rate of 6%

(sd 4%, range 0.3% to 33%). Excluding duplicate reads, mean mapping rate was 90% (sd 6%, range 41% to 98%). Finally, we re-aligned samples around indels using GATK v3.7 (Van der Auwera et al. 2013). We applied the GATK RealignerTargetCreator tool to the entire dataset analyzed for each species and applied the GATK IndelRealigner tool to each sample.

After removing samples based on the filters described above, the total number samples analyzed further was 1748.

3.3.4 Genotype likelihood bioinformatic inference: overview

We used ANGSD v0.9.40 (Korneliussen et al. 2014) to calculate genotype likelihoods from sequencing data and we analyzed our results in a genotype likelihood framework (reviewed in Lou et al 2021). Instead of calling genotypes, which would require higher-depth sequencing, this approach uses a probabilistic framework that considers the likelihood of each possible genotype for a locus, given the base composition and base quality of reads at that locus. We do not filter loci or individuals based on missing data, as is common in some bioinformatic pipelines using called genotypes (e.g. Paris et al. 2017), because missing data do not violate the assumptions of programs designed for genotype likelihoods.

We conducted analyses on two subsets of the data, which are described in further detail below. First, we used ANGSD to identify polymorphic loci (SNPs) from across the entire genome for each species and to calculate genotype likelihoods for each individual at loci identified as polymorphic. We used this dataset of SNP genotype likelihoods to create genomic PCA and admixture plots. PCA-based analyses focus on the axes of greatest genomic variation within each species, which is helpful for identifying patterns such as geographic structure (Patterson et al. 2006; Novembre et al. 2008; Shirk et al. 2010), but these axes represent only a

small fraction of genomic variation. Summary statistics such as F_{st} and genetic distance better capture the genome-wide characteristics of each sample and population but may fail to identify subtle patterns of geographic structure.

We estimated 3 genome-wide summary statistics using each species' site frequency spectrum (SFS). These are pairwise F_{st} and pairwise genetic distance (Zhao et al. 2022), which we use to characterize spatial genetic structure, and θ_π, an estimator of population genetic diversity that reflects the probability that two randomly sampled alleles in the population are identical (Tajima 1989; Korneliussen et al. 2013). Estimates of genome-wide summary statistics include invariant sites, which are necessary in low-coverage inference based on SFS because low-coverage data do not provide strong confidence that any given site is invariant (Lou et al. 2021; see also Huang and Knowles 2016; Korunes and Samuk 2021 for discussion of issues with bias in analyses that remove missing and invariant loci). Analyses that account for invariant sites are particularly important in comparisons across species that vary in their underlying levels of genetic diversity (Meirmans and Hedrick 2011). However, it is not computationally practical to calculate genomic summary statistics using entire genomes, which would require analysis of about 1.7 trillion loci in our dataset. Therefore, to capture genome-wide properties of each species, we created subsampled datasets by randomly selecting loci from across the genome. We used the subsampled datasets to calculate whole-genome summary statistics using both variant and invariant sites. Subsampled datasets used to estimate F_{st} and θ_π represent about 2% of the genome (20 million bases), while subsets used to estimate pairwise genetic distance (which is a more computationally intensive analyses) comprise about 0.2% of the genome (2 million bases).

We used the SNP and subsampled datasets to quantify spatial genetic structure across the boreal region in three different ways, as described in greater detail below. Specifically, we used

the SNP dataset to calculate isolation by distance (IBD) using genomic covariance calculated for PCA, and we used the subsampled dataset to calculate IBD using pairwise genetic distance between individuals and pairwise F_{st} between sampling regions.

3.3.5 SNP dataset: Filtering based on initial PCA

We used ANGSD to calculate genotype likelihoods across the entire genome and for all sites with a SNP p-value of less than 0.05. We applied ngsParalog v1.3.2 (Linderoth 2018) to filter out SNPs with a high likelihood of occurring within a mis-mapped or paralogous region.

Next, we used PCANGSD v1.10 (Meisner and Albrechtsen 2018) to create a PCA separately for each chromosome or scaffold (larger than 1MB). We observed many chromosomes and scaffolds with evidence of PCA clustering related to potential inversion polymorphisms (Ishigohoka et al. 2021; Harringmeyer and Hoekstra 2022), so we analyzed each chromosome and scaffold further using lostruct (Li and Ralph 2019) as implemented using PCANGSD with scripts available from https://github.com/alxsimon/local_pcangsd.

Inversion polymorphisms and other regions of suppressed recombination can obscure spatial genetic patterns (Novembre et al. 2008; Privé et al. 2020; Appendix Figure B.2-1), so we removed all putative inversions from each species' dataset (Appendix Table B.1-2). We identified regions as putative inversions when they met two criteria: 1) Lostruct identified the region as showing distinct local structure (e.g. Figure 3-3b), and 2) PCA with data from the region showed distinct clustering into two or three groups, indicating polymorphism within the species. None of the putative inversion polymorphisms we identified showed clear spatial structure. We removed entire scaffolds and microchromosomes (<35 MB in length; Waters et al. 2021) with putative inversion polymorphisms on them. To remove putative inversion

polymorphisms from macrochromosomes without discarding the entire chromosome, we used lostruct plots to identify the affected regions and we removed the region with a buffer of at least 1 MB on either side. When macrochromosomes showed evidence of more than one inversion and/or if the affected region was not clearly identifiable using lostruct, we discarded the entire chromosome. Finally, we removed all sex chromosomes and all scaffolds of less than 1 MB in length from our dataset.

We also used chromosome- and scaffold-level PCA plots to further filter individuals. We removed individuals if they presented as a strong PCA outlier on multiple macrochromosomes (47 samples total across all species). In all three of the sparrow species and 4 warbler species (*Leiothlypis peregrina, Leiothlypis ruficapilla, Setophaga castanea, Setophaga magnolia*), we detected sex-based clustering on autosomes as well as sex chromosomes. We filtered females out of these species because we have many more samples from males than females (60 female samples removed across 7 species).

3.3.6 SNP dataset: genome-wide PCA and the relationship between genetic covariance and geographic distance

Using the filtered SNP dataset, we ran PCANGSD v1.10 with the --admix option to produce genome-wide PCAs and admixture plots. We also used the genetic covariance matrix produced by PCANGSD to estimate isolation by distance (IBD) as the relationship between covariance and geographic distance. For each pair of samples, we calculated the geographic distance using the function “distGeo” from the R package “geosphere” (Hijmans 2022) on latitude/longitude coordinates. We then created a linear model using geographic distance to

assess the correlation between genetic covariance and geographic distance between all pairs of points.

3.3.7 Subsampled dataset: Filtering and estimation of genetic diversity ($\theta\pi$)

We created two subsampled sets of genome loci for each species using scripts modified from https://github.com/markravinet/genome_sampler. Each species had one larger subset used to estimate F_{st} and θ_π and one smaller subset used to estimate pairwise genetic distance. The larger subset was created by sampling random 10kb loci at least 250kb apart, while the smaller subset comprises random 2kb loci at least 500kb apart. Regions removed by the inversion filters described above were excluded prior to random locus selection. After locus selection, we removed bases flagged by ngsParalog as described above. Individuals removed from PCA-based filters described above were excluded. The subsampled loci were stored in a BED file and supplied as a site filter to ANGSD in the following analyses. We estimated θ_π by creating a species-wide SAF file in ANGSD and using winsfs to generate and fold a species-wide 1-d SFS. We then used ANGSD's saf2theta and thetaStat functions on the SAF and SFS to generate estimates of θ_π (specifically, $\hat{\theta}_\pi$ of Korneliussen et al. 2013). To calculate genome-wide θ_π, we divided the sum of θ_π across all loci by the sum of the number of sites analyzed per locus. Estimation of genetic distance and F_{st} are described below.

3.3.8 Subsampled dataset: Isolation by distance based on genetic distance and F_{st}

We estimated genetic distance for each pair of individuals within a species using distAngsd (Zhao et al. 2022). We first created genotype likelihood files with subsampled loci

using ANGSD. ANGSD emits genotype likelihoods as log-likelihoods whereas distAngsd requires likelihoods, so we exponentiated the ANGSD output before running distAngsd. We then estimated isolation by distance as the linear slope of pairwise genetic distance vs pairwise geographic distance.

We estimated F_{st} between pairs of populations using ANGSD and winsfs. Doing so required us to assign individuals *a priori* into discrete populations. We divided our sampling region into 5 sections along a longitudinal axis (Figure 3-1) and selected 3 individuals from each species in each of the sections (hereafter referred to as populations) to use for this analysis. Within a given species, we excluded populations with less than 3 individuals sampled, and we also entirely excluded species with sufficient sampling from fewer than 4 sampling regions to avoid estimating slopes based on only 3 points. We selected exactly 3 individuals from each population because we have observed that estimates of F_{st} from ANGSD are strongly biased by sample size imbalances (Appendix Figure B.2-2), and the comparative context of our analysis makes it critical for pairwise F_{st} values to be comparable not only within but also across species. A population size of 3 allows us to maximize geographic extent of usable populations for most species. It is possible to calculate pairwise F_{st} at the individual level (e.g. Singhal et al. 2022) but we chose to group individuals by sampling area because in exploratory analyses we observed that F_{st} between individuals calculated by ANGSD on low-coverage data produces results that are difficult to interpret and potentially unreliable. To estimate F_{st}, we used ANGSD estimate allele frequencies using 3 individuals in each population. We then used winsfs to generate and fold a 2-d SFS file from each pair of populations. We used ANGSD's "fst index" and "fst stats" functions with allele frequencies and SFS files to estimate pairwise F_{st} for each pair of populations within a species. In species with at least 4 sufficient populations (23 out of 34

species), we estimated isolation by distance using the method of (Rousset 1997) as the slope of F_{st} / (1-F_{st}) vs log-transformed pairwise geographic distance between populations.

3.3.9 Comparison of IBD coefficients

We quantified spatial genetic structure by relating geographic distance to three different estimates of spatial genetic variation: genetic covariance (estimated for PCA), genetic distance, and pairwise F_{st}. When populations display isolation by distance, the slope of a linear relationship between pairwise genetic distance or F_{st} versus geographic distance is expected to be positive, indicating that pairs of individuals are geographically close to each other are more genetically similar than distant pairs. Conversely, PCA covariance is expected to show a negative relationship with geographic distance such that pairs of geographically distant individuals display negative covariance to a greater degree than pairs of close individuals, which may display positive covariance. Previous work comparing IBD slopes calculated with different methods found these values to be only weakly correlated with each other (Singhal et al. 2022), so we compared IBD slopes calculated with each of the three methods using Pearson correlations. We then constructed a separate set of models for each of the three sets of IBD slopes.

3.3.10 Hypothesis testing

For each of our three estimates of IBD, we used generalized least squares model comparisons to test whether seasonal migration distance influences IBD slope across the species in our dataset. We used the function “phylosig” in the R package “phytools” (Revell 2012) to test for phylogenetic signal in the residuals of the full model for each estimate of IBD using the

phylogenetic tree described in (Pegan and Winger 2020; Winger and Pegan 2021). Phylogenetic signal was not present in any of the full models (Table 3-2), so we proceeded without using a phylogenetic covariance matrix for our main analyses. We replicate each set of models using phylogenetic generalized least squares (PGLS) in Appendix Table B.4-1.

We also included migratory status (migratory vs nonmigratory) and θ_π as predictors in the full model for each response variable. We include migratory status because whether or not a species migrates for the winter could influence dispersal and spatial genetic variation beyond the influence of variation in migration distance. We include θ_π as a proxy for effective population size (N_e) because N_e can affect the rate at which spatial genetic structure arises (Hardy and Vekemans 1999). We centered and standardized migration distance and θ_π before running models. We also centered and standardized IBD slope based on genetic distance for modeling because the raw values are extremely small (Table 3-1).

In addition to the full model, we also fit one model with only the migration predictors, one model with only θ_π, and a null (intercept-only) model. We then used the function "model.sel" from the R package "MuMIn" (Bartón 2019) to compare model AICc values. We considered the model with the lowest AICc value to be the best model and we interpret models with ∂AICc > 2 as having significantly worse fit than the best model.

3.4 Results

3.4.1 Population genomic characteristics of birds across the boreal belt

The 34 boreal bird species we analyzed varied in genetic diversity (Table 3-1). θ_π had an average value of 0.0088 (sd 0.0031) and ranged from 0.0027 in *Picoides arcticus* to 0.014 in *Leiothlypis peregrina* (Table 3-1). As a result of variation in genetic diversity, different species also showed

variation in the number of SNPs in their genomes. Appendix Table B.1-1 summarizes the number of SNPs recovered initially by ANGSD and the number of SNPs removed by filtering steps. Importantly, the number of SNPs available for each species also depends on how many genomic regions (chromosomes and scaffolds) we analyzed. Species aligned to scaffold-assembled genomes show markedly lower numbers of SNPs because we excluded scaffolds less than 1 MB in length, which comprise a large proportion of these reference genomes.

Most species had at least one genomic region that showed a PCA patterns suggesting the presence of an inversion polymorphism (Ishigohoka et al. 2021; Harringmeyer and Hoekstra 2022). During PCA filtering, we removed an average of 6 putative inversion polymorphisms from each species with a chromosome-assembled reference (range 0-16 per species), as well as many scaffolds from scaffold-assembled genomes (Appendix Table B.1-2). We found that removal of putative inversion polymorphisms was necessary to reveal geographic patterns on PCA plots in some cases (e.g. Appendix Figure B.2-1).

3.4.2 PCA and admixture analyses

Species showed various patterns on genome-wide PCA plots (Figure 3-4, Appendix Figure to B4-34). Seven species showed relatively strong geographic clustering in PCA and admixture plots (*Poecile hudsonicus, Poecile atricapillus, Regulus satrapa, Cardellina canadensis, Geothlypis philadelphia, Setophaga virens, Setophaga palmarum*). These clustering patterns tend to separate the eastern and western ends of the range, although the breadth of the clusters varies such that Great Lakes and northern Manitoba samples cluster with either the west or the east depending on the species. Other species show more continuous patterns suggestive of isolation

by distance, including *Dryobates villosus, Sphyrapicus varius, Vireo solitarius,* and *Catharus fuscescens*. PCA and admixture plots for many species show no discernable geographic pattern.

3.4.3 Comparison of IBD slopes created with PCA distance, genetic distance, and F_{st}

Many boreal bird species show weak evidence for isolation by distance, even across the 3500+ km extent of our sampling area. Slopes of geographic distance versus pairwise genetic distance or F_{st} are expected to be positive in the presence of isolation by distance, while slopes calculated with PCA covariance are expected to be negative. Twenty out of the 34 species we studied had a slope with the opposite sign as expected in at least one of the three metrics of IBD (i.e. a negative IBD slope based on F_{st} or genetic distance, or a positive IBD slope based on PCA covariance). The three metrics of IBD that we calculated are only modestly correlated (Figure 3-5). The Pearson correlation coefficient was 0.49 between genetic distance IBD and Fst IBD; -0.25 between PCA IBD and Fst IBD; and -0.17 between PCA IBD and genetic distance IBD.

3.4.4 F_{st} was relatively low between sampling regions

The mean value of pairwise F_{st} between sampling regions was 0.089 (sd 0.0044), reflecting the low levels of genetic differentiation in this system (Appendix Table B.5-1) and the fact that genetic variation tends to be continuous across space as opposed to clustered in discrete populations. The minimum value of Fst that we detected was 0.072 between Alberta and northern Manitoba samples from *Picoides arcticus*, while the maximum value was 0.10 between Alberta and Atlantic maritime individuals of *Setophaga virens*.

3.4.5 Modeling the effect of seasonal migration on IBD

Model comparison supported the hypothesis that seasonal migration influences the relationship between PCA covariance and geographic distance. The best-fit model, which included migration status and migration distance as predictors, showed an AICc value that was 11.88 AICc units lower than that of the null model and 2.74 AICc units lower than that of a model with the θ_π predictor. The best-fit model provides relatively strong support for an effect of migration status on IBD based on PCA covariance such that migratory species have greater (less negative) slopes than nonmigratory species (β=0.026, SE=0.0069; Table 3-2). This suggests a greater degree of continuous genetic structure in nonmigratory species compared to migratory species. The coefficient for migration distance in this model was negative, suggesting that longer-distance migrants have stronger continuous structure than shorter-distance migrants, but support for this relationship was weak (β=-0.0013, SE=0.0023; Table 3-2).

Our models did not provide support for the hypothesis that seasonal migration status or distance influences IBD slopes based on genetic distance or F_{st} (Table 3-2). The best model was the null model for both F_{st} IBD and genetic distance IBD.

3.5 Discussion

3.5.1 Comparative spatial population genetics of the North American boreal avifauna

Our results present an unusually complete picture of the phylogeographic structure of a continent-wide fauna. The 34 co-distributed bird species we examined show idiosyncratic spatial genetic patterns, even though they share broadly similar demographic histories (Kimmitt et al. 2023), overlapping geographic ranges, and general habitat. As expected, we did not find

evidence for strong phylogeographic splitting within the boreal region. Yet, by sampling the region evenly along its longitudinal axis, we were able to reveal patterns of isolation by distance in many species and to identify the locations of population genetic clusters in others. Many species show no identifiable geographic structure, even though sampling occurred across thousands of kilometers. These results underscore that in the absence of strong barriers to gene flow, phylogeographic patterns in co-distributed species are frequently discordant and species-specific (Smith et al. 2014; Papadopoulou and Knowles 2016).

Spatial differentiation in boreal species was most clearly identifiable in analyses based on PCA, whereas F_{st} between sampling regions and individual pairwise genetic distance was low, even among species that show distinct clustering on PCA plots. PCA methods place greater weight on alleles that capture the greatest portion of covariance within a population (Shirk et al. 2010). The presence of patterns on PCA that are less evident in summary statistics suggests that geographic structure in these species reflects a relatively small number of loci in the genome (as in Piertney et al. 2023). That boreal bird species show relatively low phylogeographic structure is unsurprising given that these species tend to be fairly mobile, especially in comparison with species at lower latitudes (Salisbury et al. 2012; Smith et al. 2017). The recent dynamic history of glaciation across the study region also likely contributes to low geographic structure in boreal species. Older spatial patterns, including patterns of isolation by distance or allopatric differentiation in refugia, may have been disrupted or erased repeatedly in relatively recent evolutionary time (Castric and Bernatchez 2003; Arenas et al. 2012; De Lafontaine et al. 2013; Hagen et al. 2015). Yet, it is notable that many of the species we examined have maintained or re-developed geographic structure that can be detected by PCA, reflecting the power of whole

genome sequencing to facilitate associations between genetic variation and geographic structure (Novembre et al. 2008).

We used the comparative framework afforded by our study to test whether variation in the strength of geographic structure across species could be explained by a movement-related trait, seasonal migration. We found evidence that migratory species tend to have weaker isolation by distance than nonmigratory species, but the effects of migration behavior on gene flow within migratory species are complex. As discussed further in the next section, we suggest that dispersal and gene flow in boreal migratory birds are shaped by traits other than migration-related mobility. Our understanding of spatial evolution in boreal migratory birds would benefit from dedicated field study to characterize aspects of natural history that vary across species and potentially influence dispersal patterns, such as reliance on particular prey species (Drever et al. 2018), distances traveled during foraging (Weeks et al. 2022) or the post-fledging period (Mitchell et al. 2010; Brown and Taylor 2015), and strength of site fidelity.

A key question about drivers of idiosyncratic spatial variation is the extent to which species' present-day spatial genetic patterns deviate from equilibrium, and why. Spatial genetic patterns are said to be at equilibrium when they reflect the steady-state outcome of dispersal patterns and population parameters (Slatkin 1993; Broquet and Petit 2009). Isolation by distance is an expected equilibrium consequence of limited dispersal (Meirmans 2012; Aguillon et al. 2017), so traits that affect dispersal theoretically have a deterministic influence on isolation by distance (Furstenau and Cartwright 2016; Smith and Weissman 2023). But deviations from equilibrium also affect spatial genetic patterns (Slatkin 1993; Lombal et al. 2020; Arranz et al. 2021), and the demographic processes that disrupt equilibrium (e.g. range expansions, population size changes) are also influenced by dispersal traits (Clark et al. 2001; Stover et al. 2014; Nürk et

al. 2018) and other aspects of ecology. Hypotheses that consider potential effects of demographic history alongside effects of traits are more realistic than those that assume equilibrium (Slatkin 1993; Hutchison and Templeton 1999).

In our models, we tested the prediction that isolation by distance is influenced by effective population size (N_e) based on the hypothesis that equilibrium conditions arise more quickly (following Pleistocene perturbations) in species with smaller N_e (Maruyama 1971; Hardy and Vekemans 1999; Irwin 2002). We did not find strong support for this hypothesis, and previous analysis suggests that boreal species show broadly concordant demographic expansion (Kimmitt et al. 2023). However, there are other more complex ways that Pleistocene population histories could influence spatial genetic patterns. For example, stable glacial refugia are associated with deep phylogeographic breaks (Hewitt 2000), but how do ephemeral glacial refugia influence continuous spatial patterns? Do species differ in the manner in which they re-colonized the current boreal landscape—e.g., through patchy vs continuous expansion (Ezard and Travis 2006; Excoffier et al. 2009; Van Strien et al. 2015)? And can variation in these demographic processes be explained by traits associated with dispersal or other aspects of ecology? These hypotheses may be profitably addressed with spatially-explicit forward-time population genetic simulation methods (Haller and Messer 2019).

3.5.2 Seasonal migration distance and spatial genetic variation

While our models did not strongly support a relationship between seasonal migration distance and isolation by distance (IBD) among boreal forest birds, our results nonetheless provide new insight into spatial evolutionary patterns within migratory birds. The weak negative correlation we found between migration distance and IBD based on PCA covariance suggests

that the enormous distances traveled by long-distance migrants do not correspond to high dispersal rates. Some extremely long-distance migrants in our study show evidence of spatial genetic structure and isolation by distance (e.g. *Catharus fuscescens, Cardellina canadensis, Geothlypis philadelphia*, all of which spend the nonbreeding season in South America). Regardless of how these patterns arose—i.e. whether they reflect equilibrium gene flow conditions or the signal of a non-equilibrium demographic expansion—they have not been erased by rampant dispersal. The distances traveled by individuals in these species during migration are roughly 1.5 to 2 times the breadth of the boreal forest ecoregion, and are also several times greater than the distance over which the boreal forest ecoregion itself shifted since the Last Glacial Maximum (Ray and Adams 2001). That these species show geographic structure despite their tremendous tendency for movement demonstrates the influence of site fidelity on spatial evolution in these cases. These results underscore the remarkable navigational precision that extreme long-distance migrants employ to travel around the globe only to return to the exact same breeding sites year after year (e.g. Schmaljohann et al. 2012; DeLuca et al. 2019).

We found that the 4 nonmigratory species in our study generally showed higher genetic structure than many of the migratory species. This supports the hypothesis that nonmigratory birds undergo higher dispersal than migratory birds (Paradis et al. 1998; Dawideit et al. 2009), although our ability to draw robust conclusions is hampered by the fact that few boreal species are nonmigratory, and those that are nonmigratory are phylogenetically clustered (comprising two out of three species of woodpeckers and both species of chickadees in this study). Further, as discussed above, several long-distance migratory species show as much geographic structure as any of the nonmigratory species. The relationship between migration behavior and spatial

genetic processes in the boreal region is complex and driven by factors beyond a simple assessment of mobility in each species.

Our understanding of spatial evolution in boreal birds would benefit from detailed study of what drives dispersal versus natal philopatry or adult site fidelity in these species. Migration is frequently used as an indicator of mobility under the assumption that higher mobility lengthens dispersal distances (e.g. Laube et al. 2013; Pigot and Tobias 2015), but dispersal tendencies also vary within migratory species for poorly-characterized reasons. For example, another axis of dispersal behavior in boreal birds is the extent to which these species rely on spatially erratic resources—in other words, the extent to which individuals follow resource variation across their breeding grounds instead of exhibiting strict site fidelity. We purposely excluded species with nomadic breeding behavior from our study, but resource-driven dispersal may influence spatial genetics in species that otherwise appear to have regular breeding seasons. Specifically, it is noteworthy that the three species of warblers in our study whose ecology is closely tied to spruce budworm outbreaks (*Setophaga castanea, Setophaga tigrina, Leiothlypis peregrina;* Drever et al. 2018) show no geographic structure in PCA. Similarly, the non-migratory species with the weakest evidence of geographic structure is *Picoides arcticus*, a woodpecker species known to follow outbreaks of bark beetles following forest fires (Pierson et al. 2013). These results suggest the possibility that the strength of site fidelity and philopatry, rather than any metric of mobility, structures spatial evolution in boreal birds. Measuring site fidelity is inherently difficult because most tracking methods cannot easily distinguish between dispersal and mortality. Nonetheless, detailed studies of directly-measured dispersal and genetic connectivity in boreal birds (e.g. Christie et al. 2023) are critical not only for understanding their evolutionary past, but also for understanding how and why their populations are connected and thus how they may respond to

rapid environmental change (Leech and Crick 2007; Scoble and Lowe 2010). Our results show that even long-distance migrants may exhibit sufficiently high site fidelity or natal philopatry to result in spatial segregation of breeding populations across a continuous landscape, a result that bears relevance for understanding differential rates of contemporary population declines within species of migratory birds (Kramer et al. 2018; Hallworth et al. 2021).

3.5.3 Whole-genome sequencing presents new opportunities for discovering and understanding population genetic patterns

Our use of whole-genome sequencing facilitated identification of spatial variation in species with very weak genetic divergence, including species that show no evident structure in prior studies of mitochondrial or microsatellite genetic variation across the eastern boreal belt (Graham and Burg 2012; Hindley et al. 2018). Whole genome data increase the likelihood that our dataset includes SNPs with geographic signal, even if these SNPs are relatively uncommon across the genome. Further, our ability to assess patterns at high resolution across regions of the genome allowed us to identify a large number of putative inversion polymorphisms (Figure 3-3). The putative inversion polymorphisms we identified are not associated with known phenotypic variation (unlike, e.g., Thomas et al. 2008; Küpper et al. 2015; Wellenreuther and Bernatchez 2018; Huang et al. 2020) and most have never been previously described. None of the newly identified polymorphisms showed geographic structure. Instead, these regions often created strong covariance axes across samples that obscured geographic patterns in PCA (Appendix Figure B.2-1). Interestingly, the comparative nature of our study revealed apparent phylogenetic signal in some putative inversion polymorphisms (Figure 3-3). Shared putative inversion polymorphisms have apparently been retained through either incomplete lineage sorting or

selection since before these species last shared a common ancestor (Wellenreuther and Bernatchez 2018). Detailed investigation of these putative inversion polymorphisms is beyond the scope of the present study but promises to contribute to our understanding of the evolution of structural variation across the genome in a comparative context. Because our dataset is mostly specimen-vouchered, the putative inversion polymorphisms we identified may be linked with morphological phenotypic variation in the future, if any such variation is discovered.

3.6 Acknowledgements

For helpful discussion, we thank the Winger and Bradburd labs at the University of Michigan, especially Eric Gulson-Castillo, Kristen Wacker, Jacob Berv, Abigail Kimmitt, Gideon Bradburd and Zachary Hancock. For permits to collect specimens in the field, we thank the United States Fish and Wildlife Service, the United States Forest Service, the Minnesota Department of Natural Resources, the Michigan Department of Natural Resources, the New York State Department of Environmental Conservation, the Vermont Fish & Wildlife Department, the Vermont Agency of Natural Resources, the Canadian Wildlife Service of Environment and Climate Change Canada, Alberta Fish and Wildlife and Manitoba Fish and Wildlife. Field sampling by the authors was approved by the University of Michigan Animal Care and Use Committee (# PRO00010608). For providing additional tissue and blood samples, we thank the American Museum of Natural History (Brian Smith, Joel Cracraft, Paul Sweet, Peter Capainolo, Tom Trombone), Cleveland Museum of Natural History (Andrew Jones and Courtney Brennan), Cornell University Museum of Vertebrates (Irby Lovette, Vanya Rohwer, Mary Margaret Ferraro, Charles Dardia), New York State Museum (Jeremy Kirchman), Royal Alberta Museum (Jocelyn Hudon), University of Minnesota Museum of Natural History (Keith Barker),

University of California, Berkeley Museum of Vertebrate Zoology (Rauri Bowie and Carla Cicero), Theresa Burg (University of Lethbridge), Yves Auby and Junior Tremblay (Environment Canada), University of Alaska Museum of the North (Kevin Winker), and University of Washington Burke Museum (Sharon Birks). For assistance in the field, we thank Susanna Campbell, Shane DuBay, Gary M. Erickson, Mary Margaret Ferraro, Laura Gooch, Eric Gulson-Castillo, Heather Skeen, Vera Ting, Kristen Wacker, and Brian Weeks. For assistance in the lab, we thank Teia Schweizer, Christine Rayne, Rachael Herman, Brian Weeks, Jessica Yan, Caleb Kaczmarek, Melanie Florkowski, Madisyn Guza, Claire Pajka, Matthew Hack, Connor Jordan, and especially Abigail Kimmitt. Next-generation sequencing for this project was partially carried out in the Advanced Genomics Core at the University of Michigan. This research was also supported in part through computational resources and services provided by Advanced Research Computing (ARC), a division of Information and Technology Services (ITS) at the University of Michigan, Ann Arbor. This material is based upon work supported by the National Science Foundation under grant no. 2146950 to B.M.W. This research was supported by the Jean Wright Cohn Endowment Fund, Robert W. Storer Endowment Fund, Mary Rhoda Swales Museum of Zoology Research Fund and William G. Fargo Fund at the University of Michigan Museum of Zoology, and the William A. and Nancy R. Klamm Endowment funds at the Cleveland Museum of Natural History. T.M.P. was supported by the NSF Graduate Research Fellowship (DGE 1256260, Fellow ID 2018240490) and a University of Michigan Rackham Graduate Student Research Grant.

3.7 Figures and Tables

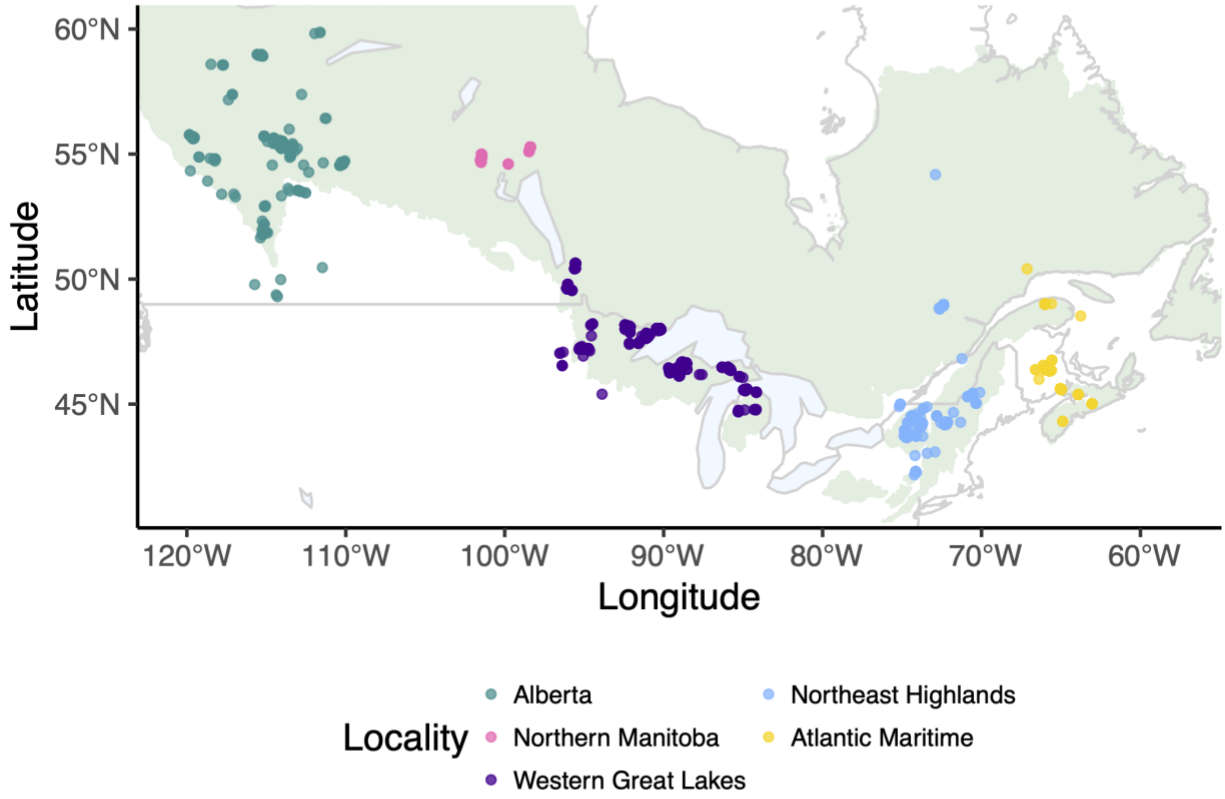

Figure 3-1. Map of sampling sites across the boreal ecoregion (shown in pale green) and some peripheral areas.

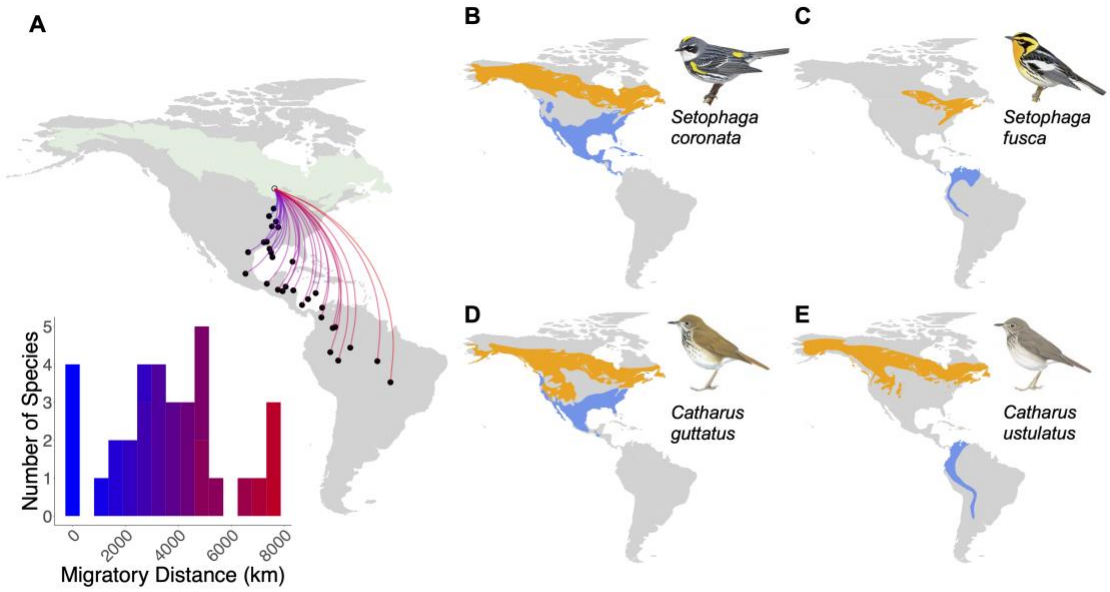

Figure 3-2. Migration distance varies in the 34 species in our study (*Table 3-1*). (A) Species broadly co-occur during the breeding season in the North American boreal forest but winter in disparate locations. Hypothetical migration routes are depicted between a single breeding location (Gunflint Trail, MN, USA) and the centroid of the winter ranges of each of the 34 migratory species, with a color scale corresponding to migration distances depicted in the histogram. (B–E) Example species representing short-distance (B and D) and long-distance (C and E) migratory species pairs in each of 2 genera. Species maps from BirdLife International and Naturserve (2014); *Setophaga coronata* and *Catharus ustulatus* maps illustrate subspecies *S. c. coronata* and *C. u. swainsoni*, respectively. Illustrations reproduced by permission of Lynx Edicions. Figure and caption adapted from Winger and Pegan 2021.

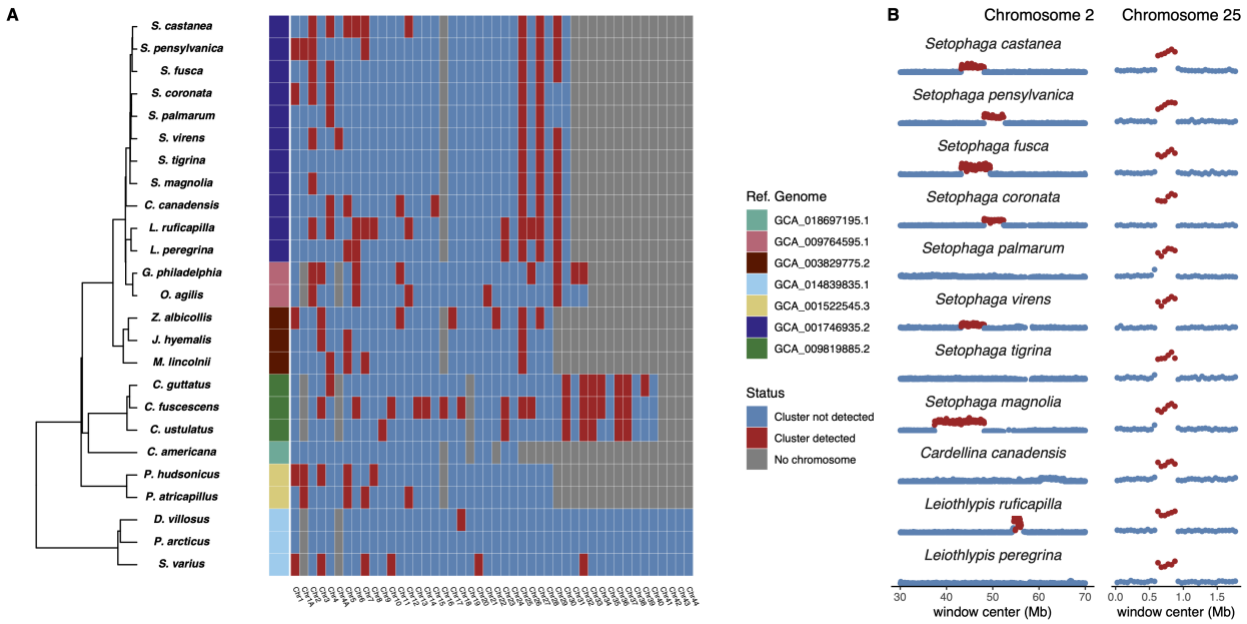

Figure 3-3. Putative inversion polymorphisms across the genomes of species in our dataset. (A) A phylogenetic tree of the 25 species in our study that were aligned to chromosome-assembled references genomes, alongside a matrix of autosomes colored based on whether they showed PCA clustering patterns indicative of inversions. Chromosomes are labeled at the bottom of the matrix based on names used by the reference genome on GenBank (i.e. we have not assessed the extent to which "Chr1" is syntenic across different reference genomes). Reference genomes contain different numbers of chromosomes, as indicated by gray cells. Putative inversion polymorphisms, as identified by clustering patterns in PCA and lostruct analyses, are common and in several cases are shared across related species mapped to the same reference genome. (B) Examples of putative inversion polymorphisms on two chromosomes among the 11 species aligned to the reference genome GCA_001746935.2. The y axis represents MDS values calculated by lostruct for windows across the region. High MDS values indicate local population structure in a given window that is strongly different from population structure in windows across the rest of the chromosome. Windows with high MDS values, colored red, likely reflect the location of putative inversion polymorphisms. Seven out of the 11 species shown have a putative inversion on chromosome 2, although the exact location (i.e. the mapped location on the reference genome) varies. *Setophaga castanea*, *Setophaga fusca*, and *Setophaga virens* appear to share a plesiomorphic putative inversion polymorphism on chromosome 2. *Setophaga magnolia* carries a putative inversion polymorphism that shares a similar border with the above-mentioned species on the 3' end but extends further on the 5' end. *Setophaga pensylvanica* and *Setophaga coronata* share a plesiomorphic putative inversion polymorphism in a different place, while *Leiothlypis ruficapilla* shows a putative inversion polymorphism in a unique location. On chromosome 25, all 11 species share a putative inversion polymorphism that appears in the exact same place.

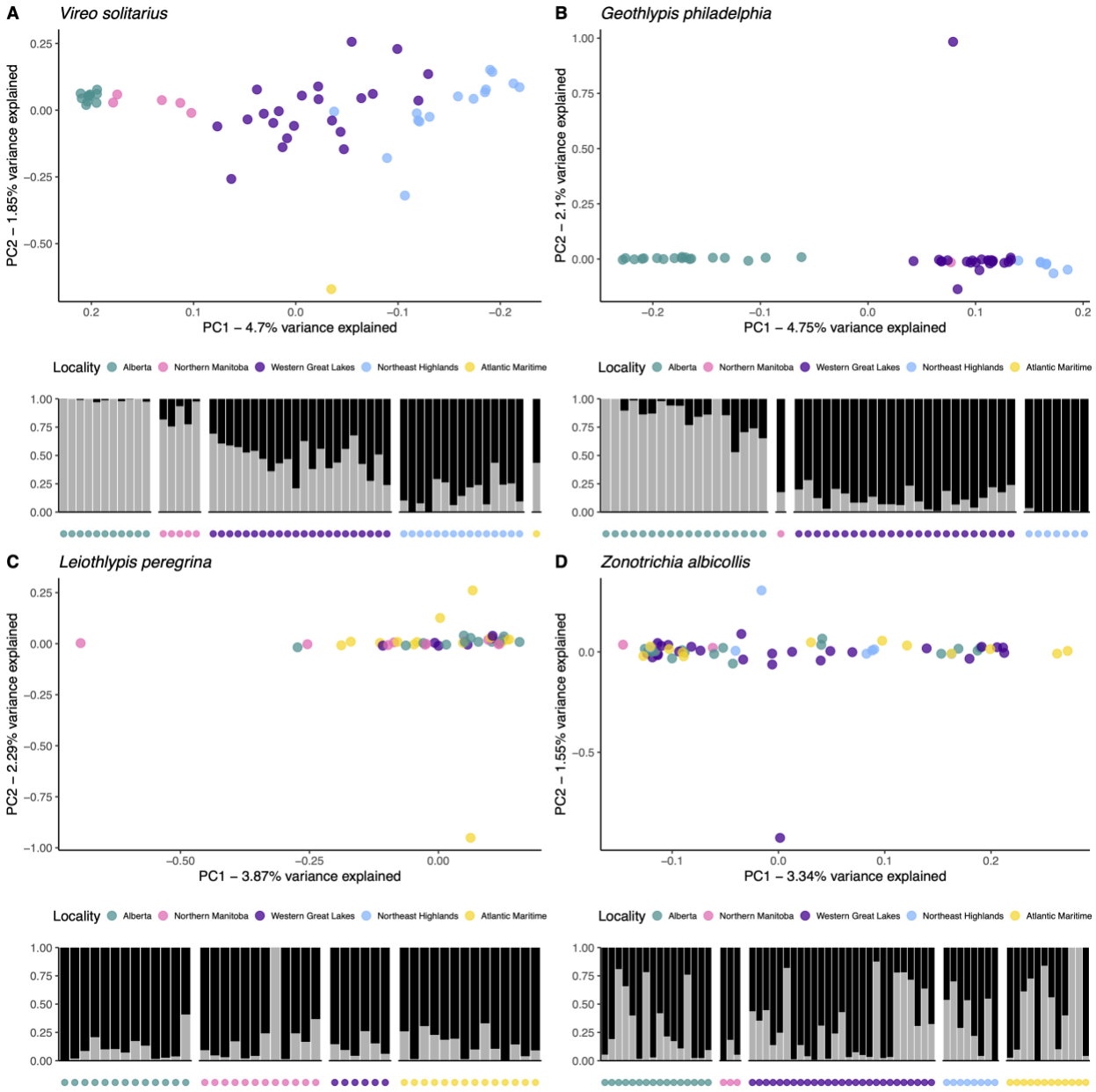

Figure 3-4. Species demonstrate a range of patterns on PCA and admixture plots. Individuals are ordered by longitude in admixture plots. *Vireo solitarius* (A) individuals from different sampling areas cluster with each other in a mostly continuous longitudinal axis on PC1. *Geothlypis philadelphia* (B) shows a similar pattern but with a clearer break between individuals from Alberta and individuals from further east. *Leiothlypis peregrina* (C) and *Zonotrichia albicollis* (D) are examples of species with no evident geographic patterns on PCA.

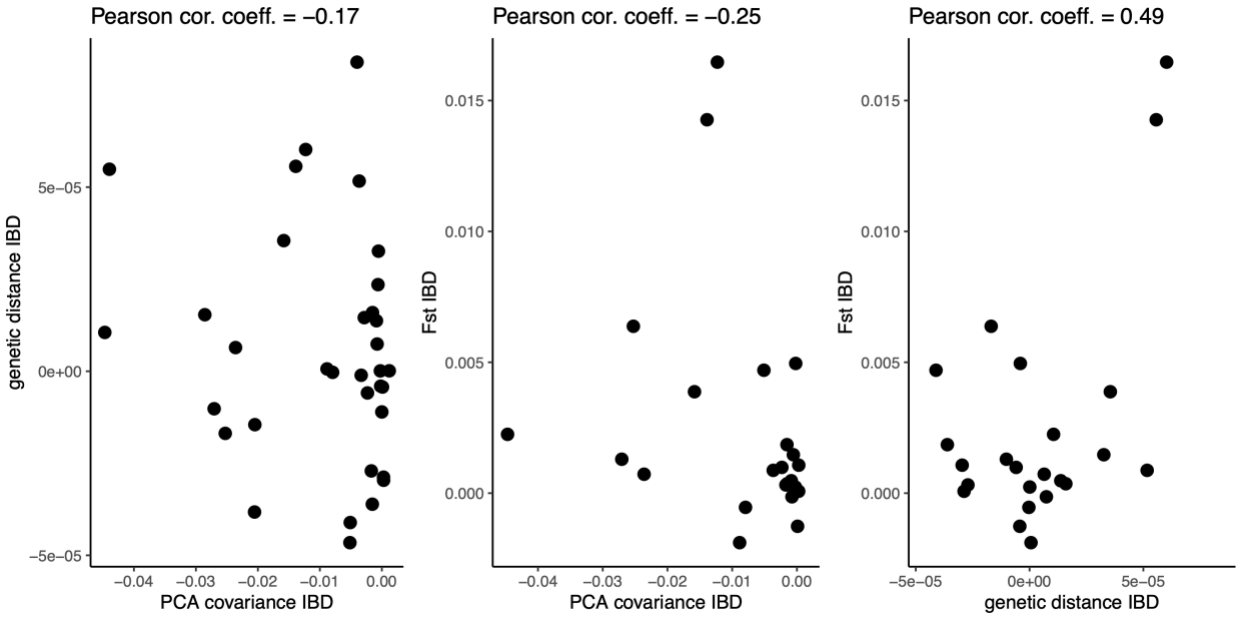

Figure 3-5. The three different methods we used to estimate IBD slope produce results that are not strongly correlated with each other.

Table 3-1. Species used in this study with migration distance, IBD slopes estimated for each species, mean pairwise genetic distance and θ_π, and the number of individuals sampled. Migration distances are from Winger and Pegan 2021.

Species	**Family**	**Migration distance (km)**	**Fst IBD slope**	**Genetic distance IBD slope**	**PCA covariance IBD slope**	**Mean genetic distance**	**θπ**	**Total sample size**
Picoides arcticus	Picidae	0	-0.00189	6.36E-07	-0.00885	0.0019	0.0027	31
Dryobates villosus	Picidae	0	NA	5.49E-05	-0.04396	0.0049	0.0056	43
Sphyrapicus varius	Picidae	2900	0.00130	-1.02E-05	-0.02706	0.0043	0.0057	62
Empidonax alnorum	Tyrannidae	7300	-0.00127	-4.29E-06	0.00010	0.0097	0.0096	49
Empidonax flaviventris	Tyrannidae	4100	0.00496	-4.05E-06	-0.00019	0.0064	0.0065	58
Empidonax minimus	Tyrannidae	4000	0.00470	-4.11E-05	-0.00510	0.0086	0.0085	44
Vireo olivaceus	Vireonidae	7600	NA	-4.66E-05	-0.00515	0.012	0.012	63
Vireo philadelphicus	Vireonidae	4200	NA	-1.09E-06	-0.00334	0.0082	0.008	17
Vireo solitarius	Vireonidae	2900	0.00072	6.43E-06	-0.02361	0.0052	0.0052	56
Poecile atricapillus	Paridae	0	0.00638	-1.69E-05	-0.02527	0.0061	0.0064	59

Poecile hudsonicus	Paridae	0	0.00225	1.05E-05	-0.04470	0.0039	0.0041	37
Corthylio calendula	Regulidae	2800	0.00185	-3.61E-05	-0.00154	0.0076	0.0078	49
Regulus satrapa	Regulidae	1600	0.01647	6.02E-05	-0.01229	0.0079	0.0079	63
Certhia americana	Certhiidae	1000	0.00007	-2.88E-05	0.00027	0.0044	0.0044	48
Troglodytes hiemalis	Troglodytidae	1700	NA	8.40E-05	-0.00400	0.0063	0.0061	26
Catharus fuscescens	Turdidae	7400	NA	1.54E-05	-0.02856	0.013	0.013	47
Catharus guttatus	Turdidae	2500	0.00098	-5.89E-06	-0.00233	0.0079	0.0087	65
Catharus ustulatus	Turdidae	7100	-0.00054	-2.97E-07	-0.00795	0.012	0.012	66
Junco hyemalis	Passerellidae	2000	0.00023	1.04E-07	-0.00025	0.0064	0.0064	59
Melospiza lincolnii	Passerellidae	3000	0.00036	1.59E-05	-0.00151	0.0098	0.01	53
Zonotrichia albicollis	Passerellidae	2100	0.00147	3.26E-05	-0.00055	0.0063	0.0066	68
Cardellina canadensis	Parulidae	5500	NA	-3.82E-05	-0.02054	0.011	0.011	31
Geothlypis philadelphia	Parulidae	5100	NA	-1.45E-05	-0.02049	0.013	0.013	52
Oporornis agilis	Parulidae	6600	NA	1.25E-07	0.00119	0.012	0.013	30
Leiothlypis peregrina	Parulidae	5000	0.00107	-2.96E-05	0.00028	0.014	0.014	47
Leiothlypis ruficapilla	Parulidae	3400	0.00031	-2.71E-05	-0.00170	0.0085	0.0086	57
Setophaga castanea	Parulidae	5000	-0.00014	7.39E-06	-0.00077	0.013	0.013	45
Setophaga coronata	Parulidae	3100	0.00048	1.37E-05	-0.00087	0.0089	0.0089	70
Setophaga fusca	Parulidae	5100	NA	2.35E-05	-0.00062	0.012	0.012	52
Setophaga magnolia	Parulidae	4100	0.00087	5.17E-05	-0.00366	0.012	0.012	56
Setophaga palmarum	Parulidae	3300	0.00387	3.55E-05	-0.01583	0.0094	0.0094	51
Setophaga pensylvanica	Parulidae	4000	NA	1.46E-05	-0.00284	0.013	0.013	46
Setophaga tigrina	Parulidae	4700	NA	-1.11E-05	-0.00001	0.0078	0.008	44
Setophaga virens	Parulidae	3900	0.01427	5.57E-05	-0.01389	0.0052	0.0054	63

Table 3-2. Generalized least squares model selection results for sets of models predicting each version of IBD. Response variables (the different versions of IBD) are indicated in bold above their respective model sets. The "type" column describes which set of predictors were included in each model. Model coefficients are listed with their standard error in parentheses within the column corresponding to each predictor. Estimates of **λ** for full models, shown with p-values, indicate no support for phylogenetic signal in model residuals of full models. Model comparison with AICc indicates that the best-fit model of IBD slope based on PCA covariance includes migration status and migration distance as predictors. In models of IBD based on genetic distance and F_{st}, predictor variables do not improve model fit compared with a null (intercept-only) model.

Type	**Migration Status: migratory**	**Migration Distance**	**θ_π**	**λ (p)**	**logLik**	**AICc**	**∂AICc**	**Weight**	**Sample size**
PCA covariance IBD									
migration	0.026 (0.0069)	-0.0013 (0.0023)			109.38	-209.4	0.00	0.794	34
migration + θ_π	0.026 (0.007)	-0.0016 (0.0033)	0.00046 (0.0029)	<0.0001 (1)	109.39	-206.6	2.74	0.202	34
θ_π			0.0033 (0.0021)		102.20	-197.6	11.77	0.002	34
null					100.94	-197.5	11.88	0.002	34
Genetic distance IBD									
null					-47.74	99.9	0.00	0.497	34
migration	0.44 (0.67)	-0.37 (0.22)			-46.07	101.5	1.65	0.218	34
θ_π			-0.131 (0.18)		-47.44	101.7	1.82	0.201	34
migration + θ_π	0.44 (0.067)	-0.57 (0.31)	0.24 (0.28)	<0.0001 (1)	-45.6	103.4	3.56	0.084	34
Fst IBD									
null					92.08	-179.6	0.00	0.691	23
θ_π			-0.0006 (0.0010)		92.23	-177.2	2.36	0.212	23
migration	0.0029 (0.0037)	-0.0015 (0.0014)			92.75	-175.3	4.29	0.081	23
migration + θ_π	0.0029 (0.0038)	-0.0016 (0.0019)	-0.000046 (0.0016)	<0.0001 (1)	92.75	-172.0	7.60	0.015	23

Chapter 4 The Pace of Mitochondrial Molecular Evolution Varies with Seasonal Migration Distance

4.1 Abstract

Species with slow life histories typically show lower rates of synonymous substitution (dS) than "fast" species, potentially due to slower rates of DNA replication or selection for mutation avoidance. Previous work has shown that long-distance seasonal migrants have a slower life history strategy than short-distance migrants, raising the possibility that rates of molecular evolution may covary with migration distance. Additionally, long-distance migrants may face strong selection on metabolically-important mitochondrial genes owing to their long-distance flights. Using 950 mitochondrial genomes, we assessed the relationship between migration distance and mitochondrial molecular evolution in 39 boreal-breeding migratory bird species. We show that migration distance correlates negatively with dS, suggesting that the slow life history associated with long-distance migration is manifest in rates of molecular evolution. Mitochondrial genes in all of our study species exhibited evidence of purifying selection, but the strength of selection was greater in short-distance migrants. This result may reflect an influence of selection for cold tolerance on mitochondrial evolution among species overwintering at high latitudes. Our study demonstrates that the pervasive correlation between life history and molecular evolutionary rate exists in the context of differential adaptations to seasonality.

4.2 Introduction

Species' traits are the product of their genome and their environment, but in turn, traits and the environment also shape the molecular evolution of the genome. In particular, traits associated with the slow-fast continuum of life history (Stearns 1983) are correlated with rates of molecular evolution (Bromham 2020) such that life history evolution is thought to alter the pace of a lineage's molecular clock (Hwang and Green 2004; Moorjani et al. 2016). Environmental pressures associated with seasonality can cause life history tradeoffs (Varpe 2017), which means that variation in adaptation to seasonality may entail variation in molecular evolutionary rates. However, the linkages between molecular evolution and differential adaptations to seasonality are little explored.

In this study, we investigate how patterns of mitochondrial molecular evolution are related to variation in seasonal migration, which has been recognized as an important and underappreciated axis of life history variation in birds (Greenberg 1980; Møller 2007; Bruderer and Salewski 2009; Winger and Pegan 2021). Migratory animals survive harsh seasonal conditions on their breeding grounds by temporarily departing until conditions improve (Winger et al. 2019). In the community of passerine birds breeding in the North American boreal forests, the life history strategy of seasonal migrants is structured by the time they spend breeding and their overwinter survival rate, both of which are correlated with migration distance (Figure 4-1, Winger and Pegan 2021). Seasonal migration also entails long-distance travel and high metabolic performance (Weber 2009), with potential implications for the dynamics of selection on the metabolically-important mitochondrial genes (Shen et al. 2009; Strohm et al. 2015). Here, we examine how migration distance correlates with mitochondrial molecular evolution within the

community of migratory birds breeding in the highly seasonal North American boreal region, focusing on the roles of life history and metabolic adaptation.

4.2.1 Life history influences molecular evolutionary rate

Associations between life history and molecular evolutionary rate are widespread across the tree of life. A species' position on the slow-fast continuum of life history is commonly characterized by traits that underly or correlate with differing rates of growth, survival, and reproduction; such "life history traits" include growth, generation time, age at maturity, metabolic rate, and the number of offspring produced per year (Read and Harvey 1989; White et al. 2022). Within major lineages of plants, bacteria, vertebrates, and invertebrates, species with "slow" life history (i.e. with long generation time, low annual fecundity, large size; Stearns 1983) also exhibit slower molecular substitution rate than "fast" species (with shorter generation time, higher annual fecundity, and smaller size) (Nabholz et al. 2008a; Smith and Donoghue 2008; Thomas et al. 2010; Weller and Wu 2015). One of the specific molecular evolutionary rates known to correlate with the slow-fast continuum is synonymous substitution rate, or dS (Nikolaev et al. 2007, Bromham et al. 2015, Hua et al. 2015; Table 4-1), which is thought to primarily reflect the underlying mutation rate when synonymous mutations are selectively neutral (Kimura 1983; Nei et al. 2010; Lanfear et al. 2014). As such, several hypotheses seek to explain the correlation between dS and life history by suggesting that life history influences mutation rate (reviewed in Bromham 2020).

The processes linking life history and mutation rate remain poorly understood, although several hypotheses exist. One hypothesis suggests that life history influences mutation rate through a "copy error" effect, which assumes that mutation rates covary with germline replication rates, and that organisms with "fast" life history strategy undergo higher rates of

germline replication per unit of time (Li et al. 1996; Thomas et al. 2010; Lehtonen and Lanfear 2014). A non-exclusive possibility is that differences in mutation rate represent a life history tradeoff at the cellular level, wherein species with slow life histories invest more resources in mutation avoidance (Bromham 2020). The "mutation avoidance" hypothesis suggests that natural selection on mutation-modulating phenotypes associated with DNA replication and repair can lead to the evolution of mutation rate variation between species (Britten 1986; Thomas and Hahn 2014; Bromham 2020). Selection for mutation avoidance may be influenced by the relationship between somatic mutation and senescence; there is evidence for selection against mutation in long-lived species in both the mitochondrial genome (Nabholz et al. 2008a; Galtier et al. 2009) and the nuclear genome (Tian et al. 2019; Zhang et al. 2021; Cagan et al. 2022).

4.2.2 Metabolic demand from locomotion may influence purifying selection in mitochondrial genes

Because most mutations are deleterious, genes influencing fundamental biological function, including mitochondrial genes, tend to show conserved molecular evolution (Nei et al. 2010; Nabholz et al. 2013; Popadin et al. 2013). While synonymous mutations may evolve neutrally, nonsynonymous mutations can alter protein phenotype and are therefore more likely to be removed by purifying natural selection (reviewed in Nei 2005), which reduces the rate of nonsynonymous vs synonymous substitution (the dN/dS ratio; Table 4-1). Prior studies have shown that purifying selection tends to be stronger in the mitochondria of mobile animals compared with less-mobile relatives. This pattern has been demonstrated in comparisons between flighted and flightless birds (Shen et al. 2009) and insects (Mitterboeck et al. 2017; Chang et al. 2020), between migratory and nonmigratory fishes (Strohm et al. 2015), and between amphibians (Chong and Mueller 2013) and mollusks (Sun et al. 2017) with different

locomotory modes. Within flighted birds, species with slow flight and those that rely heavily on soaring (rather than flapping) have been shown to experience relaxed mitochondrial purifying selection compared with faster-flying species (Shen et al. 2009; De Panis et al. 2021). A relationship between locomotion and strength of purifying selection would suggest that mitochondrial genotype plays an especially important role in fitness for organisms that rely on high-energy locomotion.

4.2.3 Long-distance migrants show slow life histories and rely on high-energy locomotion for survival, with potential implications for mitochondrial molecular evolution

Long-distance migrants breeding at temperate latitudes and wintering in equatorial latitudes exhibit lower annual fecundity and higher annual adult survival—that is, a "slower" life history—than sympatric breeding short-distance migrants, which have lower survival and higher annual fecundity (Winger and Pegan 2021, Figure 4-1). There is also evidence that migration distance scales positively with longevity (Møller 2007). Thus, long-distance migrants not only travel farther in each migratory trip, but may also make more trips per lifetime, which would allow them to achieve a similar number of lifetime offspring than short-distance migrants with higher annual fecundity but lower annual survival. Owing to the strenuousness of migration and the importance of repeated migration success for fitness in long-distance migrants, the migratory phenotypes of these species are hypothesized to be under strong variation-reducing natural selection (Conklin et al. 2017). Fitness costs of mitochondrial senescence may be especially severe in long-distance migrants for the same reason, potentially subjecting these species to strong selection for mutation avoidance. As such, we hypothesize that long-distance migrants exhibit lower dS and stronger evidence of purifying selection in their mitochondrial genes than short-distance migrants.

To test this hypothesis, we examined the relationship between migration distance and rates of molecular evolution of the mitochondrial coding genes in a community of small-bodied migratory songbirds breeding in the boreal forests of North America. The 39 co-distributed species we studied are ideal for investigating the effects of migration distance on molecular evolution because they vary greatly in migration distance (e.g., Figure 4-1, Appendix Table C.2-1), yet they otherwise share similar breeding habitat, population history, and body mass (Winger and Pegan 2021). This system allows us to test our hypotheses about migration distance while minimizing variation in other traits that could influence molecular evolution. We generated a complete mitochondrial coding sequence for each of the 39 species, which allowed us to conduct phylogenetic comparative analyses on the relationship between migration distance and molecular substitution rates (dS and dN/dS). We included body mass in our analyses to account for well-known relationships between mass and substitution rates (Figuet et al. 2014; Nabholz et al. 2016). We predicted that long-distance migrants, which have slower life history than short-distance migrants, would show lower dS. We also predicted that migration distance would correlate positively with strength of purifying selection in the mitochondria (and therefore correlate negatively with dN/dS), reflecting the metabolic pressures associated with high-energy locomotion during migration (Shen et al. 2009; Strohm et al. 2015) and the importance of metabolic performance for fitness in long-distance migrants with slow life history (Conklin et al. 2017).

To further test these hypotheses, we generated population genetic datasets for a subset of 27 species (representing a large sampling effort involving 938 mitochondrial coding sequences). These data allowed us to estimate two population genetic summary statistics to complement our analyses. First, we used the population genetic data to estimate a proxy of effective population

size (N_e; Table 4-1), which is expected to correlate with substitution rates when the sites in question are under natural selection (Ohta 1992; see Methods). These estimates allowed us to test the assumption that dS evolves neutrally in our system and to test the prediction that mitochondrial genes are generally under purifying selection. Second, we calculated population-level estimates of nonsynonymous vs synonymous polymorphism ($\pi N/\pi S$ ratios; Table 4-1), which provide additional insight into the dynamics of selection operating within populations (Kryazhimskiy and Plotkin 2008; Chen et al. 2017). Predictions about the effect of purifying selection on polymorphisms are more complex than predictions about substitution rates because within-population variation can be purged by strong directional selective sweeps in addition to purifying selection (Kryazhimskiy and Plotkin 2008). Nevertheless, we predict a negative relationship between migration distance and the $\pi N/\pi S$ ratio, which could result from either stronger purifying or stronger positive selection in long-distance migrants on mitochondrial function. In either case, such a relationship would broadly support the hypothesis that migration distance covaries with the dynamics of selection on the mitochondrial genome.

Although we framed our predictions in this study around the relationship between migration distance, metabolic demand for flight, and life history, it is worth noting that cold tolerance is also a metabolically-demanding challenge (Dawson and Yacoe 1983) that can influence the molecular evolution of the mitochondria (Chen et al. 2018a). As an adaptation for seasonal persistence in the boreal region, migration distance inversely covaries with tolerance of cold and resource scarcity. Whereas long-distance boreal migrants spend the boreal winter in tropical regions with warm temperatures and high resource availability, short-distance migrants overwinter in northern regions closer to their boreal breeding grounds with comparatively colder temperatures and scarcer resources (Winger and Pegan 2021). Therefore, we can alternatively

hypothesize that short-distance migrants exhibit strong purifying selection on mitochondrial genes, but due to the demands of cold tolerance as opposed to long-distance flight performance, which could lead to similar signatures of selection in the mitochondrial genomes of all species in the study.

4.3 Methods

4.3.1 Study system

We focused on 39 species of migratory birds breeding in the North American boreal forest, representing 11 families. These are the same species for which a correlation between migration distance and the slow-fast continuum was demonstrated using data on fecundity and survivorship (Winger and Pegan 2021). The species in the dataset exhibit broad variation in migration distance, with their geographic range centroids shifting between 1048 km and 7600 km between the breeding and non-breeding periods (Figure 4-2, Appendix Table C.2-1; Winger and Pegan 2021). These centroid shifts represent migratory strategies ranging from short-distance movements within the temperate region to the movement of an entire population across ocean and land barriers from North America to South America. The species in our study have breeding ranges co-distributed in the boreal forest ecoregion (Billerman et al. 2022), which extends from central Alaska to the maritime provinces of Canada (Omernik 1987). All species are less than 100 g in mass (range of mass for each species is 6-87 grams; Appendix Table C.2-1) and are broadly similar in habitat use. They are all forest-dwelling, territorial species with socially monogamous breeding systems. Small songbirds are typically capable of breeding in their second year, and this is true of all species in our study that have been assessed (Billerman et al. 2022). Additionally, the species share relatively similar demographic histories, with population

expansions estimated to have occurred during the period of glacial retreat that preceded the Last Glacial Maximum (~57,000 years before present; Kimmitt et al. 2023).

4.3.2 Life history covariates: Migration distance and mass

Direct measurements of migration distance of individuals are lacking for most of the species in our system, so we used the distance between the centroid of a species' breeding range and the centroid of its nonbreeding range to represent the migration distance of the species. Although the distance between centroids does not represent individual variation in migration distance within a species, this metric captures broad differences in migratory strategies between species. Our method for calculating the distance between range centroids is described in detail in Winger and Pegan 2021. We include mass as a covariate in our analyses because mass correlates strongly with life history variation (e.g., Stearns 1983). We obtained mass data from Dunning 1992 and Billerman et al. 2022.

4.3.3 Sampling and DNA sequencing

Our analysis of the relationship between migration distance and dS requires one mitochondrial genome for each species in the study, while analyses of N_e and $\pi N/\pi S$ require population-level sampling. For our analysis of dS, we obtained whole mitochondrial genomes from one individual of each of the 39 species in our study by sequencing DNA from tissue samples associated with a museum specimen as described below. These specimens were collected during the breeding season (June) from near the longitudinal center of the boreal forest (Manitoba, Minnesota, or Michigan). For two species (*Contopus cooperi* and *Euphagus carolinus*), we used specimen-vouchered tissue samples of individuals salvaged during migration in Michigan from collision mortalities.

For our population-level analyses, we generated a large dataset of 938 mitochondrial genomes for 27 of the 39 species. This dataset includes complete coding sequences for 12 to 49 individuals per species (mean 35 individuals per species; Appendix Table C.2-1). These individuals were sampled during the breeding season across a longitudinal transect of the boreal forest from Alberta to the northeastern United States. Except for 13 blood samples from New York state, all sequences we used came from frozen or ethanol-preserved tissue samples associated with museum specimens from the University of Michigan Museum of Zoology or loaned from other museum institutions. Fieldwork was approved by the University of Michigan Institutional Animal Care and Use Committee and all relevant permitting authorities.

We obtained high-depth mitochondrial genomes captured as a byproduct from low-coverage whole genome sequencing. We extracted DNA from tissue samples using DNeasy Blood and Tissue Kits (Qiagen Sciences, Germantown, MD, USA). Libraries were prepared using a modified Illumina Nextera library preparation protocol (Schweizer et al. 2021). We sequenced libraries on HiSeq or NovaSeq machines using services provided by Novogene and the University of Michigan Advanced Genomics Core. Data were demultiplexed by the sequencing core and we removed adapters with AdapterRemoval v2.3.1 (Schubert et al. 2016) using the options “trimns” and “trimqualities” to remove stretches of low-quality bases. We used NOVOPlasty v4.3.1 (Dierckxsens et al. 2016) to assemble mitochondrial contigs, specifying a target genome size of 20-30 kb and using a k-mer of 21. We provided NOVOPlasty with a conspecific mitochondrial seed sequence (Appendix Table C.2-1) for each species. We annotated the contigs built by NOVOPlasty using Geneious Prime 2020.2.2 (https://www.geneious.com) with copies of mitochondrial genes from GenBank (Appendix Table C.2-1). All 13

mitochondrial coding sequences were identified with a similarity threshold of at least 50% and were further verified through the alignment and data filtering steps described below. Whenever applicable in the filtering and analysis steps described below, we used options specifying the vertebrate mitochondrial code.

Our initial population genomic datasets contained 1155 mitochondrial samples. To ensure data quality, we used BLAST (https://blast.ncbi.nlm.nih.gov/Blast.cgi) to check species identity and we removed samples with evidence of species misidentification, chimerism, or introgression from related species (10 samples removed). We aligned and translated sequences with the R package DECIPHER v2.18.1 (Wright 2016) and we visually inspected each alignment, ensuring that sequences contained no premature stop codons or other alignment issues. We used DECIPHER to remove partial stop codons and to remove the untranslated C in the ND3 sequence of species in Picidae (Mindell et al. 1998). As our population analyses require complete data matrices, we excluded individuals with incomplete datasets (those with assemblies that were missing genes and/or with ambiguous base calls; 202 samples removed) and we concatenated the 13 genes for each remaining individual.

4.3.4 Accounting for effects of N_e on substitution rates

Many parameters of molecular evolution are fundamentally associated with effective population size (N_e), so estimating N_e provides important context for our analyses. Variation in N_e can cause variation in dS because the efficiency of natural selection in purging deleterious mutations is determined by the balance between strength of selection and strength of drift, which is reflected by N_e (Ohta 1992). For this reason, populations with small Ne typically show lower strength of purifying selection (i.e. higher dN/dS, e.g. Popadin et al. 2007, Leroy et al. 2021; and higher $\pi N/\pi S$, e.g. Chen et al 2017) in molecular analyses. Similarly, nearly neutral theory suggests that

N_e can influence dS when synonymous sites are not selectively neutral (as in Chamary et al 2006). That is, synonymous sites with weak influence on fitness may be under purifying selection in populations with large N_e and not in populations with small N_e, resulting in lower dS for species with high N_e. Several recent studies find correlations between traits associated with life history and genetic diversity, suggesting that species with "slow" life histories often have low N_e (Romiguier et al. 2014; Brüniche-Olsen et al. 2021; De Kort et al. 2021).

Effective population size (N_e) based on the mitochondrial genome can be estimated with the following formula (Watterson 1975, Nabholz et al. 2008b; Table 4-1):

$N_e = \theta / \mu$

where θ is a metric of genetic diversity and μ is mutation rate. Mutation rates are difficult to estimate directly, so many studies use substitution rates as proxies for mutation rates (Allio et al. 2017; Murray et al. 2017; Miller et al. 2021). In the absence of direct information on mutation rate variation between species, we assume that most variation in N_e estimates arises from variation in θ, not variation in μ, and we hereafter use θ as a proxy for N_e.

We used LAMARC v2.1.10 (Kuhner 2006) to estimate θ for each species. We imported our data into LAMARC after converting our concatenated fasta files into the phylip format for each species. We used the program's likelihood-based method in 10 initial chains (samples = 500, discard = 1000, interval = 20) and 2 final chains (samples = 10,000, discard = 1000, interval = 20). We used the F84 model of molecular evolution with a transition/transversion ratio of 20 (Edwards and Wilson 1990). We examined the output for each species to check for chain convergence and we ran two replicate chains for each species to make sure they produced consistent results. For 5 species (*Leiothlypis ruficapilla, Setophaga castanea, Setophaga*

coronata, *Setophaga fusca*, and *Vireo olivaceus*), we repeated LAMARC for 25 initial chains instead of 10 to improve convergence and used the values from these longer runs.

4.3.5 Population Structure

Our population-level analyses (estimation of N_e and $\pi N/\pi S$) assume that there is no geographic population genetic structure within the samples used. This assumption is reasonable given that boreal species tend to show congruent phylogeographic histories (Ralston et al. 2021). To check this assumption, we calculated mitochondrial genetic distance between all individuals within each species using "nei.dist()" from the R package poppr v2.9.3 (Kamvar et al. 2014) and created a neighbor-joining tree with "nj()" from the R package ape v5.6-2 (Paradis and Schleip 2019). We identified and removed 4 individuals from *Regulus satrapa* and one individual from *Oporornis agilis*, all from Alberta in the far western part of our sampling area, that were clearly genetically distinct from all other samples in their respective species. Otherwise, there was little evidence of geographic genetic structure in the mitochondrial genome in these species. This data filtering resulted in 950 complete mitochondrial coding sequences: 938 individuals across 27 species used in the population genomic datasets plus one sequence for each of the 12 additional species we used only in the interspecific Coevol analyses.

4.3.6 Estimating dS and dN/dS and their correlations with traits associated with life history

We used Coevol v1.6 (Lartillot and Poujol 2011) to evaluate associations between migration distance and molecular evolutionary rates using a single representative of each species. Coevol uses a Bayesian phylogenetic framework to estimate dS and dN/dS and to simultaneously measure the relationship between these values and covariates of interest (migration distance, mass, and θ). We included mass in the models to test for the expected relationship between mass

and molecular rates (Nabholz et al. 2016). Models with mass also provide a useful point of comparison, allowing us to ask whether migration distance correlates with dS and dN/dS to the same extent as (or more or less than) this well-studied life history proxy trait. Similarly, including θ in the models allows us to assess whether variation in N_e underlies differences in molecular evolutionary rates.

We provided Coevol with one complete mitochondrial coding sequence from each species and a phylogenetic tree we built with data from birdtree.org (Jetz et al. 2012) as described in Pegan and Winger 2020 (Figure 4-2). We created two data subsets for Coevol models: one subset contained all species in the study and was run with mass and migration distance as covariates. The other subset included the 27 species for which we had population-level data available, which we ran with θ as a covariate in addition to mass and migration distance. For each data subset, we ran Coevol in 4 chains: two replicate chains with the option "dnds" (estimating dS; models 1 and 2, Table 4-2) and two with "dsom" (estimating dN/dS; models 3 and 4, Table 4-2). We let each chain run for approximately 20000 steps and examined the resulting trace files to ensure convergence and evaluate estimated sample sizes (ESS). All models converged and all parameters had ESS > 300. We removed the first 500 steps of each chain and thinned the chain to retain every 10^{th} step to reduce autocorrelation. Replicate chains produced highly similar estimates, and the values we report here represent the mean value of estimates made by each replicate chain. Full Coevol model output for each chain is presented in **Error! Reference source not found.** and Appendix Table C.3-2.

The method implemented in the Coevol software provides correlation coefficients between substitution rates and each covariate, as well as partial correlation coefficients (which hold constant the effects of other covariates in the model). Each correlation or partial correlation

coefficient is accompanied by a posterior probability. Posterior probabilities near 0 indicate strong support for a negative relationship, while posterior probabilities near 1 indicate strong support for a positive relationship (Lartillot and Poujol 2021).

4.3.7 πN/πS

πN/πS is a population genetic summary statistic representing the amount of nonsynonymous vs synonymous polymorphism within a population. This value is measured by comparing individuals within a species rather than by comparing between species in a phylogenetic framework (and thus cannot be estimated by Coevol). We estimated πN/πS from each species with population-level fasta alignments, using the python package egglib v3.1.0 (De Mita and Siol 2012) to create a "CodingDiversity" class with attributes describing the number of codons with synonymous or nonsynonymous polymorphisms.

4.3.8 Linear modeling of πN/πS and θ

It is not possible to assess correlation between traits and population-level summary statistics with Coevol, so we used linear modeling to test for an effect of migration distance, mass and θ on πN/πS (Appendix Table C.3-3, Appendix Table C.3-4). Prior to linear modeling, we centered and standardized our predictors. We used a similar linear modeling approach to test whether θ exhibits a relationship with mass or migration distance to ensure that apparent relationships between these traits and molecular rates are not confounded by correlation with θ.

For each response variable (θ and πN/πS; Appendix Table C.3-3, Appendix Table C.3-4), we first created a model with all covariates of interest. We then used the function "phylosig()" from the R package phytools v0.7-70 (Revell 2010) to test for phylogenetic signal in the model's residuals (Revell 2012). For both response variables, the estimate of lambda (phylogenetic

signal) was < 0.2 and the p-value for evidence of phylogenetic signal was > 0.8, so we proceeded with linear modeling rather than using models with phylogenetic covariance matrices. For each response variable, we created a null (intercept-only) model with no predictors and models with all possible combinations of our predictors of interest, and we used the function "model.sel()" from the R package MuMIn v1.43.17 (Bartón 2019) to compare the models' AICc.

4.4 Results

4.4.1 Correlations between migration distance and molecular evolutionary rates (dS and dN/dS)

Our analyses with Coevol show that migration distance has a negative relationship with dS across the 39 species we studied, conforming to our initial predictions (Figure 4-2, Appendix Figure C.1-1). For Coevol models with the full species set, the correlation coefficient between migration distance and dS was -0.39 with a posterior probability (*pp*) of 0.018, indicating strong support for a negative relationship. The partial correlation coefficient between migration distance and dS when accounting for effects of mass was even stronger at -0.47 (*pp* = 0.0090).

We did not find strong evidence for a relationship between migration distance and dN/dS (correlation coefficient = 0.096, *pp* = 0.63). The partial correlation coefficient between migration distance and dN/dS (accounting for effects of mass) also showed only weak support for a positive relationship (partial correlation coefficient = 0.26, *pp* = 0.82).

Results from the Coevol models of the subset of 27 species for which we had estimates of θ were consistent with results produced by the full subset (39 species) models, although support for the correlation between dS and migration distance was weaker. In the model estimating dS, migration distance had a correlation coefficient of -0.36 (*pp* = 0.067) and a partial correlation coefficient of -0.26 (*pp* = 0.16). In the model estimating dN/dS, migration distance had a partial

correlation coefficient of -0.17 (*pp* = 0.31) and a partial correlation coefficient of -0.16 (*pp* = 0.32).

4.4.2 Correlations between mass and molecular evolutionary rates (dS and dN/dS)

Our Coevol models with the full species set support the expected negative relationship between mass and dS (correlation coefficient = -0.28, *pp* =0.065; Figure 4-2). This relationship weakens when effects of migration distance are accounted for (partial correlation coefficient = -0.18, *pp*=0.20). We did not find a strong correlation between mass and dN/dS (correlation coefficient = -0.25, *pp*=0.19; partial correlation coefficient = -0.072, *pp*=0.41). In models of dS with the subset of 27 species that included θ as a predictor, mass had a correlation coefficient of -0.30 (*pp* = 0.10) and a partial correlation coefficient of -0.40 (*pp* = 0.039). In models of dN/dS from this subset, mass had a correlation coefficient of 0.25 (*pp* = 0.8) and a partial correlation coefficient of 0.23 (*pp* = 0.79).

4.4.3 The influence of Ne on molecular rates and their correlation with traits of interest

In models using the subset of 27 species with population-level data, we did not find strong evidence for a correlation between θ and dS (correlation coefficient = -0.25, *pp* = 0.18; partial correlation coefficient = -0.015, *pp* = 0.47). This result is consistent with neutral evolution of synonymous sites among the species we studied. By contrast, we found strong support for the nearly neutral theory's predicted negative relationship (Ohta 1992; Popadin et al. 2007; Leroy et al. 2021) between θ and dN/dS (correlation coefficient = -0.74, *pp* = 0.0069; partial correlation coefficient = -0.69, *pp* = 0.013; Figure 4-3), indicating stronger purifying selection in species with higher N_e.

4.4.4 Linear modeling of effects of migration distance, mass and θ on πN/πS

In comparison of AICc, the highest-ranked model of πN/πS showed a strongly supported negative relationship between θ and πN/πS (Figure 4-4, Appendix Table C.3-3, model weight 0.55), as predicted if purifying selection is stronger in species with higher N_e. Compared to a model with θ alone, a model with both θ and migration distance shows an increase in multiple r^2 from 0.22 to 0.35 and a decrease in AICc by more than two units, suggesting the inclusion of migration distance improves the model. However, contrary to our prediction, migration distance has a weak positive relationship with πN/πS (Figure 4-4). The estimated effect coefficient relating θ and πN/πS in the best-fit model is -0.032 (std error = 0.01) and the estimated effect of migration distance from the best-fit model is 0.022 (std error = 0.01). Model comparison did not support the inclusion of mass as a predictor of πN/πS (Appendix Table C.3-3).

4.4.5 N_e is unlikely a confounding factor in inferred relationships

We used linear modeling to test whether migration distance or mass show a relationship with θ, our proxy of N_e. We did not find strong evidence that body mass or migration distance are correlated with θ among the 27 species we studied. The null model for θ (an intercept-only model with no predictors) showed the lowest AICc, suggesting that the addition of mass and migration distance as predictors did not substantially improve model fit (Appendix Table C.3-4, model weight 0.47). However, models with migration distance or mass as predictors were within 2 AICc units of the null model and showed model weights of 0.25 and 0.19 respectively, indicating considerable model uncertainty. The estimated effect of migration distance on θ was positive, but weakly supported, in the second-best model (estimate = 0.0016, std error = 0.0015; model multiple $r^2 = 0.045$).

4.5 Discussion

4.5.1 Seasonal migration distance correlates with mitochondrial dS

Molecular evolutionary rates are known to correlate with life history (reviewed in Bromham 2020). In this study, we examined the relationship between life history and mitochondrial molecular evolution in the context of the North American boreal region, where seasonality necessitates life history tradeoffs associated with a short breeding season and strong challenges to survival (Varpe 2017; Winger and Pegan 2021). Our results implicate the life history axis of migration distance as a novel correlate of mitochondrial synonymous substitution rate (dS). Long-distance migrants in this system have slower life history strategies than short-distance migrants, showing higher annual adult survival and lower fecundity (Winger and Pegan 2021). We found that the slow life history of long-distance migrants is accompanied by a slower rate of neutral molecular evolution in the mitochondria of these species compared with that of shorter-migrating species in the region. Indeed, among the 39 species we studied, the correlation between migration distance and dS is stronger than the correlation between mass and dS, which is notable given that the relationship between mass and substitution rate has been documented in previous work (Nabholz et al. 2016).

4.5.2 What evolutionary processes link migration distance with mitochondrial synonymous substitution rate?

Substitution rates are fundamentally influenced by mutation rate, which provides new molecular variants with potential to become substitutions, and by natural selection, which influences whether variants are fixed as substitutions or lost. The correlation between migration distance and dS therefore reflects one or both processes. dS is often treated as a proxy for

mutation rate alone based on the assumption that natural selection does not operate on synonymous sites (Nei et al. 2010), but in some cases synonymous sites are known to evolve non-neutrally (Chamary et al. 2006). If synonymous sites are not evolving neutrally, nearly neutral theory suggests that the relationship we find between dS and migration distance could hypothetically be explained by larger N_e in long-distance migrants (Ohta 1992). However, we found no strong evidence for a correlation between dS and our proxy for N_e (θ) (**Error! Reference source not found.**), nor for a correlation between θ and migration distance (Appendix Table C.3-4). Together, these results suggest that synonymous sites are evolving neutrally in our system and that variation in dS among species with different migration distances is unlikely to be driven by natural selection. Rather, we suggest that the negative relationship we found between migration distance and dS more likely reflects a negative relationship between migration distance and mutation rate.

4.5.3 Why might long-distance migrants have slower mitochondrial mutation rate?

We predicted that migration distance would correlate with dS because of the relationship between migration distance and life history (Winger and Pegan 2021), which is hypothesized to affect mutation rate (Bromham 2020). There are several potential mechanisms to explain the link between life history and mutation rate, and the relative importance of each is not clear (Bromham 2020). The “copy error effect” hypothesis suggests that the explanation is related to generation time, assuming that “fast” species with short generation times and young age at first reproduction experience higher rates of germline replication (and thus replication-induced mutation) than species with "slow” life histories (Li et al. 1996; Thomas et al. 2010; Lehtonen and Lanfear 2014). However, recent studies comparing cell division rates with directly-measured mutation rates suggest that replication-induced copy errors may not be the only driver of differences in

mutation rate between lineages (Wu et al. 2020; Wang et al. 2022). The "mutation avoidance" hypothesis offers another non-exclusive explanation for lower dS in organisms with slow life history based on higher costs of mutation in longer-lived species (Bromham 2020). Under this hypothesis, organisms with slow life history are predicted to have adaptations that reduce the introduction of mutations from DNA damage or from DNA replication and repair processes (Galtier et al. 2009; Tian et al. 2019; Zhang et al. 2021; Cagan et al. 2022). Long-distance migrants may be especially sensitive to costs of mitochondrial mutation, which may cause mitochondrial senescence (Galtier et al. 2009), because of the high physical performance demanded by their migratory behavior across their entire lifespans, which are longer than short-distance migrants breeding at the same latitudes (Møller 2007; Conklin et al. 2017). Further research is necessary to understand what processes contribute to the apparent reduction of mutation rate in species with slow life history, including long-distance migrants.

Another possible link between migration distance and mutation rate is oxidative damage from metabolism, which is recognized as a potential source of mutation rate variation (Martin and Palumbi 1993, Gillooly et al. 2005, Berv and Field 2018; but see Lanfear et al. 2007, Galtier et al. 2009). Thus, a potential explanation for our results—lower mitochondrial dS in long-distance migrants—is that long-distance migrants incur less metabolically-induced DNA damage than do short-distance migrants. This explanation is initially surprising in light of studies showing that migratory birds experience oxidative damage from endurance flight (Jenni-Eiermann et al. 2014; Skrip and McWilliams 2016). However, we suggest that there are three plausible and non-exclusive scenarios that could lead to lower metabolically-induced DNA damage in long-distance compared to short-distance migrants. First, long-distance migrants may have better adaptations for flight efficiency (Weber 2009), reducing the amount of oxidative

damage they experience per mile traveled. Second, the mutation avoidance hypothesis predicts that long-distance migrants may have more efficient DNA repair mechanisms than short-distance migrants, which could reduce metabolically-induced mutation rate even when long-distance flight does induce high oxidative stress. Last, short-distance migrants may experience greater oxidative damage arising from their increased demand for cold tolerance than long-distance migrants. The mitochondria also play an important role in the metabolic challenge of maintaining homeostasis during cold weather and resource shortages (Bicudo et al. 2001; Chen et al. 2018a). Short-distance boreal migrants likely face more of these kinds of challenges than long-distance migrants during both migration and winter (Winger and Pegan 2021). Despite the view that long-distance migration is an extreme performance challenge, its alternative—spending the winter within the temperate zone—is also a metabolic challenge in its own right (Dawson and Yacoe 1983; Winger et al. 2019). Further investigation of the comparative metabolic challenges faced by short versus long distance boreal migrants is needed to clarify whether and how migration distance influences metabolically-induced mutation in the mitochondria.

4.5.4 Purifying selection is not stronger in long-distance migrants

Whereas evolutionary rate at synonymous sites (dS) primarily reflects mutation rate, evolution at nonsynonymous sites is expected to strongly reflect natural selection because nonsynonymous mutations alter the amino acid sequence of a gene's protein product. We found that the ratio of nonsynonymous to synonymous substitutions (dN/dS) among our species is universally much less than 1 (Figure 4-3), indicating that the mitochondrial genes we studied are under purifying selection in all species in the system. We similarly found low ratios of nonsynonymous to synonymous polymorphisms within each population ($\pi N/\pi S$; Figure 4-4), which is also consistent with purifying selection. Moreover, both dN/dS and the $\pi N/\pi S$ ratio are

strongly correlated with θ, our proxy for N_e (Figure 4-3, Figure 4-4), as expected under nearly neutral theory (Ohta 1992).

Our results are consistent with the general finding that mitochondrial genes tend to experience strong purifying selection (Nabholz et al. 2013; Popadin et al. 2013). However, we did not find evidence supporting our prediction that long-distance migrants would show stronger purifying selection (i.e. lower dN/dS and $\pi N/\pi S$) than short-distance migrants. Our results are more consistent with the opposite pattern, wherein long-distance migrants show slightly higher $\pi N/\pi S$ than short-distance migrants (while accounting for the strong influence of N_e on purifying selection). This finding may reflect the fact that all species in our system face generally strong mitochondrial purifying selection, such that the endurance flights of long-distance migrants do not incur much stronger selection than the level that exists among all the species we studied. Yet, when viewed from another perspective, our results also indicate that short-distance migrants in the boreal region do not experience *relaxed* purifying selection on mitochondrial genes compared to long-distance migrants. As noted above, short-distance boreal migrants contend with metabolic challenges associated with cold winter temperatures in addition to the metabolic demands of flight, which may also exert selection on the mitochondria (Chen et al. 2018a).

4.5.5 Migration distance and the costs of mitochondrial mutations

In this study, we based our predictions on several complementary hypotheses about the costs of mutation in species with slow life history and high demand for physiological performance, such as long-distance migrants. From the perspective of molecular evolution, the mutation avoidance hypothesis (Bromham 2020) and studies on the relationship between lifespan and mutation rate (Nabholz et al. 2008a; Galtier et al. 2009; Tian et al. 2019; Zhang et al. 2021) predict that phenotype-altering genetic variation is harmful enough to induce selection for

mutation avoidance in organisms with slow life history. From the perspective of population biology, the hypothesis proposed by Conklin et al. (2017) — that long-distance migrants experience strong selective filter that truncates population-level phenotypic variation — predicts that slow species with high performance demands experience a strong selective filter on phenotypic performance in early life, reducing phenotypic variation in these populations. While Conklin et al. (2017) frame their hypothesis around reduction of phenotypic variation, a similar prediction about reduction of genetic variation emerges from a series of studies showing that mitochondrial purifying selection is stronger in species with higher locomotory metabolic demands (Shen et al. 2009; Chong and Mueller 2013; Strohm et al. 2015; Mitterboeck et al. 2017; Sun et al. 2017; Chang et al. 2020; De Panis et al. 2021). Together, these hypotheses led us to predict that costs of mitochondrial mutation in long-distance migrants, which have slow life history, would cause them to exhibit slower mitochondrial mutation rate and stronger mitochondrial purifying selection than short-distance migrants.

Our predictions about the relationship between migration distance and purifying selection were only partially supported. The negative relationship we found between migration distance and dS is consistent with lower mitochondrial mutation rate in long-distance migrants, but we did not find evidence that these species experience stronger mitochondrial purifying selection than do short-distance migrants. To reconcile these findings and advance our understanding of how long-distance migration influences molecular evolutionary dynamics, further research is needed on the relative metabolic demands of long-distance flight versus cold tolerance and on the consequences of mitochondrial genetic variation for migratory phenotype. Additionally, studying molecular rates across the nuclear genome will also help clarify which dynamics we

report here are related to selection on the mitochondrial genome and which reflect more general interactions between life history and molecular evolution.

4.5.6 Conclusions: seasonal adaptation provides novel context for studying the links between life history and molecular evolutionary rate

Adaptation to seasonality entails life history tradeoffs (Varpe 2017). Organisms balance these tradeoffs in different ways, creating variation in life history strategy within communities that inhabit seasonal environments (e.g., Winger and Pegan 2021). Our study demonstrates that life history variation related to seasonality can influence molecular evolutionary rate, which has potential implications for accurate reconstruction of evolutionary history (Shafir et al. 2020; Ritchie et al. 2022). More broadly, we suggest that communities adapted to seasonal habitats provide an interesting context in which to investigate potential drivers of the relationship between life history and molecular evolution. Co-distributed species show varying adaptations to seasonality—e.g. cold tolerance, migration, hibernation—and they express these strategies to different degrees (Auteri 2022). Cold adaptations can influence biological processes hypothesized to be relevant for germline replication rate or mutation rate (e.g. Wang et al. 2022), even among species that show little variation in commonly-studied life history proxies such as body mass. Comparative studies using seasonal communities can therefore allow us to draw new insights into how life history tradeoffs affect mutation rate, one of the most fundamental processes in evolution.

4.6 Acknowledgements

This chapter relies on the same set of genomic resources as chapter 3. Detailed acknowledgements for the generation and analysis of that dataset can be found in chapter 3.6. This paper has been submitted as a manuscript (in revision as of April 2023) with co-authorship

by Jacob Berv, Eric R Gulson-Castillo, Abigail Kimmitt, and Benjamin Winger. For helpful discussion, we thank the Winger and Smith labs at the University of Michigan.

4.7 Figures and Tables

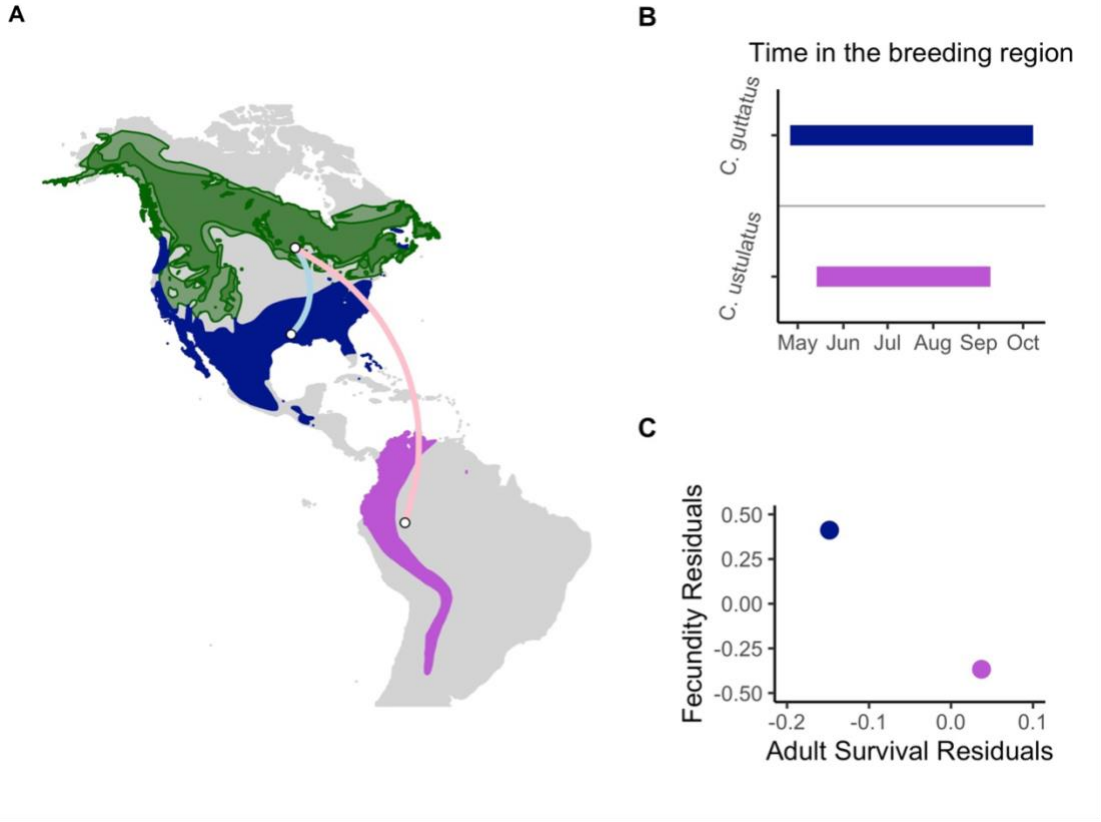

Figure 4-1. An example contrast between a shorter-distance migrant *Catharus guttatus* and a closely related longer-distance migrant *Catharus ustulatus swainsoni* illustrates the relationship between migration distance and life history in our study system. Both species have broadly overlapping breeding ranges (green), but *C. guttatus* (dark blue nonbreeding range) migrates a shorter distance (blue migratory route) than *C. u. swainsoni* (purple nonbreeding range, pink migratory route) (panel A). Accordingly, *C. guttatus* spends more time in its breeding range than *C. u. swainsoni* (panel B). With more time in the breeding range, the short-distance migrant has higher fecundity but lower adult survival—i.e., faster life history—than the long-distance migrant (panel C, showing model residuals from mass-corrected analysis of fecundity and survival). The short-distance migrant spends the winter in colder, more resource-depleted regions than the long-distance migrant. Figure and data adapted from Winger and Pegan 2021.

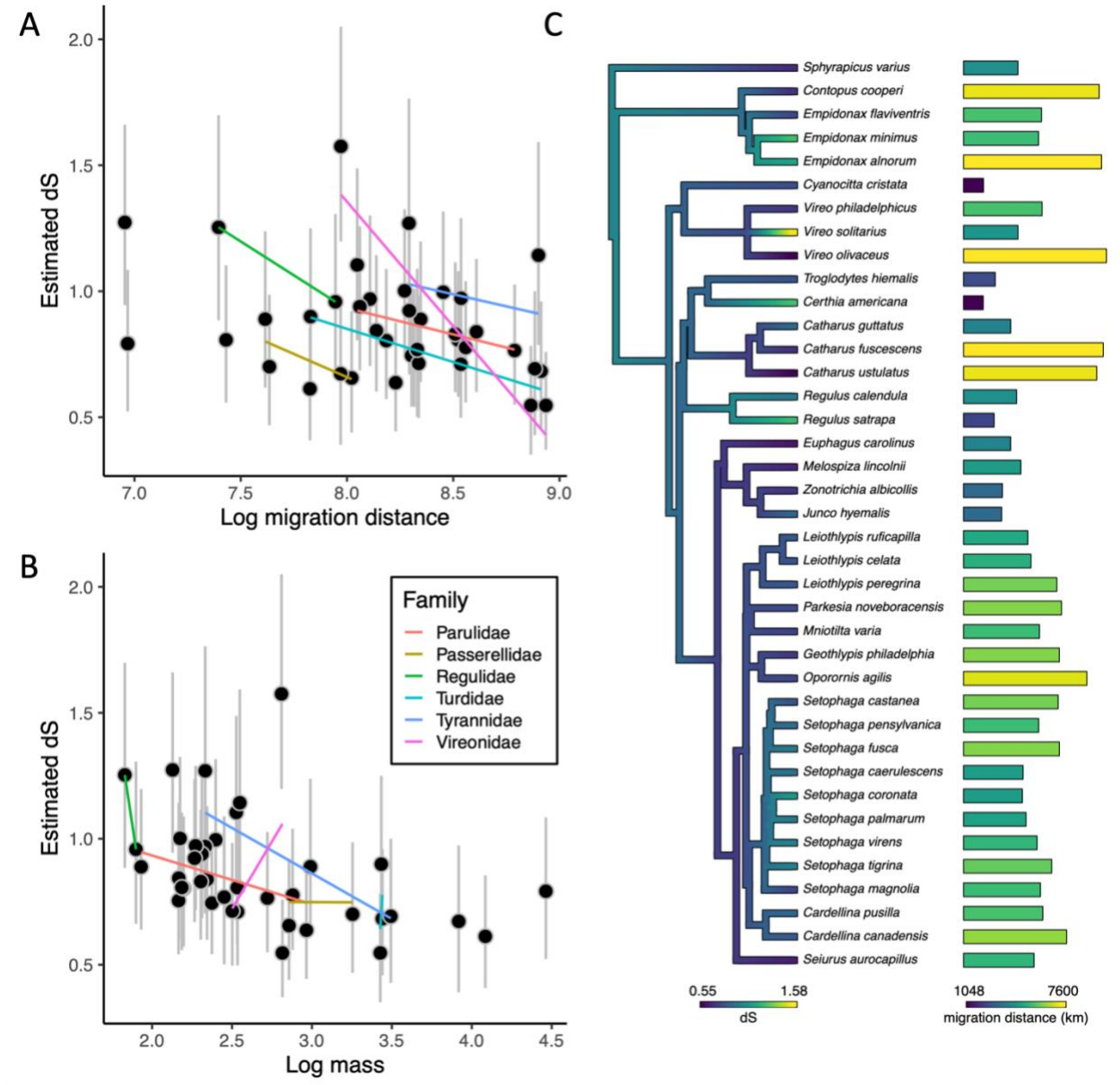

Figure 4-2. dS vs. traits associated with life history (A, B) and a phylogenetic tree showing dS and migration distance for each species (C). In panels A and B, posterior mean tip estimates of dS (black dots) from Coevol are shown compared to migration distance (A), and mass (B) from models using our full species set. Gray vertical bars indicate 95% credible intervals for each estimate. These analyses reveal that both migration distance and mass have a negative relationship with dS. Plotted lines use linear models to visualize the relationship between estimated tip dS and a given covariate within each family of birds (when represented in our dataset by two or more species), demonstrating a consistently negative relationship between dS and migration distance within and among major clades in our system. In panel C, the phylogenetic tree is colored based on posterior mean tip and node estimates of dS from Coevol.

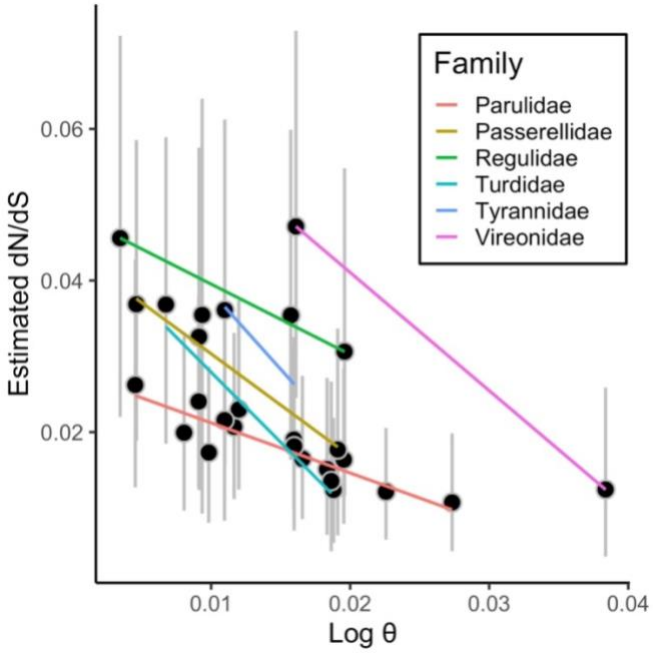

Figure 4-3. dN/dS vs. θ. Posterior mean tip estimates (black dots) of dN/dS are shown compared to θ from a Coevol model including species for which we could estimate θ. Gray vertical bars indicate 95% credible intervals for each estimate. As in *Figure 4-2*, plotted lines use linear models to visualize the relationship between mean tip dN/dS and θ within each family of birds (when represented in our dataset by two or more species), demonstrating a consistently negative relationship between θ and dN/dS within and among major clades in our system.

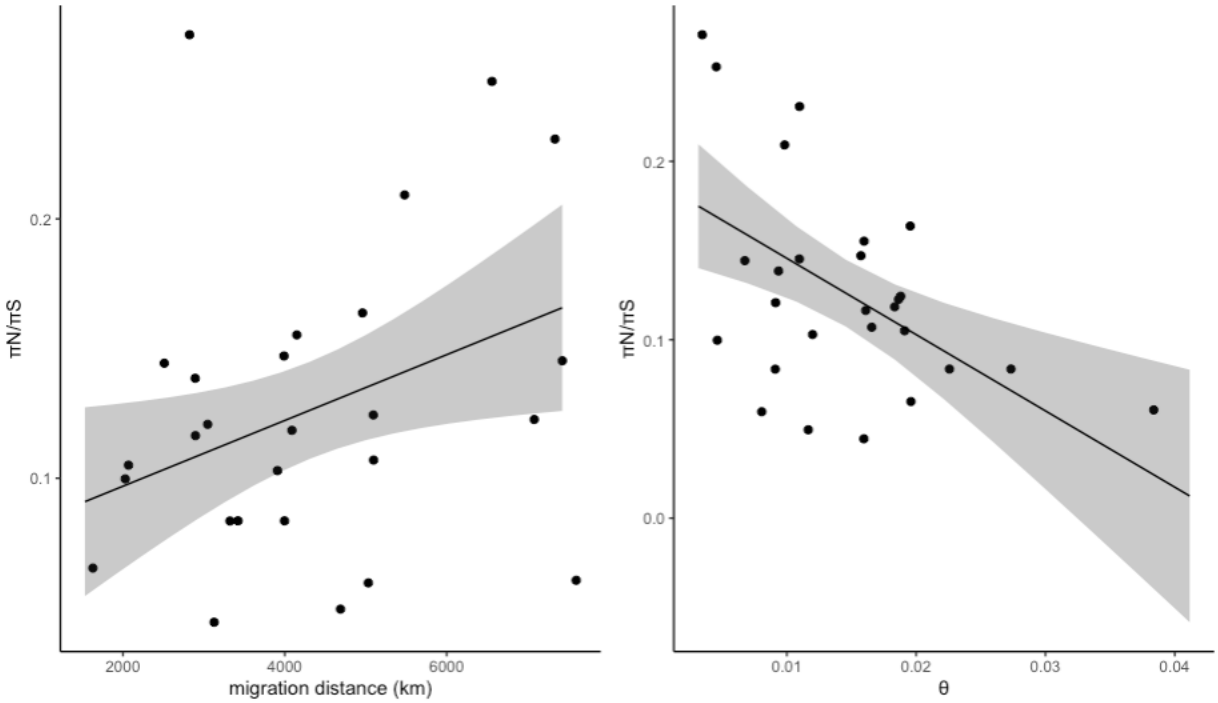

Figure 4-4. The relationship between πN/πS and migration distance (left) and θ (right). πN/πS is strongly influenced by θ, as expected if purifying selection removes more nonsynonymous variation in species with larger N_e. πN/πS increases with migration distance, after accounting for effects of θ. Regression lines and 95% confidence intervals show the marginal effect of each variable as calculated by "ggpredict()" from the R package ggeffects v0.16.0 (Lüdecke 2018) using the best-fit model, which included both predictors.

Table 4-1. Definitions of abbreviations for molecular substitution rates and population genetic parameters and predictions for their relationships with migration distance.

Concept	**Abbr.**	**Description and assumptions**	**Predictions (this study)**
Synonymous substitution rate	dS	Assuming synonymous sites evolve neutrally, dS primarily reflects μ (Nei et al. 2010; Lanfear et al. 2014)	Negative relationship between migration distance and dS
Nonsynonymous substitution rate	dN	Assuming nonsynonymous sites are generally deleterious, dN is influenced by both μ and N_e (reviewed in Nei 2005)	NA
dN/dS ratio	dN/dS	Assuming nonsynonymous mutations are generally deleterious, dN/dS reflects strength of purifying selection on dN while accounting for variation in μ. Low dN/dS = strong purifying selection. (Nei 2005; Kryazhimskiy and Plotkin 2008)	Negative relationship between θ and dN/dS, reflecting the influence of N_e on dN/dS. Negative relationship between migration distance and dN/dS, indicating positive relationship between migration distance and purifying selection strength.
Mutation rate	μ	May be influenced by life history (reviewed in Bromham 2020)	NA, μ not measurable in our data

Effective population size	N_e	Defined as the ideal population size experiencing the same level of genetic drift as observed in the data (Waples 2022). Estimated in mitochondrial data as θ / μ. (Watterson 1975; Nabholz et al. 2008a)	NA, see θ
Theta	θ	Population genetic parameter representing genetic variation. Assuming low variation in μ, variation in θ primarily reflects variation in N_e	Negative relation between θ and dN/dS and between θ and πN/πS
Synonymous nucleotide diversity	πS	Population genetic parameter representing population-level nucleotide diversity at synonymous sites.	NA
Nonsynonymous nucleotide diversity	πN	Population genetic parameter representing population-level nucleotide diversity at synonymous sites.	NA
πN/πS ratio	πN/πS	Reduction of πN compared to πS is expected to reflect natural selection, but the relationship is more complex than in dN/dS	Negative relationship between migration distance and πN/πS, indicating positive relationship between migration distance and selection. Negative relationship between θ and πN/πS, indicating purifying selection on nonsynonymous polymorphisms.

Table 4-2. A summary of analyses. Models 1 and 2 use Coevol test our hypothesis that synonymous substitution rate (dS) is influenced by migration distance, with mass and θ (model 2 only) as additional covariates. Models 3 and 4 use the same approach with Coevol to estimate correlations between traits of interest and dN/dS. Models including θ use only 27 species because we did not have population-level data available to estimate θ for all 39 species. Coevol does not analyze molecular evolutionary parameters based on population-level data, so we used linear modeling to test whether traits of interest influence πN/πS (model 5). Finally, we also used linear modeling to test for potential confounding relationships between θ and life history-associated traits of interest (mass and migration distance; model 6).

		Data subset	**Method**
1	dS ~ migration distance + mass	full (39 species)	Coevol
2	dS ~ migration distance + mass + θ	theta (27 species)	Coevol
3	dN/dS ~ migration distance + mass	full (39 species)	Coevol
4	dN/dS ~ migration distance + mass + θ	theta (27 species)	Coevol
5	πN/πS ~ migration distance + mass + θ	theta (27 species)	linear modeling
6	θ ~ migration distance + mass	27 species	linear modeling

Chapter 5 Conclusions

5.1 Evolutionary consequences of migration and seasonality in the North American avifauna

Migratory animals are among the most mobile organisms on Earth. Many species cross hemispheres on a twice-annual basis. In a global, macroevolutionary context, which is increasingly being used to understand ecology and evolution at a large scale (Tobias et al. 2022), high latitude migrants typically represent the upper extreme of mobility and dispersal ability (Blackburn and Gaston 1996; Gaston and Blackburn 1996; Pigot and Tobias 2015; Sheard et al. 2020). Yet, as I show in this dissertation, long-distance migrants do not necessarily demonstrate the expected evolutionary consequences of extreme mobility. In many contexts, mobility correlates with geographic range size and genetic connectivity (Blackburn and Gaston 1996; Claramunt et al. 2012). However, I show that mobility associated with long-distance migration is not a good predictor of spatial patterns in high latitude avian communities. In chapter 2, I demonstrate that neither migratory behavior nor dispersal ability influence range size across 306 species of North American songbirds. In chapter 3, I further show that migration distance fails to promote genetic connectivity, even though dispersal distance is usually assumed to correlate with mobility. Indeed, many long-distance migratory species show relatively strong genetic structure, which is maintained by limited dispersal and gene flow. My results suggest that among organisms with high movement capacity, costs and constraints of long-distance movement (Bonte et al. 2012) are not primary determinants of spatial evolutionary processes.

In my fourth chapter, I highlight the under-appreciated role of time-related tradeoffs in the annual cycle for evolutionary processes in high-latitude migrants. The breeding season at high latitudes is short, and high latitude animals must balance the time they spend on reproductive effort in this region against the survival risks posed by harsh conditions as the seasons change (Varpe 2017; Winger and Pegan 2021). I demonstrate that life history tradeoffs associated with time limitation are correlated with differences in molecular evolutionary rates. Long-distance migratory birds have a slower life history strategy than short-distance migrants—they prioritize survival at the cost of time spent breeding (Greenberg 1980; Böhning-Gaese et al. 2000; Bruderer and Salewski 2009; Winger and Pegan 2021)—and they show correspondingly slower rates of molecular evolution. My research adds to the rich literature on the relationship between life history and molecular evolutionary rates (reviewed in Bromham 2020) by demonstrating this pattern in a novel life history axis (seasonal migration).

The results of my analyses reveal several evolutionary consequences of seasonal migration distance and additionally highlight several important knowledge gaps for future investigation. Population-level seasonal migration distance (the major axis of migration addressed by this dissertation) can be seen as a proxy for a variety of facets of migratory strategy, including investment of time and energy into migration, the structure of annual phenology, and the location and type of wintering habitat. Yet there is much more to learn about how migration distance interacts with these other aspects of organismal biology. For example, long-distance migrants have adaptations to mitigate energetic costs of flight (Weber 2009), which may weaken the relationship between migration distance and energetic investment in migration. In my fourth chapter, I demonstrate that long-distance migrants do not experience stronger mitochondrial purifying selection than short-distance migrants, suggesting that the

relationship between migration distance and metabolic costs is complex. Similarly, detailed investigation into the annual schedule and pace of migration (e.g. Nilsson et al. 2013) in a comparative context may reveal complex relationships between these variables and migration distance across species. Tracking of individual birds' migratory journeys has produced rich information about migratory strategy, but these studies usually focus on one species at a time. Comparative analysis of migratory strategy variation across species promises to lend new insights into how migratory distance interacts with other aspects of avian biology in an evolutionary context.

5.2 Dispersal dynamics in migratory birds are influenced by complex factors other than mobility

Time-related tradeoffs also potentially play a role in dispersal evolution (Reed et al. 1999; McNamara and Dall 2011), but dispersal behavior in migratory species requires further investigation. My thesis demonstrates that variation in both genetic structure and geographic range evolution among migratory species is not predicted by increased migration distance, suggesting that long distance migration does not inherently promote higher dispersal than short-distance migration. Costs of mobility generally play an important role in dispersal evolution, but other costs associated with time, opportunity, and risk (Bonte et al. 2012) probably have stronger consequences in species with generally high mobility. The time budget of migratory birds before and after the nesting period potentially influences the information available to individuals making dispersal decisions (Mitchell et al. 2010; Brown and Taylor 2015) such that individuals with more time to explore potentially derive greater benefits from informed long-distance dispersal. In chapter 3, I found that long-distance migrants—species that spend the least time on

the breeding grounds (Winger and Pegan 2021)—show some evidence of having stronger genetic structure than short-distance migrants. An effect of limited time on informed dispersal potentially explains this pattern. Investigation of species' time budgets and exploratory behavior during their time on their breeding grounds may be a fruitful way to develop our understanding of how migration behavior, seasonality and life history impact dispersal evolution in these species.

To better understand spatial evolution in migratory birds, it would be beneficial to test hypotheses about how migration and dispersal interact within individual wild organisms. Migratory birds typically show greater dispersal distances than non-migratory birds (Paradis et al. 1998; Dawideit et al. 2009). To the extent that seasonal migration promotes dispersal, is this because high dispersal ability promotes exploration over large spatial areas during assessment of potential breeding sites (Reed et al. 1999; Delgado et al. 2014), or is this a result of navigation error in migrants that are otherwise attempting to return to their former breeding locality (Wynn et al. 2022; Vickers et al. 2023)? When the breeding ranges of migratory birds appear to be smaller than their expected suitable habitat, is this because philopatry drives them to return to their former breeding sites (Pearce 2007; Winger et al. 2019), or because individuals that attempt to disperse further away fail to breed or survive (Böhning-Gaese et al. 1998; Toews 2017)? Dispersal behavior also varies with age, and several studies suggest that the behavior of young individuals is particularly important for understanding spatial evolution of migrant species (Gill et al. 2019; Christie et al. 2023). Dispersal processes may vary across species and they likely affect the shape of the population dispersal kernel, which influences spatial evolution (Clark et al. 2001; Furstenau and Cartwright 2016; Smith and Weissman 2023). Parameterizing the dispersal kernel of migratory species requires long-term tracking studies. While such studies

remain technologically intractable for small species, especially in a comparative context, the answer to these questions would significantly inform our ability to make predictions about spatial evolution in migratory birds.

5.3 Genetic diversity within species informs comparisons across species

In this dissertation, I used data on genetic variation within species to inform comparisons between species. Evolutionary patterns are influenced both by species' traits and by the effective size and demographic history of their populations (Ohta 1992; Slatkin 1993; Hutchison and Templeton 1999), which are reflected in their genetic diversity. By conducting analyses that include species' traits and their genetic diversity (as a proxy for effective population size) as predictors for evolutionary outcomes, I explicitly test hypotheses about how both of these processes affect present-day genetic patterns. In chapter 3, I found that effective population size is not correlated with spatial genetic structure, but more sophisticated modeling of species' demographic histories is potentially a promising avenue to explain species-level variation in their spatial patterns (Haller and Messer 2019). In chapter 4, I showed that effective population size influences efficiency of purifying selection on the mitochondria, as expected based on nearly neutral theory (Ohta 1992). I also showed that effective population size variation does not correlate with synonymous substitution rate. This suggests that the influence of migration distance on molecular evolution is not confounded by variation in genetic drift across species, but more likely reflects links between migration and life history. My ability to test these nuanced hypotheses was facilitated by the substantial multi-species population genetic dataset that I generated during my dissertation.

Bibliography

Acevedo, P., A. Jiménez-Valverde, J. M. Lobo, and R. Real. 2012. Delimiting the geographical background in species distribution modelling. J. Biogeogr. 39:1383–1390.

Adamík, P., T. Emmenegger, M. Briedis, L. Gustafsson, I. Henshaw, M. Krist, T. Laaksonen, F. Liechti, P. Procházka, V. Salewski, and S. Hahn. 2016. Barrier crossing in small avian migrants: Individual tracking reveals prolonged nocturnal flights into the day as a common migratory strategy. Sci. Rep. 6:1–9.

Aguillon, S. M., J. W. Fitzpatrick, R. Bowman, S. J. Schoech, A. G. Clark, G. Coop, and N. Chen. 2017. Deconstructing isolation-by-distance: The genomic consequences of limited dispersal. PLoS Genet. 13:1–27.

Allio, R., S. Donega, N. Galtier, and B. Nabholz. 2017. Large variation in the ratio of mitochondrial to nuclear mutation rate across animals: Implications for genetic diversity and the use of mitochondrial DNA as a molecular marker. Mol. Biol. Evol. 34:2762–2772.

Angert, A. L. 2009. The niche, limits to species' distributions, and spatiotemporal variation in demography across the elevation ranges of two monkeyflowers. Proc. Natl. Acad. Sci. U. S. A. 106:19693–19698.

Angert, A. L., L. G. Crozier, L. J. Rissler, S. E. Gilman, J. J. Tewksbury, and A. J. Chunco. 2011. Do species' traits predict recent shifts at expanding range edges? Ecol. Lett. 14:677–689.

Arenas, M., N. Ray, M. Currat, and L. Excoffier. 2012. Consequences of range contractions and

range shifts on molecular diversity. Mol. Biol. Evol. 29:207–218.

Arguedas, N., and P. G. Parker. 2012. Seasonal Migration and Genetic Population Structure in House Wrens. Condor 102:517–528.

Arita, H. T., and P. Rodríguez. 2002. Geographic range, turnover rate and the scaling of species diversity. Ecography 25:541–550.

Arranz, V., V. Thakur, and S. D. Lavery. 2021. Demographic history , not larval dispersal potential , explains differences in population structure of two New Zealand intertidal species. Mar. Biol. 168:1–14.

Auteri, G. G. 2022. A conceptual framework to integrate cold-survival strategies: Torpor, resistance and seasonal migration. Biol. Lett. 18:20220050.

Avise, J. C. 1987. Intraspecific phylogeography: the mitochondrial DNA bridge between population genetics and systematics. Annu. Rev. Ecol. Syst. Vol. 18 489–522.

Bartón, K. 2019. MuMIn: Multi-Model Inference. R package.

Barve, N., V. Barve, A. Jiménez-Valverde, A. Lira-Noriega, S. P. Maher, A. T. Peterson, J. Soberón, and F. Villalobos. 2011. The crucial role of the accessible area in ecological niche modeling and species distribution modeling. Ecol. Modell. 222:1810–1819. Elsevier B.V.

Bears, H., K. Martin, and G. C. White. 2009. Breeding in high-elevation habitat results in shift to slower life-history strategy within a single species. J. Anim. Ecol. 78:365–375.

Bensch, S. 1999. Is the range size of migratory birds constrained by their migratory program? J. Biogeogr. 26:1225–1235.

Benson, A. M., and K. Winker. 2001. Timing of breeding range occupancy among high-latitude passerine migrants. Auk 118:513–519.

Berthold, P., E. Gwinner, and E. Sonnenschein. 2003. Avian Migration. Springer.

Berthold, P., and U. Querner. 1981. Genetic basis of migratory behavior in European warblers. Science 212:77–79.

Berv, J. S., and D. J. Field. 2018. Genomic Signature of an Avian Lilliput Effect across the K-Pg Extinction. Syst. Biol. 67:1–13.

Bhatia, G., N. Patterson, S. Sankararaman, and A. L. Price. 2013. Estimating and interpreting FST: The impact of rare variants. Genome Res. 23:1514–1521.

Bicudo, J. E. P. W., C. R. Vianna, and J. G. Chaui-Berlinck. 2001. Thermogenesis in birds. Biosci. Rep. 21:181–188.

Billerman, S., B. Keeney, P. Rodewald, and T. Schulenberg (eds). 2022. Birds of the World. Cornell Lab of Ornithology, Ithaca, NY.

BirdLife International. 2015. IUCN Red List for birds.

Bivand, R., T. Keitt, and B. Rowlingson. 2019. rgdal: Bindings for the “Geospatial” Data Abstraction Library.

Bivand, R., and C. Rundel. 2019. rgeos: Interface to Geometry Engine - Open Source ('GEOS’).

Blackburn, T. M., and K. J. Gaston. 1996. Spatial patterns in the geographic range sizes of bird species in the New World. Philos. Trans. R. Soc. B Biol. Sci. 351:897–912.

Blanck, A., and N. Lamouroux. 2007. Large-scale intraspecific variation in life-history traits of European freshwater fish. J. Biogeogr. 34:862–875.

Böhning-Gaese, K., T. Caprano, K. van Ewijk, and M. Veith. 2006. Range Size: Disentangling Current Traits and Phylogenetic and Biogeographic Factors. Am. Nat. 167:555–567.

Böhning-Gaese, K., L. I. González-Guzmán, and J. H. Brown. 1998. Constraints on dispersal and the evolution of the avifauna of the Northern Hemisphere. Evol. Ecol. 12:767–783.

Böhning-Gaese, K., B. Halbe, N. Lemoine, and R. Oberrath. 2000. Factors influencing the clutch

size, number of broods and annual fecundity of North American and European land birds. Evol. Ecol. Res. 2:823–839.

Bonte, D., H. Van Dyck, J. M. Bullock, A. Coulon, M. Delgado, M. Gibbs, V. Lehouck, E. Matthysen, K. Mustin, M. Saastamoinen, N. Schtickzelle, V. M. Stevens, S. Vandewoestijne, M. Baguette, K. Barton, T. G. Benton, A. Chaput-Bardy, J. Clobert, C. Dytham, T. Hovestadt, C. M. Meier, S. C. F. Palmer, C. Turlure, and J. M. J. Travis. 2012. Costs of dispersal. Biol. Rev. 87:290–312.

Boria, R. A., L. E. Olson, S. M. Goodman, and R. P. Anderson. 2014. Spatial filtering to reduce sampling bias can improve the performance of ecological niche models. Ecol. Modell. 275:73–77. Elsevier B.V.

Boucher-Lalonde, V., and D. J. Currie. 2016. Spatial autocorrelation can generate stronger correlations between range size and climatic niches than the biological signal - A demonstration using bird and mammal range maps. PLoS One 11:1–15.

Bowler, D. E., and T. G. Benton. 2005. Causes and consequences of animal dispersal strategies: Relating individual behaviour to spatial dynamics. Biol. Rev. Camb. Philos. Soc. 80:205–225.

Bowlin, M. S., and M. Wikelski. 2008. Pointed wings, low wingloading and calm air reduce migratory flight costs in songbirds. PLoS One 3.

Boyce, A. J., and T. E. Martin. 2017. Contrasting latitudinal patterns of life-history divergence in two genera of new world thrushes (Turdinae). J. Avian Biol. 48:581–590.

Bradburd, G. S., G. M. Coop, and P. L. Ralph. 2018. Inferring continuous and discrete population genetic structure across space. Genetics 210:33–52.

Brandt, J. P. 2009. The extent of the North American boreal zone. Environ. Rev. 17:101–161.

Britten, R. J. 1986. Rates of DNA sequence evolution differ between taxonomic groups. Science 231:1393–1398.

Bromham, L. 2020. Causes of Variation in the Rate of Molecular Evolution. Pp. 45–64 *in* S. Y. W. Ho, ed. The Molecular Evolutionary Clock. Springer Cham.

Bromham, L. 2011. The genome as a life-history character: Why rate of molecular evolution varies between mammal species. Philos. Trans. R. Soc. B Biol. Sci. 366:2503–2513.

Bromham, L., X. Hua, R. Lanfear, and P. F. Cowman. 2015. Exploring the Relationships between Mutation Rates, Life History, Genome Size Environment, and Species Richness in Flowering Plants. Am. Nat. 185.

Brommer, J. E. 2008. Extent of recent polewards range margin shifts in Finnish birds depends on their body mass and feeding ecology. Ornis Fenn. 85:109–117.

Brommer, J. E., and A. P. Møller. 2010. Range margin changes, life history and ecology. P. *in* A. P. Møller, W. Fiedler, and P. Berthold, eds. Climate Change and Birds. Oxford University Press.

Broquet, T., and E. J. Petit. 2009. Molecular Estimation of Dispersal for Ecology and Population Genetics. Annu. Rev. Ecol. Evol. Syst. 40:193–216.

Brown, J. M., and P. D. Taylor. 2015. Adult and hatch-year blackpoll warblers exhibit radically different regional-scale movements during post-fledging dispersal. Biol. Lett. 11:2015–2018.

Bruderer, B., and V. Salewski. 2009. Lower annual fecundity in long-distance migrants than in less migratory birds of temperate Europe. J. Ornithol. 150:281–286.

Brüniche-Olsen, A., K. F. Kellner, J. L. Belant, and J. A. Dewoody. 2021. Life-history traits and habitat availability shape genomic diversity in birds: Implications for conservation. Proc. R.

Soc. B Biol. Sci. 288:20211441.

Burg, T. M., S. A. Taylor, K. D. Lemmen, A. J. Gaston, and V. L. Friesen. 2014. Postglacial population genetic differentiation potentially facilitated by a flexible migratory strategy in golden-crowned Kinglets (Regulus satrapa). Can. J. Zool. 92:163–172.

Bürkner, P.-C. 2017. brms : An R Package for Bayesian Multilevel Models using Stan. J. Stat. Softw. 80:1–28.

Burney, and Brumfield. 2009. Ecology Predicts Levels of Genetic Differentiation in Neotropical Birds. Am. Nat. 174:358–368.

Cagan, A., A. Baez-Ortega, N. Brzozowska, F. Abascal, T. H. H. Coorens, M. A. Sanders, A. R. J. Lawson, L. M. R. Harvey, S. Bhosle, D. Jones, R. E. Alcantara, T. M. Butler, Y. Hooks, K. Roberts, E. Anderson, S. Lunn, E. Flach, S. Spiro, I. Januszczak, E. Wrigglesworth, H. Jenkins, T. Dallas, N. Masters, M. W. Perkins, R. Deaville, M. Druce, R. Bogeska, M. D. Milsom, B. Neumann, F. Gorman, F. Constantino-Casas, L. Peachey, D. Bochynska, E. S. J. Smith, M. Gerstung, P. J. Campbell, E. P. Murchison, M. R. Stratton, and I. Martincorena. 2022. Somatic mutation rates scale with lifespan across mammals. Nature 604:517–524.

Cain, M. L., B. G. Milligan, and A. E. Strand. 2000. Long-distance seed dispersal in plant populations. Am. J. Bot. 87:1217–1227.

Canestrelli, D., R. Bisconti, and C. Carere. 2016. Bolder Takes All? The Behavioral Dimension of Biogeography. Trends Ecol. Evol. 31:35–43. Elsevier Ltd.

Castric, V., and L. Bernatchez. 2003. The rise and fall of isolation by distance in the anadromous brook charr (Salvelinus fontinalis Mitchill). Genetics 163:983–996.

Catchpole, C. K. 1980. Sexual Selection and the Evolution of Complex Songs among European Warblers of the Genus Acrocephalus. Behaviour 74:149–166.

Cava, J. A., N. G. Perlut, and S. E. Travis. 2016. Why come back home? Investigating the proximate factors that influence natal philopatry in migratory passerines. Anim. Behav. 118:39–46.

Cavender-Bares, J., K. H. Kozak, P. V. A. Fine, and S. W. Kembel. 2009. The merging of community ecology and phylogenetic biology. Ecol. Lett. 12:693–715.

Chamary, J. V., J. L. Parmley, and L. D. Hurst. 2006. Hearing silence: Non-neutral evolution at synonymous sites in mammals. Nat. Rev. Genet. 7:98–108.

Chang, H., Z. Qiu, H. Yuan, X. Wang, X. Li, H. Sun, X. Guo, Y. Lu, X. Feng, M. Majid, and Y. Huang. 2020. Evolutionary rates of and selective constraints on the mitochondrial genomes of Orthoptera insects with different wing types. Mol. Phylogenet. Evol. 145:106734.

Chen, J., S. Glémin, and M. Lascoux. 2017. Genetic diversity and the efficacy of purifying selection across plant and animal species. Mol. Biol. Evol. 34:1417–1428.

Chen, J., P. Ni, T. N. T. Thi, E. V. Kamaldinov, V. L. Petukhov, J. Han, X. Liu, N. Sprem, and S. Zhao. 2018a. Selective constraints in cold-region wild boars may defuse the effects of small effective population size on molecular evolution of mitogenomes. Ecol. Evol. 17:8102–8114.

Chen, S., Y. Zhou, Y. Chen, and J. Gu. 2018b. fastp: an ultra-fast all-in-one FASTQ preprocessor. Bioinformatics 34:i884–i890.

Chong, R. A., and R. L. Mueller. 2013. Low metabolic rates in salamanders are correlated with weak selective constraints on mitochondrial genes. Evolution 67:894–899.

Christie, K., R. E. Wilson, J. A. Johnson, C. Friis, C. M. Harwood, L. A. Mcduffie, E. Nol, and S. A. Sonsthagen. 2023. Movement and Genomic Methods Reveal Mechanisms Promoting Connectivity in a Declining Shorebird : The Lesser Yellowlegs. Diversity 15:595.

Claramunt, S., E. P. Derryberry, J. V. Remsen, and R. T. Brumfield. 2012. High dispersal ability inhibits speciation in a continental radiation of passerine birds. Proc. R. Soc. B Biol. Sci. 279:1567–1574.

Claramunt, S., and N. A. Wright. 2017. Using museum specimens to study flight and dispersal. Pp. 127–142 *in* The Extended Specimen: Emerging Frontiers in Collections-Based Ornithological Research.

Clark, J. S., M. Lewis, and L. Horvath. 2001. Invasion by extremes: Population spread with variation in dispersal and reproduction. Am. Nat. 157:537–554.

Clark, M. E., and T. E. Martin. 2007. Modeling tradeoffs in avian life history traits and consequences for population growth. Ecol. Modell. 209:110–120.

Clark, P. U., A. S. Dyke, J. D. Shakun, A. E. Carlson, J. Clark, B. Wohlfarth, A. M. McCabe, J. X. Mitrovica, and S. W. Hostetler. 2009. The Last Glacial Maximum. Science 325:710–714.

Colbeck, G. J., H. L. Gibbs, P. P. Marra, K. Hobson, and M. S. Webster. 2008. Phylogeography of a widespread North American migratory songbird (Setophaga ruticilla). J. Hered. 99:453–463.

Conklin, J. R., N. R. Senner, P. F. Battley, and T. Piersma. 2017. Extreme migration and the individual quality spectrum. J. Avian Biol. 48:19–36.

Cox, G. W. 1985. The Evolution of Avian Migration Systems between Temperate and Tropical Regions of the New World. Am. Nat. 126:451–474.

Cox, G. W. 1968. The Role of Competition in the Evolution of Migration. Evolution 22:180–192.

Cribari-Neto, F., and A. Zeileis. 2010a. Beta Regression in R. J. Stat. Softw. 34:1–24.

Cribari-Neto, F., and A. Zeileis. 2010b. Journal of Statistical SoftwareBeta Regression in R. J.

Stat. Softw. 34:1–24.

Crispo, E., and A. P. Hendry. 2005. Does time since colonization influence isolation by distance? A meta-analysis. Conserv. Genet. 6:665–682.

Cumming, S. G., D. Stralberg, K. L. Lefevre, P. S, E. M. Bayne, S. Fang, T. Fontaine, D. Mazerolle, F. K. A. Schmiegelow, and S. J. Song. 2014. Climate and vegetation hierarchically structure patterns of songbird distribution in the Canadian boreal region. Ecography 137–151.

Danecek, P., J. K. Bonfield, J. Liddle, J. Marshall, V. Ohan, M. O. Pollard, A. Whitwham, T. Keane, S. A. McCarthy, and R. M. Davies. 2021. Twelve years of SAMtools and BCFtools. Gigascience 10:1–4.

Davis, J. M., and J. A. Stamps. 2004. The effect of natal experience on habitat preferences. Trends Ecol. Evol. 19:411–416.

Davis, L. A., E. H. Roalson, K. L. Cornell, K. D. Mcclanahan, and M. S. Webster. 2006. Genetic divergence and migration patterns in a North American passerine bird: Implications for evolution and conservation. Mol. Ecol. 15:2141–2152.

Dawideit, B. A., A. B. Phillimore, I. Laube, B. Leisler, and K. Böhning-Gaese. 2009. Ecomorphological predictors of natal dispersal distances in birds. J. Anim. Ecol. 78:388–395.

Dawson, W. R., and M. E. Yacoe. 1983. Metabolic adjustments of small passerine birds for migration and cold. Am. J. Physiol. - Regul. Integr. Comp. Physiol. 14:R755–R767.

De Kort, H., J. G. Prunier, S. Ducatez, O. Honnay, M. Baguette, V. M. Stevens, and S. Blanchet. 2021. Life history, climate and biogeography interactively affect worldwide genetic diversity of plant and animal populations. Nat. Commun. 12:1–11.

De Lafontaine, G., A. Ducousso, S. Lefèvre, E. Magnanou, and R. J. Petit. 2013. Stronger spatial genetic structure in recolonized areas than in refugia in the European beech. Mol. Ecol. 22:4397–4412.

De Mita, S., and M. Siol. 2012. EggLib : processing , analysis and simulation tools for population genetics and genomics. BMC Genet. 13:1–12.

De Panis, D., S. A. Lambertucci, G. Wiemeyer, H. Dopazo, F. C. Almeida, C. J. Mazzoni, M. Gut, I. Gut, and J. Padró. 2021. Mitogenomic analysis of extant condor species provides insight into the molecular evolution of vultures. Sci. Rep. 11:17109.

Delgado, M. M., K. A. Barton, D. Bonte, and J. M. J. Travis. 2014. Prospecting and dispersal : their eco-evolutionary dynamics and implications for population patterns. Proc. R. Soc. B Biol. Sci. 281:20132851.

Delmore, K. E., and D. E. Irwin. 2014. Hybrid songbirds employ intermediate routes in a migratory divide. Ecol. Lett. 17:1211–1218.

DeLuca, W. V., B. K. Woodworth, S. A. Mackenzie, A. E. M. Newman, H. A. Cooke, L. M. Phillips, N. E. Freeman, A. O. Sutton, L. Tauzer, C. McIntyre, I. J. Stenhouse, S. Weidensaul, P. D. Taylor, and D. R. Norris. 2019. A boreal songbird's 20,000 km migration across North America and the Atlantic Ocean. Ecology 0:e02651.

Detsch, F. 2018. gimms: Download and Process GIMMS NDVI3g Data. R package.

Dierckxsens, N., P. Mardulyn, and G. Smits. 2016. NOVOPlasty : de novo assembly of organelle genomes from whole genome data. Nucleic Acids Res. 45:10.1093/nar/gkw955.

Drever, M. C., A. C. Smith, L. A. Venier, D. J. H. Sleep, and D. A. MacLean. 2018. Cross-scale effects of spruce budworm outbreaks on boreal warblers in eastern Canada. Ecol. Evol. 8:7334–7345.

Dunning, J. B. J. 1992. CRC Handbook of Avian Body Masses. CRC Press.

Dyke, A. S., and V. K. Prest. 1987. Late Wisconsinan and Holocene History of the Laurentide Ice Sheet. Géographie Phys. Quat. 41:237–263.

Dytham, C. 2009. Evolved dispersal strategies at range margins. Proc. R. Soc. B Biol. Sci. 276:1407–1413.

Edwards, S. V., V. V. Robin, N. Ferrand, and C. Moritz. 2022. The Evolution of Comparative Phylogeography: Putting the Geography (and More) into Comparative Population Genomics. Genome Biol. Evol. 14:1–16. Oxford University Press.

Edwards, S. V., and A. C. Wilson. 1990. Phylogenetically informative length polymorphism and sequence variability in mitochondrial DNA of Australian songbirds (Pomatostomus). Genetics 126:695–711.

Elith, J., S. J. Phillips, T. Hastie, M. Dudík, Y. E. Chee, and C. J. Yates. 2010. A statistical explanation of MaxEnt for ecologists. Divers. Distrib. 17:43–57.

Engelmark, O. 1999. Boreal forest disturbances. Pp. 161–186 *in* Ecosystems of the World 16: Ecosystems of Disturbed Ground. Elsevier.

Engler, J. O., D. Rödder, D. Stiels, and M. I. Förschler. 2014. Suitable, reachable but not colonised: Seasonal niche duality in an endemic mountainous songbird. J. Ornithol. 155:657–669.

Eo, S. H., J. M. Doyle, and J. A. Dewoody. 2011. Genetic diversity in birds is associated with body mass and habitat type. J. Zool. Syst. Evol. Res. 283:220–226.

Estrada, A., I. Morales-Castilla, C. Meireles, P. Caplat, and R. Early. 2017. Equipped to cope with climate change: traits associated with range filling across European taxa. Ecography 41:770–781.

Estrada, A., I. Morales-Castilla, C. Meireles, P. Caplat, and R. Early. 2018. Equipped to cope with climate change: traits associated with range filling across European taxa. Ecography 41:770–781.

Excoffier, L., M. Foll, and R. J. Petit. 2009. Genetic Consequences of Range Expansions. Annu. Rev. Ecol. Evol. Syst. 40:481–501.

Ezard, T. H. G., and J. M. J. Travis. 2006. The impact of habitat loss and fragmentation on genetic drift and fixation time. Oikos 114:367–375.

Felsenstein, J. 1985. Phylogenies and the comparative method. Am. Nat. 125:1–15.

Feng, S., J. Stiller, Y. Deng, J. Armstrong, Q. Fang, A. H. Reeve, D. Xie, G. Chen, C. Guo, B. C. Faircloth, B. Petersen, Z. Wang, Q. Zhou, M. Diekhans, W. Chen, S. Andreu-Sánchez, A. Margaryan, J. T. Howard, C. Parent, G. Pacheco, M. H. S. Sinding, L. Puetz, E. Cavill, Â. M. Ribeiro, L. Eckhart, J. Fjeldså, P. A. Hosner, R. T. Brumfield, L. Christidis, M. F. Bertelsen, T. Sicheritz-Ponten, D. T. Tietze, B. C. Robertson, G. Song, G. Borgia, S. Claramunt, I. J. Lovette, S. J. Cowen, P. Njoroge, J. P. Dumbacher, O. A. Ryder, J. Fuchs, M. Bunce, D. W. Burt, J. Cracraft, G. Meng, S. J. Hackett, P. G. Ryan, K. A. Jønsson, I. G. Jamieson, R. R. da Fonseca, E. L. Braun, P. Houde, S. Mirarab, A. Suh, B. Hansson, S. Ponnikas, H. Sigeman, M. Stervander, P. B. Frandsen, H. van der Zwan, R. van der Sluis, C. Visser, C. N. Balakrishnan, A. G. Clark, J. W. Fitzpatrick, R. Bowman, N. Chen, A. Cloutier, T. B. Sackton, S. V. Edwards, D. J. Foote, S. B. Shakya, F. H. Sheldon, A. Vignal, A. E. R. Soares, B. Shapiro, J. González-Solís, J. Ferrer-Obiol, J. Rozas, M. Riutort, A. Tigano, V. Friesen, L. Dalén, A. O. Urrutia, T. Székely, Y. Liu, M. G. Campana, A. Corvelo, R. C. Fleischer, K. M. Rutherford, N. J. Gemmell, N. Dussex, H. Mouritsen, N. Thiele, K. Delmore, M. Liedvogel, A. Franke, M. P. Hoeppner, O. Krone, A. M. Fudickar,

B. Milá, E. D. Ketterson, A. E. Fidler, G. Friis, Á. M. Parody-Merino, P. F. Battley, M. P. Cox, N. C. B. Lima, F. Prosdocimi, T. L. Parchman, B. A. Schlinger, B. A. Loiselle, J. G. Blake, H. C. Lim, L. B. Day, M. J. Fuxjager, M. W. Baldwin, M. J. Braun, M. Wirthlin, R. B. Dikow, T. B. Ryder, G. Camenisch, L. F. Keller, J. M. DaCosta, M. E. Hauber, M. I. M. Louder, C. C. Witt, J. A. McGuire, J. Mudge, L. C. Megna, M. D. Carling, B. Wang, S. A. Taylor, G. Del-Rio, A. Aleixo, A. T. R. Vasconcelos, C. V. Mello, J. T. Weir, D. Haussler, Q. Li, H. Yang, J. Wang, F. Lei, C. Rahbek, M. T. P. Gilbert, G. R. Graves, E. D. Jarvis, B. Paten, and G. Zhang. 2020. Dense sampling of bird diversity increases power of comparative genomics. Nature 587:252–257.

Fick, S. E., and R. J. Hijmans. 2017. WorldClim 2: new 1-km spatial resolution climate surfaces for global land areas. Int. J. Climatol. 37:4302–4315.

Figuet, E., J. Romiguier, J. Y. Dutheil, and N. Galtier. 2014. Mitochondrial DNA as a tool for reconstructing past life-history traits in mammals. J. Evol. Biol. 27:899–910.

Förschler, M. I., E. del Val, and F. Bairlein. 2010. Extraordinary high natal philopatry in a migratory passerine. J. Ornithol. 151:745–748.

Forsyth, D. M., R. P. Duncan, M. Bomford, G. Moore, D. M. Forsyth, R. P. Duncan, M. Bomford, and G. Moore. 2004. Climatic Suitability, Life-History Traits, Introduction Effort, and the Establishment and Climatic Suitability, Life-History Traits, Introduction Effort, and the Establishment and Spread of Introduced Mammals in Australia. Conserv. Biol. 18:557–569.

Freeman, B. G., G. A. Montgomery, J. Heavyside, A. E. Moncrieff, O. Johnson, and B. M. Winger. 2023. On the predictability of phenotypic divergence in geographic isolation. 77:26–35.

Friis, G., J. Vizueta, E. D. Ketterson, and B. Milá. 2022. A high-quality genome assembly and annotation of the dark-eyed junco Junco hyemalis, a recently diversified songbird. G3 Genes, Genomes, Genet. 12.

Furstenau, T. N., and R. A. Cartwright. 2016. The effect of the dispersal kernel on isolation-by-distance in a continuous population. PeerJ 4:e1848.

Gagnaire, P. A. 2020. Comparative genomics approach to evolutionary process connectivity. Evol. Appl. 13:1320–1334.

Galtier, N., R. W. Jobson, B. Nabholz, S. Glémin, and P. U. Blier. 2009. Mitochondrial whims: Metabolic rate, longevity and the rate of molecular evolution. Biol. Lett. 5:413–416.

Gaston, K. J., and T. M. Blackburn. 1996. Global Scale Macroecology: Interactions between Population Size, Geographic Range Size and Body Size in the Anseriformes. J. Anim. Ecol. 65:701–714.

Gaston, K. J., T. M. Blackburn, and J. I. Spicer. 1998. Rapoport's rule: Time for an epitaph? Trends Ecol. Evol. 13:70–74.

Gaughran, S. J., M. C. Quinzin, J. M. Miller, R. C. Garrick, D. L. Edwards, M. A. Russello, N. Poulakakis, C. Ciofi, L. B. Beheregaray, and A. Caccone. 2018. Theory , practice , and conservation in the age of genomics : The Galápagos giant tortoise as a case study. 1084–1093.

Gill, J. A., J. A. Alves, and T. G. Gunnarsson. 2019. Mechanisms driving phenological and range change in migratory species. Philos. Trans. R. Soc. B Biol. Sci. 374:20180047.

Gillooly, J. F., A. P. Allen, G. B. West, and J. H. Brown. 2005. The rate of DNA evolution : Effects of body size and temperature on the molecular clock. Proc. Natl. Acad. Sci. 102:140–145.

Gómez-Bahamón, V., R. Márquez, A. E. Jahn, C. Y. Miyaki, D. T. Tuero, O. Laverde-R, S. Restrepo, and C. D. Cadena. 2020. Speciation Associated with Shifts in Migratory Behavior in an Avian Radiation. Curr. Biol. 30:1312-1321.e6.

Gómez, C., E. A. Tenorio, P. Montoya, and C. D. Cadena. 2016. Niche-tracking migrants and nicheswitching residents: Evolution of climatic niches in new world warblers (Parulidae). Proc. R. Soc. B Biol. Sci. 283:1–9.

Gove, A. D., M. C. Fitzpatrick, J. D. Majer, and R. R. Dunn. 2009. Dispersal traits linked to range size through range location, not dispersal ability, in Western Australian angiosperms. Glob. Ecol. Biogeogr. 18:596–606.

Graham, B. A., and T. M. Burg. 2012. Molecular markers provide insights into contemporary and historic gene flow for a non-migratory species. J. Avian Biol. 43:198–214.

Graves, G. R., and C. Rahbek. 2005. Source pool geometry and the assembly of continental avifaunas. Proc. Natl. Acad. Sci. U. S. A. 102:7871–7876.

Greenberg, R. 1980. Demographic aspects of long-distance migration. Pp. 493–504 *in* A. Keast and E. S. Morton, eds. Migrant Birds in the Neotropics. Smithsonian Institution.

Guillot, G., R. Leblois, A. Coulon, and A. C. Frantz. 2009. Statistical methods in spatial genetics. Mol. Ecol. 18:4734–4756.

Haché, S., E. M. Bayne, M.-A. A. Villard, H. Proctor, C. S. Davis, D. Stralberg, J. K. Janes, M. T. Hallworth, K. R. Foster, E. Chidambara-vasi, A. A. Grossi, J. C. Gorrell, and R. Krikun. 2017. Phylogeography of a migratory songbird across its Canadian breeding range: Implications for conservation units. Ecol. Evol. 7:6078–6088. John Wiley and Sons Ltd.

Hagen, S. B., A. Kopatz, J. Aspi, I. Kojola, and H. Geir Eiken. 2015. Evidence of rapid change in genetic structure and diversity during range expansion in a recovering large terrestrial

carnivore. Proc. R. Soc. B Biol. Sci. 282:13–16.

Haller, B. C., and P. W. Messer. 2019. SLiM 3: Forward Genetic Simulations Beyond the Wright-Fisher Model. Mol. Biol. Evol. 36:632–637.

Hallworth, M. T., E. Bayne, E. Mckinnon, O. Love, J. A. Tremblay, B. Drolet, J. Ibarzabal, S. Van Wilgenburg, and P. P. Marra. 2021. Habitat loss on the breeding grounds is a major contributor to population declines in a long-distance migratory songbird.

Hanski, I. 1998. Metapolulation dynamics. Nature 396:41–49.

Hansson, B., S. Bensch, D. Hasselquist, and B. Nielsen. 2002. Restricted dispersal in a long-distance migrant bird with patchy distribution, the great reed warbler.

Hardy, O. J., and X. Vekemans. 1999. Isolation by distance in a continuous population: Reconciliation between spatial autocorrelation analysis and population genetics models. Heredity (Edinb). 83:145–154.

Hargreaves, A. L., K. E. Samis, and C. G. Eckert. 2014. Are Species' Range Limits Simply Niche Limits Writ Large? A Review of Transplant Experiments beyond the Range. Am. Nat. 183:157–173.

Harringmeyer, O. S., and H. E. Hoekstra. 2022. Chromosomal inversion polymorphisms shape the genomic landscape of deer mice. Nat. Ecol. Evol. 6:1965–1979.

Hawkins, B. A., and J. A. Felizola Diniz-Filho. 2006. Beyond Rapoport's rule: Evaluating range size patterns of New World birds in a two-dimensional framework. Glob. Ecol. Biogeogr. 15:461–469.

Heckscher, C. M. 2018. A Nearctic-Neotropical Migratory Songbird's Nesting Phenology and Clutch Size are Predictors of Accumulated Cyclone Energy. Sci. Rep. 8:1–6.

Helbig, A. J. 1991. SE- and SW-migrating Blackcap (Sylvia atricapilla) populations in Central

Europe: Orientation of birds in the contact zone. J. Evol. Biol. 4:657–670.

Heldstab, S. A. 2021. Latitude, life history and sexual size dimorphism correlate with reproductive seasonality in rodents. Mamm. Rev. 51:256–271.

Henningsson, S. S., and T. Alerstam. 2008. Does migration promote or restrict circumpolar breeding ranges of arctic birds? J. Biogeogr. 35:78.

Henningsson, S. S., and T. Alerstam. 2006. Implications of migratory connectivity for species ' ranges and subspeciation of arctic shorebirds. Ardea 94:499–509.

Hewitt, G. 2000. The genetic legacy of the quaternary ice ages. Nature 405:907–913.

Hijmans, R. J. 2019a. geosphere: Spherical Trigonometry. R package.

Hijmans, R. J. 2022. Package "geosphere." CRAN.

Hijmans, R. J. 2019b. raster: Geographic Data Analysis and Modeling.

Hijmans, R. J., S. Phillips, J. Leathwick, and J. Elith. 2017. dismo: Species Distribution Modeling. R package.

Hindley, J., B. A. Graham, and T. M. Burg. 2018. Pleistocene glacial cycles and physical barriers influence phylogeographic structure in Black-capped Chickadees (Poecile atricapillus), a widespread North American passerine . Can. J. Zool. 96:1366–1377.

Hofreiter, M., and J. Stewart. 2009. Ecological Change , Range Fluctuations and Population Dynamics during the Pleistocene Review. Curr. Biol. 19:R584–R594.

Hua, X., P. Cowman, D. Warren, and L. Bromham. 2015. Longevity is linked to mitochondrial mutation rates in rockfish: A test using poisson regression. Mol. Biol. Evol. 32:2633–2645.

Huang, H., and L. L. Knowles. 2016. Unforeseen consequences of excluding missing data from next-generation sequences: Simulation study of rad sequences. Syst. Biol. 65:357–365.

Huang, K., R. L. Andrew, G. L. Owens, K. L. Ostevik, and L. H. Rieseberg. 2020. Multiple

chromosomal inversions contribute to adaptive divergence of a dune sunflower ecotype. Mol. Ecol. 29:2535–2549. Blackwell Publishing Ltd.

Hubbell, S. P. 1997. A unified theory of biogeography and relative species abundance and its application to tropical rain forests and coral reefs. Coral Reefs 16:9–21.

Hung, C. M., S. V. Drovetski, and R. M. Zink. 2017. The roles of ecology, behaviour and effective population size in the evolution of a community. Mol. Ecol. 26:3775–3784.

Huntington, C. E. 1951. Review: "Ortstreue " and Subspecies Formation in the Pied Flycatcher. Ecology 32:352–355.

Hutchinson, G. E. 1957. Concluding remarks: The demographic symposium as a heterogeneous unstable population. Cold Spring Harb. Symp. Quant. Biol. 22:415–427.

Hutchison, D. W., and A. R. Templeton. 1999. Correlation of pairwise genetic and geographic distance measures: Inferring the relative influences of gene flow and drift on the distribution of genetic variability. Evolution 53:1898–1914.

Hwang, D. G., and P. Green. 2004. Bayesian Markov chain Monte Carlo sequence analysis reveals varying neutral substitution patterns in mammalian evolution. Proc. Natl. Acad. Sci. U. S. A. 101:13994–14001.

Iannucci, A., A. Benazzo, C. Natali, E. Ayu, M. Samsul, A. Zein, T. S. Jessop, G. Bertorelle, and C. Ciofi. 2021. Population structure , genomic diversity and demographic history of Komodo dragons inferred from whole- - genome sequencing. Mol. Ecol. 30:6309–6324.

Irwin, D. E. 2002. Phylogeographic breaks without geographic barriers to gene flow. Evolution 56:2383–2394.

Irwin, D. E. 2009. Speciation: New Migratory Direction Provides Route toward Divergence. Curr. Biol. 19:R1111–R1113.

Ishigohoka, J., K. Bascón-Cardozo, A. Bours, J. Fuß, A. Rhie, J. Mountcastle, B. Haase, W. Chow, J. Collins, K. Howe, M. Uliano-Silva, O. Fedrigo, E. D. Jarvis, J. Pérez-Tris, J. Carlos Illera, and M. Liedvogel. 2021. Recombination suppression and selection affect local ancestries in genomes of a migratory songbird. bioRxiv, doi: 10.1101/2021.12.22.473882.

Jablonski, D. 2005. Mass Extinctions and Macroevolution. Paleobiology 31:192–210.

Jahn, A. E., and V. R. Cueto. 2012. The potential for comparative research across New World bird migration systems. J. Ornithol. 153:199–205.

Jahn, A. E., V. R. Cueto, C. S. Fontana, A. C. Guaraldo, D. J. Levey, P. P. Marra, and T. B. Ryder. 2020. Bird migration within the Neotropics. Auk 137:1–23.

Jangjoo, M., S. F. Matter, J. Roland, and N. Keyghobadi. 2020. Demographic fluctuations lead to rapid and cyclic shifts in genetic structure among populations of an alpine butterfly, Parnassius smintheus. J. Evol. Biol. 33:668–681.

Jenni-Eiermann, S., L. Jenni, S. Smith, and D. Costantini. 2014. Oxidative stress in endurance flight: An unconsidered factor in bird migration. PLoS One 9:1–6.

Jetz, W., G. H. Thomas, J. B. Joy, K. Hartmann, and A. O. Mooers. 2012. The global diversity of birds in space and time. Nature 491:444–448.

Johnson, O., C. C. Ribas, A. Aleixo, L. N. Naka, M. G. Harvey, and R. T. Brumfield. 2023. Amazonian birds in more dynamic habitats have less population genetic structure and higher gene flow. Mol. Ecol. 1–21.

Jønsson, K. A., A. P. Tøttrup, M. K. Borregaard, S. A. Keith, C. Rahbek, and K. Thorup. 2016. Tracking Animal Dispersal: From Individual Movement to Community Assembly and Global Range Dynamics. Trends Ecol. Evol. 31:204–214. Elsevier Ltd.

Jun, G., M. K. Wing, G. Abecasis, and H. M. Kang. 2015. An efficient and scalable analysis

framework for variant extraction and refinement from population scale DNA sequence data. Genome Res., doi: 10.1101/gr.176552.114.

Kamvar, Z. N., J. F. Tabima, and N. J. Gŕunwald. 2014. Poppr: An R package for genetic analysis of populations with clonal, partially clonal, and/or sexual reproduction. PeerJ 2014:1–14.

Kapusta, A., A. Suh, and C. Feschotte. 2017. Dynamics of genome size evolution in birds and mammals. Proc. Natl. Acad. Sci. U. S. A. 114:E1460–E1469.

Kimmitt, A. A., T. M. Pegan, A. W. Jones, K. S. Wacker, C. L. Brennan, J. Hudon, J. J. Kirchman, K. Ruegg, B. W. Benz, R. R. Herman, and B. M. Winger. 2023. Genetic evidence for widespread population size expansion in North American boreal birds prior to the Last Glacial Maximum. Proc. R. Soc. B Biol. Sci. 290:20221334.

Kimura, M. 1983. The neutral theory of molecular evolution. Cambridge University Press.

Kisel, Y., and T. G. Barraclough. 2010. Speciation Has a Spatial Scale That Depends on Levels of Gene Flow. Am. Nat. 175:316–334.

Knowles, L. L. 2009. Statistical phylogeography. Annu. Rev. Ecol. Evol. Syst. 40:593–612.

Korneliussen, T. S., A. Albrechtsen, and R. Nielsen. 2014. ANGSD: Analysis of Next Generation Sequencing Data. BMC Bioinformatics 15:1–13.

Korneliussen, T. S., I. Moltke, A. Albrechtsen, and R. Nielsen. 2013. Calculation of Tajima's D and other neutrality test statistics from low depth next-generation sequencing data. BMC Bioinformatics 14.

Korunes, K. L., and K. Samuk. 2021. pixy: Unbiased estimation of nucleotide diversity and divergence in the presence of missing data. Mol. Ecol. Resour. 21:1359–1368.

Kramer-Schadt, S., J. Niedballa, J. D. Pilgrim, B. Schröder, J. Lindenborn, V. Reinfelder, M.

Stillfried, I. Heckmann, A. K. Scharf, D. M. Augeri, S. M. Cheyne, A. J. Hearn, J. Ross, D. W. Macdonald, J. Mathai, J. Eaton, A. J. Marshall, G. Semiadi, R. Rustam, H. Bernard, R. Alfred, H. Samejima, J. W. Duckworth, C. Breitenmoser-Wuersten, J. L. Belant, H. Hofer, and A. Wilting. 2013. The importance of correcting for sampling bias in MaxEnt species distribution models. Divers. Distrib. 19:1366–1379.

Kramer, G. R., D. E. Andersen, D. A. Buehler, P. B. Wood, S. M. Peterson, J. A. Lehman, K. R. Aldinger, L. P. Bulluck, S. Harding, J. A. Jones, J. P. Loegering, and C. Smalling. 2018. Population trends in Vermivora warblers are linked to strong migratory connectivity. Proc. Natl. Acad. Sci. 115.

Krauel, J. J., and G. F. McCracken. 2013. Recent advances in bat migration research. P. *in* R. A. Adams and S. C. Pederson, eds. Bat Evolution, Ecology, and Conservation. Springer, New York, NY.

Kryazhimskiy, S., and J. B. Plotkin. 2008. The population genetics of dN/dS. PLoS Genet. 4:e1000304.

Kubisch, A., R. D. Holt, H. J. Poethke, and E. A. Fronhofer. 2014. Where am I and why? Synthesizing range biology and the eco-evolutionary dynamics of dispersal. Oikos 123:5–22.

Kuhner, M. K. 2006. LAMARC 2.0: Maximum likelihood and Bayesian estimation of population parameters. Bioinformatics 22:768–770.

Küpper, C., M. Stocks, J. E. Risse, N. Dos Remedios, L. L. Farrell, S. B. McRae, T. C. Morgan, N. Karlionova, P. Pinchuk, Y. I. Verkuil, A. S. Kitaysky, J. C. Wingfield, T. Piersma, K. Zeng, J. Slate, M. Blaxter, D. B. Lank, and T. Burke. 2015. A supergene determines highly divergent male reproductive morphs in the ruff. Nat. Genet. 48:79–83. Nature Publishing

Group.

Kutschera, V. E., J. W. Poelstra, F. Botero-Castro, N. Dussex, N. J. Gemmell, G. R. Hunt, M. G. Ritchie, C. Rutz, R. A. W. Wiberg, and J. B. W. Wolf. 2020. Purifying Selection in Corvids Is Less Efficient on Islands. Mol. Biol. Evol. 37:469–474.

Lack, D. 1948. The significance of clutch-size. Part III.-Some interspecific comparisons. Ibis (Lond. 1859). 90:25–45.

Laine, V. N., T. I. Gossmann, K. M. Schachtschneider, C. J. Garroway, O. Madsen, K. J. F. Verhoeven, V. De Jager, H. J. Megens, W. C. Warren, P. Minx, R. P. M. A. Crooijmans, P. Corcoran, F. Adriaensen, E. Belda, A. Bushuev, M. Cichon, A. Charmantier, N. Dingemanse, B. Doligez, T. Eeva, K. E. Erikstad, S. Fedorov, M. Hau, S. Hille, C. Hinde, B. Kempenaers, A. Kerimov, M. Krist, R. Mand, E. Matthysen, R. Nager, C. Norte, M. Orell, H. Richner, T. Slagsvold, V. Tilgar, J. Tinbergen, J. Torok, B. Tschirren, T. Yuta, B. C. Sheldon, J. Slate, K. Zeng, K. Van Oers, M. E. Visser, and M. A. M. Groenen. 2016. Evolutionary signals of selection on cognition from the great tit genome and methylome. Nat. Commun. 7:1–9.

Lanfear, R., H. Kokko, and A. Eyre-Walker. 2014. Population size and the rate of evolution. Trends Ecol. Evol. 29:33–41.

Lanfear, R., J. A. Thomas, J. J. Welch, T. Brey, and L. Bromham. 2007. Metabolic rate does not calibrate the molecular clock. Proc. Natl. Acad. Sci. 104:15388–15393.

Lartillot, N., and R. Poujol. 2011. A phylogenetic model for investigating correlated evolution of substitution rates and continuous phenotypic characters. Mol. Biol. Evol. 28:729–744.

Lartillot, N., and R. Poujol. 2021. Coevol: Correlated evolution of substitution rates and quantitative traits (v1.6 manual).

Laube, I., C. H. Graham, and K. Böhning-Gaese. 2013a. Intra-generic species richness and dispersal ability interact to determine geographic ranges of birds. Glob. Ecol. Biogeogr. 22:223–232.

Laube, I., H. Korntheuer, M. Schwager, S. Trautmann, C. Rahbek, and K. Böhning-Gaese. 2013b. Towards a more mechanistic understanding of traits and range sizes. Glob. Ecol. Biogeogr. 22:233–241.

Lawton, J. 1993. Population Abu ante and Conservation. Oikos 8:409–413.

Leech, D. I., and H. Q. P. Crick. 2007. Influence of climate change on the abundance , distribution and phenology of woodland bird species in temperate regions. Ibis (Lond. 1859). 149:128–145.

Lees, A. C., and J. J. Gilroy. 2014. Vagrancy fails to predict colonization of oceanic islands. Glob. Ecol. Biogeogr. 23:405–413.

Lehtonen, J., and R. Lanfear. 2014. Generation time, life history and the substitution rate of neutral mutations. Biol. Lett. 10:3–6.

Leroy, T., M. Rousselle, M. K. Tilak, A. E. Caizergues, C. Scornavacca, M. Recuerda, J. Fuchs, J. C. Illera, D. H. De Swardt, G. Blanco, C. Thébaud, B. Milá, and B. Nabholz. 2021. Island songbirds as windows into evolution in small populations. Curr. Biol. 31:1303–1310.

Lessa, E. P., J. A. Cook, and J. L. Patton. 2003. Genetic footprints of demographic expansion in North America, but not Amazonia, during the Late Quaternary. Proc. Natl. Acad. Sci. U. S. A. 100:10331–10334.

Levey, D. J., and G. F. Stiles. 1992. Evolutionary Precursors of Long-Distance Migration : Resource Availability and Movement Patterns in Neotropical Landbirds. Am. Nat. 140:447–476.

Li, H. 2013. Aligning sequence reads, clone sequences and assembly contigs with BWA-MEM. 00:1–3.

Li, H., and P. Ralph. 2019. Local PCA shows how the effect of population structure differs along the genome. Genetics 211:289–304.

Li, W. H., D. L. Ellsworth, J. Krushkal, B. H. J. Chang, and D. Hewett-Emmett. 1996. Rates of nucleotide substitution in primates and rodents and the generation-time effect hypothesis. Mol. Phylogenet. Evol. 5:182–187.

Linderoth, T. 2018. Identifying Population Histories, Adaptive Genes, and Genetic Duplication from Population-scale Next Generation Sequencing. University of California, Berkeley.

Lombal, A. J., E. O. James, V. Friesen, E. J. Woehler, and C. P. Burridge. 2020. Identifying mechanisms of genetic differentiation among populations in vagile species : historical factors dominate genetic differentiation in seabirds. Biol. Rev. 2.

Londoño, G. A., M. A. Chappell, M. del R. Castañeda, J. E. Jankowski, and S. K. Robinson. 2015. Basal metabolism in tropical birds: Latitude, altitude, and the "pace of life." Funct. Ecol. 29:338–346.

Lou, R. N., A. Jacobs, A. P. Wilder, and N. O. Therkildsen. 2021. A beginner's guide to low-coverage whole genome sequencing for population genomics. Mol. Ecol. 30:5966–5993.

Lou, R. N., and N. O. Therkildsen. 2021. Batch effects in population genomic studies with low-coverage whole genome sequencing data: Causes, detection and mitigation. Mol. Ecol. Resour. 1–15.

Lüdecke, D. 2018. ggeffects: Tidy Data Frames of Marginal Effects from Regression Models. J. Open Source Softw. 3:772.

Luo, B., S. E. Santana, Y. Pang, M. Wang, Y. Xiao, and J. Feng. 2019. Wing morphology

predicts geographic range size in vespertilionid bats. Sci. Rep. 9:4526.

MacArthur, R. H., and E. O. Wilson. 1967. Theory of Island Biogeography. Princeton University Press, Princeton, NJ.

Manthey, J. D., J. Klicka, and G. M. Spellman. 2021. The Genomic Signature of Allopatric Speciation in a Songbird Is Shaped by Genome Architecture (Aves: Certhia americana). Genome Biol. Evol. 13:1–21.

Martin, A. E., and L. Fahrig. 2018. Habitat specialist birds disperse farther and are more migratory than habitat generalist birds. Ecology 99:2058–2066.

Martin, A. P., and S. R. Palumbi. 1993. Body size, metabolic rate, generation time, and the molecular clock. Proc. Natl. Acad. Sci. U. S. A. 90:4087–4091.

Martin, T. E. 2004. Avian life-history evolution has an eminent past: does it have a bright future? Auk 121:289–301.

Maruyama, T. 1971. Analysis of population structure II. Two-dimensional stepping stone models of finite length and other geographically structured populations. Ann. Hum. Genet. 35:179–196.

May, M. L. 2013. A critical overview of progress in studies of migration of dragonflies (Odonata: Anisoptera), with emphasis on North America. J. Insect Conserv. 17:1–15.

Mayr, E. 1942. Systematics and the Origin of Species, from the Viewpoint of a Zoologist. Columbia University Press.

McKinnon, E. A., and O. P. Love. 2018. Ten years tracking the migrations of small landbirds: Lessons learned in the golden age of bio-logging. Auk 135:834–856.

McNamara, J. M., Z. Barta, M. Wikelski, and A. I. Houston. 2008. A theoretical investigation of the effect of latitude on avian life histories. Am. Nat. 172:331–345.

McNamara, J. M., and S. R. X. Dall. 2011. The evolution of unconditional strategies via the "multiplier effect." Ecol. Lett. 14:237–243.

Medina, I., G. M. Cooke, and T. J. Ord. 2018. Walk, swim or fly? Locomotor mode predicts genetic differentiation in vertebrates. Ecol. Lett. 21:638–645.

Meirmans, P. G. 2012. The trouble with isolation by distance. Mol. Ecol. 21:2839–2846.

Meirmans, P. G., and P. W. Hedrick. 2011. Assessing population structure: FST and related measures. Mol. Ecol. Resour. 11:5–18.

Meisner, J., and A. Albrechtsen. 2018. Inferring population structure and admixture proportions in low-depth NGS data. Genetics 210:719–731.

Merlin, C., and M. Liedvogel. 2019. The genetics and epigenetics of animal migration and orientation: Birds, butterflies and beyond. J. Exp. Biol. 222:1–12.

Meyer, C. F. J., E. K. V. Kalko, and G. Kerth. 2009. Small-scale fragmentation effects on local genetic diversity in two phyllostomid bats with different dispersal abilities in Panama. Biotropica 41:95–102.

Milá, B., J. E. McCormack, G. Castañeda, R. K. Wayne, and T. B. Smith. 2007a. Recent postglacial range expansion drives the rapid diversification of a songbird lineage in the genus Junco. Proc. R. Soc. B Biol. Sci. 274:2653–2660.

Milá, B., T. B. Smith, and R. K. Wayne. 2007b. Speciation and rapid phenotypic differentiation in the yellow-rumped warbler Dendroica coronata complex. Mol. Ecol. 16:159–173.

Miller, E. F., R. E. Green, A. Balmford, P. Maisano Delser, R. Beyer, M. Somveille, M. Leonardi, W. Amos, and A. Manica. 2021. Bayesian Skyline Plots disagree with range size changes based on Species Distribution Models for Holarctic birds. Mol. Ecol. 30:3993–4004.

Milot, E., H. Lisle Gibbs, and K. A. Hobson. 2000. Phylogeography and genetic structure of northern populations of the yellow warbler (Dendroica petechia). Mol. Ecol. 9:667–681.

Mindell, D. P., M. D. Sorenson, and D. E. Dimcheff. 1998. An extra nucleotide is not translated in mitochondrial ND3 of some birds and turtles. Mol. Biol. Evol. 15:1568–1571.

Mitchell, G. W., P. D. Taylor, and I. G. Warkentin. 2010. Assessing the Function of Broad-Scale Movements Made by Juvenile Songbirds Prior to Migration. Condor 112:644–654.

Mitterboeck, T. F., S. Liu, S. J. Adamowicz, J. Fu, R. Zhang, W. Song, K. Meusemann, and X. Zhou. 2017. Positive and relaxed selection associated with flight evolution and loss in insect transcriptomes. Gigascience 6:1–14.

Møller, A. P. 2007. Senescence in relation to latitude and migration in birds. J. Evol. Biol. 20:750–757.

Moore, R. P., W. D. Robinson, I. J. Lovette, and T. R. Robinson. 2008. Experimental evidence for extreme dispersal limitation in tropical forest birds. Ecol. Lett. 11:960–968.

Moore, T. E., R. Bagchi, M. E. Aiello-Lammens, and C. D. Schlichting. 2018. Spatial autocorrelation inflates niche breadth–range size relationships. Glob. Ecol. Biogeogr. 27:1426–1436.

Moorjani, P., C. E. G. Amorim, P. F. Arndt, and M. Przeworski. 2016. Variation in the molecular clock of primates. Proc. Natl. Acad. Sci. U. S. A. 113:10607–10612.

Morrone, J. J. 2015. Halffter's Mexican transition zone (1962-2014), cenocrons and evolutionary biogeography. J. Zool. Syst. Evol. Res. 53:249–257.

Murray, G. G. R., A. E. R. Soares, B. J. Novak, N. K. Schaefer, J. A. Cahill, A. J. Baker, J. R. Demboski, A. Doll, R. R. Da Fonseca, T. L. Fulton, T. P. Gilbert, P. D. Heintzman, B. Letts, G. McIntosh, B. L. O'Connell, M. Peck, M. L. Pipes, E. S. Rice, K. M. Santos, A. G.

Sohrweide, S. H. Vohr, R. B. Corbett-Detig, R. E. Green, and B. Shapiro. 2017. Natural selection shaped the rise and fall of passenger pigeon genomic diversity. Science 358:951–954.

Nabholz, B., H. Ellegren, and J. B. W. Wolf. 2013. High levels of gene expression explain the strong evolutionary constraint of mitochondrial protein-coding genes. Mol. Biol. Evol. 30:272–284.

Nabholz, B., S. Glémin, and N. Galtier. 2008a. Strong variations of mitochondrial mutation rate across mammals - The longevity hypothesis. Mol. Biol. Evol. 25:120–130.

Nabholz, B., R. Lanfear, and J. Fuchs. 2016. Body mass-corrected molecular rate for bird mitochondrial DNA. Mol. Ecol. 25:4438–4449.

Nabholz, B., J. F. Mauffrey, E. Bazin, N. Galtier, and S. Glemin. 2008b. Determination of mitochondrial genetic diversity in mammals. Genetics 178:351–361.

Nei, M. 2005. Selectionism and neutralism in molecular evolution. Mol. Biol. Evol. 22:2318–2342.

Nei, M., Y. Suzuki, and M. Nozawa. 2010. The Neutral Theory of Molecular Evolution in the Genomic Era. Annu. Rev. Genomics Hum. Genet. 11:265–289.

Newton, I. 2007. The Migration Ecology of Birds. Academic Press.

Newton, I., and L. C. Dale. 1996. Bird migration at different latitudes in Eastern North America. Auk 113:626–635.

Nikolaev, S. I., J. I. Montoya-Burgos, K. Popadin, L. Parand, E. H. Margulies, S. E. Antonarakis, G. G. Bouffard, J. R. Idol, V. V. B. Maduro, R. W. Blakesley, X. Guan, N. F. Hansen, B. Maskeri, J. C. McDowell, M. Park, P. J. Thomas, and A. C. Young. 2007. Life-history traits drive the evolutionary rates of mammalian coding and noncoding genomic elements. Proc.

Natl. Acad. Sci. U. S. A. 104:20443–20448.

Nilsson, C., R. H. G. Klaassen, and T. Alerstam. 2013. Differences in speed and duration of bird migration between spring and autumn. Am. Nat. 181:837–845.

Normand, S., R. E. Ricklefs, F. Skov, J. Bladt, O. Tackenberg, and J. C. Svenning. 2011. Postglacial migration supplements climate in determining plant species ranges in Europe. Proc. R. Soc. B Biol. Sci. 278:3644–3653.

Norris, D. R., P. P. Marra, T. K. Kyser, T. W. Sherry, and L. M. Ratcliffe. 2004. Tropical winter habitat limits reproductive success on the temperate breeding grounds in a migratory bird. Proc. R. Soc. B Biol. Sci. 271:59–64.

Novembre, J., T. Johnson, K. Bryc, Z. Kutalik, A. R. Boyko, A. Auton, A. Indap, K. S. King, S. Bergmann, M. R. Nelson, M. Stephens, and C. D. Bustamante. 2008. Genes mirror geography within Europe. Nature 456:98–102.

Nürk, N. M., F. Michling, and H. P. Linder. 2018. Are the radiations of temperate lineages in tropical alpine ecosystems pre-adapted? Glob. Ecol. Biogeogr. 27:334–345.

Ohta, T. 1992. The nearly neutral theory of molecular evolution. Annu. Rev. Ecol. Syst. 23:263–286.

Omernik, J. M. 1987. Ecoregions of the conterminous United States. Map (scale 1:7,500,000). Ann. Assoc. Am. Geogr. 77:118–125.

Omernik, J. M., and G. E. Griffith. 2014. Ecoregions of the Conterminous United States: Evolution of a Hierarchical Spatial Framework. Environ. Manage. 54:1249–1266.

Orme, C. D. L., R. G. Davies, V. A. Olson, G. H. Thomas, T. S. Ding, P. C. Rasmussen, R. S. Ridgely, A. J. Stattersfield, P. M. Bennett, I. P. F. Owens, T. M. Blackburn, and K. J. Gaston. 2006. Global patterns of geographic range size in birds. PLoS Biol. 4:1276–1283.

Outomuro, D., and F. Johansson. 2019. Wing morphology and migration status, but not body size, habitat or Rapoport's rule predict range size in North-American dragonflies (Odonata: Libellulidae). Ecography 42:309–320.

Papadopoulou, A., I. Anastasiou, B. Keskin, and A. P. Vogler. 2009. Comparative phylogeography of tenebrionid beetles in the Aegean archipelago: The effect of dispersal ability and habitat preference. Mol. Ecol. 18:2503–2517.

Papadopoulou, A., and L. L. Knowles. 2016. Toward a paradigm shift in comparative phylogeography driven by trait-based hypotheses. PNAS 113:8018–8024. National Academy of Sciences.

Paradis, E., S. R. Baillie, W. J. Sutherland, and R. D. Gregory. 1998. Patterns of natal and breeding dispersal in birds. J. Anim. Ecol. 67:518–536.

Paradis, E., and K. Schleip. 2019. ape 5.0: an environment for modern phylogenetics and evolutionary analyses in R. Bioinformatics 35:526–528.

Paris, J. R., J. R. Stevens, and J. M. Catchen. 2017. Lost in parameter space: a road map for stacks. Methods Ecol. Evol. 8:1360–1373.

Patterson, N., A. L. Price, and D. Reich. 2006. Population Structure and Eigenanalysis. 2.

Pearce, J. M. 2007. Philopatry: A return to origins. Auk 124:1085–1087.

Pegan, T. M., and B. M. Winger. 2020. The influence of seasonal migration on range size in temperate North American passerines. Ecography 43:1191–1202.

Peterson, A. T., J. Soberón, R. G. Pearson, R. P. Anderson, E. Martínez-Meyer, M. Nakamura, and M. B. Araújo. 2011. Ecological Niches and Geographic Distributions. Princeton University Press.

Peterson, M. A., and R. F. Denno. 1998. The influence of dispersal and diet breadth on patterns

of genetic isolation by distance in phytophagous insects. Am. Nat. 152:428–446.

Phillips, A. G., T. Töpfer, K. Böhning-Gaese, and S. A. Fritz. 2018. Evidence for distinct evolutionary optima in the morphology of migratory and resident birds. J. Avian Biol. 49:1–12.

Phillips, S. 2010. "A Brief Tutorial on Maxent" in Species Distribution Modeling for Educators and Practitioners. Lessons Conserv. 3:107–135.

Phillips, S. J. 2017. maxnet: Fitting "Maxent" Species Distribution Models with "glmnet." R package.

Pierson, J. C., F. W. Allendorf, P. Drapeau, and M. K. Schwartz. 2013. Breed Locally, Disperse Globally: Fine-Scale Genetic Structure Despite Landscape-Scale Panmixia in a Fire-Specialist. PLoS One 8:1–8.

Piertney, S. B., M. Wenzel, and A. J. Jamieson. 2023. Large effective population size masks population genetic structure in *Hirondellea* amphipods within the deepest marine ecosystem, the Mariana Trench. Mol. Ecol., doi: 10.1111/mec.16887.

Pigot, A. L., and J. A. Tobias. 2015. Dispersal and the transition to sympatry in vertebrates. Proc. R. Soc. B Biol. Sci. 282.

Pinzon, J. E., and C. J. Tucker. 2014. A Non-Stationary 1981–2012 AVHRR NDVI3g Time Series. Remote Sens. 6:6929–6960.

Polato, N. R., B. A. Gill, A. A. Shah, M. M. Gray, K. L. Casner, A. Barthelet, P. W. Messer, M. P. Simmons, J. M. Guayasamin, A. C. Encalada, B. C. Kondratieff, A. S. Flecker, S. A. Thomas, C. K. Ghalambor, N. L. Poff, W. C. Funk, and K. R. Zamudio. 2018. Narrow thermal tolerance and low dispersal drive higher speciation in tropical mountains. Proc. Natl. Acad. Sci. 115:12471–12476.

Ponti, R., A. Arcones, X. Ferrer, and D. R. Vieites. 2019. Seasonal climatic niches diverge in migratory birds. Ibis (Lond. 1859)., doi: 10.1111/ibi.12784.

Popadin, K., L. V. Polishchuk, L. Mamirova, D. Knorre, and K. Gunbin. 2007. Accumulation of slightly deleterious mutations in mitochondrial protein-coding genes of large versus small mammals. Proc. Natl. Acad. Sci. U. S. A. 104:13390–13395.

Popadin, K. Y., S. I. Nikolaev, T. Junier, M. Baranova, and S. E. Antonarakis. 2013. Purifying selection in mammalian mitochondrial protein-coding genes is highly effective and congruent with evolution of nuclear genes. Mol. Biol. Evol. 30:347–355.

Price, T. D., and M. Kirkpatrick. 2009. Evolutionarily stable range limits set by interspecific competition. Proc. R. Soc. B Biol. Sci. 276:1429–1434.

Privé, F., K. Luu, M. G. B. Blum, J. J. McGrath, and B. J. Vilhjálmsson. 2020. Efficient toolkit implementing best practices for principal component analysis of population genetic data. Bioinformatics 36:4449–4457.

Promislow, D. E. L., and P. H. Harvey. 1990. Living fast and dying young: A comparative analysis of life-history variation among mammals. J. Zool. 220:417–437.

Ralston, J., A. M. FitzGerald, T. M. Burg, N. C. Starkloff, I. G. Warkentin, and J. J. Kirchman. 2021. Comparative phylogeographic analysis suggests a shared history among eastern North American boreal forest birds. Ornithology 138:1–16.

Ralston, J., and J. J. Kirchman. 2012. Continent-scale genetic structure in a boreal forest migrant, the Blackpoll Warbler (Setophaga striata). Auk 129:467–478.

Ray, N., and J. M. Adams. 2001. A GIS-based Vegetation Map of the World at the Last Glacial Maximum (25,000-15,000 BP). Internet Archaeol. 11.

Read, A. F., and P. H. Harvey. 1989. Life history differences among the eutherian radiations. J.

Zool. 219:329–353.

Reed, J. M., T. Boulinier, E. Danchin, and L. W. Oring. 1999. Informed Dispersal. Pp. 189–259 *in* Current Ornithology.

Reif, J., D. Hořák, A. Krištín, L. Kopsová, and V. Devictor. 2016. Linking habitat specialization with species' traits in European birds. Oikos 125:405–413.

Reudink, M. W., P. P. Marra, T. K. Kyser, P. T. Boag, K. M. Langin, and L. M. Ratcliffe. 2009. Non-breeding season events influence sexual selection in a long-distance migratory bird. Proc. R. Soc. B Biol. Sci. 276:1619–1626.

Revell, L. J. 2010. Phylogenetic signal and linear regression on species data. Methods Ecol. Evol. 1:319–329.

Revell, L. J. 2012. phytools: An R package for phylogenetic comparative biology (and other things). Methods Ecol. Evol. 3:217–223.

Reynolds, J., B. S. Weir, and C. C. Cockerham. 1983. Estimation of the coancestry coefficient basis for a short-term genetic distance. Genetics 105:767–779.

Rissler, L. J. 2016. Union of Phylogeography and landscape genetics. Proc. Natl. Acad. Sci. U. S. A. 113:8079–8086. National Academy of Sciences.

Ritchie, A. M., X. Hua, and L. Bromham. 2022. Investigating the reliability of molecular estimates of evolutionary time when substitution rates and speciation rates vary. BMC Ecol. Evol. 22:1–19. BioMed Central.

Rodewald, P. (ed). 2015. The Birds of North America: https://birdsna.org. Cornell Lab of Ornithology, Ithaca, NY.

Romiguier, J., P. Gayral, M. Ballenghien, A. Bernard, V. Cahais, A. Chenuil, Y. Chiari, R. Dernat, L. Duret, N. Faivre, E. Loire, J. M. Lourenco, B. Nabholz, C. Roux, G.

Tsagkogeorga, L. A. Weinert, K. Belkhir, N. Bierne, N. Galtier, S. Gle, A. A. T. Weber, L. A. Weinert, K. Belkhir, N. Bierne, S. Glémin, and N. Galtier. 2014. Comparative population genomics in animals uncovers the determinants of genetic diversity. Nature 515:261–263.

Ronce, O. 2007. How Does It Feel to Be Like a Rolling Stone? Ten Questions About Dispersal Evolution. Annu. Rev. Ecol. Evol. Syst. 38:231–253.

Rousset, F. 1997. Genetic differentiation and estimation of gene flow from F-statistics under isolation by distance. Genetics 145:1219–1228.

Ruegg, K., R. A. Bay, E. C. Anderson, J. F. Saracco, R. J. Harrigan, M. Whitfield, E. H. Paxton, and T. B. Smith. 2018. Ecological genomics predicts climate vulnerability in an endangered southwestern songbird. Ecol. Lett. 21:1085–1096.

Ruegg, K. C., E. C. Anderson, K. L. Paxton, V. Apkenas, S. Lao, R. B. Siegel, D. F. DeSante, F. Moore, and T. B. Smith. 2014. Mapping migration in a songbird using high-resolution genetic markers. Mol. Ecol. 23:5726–5739.

Ruegg, K. C., and T. B. Smith. 2002. Not as the crow flies: A historical explanation for circuitous migration in Swainson's thrush (Catharus ustulatus). Proc. R. Soc. B Biol. Sci. 269:1375–1381.

Rundle, S. D., D. T. Bilton, J. C. Abbott, and A. Foggo. 2007. Range size in North American Enallagma damselflies correlates with wing size. Freshw. Biol. 52:471–477.

Salisbury, C. L., N. Seddon, C. R. Cooney, and J. A. Tobias. 2012. The latitudinal gradient in dispersal constraints: Ecological specialisation drives diversification in tropical birds. Ecol. Lett. 15:847–855.

Sanín, C., and R. P. Anderson. 2018. A framework for simultaneous tests of abiotic, biotic, and historical drivers of species distributions: Empirical tests for north american wood warblers

based on climate and pollen. Am. Nat. 192:E48–E61.

Schmaljohann, H., M. Buchmann, J. W. Fox, and F. Bairlein. 2012. Tracking migration routes and the annual cycle of a trans-Sahara songbird migrant. Behav. Ecol. Sociobiol. 66:915–922.

Schubert, M., S. Lindgreen, and L. Orlando. 2016. AdapterRemoval v2: rapid adapter trimming, identification, and read merging. BMC Res. Notes 9:1–7. BioMed Central.

Schweizer, T., M. G. DeSaix, and K. C. Ruegg. 2021. LI-Seq: A Cost-Effective, Low Input DNA method for Whole Genome Library Preparation. bioRxiv, doi: https://doi.org/10.1101/2021.07.06.451326.

Scoble, J., and A. J. Lowe. 2010. A case for incorporating phylogeography and landscape genetics into species distribution modelling approaches to improve climate adaptation and conservation planning. Divers. Distrib. 16:343–353.

Serre, D., and S. Pääbo. 2004. Evidence for gradients of human genetic diversity within and among continents. Genome Res. 14:1679–1685.

Sexton, J. P., P. J. McIntyre, A. L. Angert, and K. J. Rice. 2009. Evolution and Ecology of Species Range Limits. Annu. Rev. Ecol. Evol. Syst. 40:415–436.

Shafir, A., D. Azouri, E. E. Goldberg, and I. Mayrose. 2020. Heterogeneity in the rate of molecular sequence evolution substantially impacts the accuracy of detecting shifts in diversification rates. Evolution 74:1620–1639.

Sheard, C., M. H. C. Neate-Clegg, N. Alioravainen, S. E. I. Jones, C. Vincent, H. E. A. MacGregor, T. P. Bregman, S. Claramunt, and J. A. Tobias. 2020. Ecological drivers of global gradients in avian dispersal inferred from wing morphology. Nat. Commun. 11. Springer US.

Shen, Y. Y., P. Shi, Y. B. Sun, and Y. P. Zhang. 2009. Relaxation of selective constraints on avian mitochondrial DNA following the degeneration of flight ability. Genome Res. 19:1760–1765.

Shirk, A. J., D. O. Wallin, S. A. Cushman, C. G. Rice, and K. I. Warheit. 2010. Inferring landscape effects on gene flow: A new model selection framework. Mol. Ecol. 19:3603–3619.

Sibly, R. M., C. C. Witt, N. A. Wright, C. Venditti, W. Jetz, and J. H. Brown. 2012. Energetics, lifestyle, and reproduction in birds. Proc. Natl. Acad. Sci. U. S. A. 109:10937–10941.

Singhal, S., G. R. Colli, M. R. Grundler, G. C. Costa, I. Prates, and D. L. Rabosky. 2022. No link between population isolation and speciation rate in squamate reptiles. Proc. Natl. Acad. Sci. U. S. A. 119.

Singhal, S., H. Huang, M. R. Grundler, M. R. Marchán-Rivadeneira, I. Holmes, P. O. Title, S. C. Donnellan, and D. L. Rabosky. 2018. Does population structure predict rate of speciation? A comparative test across Australia's most diverse vertebrate radiation. Am. Nat. 192.

Skrip, M. M., and S. R. McWilliams. 2016. Oxidative balance in birds: An atoms-to-organisms-to-ecology primer for ornithologists. J. F. Ornithol. 87:1–20.

Slatkin, M. 1993. Isolation by Distance in Equilibrium and Non-Equilibrium Populations. Evolution 47:264–279.

Sly, N. D., C. R. Freeman-Gallant, A. E. Henschen, P. Minias, L. A. Whittingham, and P. O. Dunn. 2022. Molecular parallelism in signaling function across different sexually selected ornaments in a warbler. Proc. Natl. Acad. Sci. U. S. A. 119:1–7.

Smith, B. T., J. E. McCormack, A. M. Cuervo, M. J. Hickerson, A. Aleixo, D. A. Cadena, J. Pérez-Emán, C. W. Burney, X. Xie, M. G. Harvey, B. C. Faircloth, T. C. Glenn, E. P.

Derryberry, J. Prejean, S. Fields, and R. T. Brumfield. 2014. The drivers of tropical speciation. Nature 515:406–409.

Smith, B. T., G. F. Seeholzer, M. G. Harvey, A. M. Cuervo, and R. T. Brumfield. 2017. A latitudinal phylogeographic diversity gradient in birds. PLoS Biol. 15:1–24.

Smith, S. A., and M. J. Donoghue. 2008. Rates of molecular evolution are linked to life history in flowering plants. Science 322:86–89.

Smith, T. B., and D. B. Weissman. 2023. Isolation by distance in populations with power-law dispersal. G3 Genes, Genomes, Genet. 13:1–21. Oxford University Press.

Soberón, J., and A. T. Peterson. 2005. Interpretation of Models of Fundamental Ecological Niches and Species ' Distributional Areas. Biodivers. Informatics 2:1–10.

Somveille, M., A. Manica, S. H. M. Butchart, and A. S. L. Rodrigues. 2013. Mapping Global Diversity Patterns for Migratory Birds. PLoS One 8.

Somveille, M., A. Manica, and A. S. L. Rodrigues. 2019. Where the wild birds go: explaining the differences in migratory destinations across terrestrial bird species. Ecography 42:225–236.

Somveille, M., A. S. L. Rodrigues, and A. Manica. 2015. Why do birds migrate? A macroecological perspective. Glob. Ecol. Biogeogr. 24:664–674.

Stearns, S. C. 1983. The Influence of Size and Phylogeny on Patterns of Covariation among Life-History Traits in the Mammals. Oikos 41:173–187.

Stevens, G. C. 1989. The Latitudinal Gradient in Geographical Range: How so Many Species Coexist in the Tropics. Am. Nat. 133:240–256.

Stover, J. P., B. E. Kendall, and R. M. Nisbet. 2014. Consequences of Dispersal Heterogeneity for Population Spread and Persistence. Bull. Math. Biol. 76:2681–2710.

Stralberg, D., S. M. Matsuoka, C. M. Handel, F. K. A. Schmiegelow, A. Hamann, and E. M.

Bayne. 2017. Biogeography of boreal passerine range dynamics in western North America: past, present, and future. Ecography 40:1050–1066.

Strimas-Mackey, M., E. Miller, and W. Hochachka. 2018. auk: eBird Data Extraction and Processing with AWK.

Strohm, J. H. T., R. A. Gwiazdowski, and R. Hanner. 2015. Fast fish face fewer mitochondrial mutations: Patterns of dN/dS across fish mitogenomes. Gene 572:27–34.

Studds, C. E., T. K. Kyser, and P. P. Marra. 2008. Natal dispersal driven by environmental conditions interacting across the annual cycle of a migratory songbird. Proc. Natl. Acad. Sci. U. S. A. 105:2929.

Sukumaran, J., and M. T. Holder. 2010. DendroPy: A Python library for phylogenetic computing. Bioinformatics 26:1569–1571.

Sullivan, B. L., C. L. Wood, M. J. Iliff, R. E. Bonney, D. Fink, and S. Kelling. 2009. eBird: A citizen-based bird observation network in the biological sciences. Biol. Conserv. 142:2282–2292. Elsevier Ltd.

Sun, S., Q. Li, L. Kong, and H. Yu. 2017. Limited locomotive ability relaxed selective constraints on molluscs mitochondrial genomes. Sci. Rep. 7:1–8.

Svenning, J. C., and F. Skov. 2004. Limited filling of the potential range in European tree species. Ecol. Lett. 7:565–573.

Tajima, F. 1989. Statistical method for testing the neutral mutation hypothesis by DNA polymorphism. Genetics 123:585–595.

Therkildsen, N. O., and S. R. Palumbi. 2017. Practical low-coverage genomewide sequencing of hundreds of individually barcoded samples for population and evolutionary genomics in nonmodel species. Mol. Ecol. Resour. 17:194–208.

Thomas, G. W. C., and M. W. Hahn. 2014. The human mutation rate is increasing, even as it slows. Mol. Biol. Evol. 31:253–257.

Thomas, J. A., J. J. Welch, R. Lanfear, and L. Bromham. 2010. A generation time effect on the rate of molecular evolution in invertebrates. Mol. Biol. Evol. 27:1173–1180.

Thomas, J. W., M. Cáceres, J. J. Lowman, C. B. Morehouse, M. E. Short, E. L. Baldwin, D. L. Maney, and C. L. Martin. 2008. The chromosomal polymorphism linked to variation in social behavior in the white-throated sparrow (Zonotrichia albicollis) is a complex rearrangement and suppressor of recombination. Genetics 179:1455–1468.

Thorup, K. 2006. Does the migration programme constrain dispersal and range sizes of migratory birds? J. Biogeogr. 33:1166–1171.

Tian, X., D. Firsanov, Z. Zhang, Y. Cheng, L. Luo, R. Tan, M. Simon, S. Henderson, J. Steffan, J. Tam, K. Zheng, A. Cornwell, A. Johnson, Z. Mao, B. Manta, W. Dang, Z. Zhang, J. Vijg, K. Moody, B. Kennedy, D. Bohmann, and V. N. Gladyshev. 2019. SIRT6 is Responsible for More Efficient DNA Double-Strand Break Repair in Long-Lived Species. Cell 177:622–638.

Tingley, M. W., M. S. Koo, C. Moritz, A. C. Rush, and S. R. Beissinger. 2012. The push and pull of climate change causes heterogeneous shifts in avian elevational ranges. Glob. Chang. Biol. 18:3279–3290.

Tobias, J. A., C. Sheard, A. L. Pigot, and et al. 2022. AVONET : morphological , ecological and geographical data for all birds. Ecol. Lett. 25:581–597.

Toews, D. P. L. 2017. Habitat suitability and the constraints of migration in New World warblers. J. Avian Biol. 48:1614–1623.

Toews, D. P. L., S. A. Taylor, R. Vallender, A. Brelsford, B. G. Butcher, P. W. Messer, and I. J.

Lovette. 2016. Plumage Genes and Little Else Distinguish the Genomes of Hybridizing Warblers. Curr. Biol. 26:2313–2318. Elsevier Ltd.

Turbek, S. P., E. S. C. Scordato, and R. J. Safran. 2018. The Role of Seasonal Migration in Population Divergence and Reproductive Isolation. Trends Ecol. Evol. 33:164–175. Elsevier Ltd.

Uy, J. A. C., D. E. Irwin, and M. S. Webster. 2018. Behavioral isolation and incipient speciation in birds. Annu. Rev. Ecol. Evol. Syst. 49:1–24.

Van der Auwera, G. A., M. O. Carneiro, C. Hartl, R. Poplin, G. del Angel, A. Levy-Moonshine, T. Jordan, K. Shakir, D. Roazen, J. Thibault, E. Banks, K. V. Garimella, D. Altshuler, S. Gabriel, and M. A. DePristo. 2013. From fastQ data to high-confidence variant calls: The genome analysis toolkit best practices pipeline.

van Els, P., C. Cicero, and J. Klicka. 2012. High latitudes and high genetic diversity: Phylogeography of a widespread boreal bird, the gray jay (Perisoreus canadensis). Mol. Phylogenet. Evol. 63:456–465. Elsevier Inc.

van Els, P., G. M. Spellman, B. T. Smith, and J. Klicka. 2014. Extensive gene flow characterizes the phylogeography of a North American migrant bird: Black-headed Grosbeak (Pheucticus melanocephalus). Mol. Phylogenet. Evol. 78:148–159. Elsevier Inc.

Van Strien, M. J., R. Holderegger, and H. J. Van Heck. 2015. Isolation-by-distance in landscapes: Considerations for landscape genetics. Heredity (Edinb). 114:27–37. Nature Publishing Group.

Varpe, Ø. 2017. Life history adaptations to seasonality. Integr. Comp. Biol. 57:943–960.

Verhoeven, M. A., A. H. J. Loonstra, J. C. E. W. Hooijmeijer, J. A. Masero, T. Piersma, and N. R. Senner. 2018. Generational shift in spring staging site use by a long-distance migratory

bird. Biol. Lett. 14:2009–2012.

Vickers, S. H., A. M. A. Franco, and J. J. Gilroy. 2023. Non-reproductive dispersal: an important driver of migratory range dynamics and connectivity. Ecography 1–13.

Wang, R. J., Y. Peña-Garcia, M. G. Bibby, M. Raveendran, R. A. Harris, H. T. Jansen, C. T. Robbins, J. Rogers, J. L. Kelley, and M. W. Hahn. 2022. Examining the Effects of Hibernation on Germline Mutation Rates in Grizzly Bears. Genome Biol. Evol. 14:1–12.

Waples, R. S. 2022. What is Ne, anyway? J. Hered. 113:371–379.

Waples, R. S., G. Luikart, J. R. Faulkner, and D. A. Tallmon. 2013. Simple life-history traits explain key effective population size ratios across diverse taxa. Proc. R. Soc. B Biol. Sci. 280.

Warren, D. L., M. Cardillo, D. F. Rosauer, and D. I. Bolnick. 2014. Mistaking geography for biology: Inferring processes from species distributions. Trends Ecol. Evol. 29:572–580. Elsevier Ltd.

Waters, P. D., H. R. Patel, A. Ruiz-Herrera, L. Alvarez-Gonzalez, N. C. Lister, O. Simakov, T. Ezaz, P. Kaur, C. Frere, F. Grutzner, A. Georges, and J. A. Marshall Graves. 2021. Microchromosomes are building blocks of bird, reptile, and mammal chromosomes. Proc. Natl. Acad. Sci. U. S. A. 118:1–11.

Watterson, G. A. 1975. On the Number of Segregating Sites in Genetical Models without Recombination. Theor. Popul. Biol. 7:256–276.

Weber, J. M. 2009. The physiology of long-distance migration: Extending the limits of endurance metabolism. J. Exp. Biol. 212:593–597.

Weeks, B. C., and S. Claramunt. 2014. Dispersal has inhibited avian diversification in Australasian archipelagoes. Proc. R. Soc. B Biol. Sci. 281.

Weeks, B. C., B. K. O'Brien, J. J. Chu, S. Claramunt, C. Sheard, and J. A. Tobias. 2022. Morphological adaptations linked to flight efficiency and aerial lifestyle determine natal dispersal distance in birds. Funct. Ecol. 1681–1689.

Weir, J. T., and D. Schluter. 2004. Ice sheets promote speciation in boreal birds. Proc. R. Soc. B Biol. Sci. 271:1881–1887.

Wellenreuther, M., and L. Bernatchez. 2018. Eco-Evolutionary Genomics of Chromosomal Inversions. Trends Ecol. Evol. 33:427–440. Elsevier Ltd.

Weller, C., and M. Wu. 2015. A generation-time effect on the rate of molecular evolution in bacteria. Evolution 69:643–652.

White, A. E. 2016. Geographical Barriers and Dispersal Propensity Interact to Limit Range Expansions of Himalayan Birds. Am. Nat. 188:99–112.

White, A. E., K. K. Dey, D. Mohan, M. Stephens, and T. D. Price. 2019. Regional influences on community structure across the tropical-temperate divide. Nat. Commun. 10:1–8. Springer US.

White, C. R., L. A. Alton, C. L. Bywater, E. J. Lombardi, and D. J. Marshall. 2022. Metabolic scaling is the product of life-history optimization. Science 377:834–839.

Whitlock, M. C., and D. E. McCauley. 1999. Indirect measures of gene flow and migration: F(ST) ≠ 1/(4Nm + 1). Heredity (Edinb). 82:117–125.

Williams, T. C., J. M. Williams, P. G. Williams, and P. Stokstad. 2001. Bird migration through a mountain pass studied with high resolution radar, ceilometers, and census. Auk 118:389–403.

Wilson, R. E., S. M. Matsuoka, L. L. Powell, J. A. Johnson, D. W. Demarest, D. Stralberg, and S. A. Sonsthagen. 2021. Implications of historical and contemporary processes on genetic

differentiation of a declining boreal songbird: The rusty blackbird. Diversity 13:1–22. MDPI AG.

Winger, B. M., G. G. Auteri, T. M. Pegan, and B. C. Weeks. 2019. A long winter for the Red Queen: rethinking the evolution of seasonal migration. Biol. Rev. 94:737–752.

Winger, B. M., F. K. Barker, and R. H. Ree. 2014. Temperate origins of long-distance seasonal migration in New World songbirds. Proc. Natl. Acad. Sci. 111:12115–12120.

Winger, B. M., and J. M. Bates. 2015. The tempo of trait divergence in geographic isolation: Avian speciation across the Marañon Valley of Peru. Evolution 69:772–787.

Winger, B. M., I. J. Lovette, and D. W. Winkler. 2012. Ancestry and evolution of seasonal migration in the Parulidae. Proc. R. Soc. B Biol. Sci. 279:610–618.

Winger, B. M., and T. M. Pegan. 2021. Migration distance is a fundamental axis of the slow-fast continuum of life history in boreal birds. Ornithology 138:1–18.

Winker, K. 2010. On the origin of species through heteropatric differentiation: A review and a model of speciation in migratory animals. Ornithol. Monogr. 1–30.

Winkler, D. 2005. How do migration and dispersal interact? Pp. 401–413 *in* Ecology and Evolution of Migration.

Wright, E. S. 2016. Using DECIPHER v2.0 to Analyze Big Biological Sequence Data in R. R J. 8:352–359.

Wright, S. 1969. Evolution and the Genetics of Populations. University of Chicago Press.

Wright, S. 1943. Isolation by distance. Genetics 28.

Wu, F. L., M. Przeworski, P. Moorjani, M. Przeworski, A. I. Strand, L. A. Cox, L. A. Cox, C. Ober, J. D. Wall, A. I. Strand, and P. Moorjani. 2020. A comparison of humans and baboons suggests germline mutation rates do not track cell divisions. PLoS Biol. 18:1–38.

Wynn, J., O. Padget, H. Mouritsen, J. Morford, P. Jaggers, and T. Guilford. 2022. Magnetic stop signs signal a European songbird's arrival at the breeding site after migration. Science 375:446–449.

Zhang, G., C. Li, Q. Li, B. Li, D. M. Larkin, C. Lee, J. F. Storz, A. Antunes, M. J. Greenwold, R. W. Meredith, Y. Zeng, Z. Xiong, S. Liu, L. Zhou, Z. Huang, N. An, J. J. Wang, Q. Zheng, Y. Xiong, G. Wang, B. Wang, J. J. Wang, Y. Fan, R. R. Fonseca, A. Alfaro-núñez, M. Schubert, L. Orlando, T. Mourier, J. T. Howard, and G. Ganapathy. 2014. Comparative genomics reveals insights into avian genome evolution and adaptation. Science 1311–1321.

Zhang, L., X. Dong, X. Tian, M. Lee, J. Ablaeva, D. Firsanov, S. G. Lee, A. Y. Maslov, V. N. Gladyshev, A. Seluanov, V. Gorbunova, and J. Vijg. 2021. Maintenance of genome sequence integrity in long- and short-lived rodent species. Sci. Adv. 7:eabj3284.

Zhao, L., R. Nielsen, and T. S. Korneliussen. 2022. DistAngsd: Fast and Accurate Inference of Genetic Distances for Next-Generation Sequencing Data. Mol. Biol. Evol. 39:1084–1097.

Zuckerberg, B., A. M. Woods, and W. F. Porter. 2009. Poleward shifts in breeding bird distributions in New York State. Glob. Chang. Biol. 15:1866–1883.

Zuur, A. F., E. N. Ieno, and C. S. Elphick. 2010. A protocol for data exploration to avoid common statistical problems. Methods Ecol. Evol. 1:3–14.

Appendices

Appendix A Supplemental Material for Chapter 2

A.1 Table of species used in chapter 2

Appendix Table A.1-1 Species used in chapter 2. This large table is available at http://www.ecography.org/appendix/ecog-05070 as Appendix 1. For each species, we report the AUC of the species distribution model used to calculate range filling, and each of the response and predictor variables used in our main analyses (see Methods). We also indicate which species are endemic to North America (see *Appendix Table A.6-1*).

A.2 Figures showing relationships between range size, migration distance, and latitude

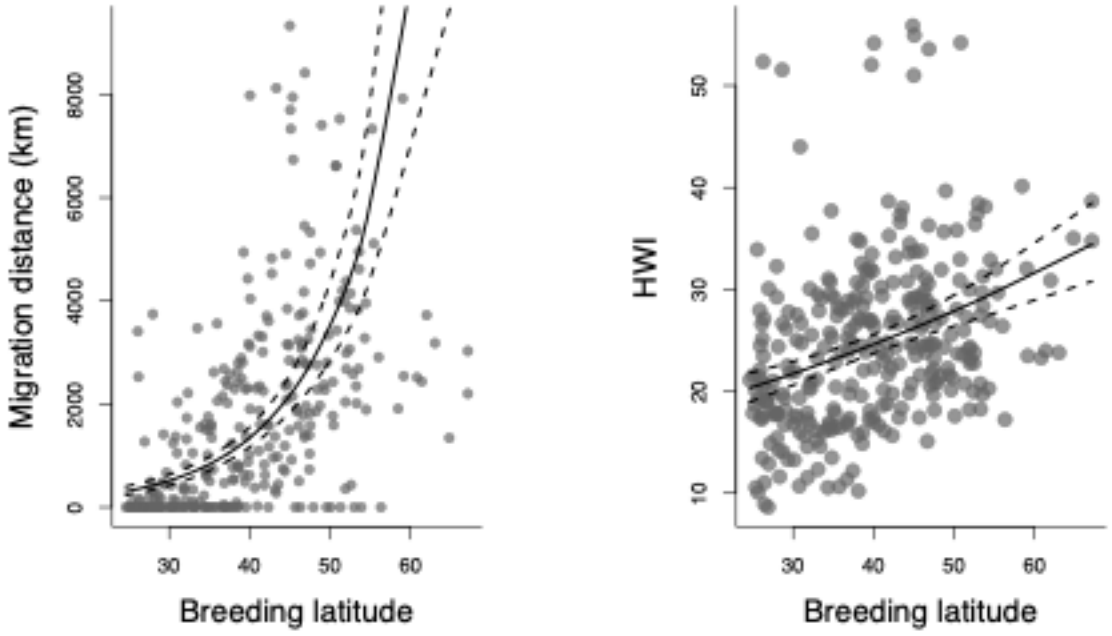

Appendix Figure A.2-1. Migration distance and wing shape are positively correlated with breeding latitude. Each point represents one species. Lines shown with 95% confidence intervals were predicted using a generalized linear model gamma family, log link.

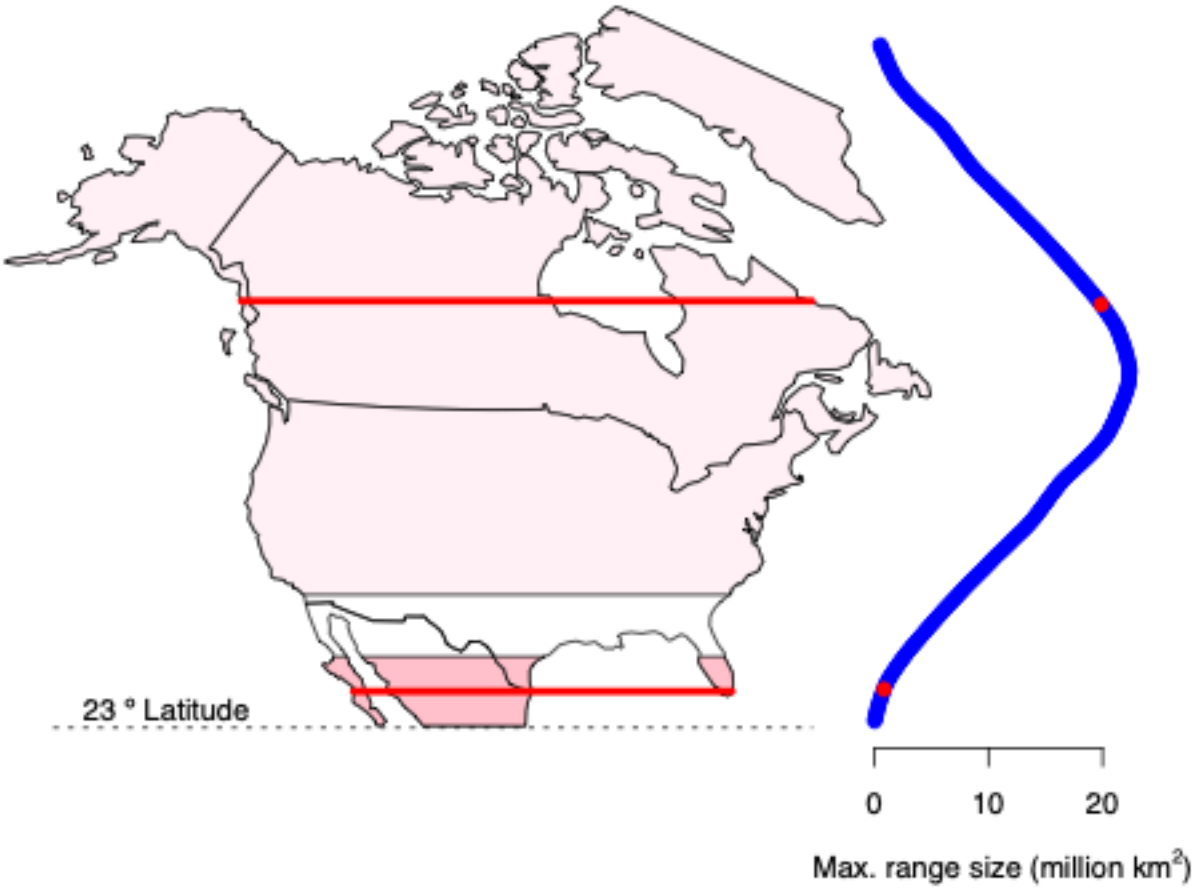

Appendix Figure A.2-2. Maximum attainable range size within our study area depends on latitude. In our main analyses, we use the latitudinal midpoint of species' breeding ranges to capture their latitudinal position and placed the southern bound of the continent at 23º. The bounded nature of our study (and, to a lesser extent, the longitudinal width of the continent) produce a pattern wherein maximum range size is strongly related to latitudinal midpoint. The two horizontal red lines on the map represent examples of latitudinal midpoints of a high latitude species and a low latitude species. By definition, the latitudinal extent of a range can be no more than twice the distance between the midpoint and the closest edge of the bounded region, so the species whose midpoint is close to the edge of the region has a smaller maximum range size (shown in the south in dark pink) than that of the other species, whose midpoint is closer to the middle of the continent (shown in light pink). The corresponding maximum range size at each of these example latitudes is highlighted in red in the plot to the right of the map. All measurements take the curvature of the Earth into account. Map shown in Lambert azimuthal equal area projection.

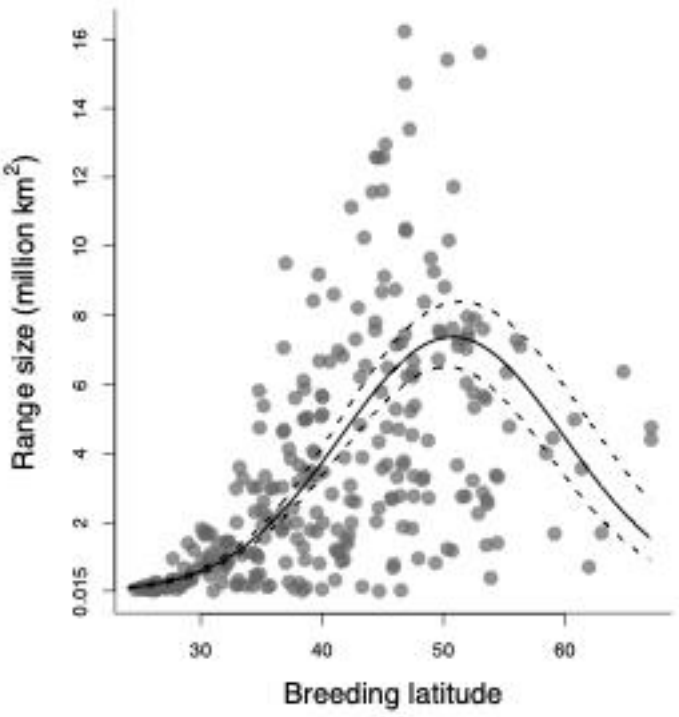

Appendix Figure A.2-3 Range size in our study species shows a hump-shaped relationship with latitude, likely for reasons described in **Error! Reference source not found.**. The line with 95% confidence intervals is predicted from a generalized linear model (gamma family, log link) with latitude as a quadratic predictor. Each point represents one species.

A.3 Detailed species distribution modeling methods

Geographic manipulation of points, geographic range polygons, and species distribution modeling output used the following R packages: *rgdal* (Bivand et al. 2019), *rgeos* (Bivand and Rundel 2019), *geosphere* (Hijmans 2019a), and *raster* (Hijmans 2019b). We transformed all of our geographic data to the Lambert azimuthal equal area projection, which accurately represents area even at high latitudes.

We calculated species distribution models using Maxent as implemented in the R package *maxnet* (Phillips 2017) with some preparatory steps carried out with the package *dismo* (Hijmans et al. 2017). We downloaded presence points for all of our species from the citizen science database eBird (Sullivan et al. 2009) and used the R package *auk* (Strimas-Mackey et al. 2018) to filter the data. Because we were interested in the size of breeding ranges (and not migratory or wintering ranges), we only used presence points recorded in the month of June (from all years in the database). Although some southern non-migratory species may complete breeding by June, these species are present in the same ranges year-round. We removed vagrant or erroneous presence points for each species by including only the eBird presence points that fell within the BirdLife International breeding range polygon for that species. We then spatially thinned the presence points to reduce sampling bias (Kramer-Schadt et al. 2013; Boria et al. 2014) by creating a 20x20 km grid (with a Lambert azimuthal equal area projection) and retained only up to one eBird presence point per 20 by 20 km (400 km^2) grid cell. All of the species listed in the Table A1 had at least 10 presence points from the month of June north of 23º after we removed vagrant records and thinned the data. The number of presence points north of 23º for each species ranged from 10 to 17,892 (mean 2,472, sd 3,418).

The sampling of background points for Maxent models can affect model output (Elith et al. 2010; Barve et al. 2011; Acevedo et al. 2012). We explored two different methods for defining background, each of which reflects a different assumption about the dispersal ability of North American passerines. First, we created Maxent models using 100,000 background points sampled from throughout North America north of 23º for each species (hereafter, "full background"). This method assumes that North American passerines generally have high dispersal ability and have had the opportunity to sample the majority of the continent, and also keeps the background consistent between species. Second, we created Maxent models using up to 100,000 background points sampled from only within each species' breeding range and a 500km buffer around that range (a technique similar to those used by Acevedo et al. 2012, Sanín and Anderson 2018; hereafter, "buffered background"). We did not include any portions of species' ranges or buffered background lying south of 23º. When the buffered background contained fewer than 100,000 raster cells, we drew as many background points as there were cells in the raster (although multiple points can be drawn from within a cell, depending on sampling effort: see below). This method assumes that North American passerines generally have not had the opportunity to disperse more than 500km from their range edges and results in background areas that vary in size depending on the species' breeding range size. In all cases, we sampled these points randomly from the predictor rasters, but we adjusted the probability that a point would be sampled from a given 20 by 20 km cell based on the number of eBird checklists reported from that cell to give the background points the same spatial biases as the presence points. We sampled background points only from terrestrial areas (not from the ocean or lakes). Predicted suitable habitat was projected onto a full raster of North America (north of 23º) regardless of background type.

We compared the results of full vs buffered background on the SDMs and on our downstream analyses of the relationship between migration, wing shape and range filling. The two different background point selection methods produced consistent results: migration and wing shape are not significant predictors of range filling in either case. Species with small ranges were most likely to have large differences between the range filling estimate from a buffered background compared to the estimate from a full background, which is likely related to artifactual effects of the small buffered background used for these species. Because our main analyses focus on comparisons between species, we chose to present results that used the full background method, where a consistent area was used for background point selection for each species.

We used 24 predictor variables for each species: all 19 WorldClim bioclimatic variables (Fick and Hijmans 2017); elevation data; and NDVI data from 2010-2012 and 2014-2015 obtained with the R package *gimms* (Pinzon and Tucker 2014; Detsch 2018). We calculated annual mean, minimum, maximum and range of NDVI and used these four annual metrics as predictor variables. All predictors were in raster format with 3600 columns and 1440 rows and with boundaries at -180º and -30º longitude and 23º and 83º latitude. We converted predictor rasters to the Lambert azimuthal equal area prior to analyses.

We used k-fold data partitioning to split the presence and background points into five groups: four training groups and one testing group (Hijmans et al. 2017). We then extracted climatic and environmental data from our predictor rasters for all background and presence points. After running a Maxent model, we made a raster of climatically suitable habitat area for each species indicating which areas are suitable using the function “threshold” (from the R package *dismo*). This function counts a cell as suitable if its predicted suitability value is as high or higher than

the value of the cells which have the highest sum of the sensitivity (proportion of correctly-predicted presences) and specificity (proportion of correctly-predicted absences) for that model. For a small number of species, the Maxent model failed to converge after the default 200 iterations; we used 400 iterations for these species and all models converged.

A.4 Full model results from main analyses

The effect of the phylogenetic covariance matrix on model results. We tested whether phylogenetic relatedness had an influence on our model results by fitting a full model (i.e. with all predictors) with a phylogenetic covariance matrix and a full model without the matrix using the Bayesian R package *brms* (Bürkner 2017) and comparing the results. As in the main analyses, we centered/standardized predictors with mean=0 and sd=1. Range size is rescaled to be between 1 and 10 and range filling is a proportion. For models of range size, we used the gamma family with a log link and we set the priors for each parameter as a normal distribution with a mean of 0 and standard deviation of 10 (except for the intercept parameter, which we set as a normal distribution with a mean of 0 and a standard deviation of 1). For models of range filling, we used the beta family with a logit link and a log link for the parameter phi, and we set the priors for each parameter as a normal distribution with a mean of 0 and standard deviation of 1. We found that the addition of the phylogenetic covariance matrix had little influence on any of the models' output. This was true both for models of range size and of range filling.

Appendix Table A.4-1. Model results from brms models of range size, using all predictors, fit with a phylogenetic covariance matrix (white rows) and without the matrix (gray rows). Model coefficients were calculated with centered/standardized predictors with mean=0 and sd=1. Range size is rescaled to be between 1 and 10. Rhat=1 indicates that the model converged.

	Estimate	**Est. Error**	**Lower 95% CI**	**Upper 95% CI**	**Rhat**
Intercept	0.92	0.06	0.80	1.04	1.00
Intercept	0.92	0.06	0.81	1.04	1.00

Migratory status	0.02	0.07	-0.12	0.16	1.00
Migratory status	0.02	0.07	-0.13	0.16	1.00
Migration distance	0.01	0.03	-0.05	0.07	1.00
Migration distance	0.01	0.03	-0.05	0.07	1.00
Wing shape	0.05	0.03	-0.01	0.11	1.00
Wing shape	0.05	0.03	-0.01	0.11	1.00
Mass	0.05	0.03	0	0.10	1.00
Mass	0.05	0.03	0	0.10	1.00
Latitude	7.05	0.54	5.98	8.08	1.00
Latitude	7.07	0.56	6.00	8.15	1.00
Latitude^2	-3.77	0.44	-4.62	-2.90	1.00
Latitude^2	-3.79	0.43	-4.63	-2.91	1.00

Appendix Table A.4-2 Model results from brms models of range filling, using all predictors, fit with a phylogenetic covariance matrix (white rows) and without the matrix (gray rows). Model coefficients were calculated with centered/standardized predictors with mean=0 and sd=1. Range filling is a proportion. Rhat=1 indicates that the model converged.

	Estimate	**Est. Error**	**Lower 95% CI**	**Upper 95% CI**	**Rhat**
Intercept	0.85	0.12	0.60	1.10	1.00
Intercept	0.84	0.13	0.58	1.11	1.00
Migratory status	0.17	0.15	-0.12	0.47	1.00
Migratory status	0.17	0.16	-0.15	0.47	1.00
Migration distance	0.09	0.08	-0.06	0.24	1.00
Migration distance	0.09	0.07	-0.06	0.23	1.00
Wing shape	-0.03	0.07	-0.15	0.10	1.00
Wing shape	-0.03	0.07	-0.15	0.10	1.00
Mass	0.08	0.06	-0.03	0.22	1.00
Mass	0.08	0.06	-0.03	0.21	1.00
Latitude	-0.03	0.07	-0.17	0.11	1.00
Latitude	-0.03	0.07	-0.16	0.11	1.00

A.5 Detailed model results from main analyses

Appendix Table A.5-1. Detailed model results from models predicting range size. Model coefficients were calculated with centered/standardized predictors with mean=0 and sd=1. Range size is rescaled to be between 1 and 10.

Predictor	Estimate	Std Error	t value	Pr(>|t|)
Intercept	0.74	0.083	8.93	<0.0001
Migratory status	0.37	0.099	3.75	0.00021
Migration distance	0.15	0.043	3.54	0.0005
Intercept	1.03	0.036	29.00	<0.0001
Wing shape	0.21	0.036	5.78	<0.0001
Mass	0.017	0.036	0.46	0.65
Intercept	0.95	0.024	39.70	<0.0001
Latitude	7.67	0.42	18.40	<0.0001
Latitude^2	-3.97	0.42	-9.52	<0.0001
Intercept	0.93	0.057	16.17	<0.0001
Migratory status	0.017	0.070	0.24	0.81
Migration distance	0.0068	0.033	0.21	0.83
Wing shape	0.051	0.030	1.78	0.076
Mass	0.046	0.026	1.76	0.079
Latitude	7.18	0.51	14.01	<0.0001
Latitude^2	-3.90	0.43	-9.08	<0.0001

Appendix Table A.5-2. Detailed model results from models predicting range filling. Model coefficients were calculated with centered/standardized predictors with mean=0 and sd=1. Range filling is a proportion.

Predictor	Estimate	Std Error	z value	Pr(>|z|)
Intercept	0.90	0.11	7.93	<0.0001
Migratory status	0.12	0.14	0.91	0.36
Migration distance	0.059	0.060	0.98	0.33
Intercept	0.99	0.054	18.42	<0.0001
Wing shape	0.042	0.052	0.82	0.41
Mass	0.031	0.053	0.59	0.56
Intercept	0.99	0.054	18.41	<0.0001
Latitude	0.050	0.051	0.98	0.33
Intercept	0.86	0.12	7.16	<0.0001
Migratory status	0.18	0.15	1.22	0.22
Migration distance	0.092	0.071	1.30	0.19
Wing shape	-0.033	0.062	-0.53	0.60
Mass	0.078	0.058	1.33	0.18
Latitude	-0.028	0.063	-0.44	0.66

A.6 Main analyses repeated with two subsets of the full species list

Appendix Table A.6-1. Comparison of models predicting range size and range filling using only species endemic to North America (ranges are entirely north of 23º latitude). Model coefficients were calculated with centered/standardized predictors with mean=0 and sd=1. Range size is rescaled to be between 1 and 10 and range filling is a proportion. R^2 shown for models of range size are trigamma estimates calculated using the R package *MuMIn*. For models of range filling, we show pseudo R^2 calculated by the R package *betareg*.

Response	Migrat-ory status	Migrat-ion distance	Wing shape	Mass	Latitude	Latitude^2	logLik	AICc	Delta	Weight	R^2
Range size	-	-	-	-	3.84	-2.24	-238.4	485.1	0	0.88	0.40
Range size	0.025	0.068	-0.016	0.08	3.54	-2.06	-236.1	489.1	4.0	0.19	0.41
Range size	0.15	0.14	-	-	-	-	-268.8	545.8	60.8	0	0.10
Range size	-	-	0.14	0.022	-	-	-274.2	556.7	71.6	0	0.045
Range filling	-	-	-	-	- 0.088	-	59.3	-112.5	0	0.57	0.0052
Range filling	0.012	0.070	-	-	-	-	59.4	-110.5	2.03	0.21	0.0066
Range filling	-	-	0.0045	0.058	-	-	59.1	-110.0	2.54	0.16	0.0033
Range filling	0.098	0.16	-0.087	0.13	-0.16	-	61.3	-108.0	4.58	0.06	0.036

Appendix Table A.6-2. Comparison of models predicting range size and range filling using only non-migrants. Model coefficients were calculated with centered/standardized predictors with mean=0 and sd=1. Range size is rescaled to be between 1 and 10 and range filling is a proportion. R^2 shown for models of range size are trigamma estimates calculated using the R package *MuMIn*. For models of range filling, we show pseudo R^2 calculated by the R package *betareg*.

Response	Wing shape	Mass	Latitude	Latitude^2	logLik	AICc	Delta	Weight	R^2
Range size	-	-	4.74	-3.58	-55.8	120.1	0	0.74	0.66
Range size	0.004	0.034	4.92	-3.59	-372.1	122.2	2.16	0.25	0.66
Range size	0.070	0.090	-	-	-428.6	202.3	82.22	0	0.10
Range filling	-	-	0.27	-	32.7	-59.1	0	0.85	0.065
Range filling	-0.081	0.0032	0.29	-	33.0	-55.2	3.95	0.12	0.0081
Range filling	-0.062	0.049	-	-	30.4	-52.2	6.91	0.03	0.071

Appendix B Supplemental Material for Chapter 3

B.1 Additional bioinformatic metadata

Appendix Table B.1-1. Species used in this study are presented with bioinformatic metadata, including details about reference genomes, mean mapping rate (i.e. rate of alignment to the reference genome by bwa-mem), and mean depth of coverage. The final five columns describe the number of loci in each dataset for each species. The total number of SNPs identified by ANGSD is shown in "Raw SNP number," and the next two columns indicate the number of SNPs remaining after filters were applied based on ngsParalog and putative inversion clustering, respectively. The number of SNPs used in analyses is shown in "SNPs after inversion filter." The final two columns give the size of the subsampled datasets used for calculating summary statistics, which include both SNPs and invariant sites.

Species	Reference genome GenBank assembly	Reference genome associated publication	Assembly level	Reference genome species	Mean map rate	Mean depth of coverage	Raw SNP number	SNPs after ngs Paralog	SNPs after inversion filter	Subsample, genetic distance	Sub-sample, Fst and θ_π
Picoides arcticus	GCA_014839835.1	Zhang et al 2014	Chromo-some	*Picoides pubescens*	0.95	4	12056881	10881723	9325085	2804131	27188828
Dryobates villosus	GCA_014839835.1	Zhang et al 2014	Chromo-some	*Picoides pubescens*	0.95	3.6	21727984	20526591	17720295	2733354	26239950
Sphyrapicus varius	GCA_014839835.1	Zhang et al 2014	Chromo-some	*Picoides pubescens*	0.91	3.5	22941999	20830084	15445280	2361400	22992060
Empidonax alnorum	GCF_003031625.1	Ruegg et al 2018	Scaffold	*Empidonax traillii*	0.95	4	32264867	31372546	13932313	1673806	14836614
Empidonax flaviventris	GCF_003031625.1	Ruegg et al 2018	Scaffold	*Empidonax traillii*	0.95	4.2	24243976	23151566	8552886	1461399	12924657
Empidonax minimus	GCF_003031625.1	Ruegg et al 2018	Scaffold	*Empidonax traillii*	0.93	4.5	31182957	30107477	12927246	1659534	14875454
Vireo olivaceus	GCA_013396875.1	Feng et al 2020	Scaffold	*Vireo altiloquus*	0.92	3.3	36668099	36668099	10922102	1217856	10656866
Vireo philadelphicus	GCA_013396875.1	Feng et al 2020	Scaffold	*Vireo altiloquus*	0.93	5.1	31473620	30901578	9298677	1229383	10748633
Vireo solitarius	GCA_013396875.1	Feng et al 2020	Scaffold	*Vireo altiloquus*	0.9	3.3	20958533	19987935	5229041	1211061	10675151
Poecile atricapillus	GCA_001522545.3	Laine et al 2016	Chromo-some	*Parus major*	0.91	3.8	20545862	19505859	17248392	2341066	22955650
Poecile hudsonicus	GCA_001522545.3	Laine et al 2016	Chromo-some	*Parus major*	0.9	3.4	13482980	12739724	9578889	2086503	20256005
Corthylio calendula	GCA_013396955.1	Feng et al 2020	Scaffold	*Regulus satrapa*	0.9	3.8	21399431	21399174	3483471	518000	4420000

Regulus satrapa	GCA_013396955.1	Feng et al 2020	Scaffold	*Regulus satrapa*	0.92	4.2	21812486	21272531	3587975	551960	4878740
Certhia americana	GCA_018697195.1	Manthey et al 2021	Chromo-some	*Certhia americana*	0.95	4.1	14722943	13937070	11338226	2814686	26982445
Troglodytes hiemalis	GCA_013397245.1	Feng et al 2020	Scaffold	*Thryothorus ludovicianus*	0.91	3.7	21239634	20823812	4792113	797988	6988890
Catharus fuscescens	GCA_009819885.2	NA	Chromo-some	*Catharus ustulatus*	0.96	4.7	47549705	45435269	35677180	2402625	23280960
Catharus guttatus	GCA_009819885.2	NA	Chromo-some	*Catharus ustulatus*	0.94	3.7	27609103	25820254	23301650	2746706	26415709
Catharus ustulatus	GCA_009819885.2	NA	Chromo-some	*Catharus ustulatus*	0.96	3.8	38764475	37007330	32394561	2670000	25633393
Junco hyemalis	GCA_003829775.2	Friis et al 2022	Chromo-some	*Junco hyemalis*	0.94	5.1	15372806	13808922	11889443	2401187	23144538
Melospiza lincolnii	GCA_003829775.2	Friis et al 2022	Chromo-some	*Junco hyemalis*	0.91	4.1	31139305	29362108	23709552	2226036	21362385
Zonotrichia albicollis	GCA_003829775.2	Friis et al 2022	Chromo-some	*Junco hyemalis*	0.93	4.5	17737289	16507633	11851497	1802411	17606683
Cardellina canadensis	GCA_001746935.2	Toews et al 2016	Chromo-some	*Setophaga coronata*	0.81	4.3	31263642	30389157	24179480	2052000	19932143
Geothlypis philadelphia	GCA_009764595.1	Sly et al 2022	Chromo-some	*Geothlypis trichas*	0.86	4	41705964	39350849	33930269	2356114	23009330
Oporornis agilis	GCA_009764595.1	Sly et al 2022	Chromo-some	*Geothlypis trichas*	0.86	4.1	43492691	41633829	35593575	2363437	23206827
Leiothlypis peregrina	GCA_001746935.2	Toews et al 2016	Chromo-some	*Setophaga coronata*	0.82	3.2	38601252	37772294	32637118	2377809	22784790
Leiothlypis ruficapilla	GCA_001746935.2	Toews et al 2016	Chromo-some	*Setophaga coronata*	0.82	3.1	21604171	20649668	17403822	2292913	22119717
Setophaga castanea	GCA_001746935.2	Toews et al 2016	Chromo-some	*Setophaga coronata*	0.81	3.2	35522605	34727422	28526191	2149058	20905308
Setophaga coronata	GCA_001746935.2	Toews et al 2016	Chromo-some	*Setophaga coronata*	0.86	3.2	22794604	21926073	18673928	2338926	22551104
Setophaga fusca	GCA_001746935.2	Toews et al 2016	Chromo-some	*Setophaga coronata*	0.85	3.1	34851489	34112569	30620914	2389366	23386491
Setophaga magnolia	GCA_001746935.2	Toews et al 2016	Chromo-some	*Setophaga coronata*	0.82	3.9	34698342	33593437	30025527	2362767	23209897
Setophaga palmarum	GCA_001746935.2	Toews et al 2016	Chromo-some	*Setophaga coronata*	0.86	3.9	26951076	26001331	23008752	2408310	23274551
Setophaga pensylvanica	GCA_001746935.2	Toews et al 2016	Chromo-some	*Setophaga coronata*	0.8	3.6	35898041	34999133	30693752	2371560	22830485
Setophaga tigrina	GCA_001746935.2	Toews et al 2016	Chromo-some	*Setophaga coronata*	0.84	3.7	22413208	22407383	20673474	2495993	24239479
Setophaga virens	GCA_001746935.2	Toews et al 2016	Chromo-some	*Setophaga coronata*	0.86	4.1	14938759	13746372	12214860	2417412	23127715

Appendix Table B.1-2. A list of regions (chromosomes or scaffolds) filtered out of the dataset due to evidence of putative inversion polymorphisms. Microchromosomes and scaffolds (as indicated by "Region type") were entirely discarded. When possible, we removed putative inversion regions from macrochromosomes while leaving the remaining parts of the chromosome in the dataset. "Filter start" and "Filter end" columns show genome coordinates

filtered out of macrochromosomes. When the affected region was too large or poorly defined to allow confidence in the location of the putatively inverted region, we discarded the entire macrochromosome.

Species	Region name (GenBank accession)	Region type	Filter start	Filter end
Dryobates villosus	CM026011.1	Micro		
Sphyrapicus varius	CM025994.1	Macro	40000000	50000000
Sphyrapicus varius	CM025996.1	Macro	Affected region too large to filter	
Sphyrapicus varius	CM026000.1	Macro	10000000	30000000
Sphyrapicus varius	CM026003.1	Macro	Affected region too large to filter	
Sphyrapicus varius	CM026013.1	Micro		
Sphyrapicus varius	CM026025.1	Micro		
Empidonax alnorum	NW_020955207.1	Scaffold		
Empidonax alnorum	NW_020955239.1	Scaffold		
Empidonax alnorum	NW_020955251.1	Scaffold		
Empidonax alnorum	NW_020955278.1	Scaffold		
Empidonax alnorum	NW_020955314.1	Scaffold		
Empidonax alnorum	NW_020955356.1	Scaffold		
Empidonax alnorum	NW_020955369.1	Scaffold		
Empidonax alnorum	NW_020955396.1	Scaffold		
Empidonax alnorum	NW_020955429.1	Scaffold		
Empidonax alnorum	NW_020955664.1	Scaffold		
Empidonax alnorum	NW_020955753.1	Scaffold		
Empidonax flaviventris	NW_020955202.1	Scaffold		
Empidonax flaviventris	NW_020955214.1	Scaffold		
Empidonax flaviventris	NW_020955239.1	Scaffold		
Empidonax flaviventris	NW_020955241.1	Scaffold		
Empidonax flaviventris	NW_020955253.1	Scaffold		
Empidonax flaviventris	NW_020955254.1	Scaffold		

Empidonax flaviventris	NW_020955261.1	Scaffold		
Empidonax flaviventris	NW_020955271.1	Scaffold		
Empidonax flaviventris	NW_020955272.1	Scaffold		
Empidonax flaviventris	NW_020955278.1	Scaffold		
Empidonax flaviventris	NW_020955281.1	Scaffold		
Empidonax flaviventris	NW_020955285.1	Scaffold		
Empidonax flaviventris	NW_020955287.1	Scaffold		
Empidonax flaviventris	NW_020955291.1	Scaffold		
Empidonax flaviventris	NW_020955293.1	Scaffold		
Empidonax flaviventris	NW_020955305.1	Scaffold		
Empidonax flaviventris	NW_020955306.1	Scaffold		
Empidonax flaviventris	NW_020955308.1	Scaffold		
Empidonax flaviventris	NW_020955312.1	Scaffold		
Empidonax flaviventris	NW_020955314.1	Scaffold		
Empidonax flaviventris	NW_020955316.1	Scaffold		
Empidonax flaviventris	NW_020955318.1	Scaffold		
Empidonax flaviventris	NW_020955329.1	Scaffold		
Empidonax flaviventris	NW_020955330.1	Scaffold		
Empidonax flaviventris	NW_020955337.1	Scaffold		
Empidonax flaviventris	NW_020955347.1	Scaffold		
Empidonax flaviventris	NW_020955356.1	Scaffold		
Empidonax flaviventris	NW_020955358.1	Scaffold		
Empidonax flaviventris	NW_020955360.1	Scaffold		
Empidonax flaviventris	NW_020955363.1	Scaffold		
Empidonax flaviventris	NW_020955369.1	Scaffold		
Empidonax flaviventris	NW_020955379.1	Scaffold		

Empidonax flaviventris	NW_020955380.1	Scaffold		
Empidonax flaviventris	NW_020955382.1	Scaffold		
Empidonax flaviventris	NW_020955389.1	Scaffold		
Empidonax flaviventris	NW_020955391.1	Scaffold		
Empidonax flaviventris	NW_020955396.1	Scaffold		
Empidonax flaviventris	NW_020955398.1	Scaffold		
Empidonax flaviventris	NW_020955408.1	Scaffold		
Empidonax flaviventris	NW_020955409.1	Scaffold		
Empidonax flaviventris	NW_020955418.1	Scaffold		
Empidonax flaviventris	NW_020955424.1	Scaffold		
Empidonax flaviventris	NW_020955425.1	Scaffold		
Empidonax flaviventris	NW_020955429.1	Scaffold		
Empidonax flaviventris	NW_020955431.1	Scaffold		
Empidonax flaviventris	NW_020955433.1	Scaffold		
Empidonax flaviventris	NW_020955437.1	Scaffold		
Empidonax flaviventris	NW_020955440.1	Scaffold		
Empidonax flaviventris	NW_020955442.1	Scaffold		
Empidonax flaviventris	NW_020955457.1	Scaffold		
Empidonax flaviventris	NW_020955458.1	Scaffold		
Empidonax flaviventris	NW_020955461.1	Scaffold		
Empidonax flaviventris	NW_020955474.1	Scaffold		
Empidonax flaviventris	NW_020955503.1	Scaffold		
Empidonax flaviventris	NW_020955505.1	Scaffold		
Empidonax flaviventris	NW_020955506.1	Scaffold		
Empidonax flaviventris	NW_020955507.1	Scaffold		
Empidonax flaviventris	NW_020955524.1	Scaffold		

Empidonax flaviventris	NW_020955566.1	Scaffold		
Empidonax flaviventris	NW_020955579.1	Scaffold		
Empidonax flaviventris	NW_020955589.1	Scaffold		
Empidonax flaviventris	NW_020955604.1	Scaffold		
Empidonax flaviventris	NW_020955616.1	Scaffold		
Empidonax flaviventris	NW_020955664.1	Scaffold		
Empidonax flaviventris	NW_020955697.1	Scaffold		
Empidonax flaviventris	NW_020955753.1	Scaffold		
Empidonax minimus	NW_020955202.1	Scaffold		
Empidonax minimus	NW_020955203.1	Scaffold		
Empidonax minimus	NW_020955207.1	Scaffold		
Empidonax minimus	NW_020955210.1	Scaffold		
Empidonax minimus	NW_020955212.1	Scaffold		
Empidonax minimus	NW_020955214.1	Scaffold		
Empidonax minimus	NW_020955223.1	Scaffold		
Empidonax minimus	NW_020955228.1	Scaffold		
Empidonax minimus	NW_020955234.1	Scaffold		
Empidonax minimus	NW_020955239.1	Scaffold		
Empidonax minimus	NW_020955257.1	Scaffold		
Empidonax minimus	NW_020955261.1	Scaffold		
Empidonax minimus	NW_020955271.1	Scaffold		
Empidonax minimus	NW_020955272.1	Scaffold		
Empidonax minimus	NW_020955274.1	Scaffold		
Empidonax minimus	NW_020955278.1	Scaffold		
Empidonax minimus	NW_020955281.1	Scaffold		
Empidonax minimus	NW_020955289.1	Scaffold		

Empidonax minimus	NW_020955290.1	Scaffold		
Empidonax minimus	NW_020955308.1	Scaffold		
Empidonax minimus	NW_020955313.1	Scaffold		
Empidonax minimus	NW_020955314.1	Scaffold		
Empidonax minimus	NW_020955316.1	Scaffold		
Empidonax minimus	NW_020955321.1	Scaffold		
Empidonax minimus	NW_020955324.1	Scaffold		
Empidonax minimus	NW_020955327.1	Scaffold		
Empidonax minimus	NW_020955356.1	Scaffold		
Empidonax minimus	NW_020955369.1	Scaffold		
Empidonax minimus	NW_020955396.1	Scaffold		
Empidonax minimus	NW_020955410.1	Scaffold		
Empidonax minimus	NW_020955416.1	Scaffold		
Empidonax minimus	NW_020955425.1	Scaffold		
Empidonax minimus	NW_020955429.1	Scaffold		
Empidonax minimus	NW_020955440.1	Scaffold		
Empidonax minimus	NW_020955458.1	Scaffold		
Empidonax minimus	NW_020955477.1	Scaffold		
Empidonax minimus	NW_020955550.1	Scaffold		
Empidonax minimus	NW_020955566.1	Scaffold		
Empidonax minimus	NW_020955577.1	Scaffold		
Empidonax minimus	NW_020955616.1	Scaffold		
Empidonax minimus	NW_020955664.1	Scaffold		
Empidonax minimus	NW_020955720.1	Scaffold		
Empidonax minimus	NW_020955753.1	Scaffold		
Empidonax minimus	NW_020955927.1	Scaffold		
Vireo olivaceus	VZRF01012750.1	Scaffold		

Poecile atricapillus	CM003714.1	Macro	55000000	71365269 (chromosome end)
Poecile atricapillus	CM003715.1	Macro	1	20000000
Poecile atricapillus	CM003717.2	Macro	1	10000000
Poecile atricapillus	CM003722.1	Micro		
Poecile hudsonicus	CM003709.1	Macro	80000000	101000000
Poecile hudsonicus	CM003711.1	Macro	1	60000000
Poecile hudsonicus	CM003714.1	Macro	50000000	71365269 (chromosome end)
Poecile hudsonicus	CM003715.1	Macro	1	20000000
Poecile hudsonicus	CM003718.2	Micro		
Corthylio calendula	VWZN01001582.1	Scaffold		
Corthylio calendula	VWZN01002012.1	Scaffold		
Corthylio calendula	VWZN01003768.1	Scaffold		
Corthylio calendula	VWZN01003785.1	Scaffold		
Corthylio calendula	VWZN01014447.1	Scaffold		
Corthylio calendula	VWZN01016700.1	Scaffold		
Corthylio calendula	VWZN01017393.1	Scaffold		
Corthylio calendula	VWZN01018494.1	Scaffold		
Corthylio calendula	VWZN01021048.1	Scaffold		
Regulus satrapa	VWZN01013934.1	Scaffold		
Regulus satrapa	VWZN01015879.1	Scaffold		
Regulus satrapa	VWZN01022086.1	Scaffold		
Troglodytes hiemalis	VZTB01003382.1	Scaffold		
Troglodytes hiemalis	VZTB01004761.1	Scaffold		
Troglodytes hiemalis	VZTB01010552.1	Scaffold		
Troglodytes hiemalis	VZTB01013914.1	Scaffold		
Catharus fuscescens	CM020338.1	Macro	1	2000000
Catharus fuscescens	CM020341.1	Macro	1	2000000
Catharus fuscescens	CM020345.1	Micro		
Catharus fuscescens	CM020348.1	Micro		

Catharus fuscescens	CM020349.1	Micro		
Catharus fuscescens	CM020351.1	Micro		
Catharus fuscescens	CM020353.1	Micro		
Catharus fuscescens	CM020358.1	Micro		
Catharus fuscescens	CM020360.1	Micro		
Catharus fuscescens	CM020361.1	Micro		
Catharus fuscescens	CM020365.1	Micro		
Catharus fuscescens	CM020367.1	Micro		
Catharus fuscescens	CM020368.1	Micro		
Catharus fuscescens	CM020369.1	Micro		
Catharus fuscescens	CM020371.1	Micro		
Catharus fuscescens	CM020372.1	Micro		
Catharus guttatus	CM020339.1	Macro	70000000	77026709 (chromosome end)
Catharus guttatus	CM020365.1	Micro		
Catharus guttatus	CM020367.1	Micro		
Catharus guttatus	CM020368.1	Micro		
Catharus guttatus	CM020369.1	Micro		
Catharus guttatus	CM020371.1	Micro		
Catharus guttatus	CM020372.1	Micro		
Catharus guttatus	CM020374.1	Micro		
Catharus ustulatus	CM020344.1	Micro		
Catharus ustulatus	CM020358.1	Micro		
Catharus ustulatus	CM020365.1	Micro		
Catharus ustulatus	CM020367.1	Micro		
Catharus ustulatus	CM020368.1	Micro		
Catharus ustulatus	CM020371.1	Micro		
Catharus ustulatus	CM020372.1	Micro		
Junco hyemalis	CM042576.1	Macro	10000000	40000000
Junco hyemalis	CM042579.1	Macro	1	30000000
Junco hyemalis	CM042598.1	Micro		
Melospiza lincolnii	CM042577.1	Macro	20000000	40000000
Melospiza lincolnii	CM042579.1	Macro	Affected region too large to filter	

Melospiza lincolnii	CM042581.1	Macro	Affected region too large to filter	
Melospiza lincolnii	CM042598.1	Micro		
Zonotrichia albicollis	CM042573.1	Macro	Affected region too large to filter	
Zonotrichia albicollis	CM042576.1	Macro	Affected region too large to filter	
Zonotrichia albicollis	CM042585.1	Micro		
Zonotrichia albicollis	CM042590.1	Micro		
Zonotrichia albicollis	CM042595.1	Micro		
Zonotrichia albicollis	CM042598.1	Micro		
Zonotrichia albicollis	CM042600.1	Micro		
Cardellina canadensis	CM027510.1	Macro	Affected region too large to filter	
Cardellina canadensis	CM027511.1	Macro	Affected region too large to filter	
Cardellina canadensis	CM027517.1	Micro		
Cardellina canadensis	CM027521.1	Micro		
Cardellina canadensis	CM027530.1	Micro		
Cardellina canadensis	CM027532.1	Micro		
Cardellina canadensis	CM027534.1	Micro		
Geothlypis philadelphia	CM019902.1	Macro	95000000	116842828 (chromosome end)
Geothlypis philadelphia	CM019903.1	Macro	15000000	50000000
Geothlypis philadelphia	CM019906.1	Macro	1	28000000
Geothlypis philadelphia	CM019911.1	Micro		
Geothlypis philadelphia	CM019926.1	Micro		
Geothlypis philadelphia	CM019929.1	Micro		
Geothlypis philadelphia	CM019931.1	Micro		

Geothlypis philadelphia	CM019932.1	Micro		
Leiothlypis peregrina	CM027511.1	Macro	Affected region too large to filter	
Leiothlypis peregrina	CM027512.1	Macro	1	5000000
Leiothlypis peregrina	CM027528.1	Micro		
Leiothlypis peregrina	CM027530.1	Micro		
Leiothlypis peregrina	CM027532.1	Micro		
Leiothlypis peregrina	CM027534.1	Micro		
Leiothlypis ruficapilla	CM027508.1	Macro	50000000	60000000
Leiothlypis ruficapilla	CM027510.1	Macro	60000000	70957965 (chromosome end)
Leiothlypis ruficapilla	CM027512.1	Macro	1	5000000
Leiothlypis ruficapilla	CM027513.1	Macro	30000000	38264695 (chromosome end)
Leiothlypis ruficapilla	CM027514.1	Micro		
Leiothlypis ruficapilla	CM027518.1	Micro		
Leiothlypis ruficapilla	CM027528.1	Micro		
Leiothlypis ruficapilla	CM027530.1	Micro		
Leiothlypis ruficapilla	CM027531.1	Micro		
Leiothlypis ruficapilla	CM027532.1	Micro		
Leiothlypis ruficapilla	CM027534.1	Micro		
Oporornis agilis	CM019902.1	Macro	100000000	116842828 (chromosome end)
Oporornis agilis	CM019906.1	Macro	40000000	63300891 (chromosome end)
Oporornis agilis	CM019912.1	Micro		
Oporornis agilis	CM019921.1	Micro		
Oporornis agilis	CM019929.1	Micro		
Setophaga castanea	CM027508.1	Macro	40000000	60000000
Setophaga castanea	CM027510.1	Macro	60000000	70957965 (chromosome end)

Setophaga castanea	CM027511.1	Macro	Affected region too large to filter	
Setophaga castanea	CM027512.1	Macro	1	10000000
Setophaga castanea	CM027513.1	Macro	30000000	38264695 (chromosome end)
Setophaga castanea	CM027518.1	Micro		
Setophaga castanea	CM027530.1	Micro		
Setophaga castanea	CM027532.1	Micro		
Setophaga castanea	CM027534.1	Micro		
Setophaga coronata	CM027507.1	Macro	65000000	100000000
Setophaga coronata	CM027508.1	Macro	40000000	60000000
Setophaga coronata	CM027510.1	Macro	1	15000000
Setophaga coronata	CM027530.1	Micro		
Setophaga coronata	CM027532.1	Micro		
Setophaga fusca	CM027508.1	Macro	40000000	60000000
Setophaga fusca	CM027510.1	Macro	1	15000000
Setophaga fusca	CM027530.1	Micro		
Setophaga fusca	CM027532.1	Micro		
Setophaga fusca	CM027534.1	Micro		
Setophaga magnolia	CM027508.1	Macro	30000000	70000000
Setophaga magnolia	CM027530.1	Micro		
Setophaga magnolia	CM027532.1	Micro		
Setophaga magnolia	CM027534.1	Micro		
Setophaga palmarum	CM027510.1	Macro	1	40000000
Setophaga palmarum	CM027530.1	Micro		
Setophaga palmarum	CM027532.1	Micro		
Setophaga pensylvanica	CM027507.1	Macro	100000000	114062283 (chromosome end)
Setophaga pensylvanica	CM027508.1	Macro	40000000	60000000

Setophaga pensylvanica	CM027513.1	Macro	33000000	38264695 (chromosome end)
Setophaga pensylvanica	CM027530.1	Micro		
Setophaga pensylvanica	CM027532.1	Micro		
Setophaga pensylvanica	CM027534.1	Micro		
Setophaga pensylvanica	CM027536.1	Macro	45000000	60000000
Setophaga tigrina	CM027530.1	Micro		
Setophaga tigrina	CM027532.1	Micro		
Setophaga tigrina	CM027534.1	Micro		
Setophaga virens	CM027508.1	Macro	40000000	60000000
Setophaga virens	CM027530.1	Micro		
Setophaga virens	CM027532.1	Micro		
Setophaga virens	CM027534.1	Micro		
Setophaga virens	CM027537.1	Micro		

B.2 Supplemental figures for chapter 3

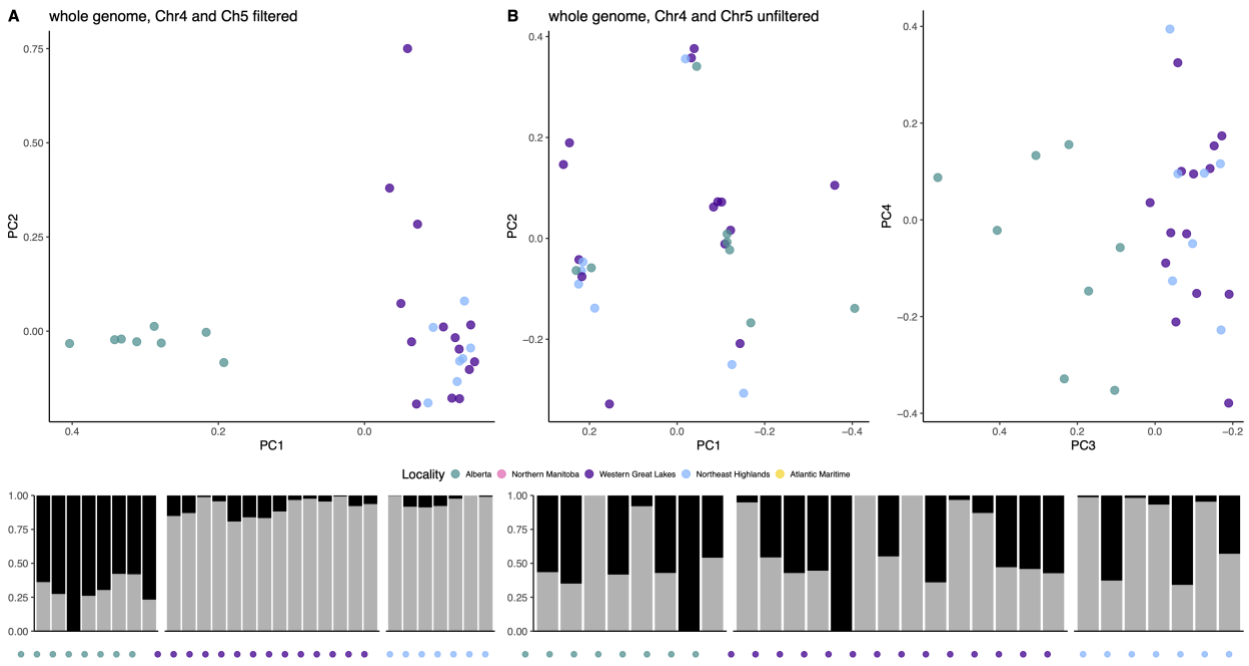

Appendix Figure B.2-1. PCA and admixture plots demonstrate the influence of chromosomes with putative inversion polymorphisms in an example species, *Cardellina canadensis*. In this species, chromosomes 4 and 5 demonstrate clustering patterns potentially caused by inversion polymorphisms. When chromosomes 4 and 5 are filtered as described in the methods section to remove a putative inversion polymorphism (A), a relatively strong geographic pattern is evident on PC1 and on the admixture plot, where samples are ordered by longitude. When chromosomes 4

and 5 are present in their entirety (B), PC1 and PC2 each capture structure from the putative inversion polymorphisms on each of these chromosomes, clustering points into a 3-by-3 grid (B, left PCA). The grid appears to reflect inversion genotypes—homozygous major, heterozygous, homozygous minor—in all possible combinations for chromosomes 4 and 5 on PC1 and PC2, except that we have no individuals with one of the genotype combinations (empty upper right corner of the grid). Geographic structure is evident on PC3 in this case (B, right PCA plot), albeit more subtly than shown in (A). The admixture plot made using the unfiltered dataset also reflects putative inversion genotype rather than geography.

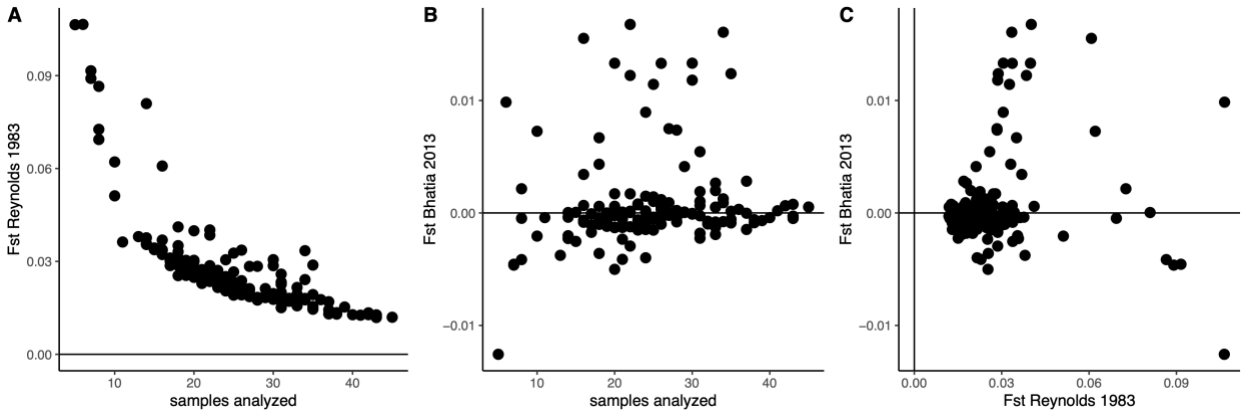

Appendix Figure B.2-2. Fst calculations made by ANGSD using all possible samples from each sampling area. (A) demonstrates strong bias based on the number of samples analyzed to estimate pairwise Fst using ANGSD's default Fst estimator from Reynolds et al. 1983. Comparisons based on more samples receive lower estimates of Fst. The points in (A) represents pairwise Fst values from all species plotted together, which further underscores the strength of this bias. ANGSD provides the option to calculate Fst using the estimator of Bhatia et al. 2013, which is designed to reduce bias from sample size. (B) The estimator successfully reduces bias, as there appears to be no relationship between samples analyzed and pairwise Fst across species. However, this estimator presents a new challenge for interpretation, which is that 54% of pairwise Fst values across all species are assigned negative values of Fst. Lines at Fst=0 are shown on all plots. Typically, negative values of Fst are treated as equivalent to Fst ~ 0. Negative Fst values produced by the Bhatia 2013 estimator are not distributed evenly across species. There are 6 species for which all possible Bhatia Fst values are negative, and a further 7 species for which only 1 or 2 pairwise comparisons have positive values. The two Fst estimators are not evidently correlated with each other (C), although this may be related to the strength of the bias shown in (A). We chose to mitigate the effect of sample size bias by using the Reynolds 1983 estimator on exactly the same number of samples across all species and populations, rather than by using the Bhatia 2013 estimator on unbalanced sample sizes, because we felt that doing so produced results that were easier to interpret.

B.3 Spatial genetic patterns in each species

Appendix Figure B3-1 to B3-34. Spatial genetic patterns for each species as shown with PCA (A) and admixture plots (B) generated by PCANGSD; and the relationship between geographic distance and PCA covariance (C), genetic distance (D), and F_{st} (E). Samples are ordered by longitude in admixture plots. Genetic distance and F_{st}

estimates in D and E come from the subsampled datasets whereas PCA-based analyses use the SNP dataset. We did not calculate IBD slope based on F_{st} in species.

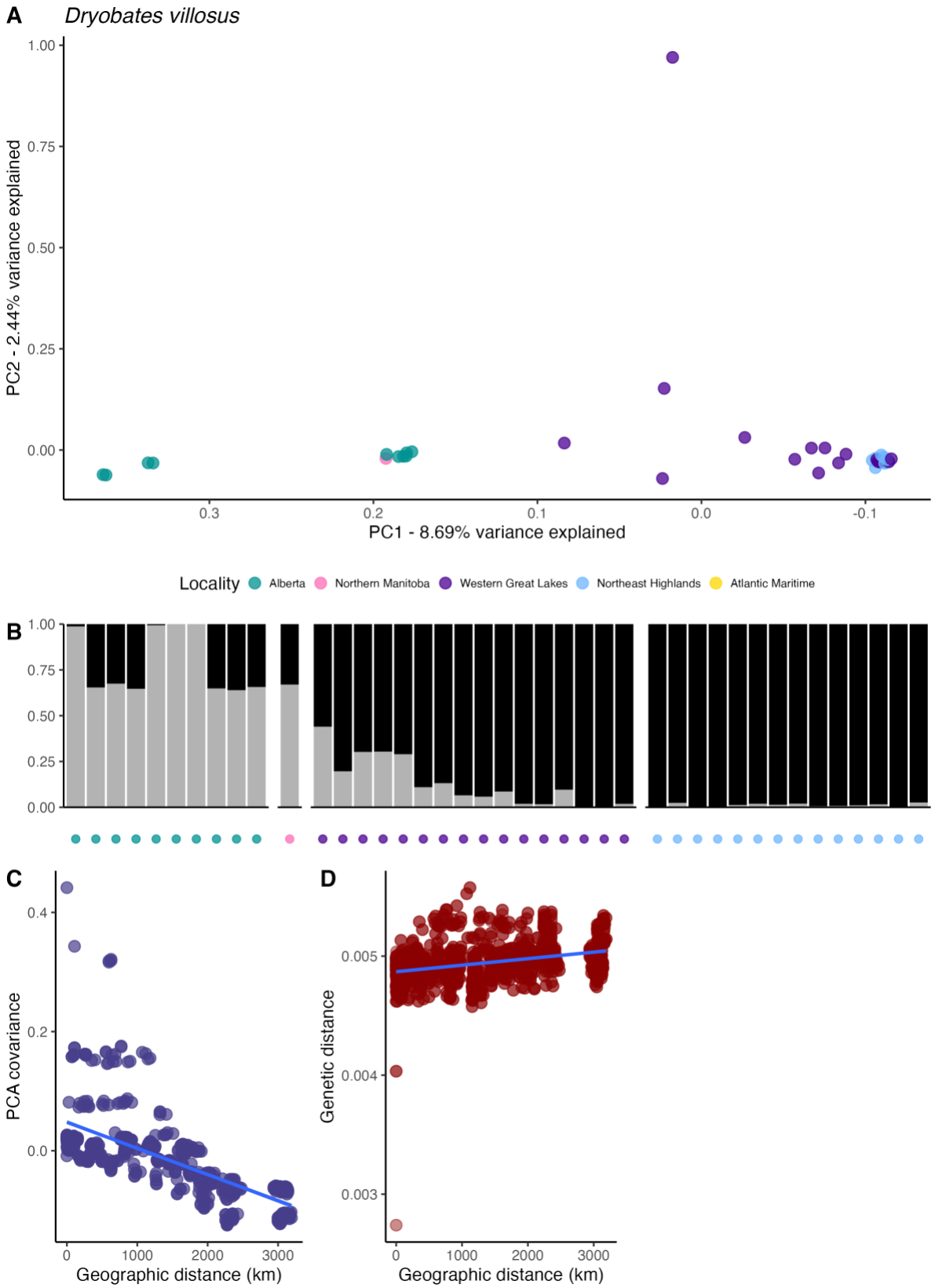

Appendix Figure B.3-1. Spatial genetic patterns for *Dryobates villosus*.

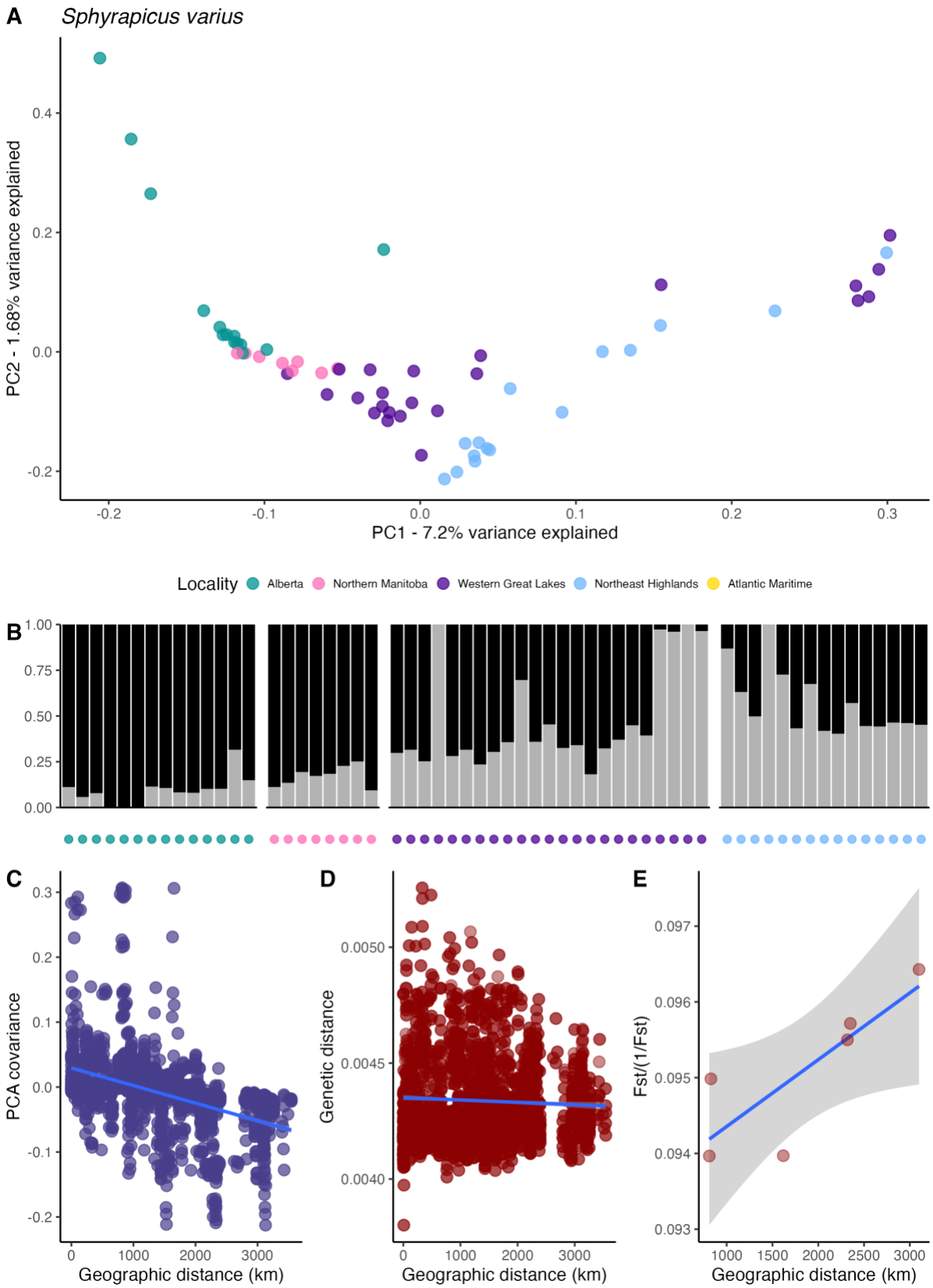

*Appendix Figure B.3-2.*Spatial genetic patterns for *Sphyrapicus varius*.

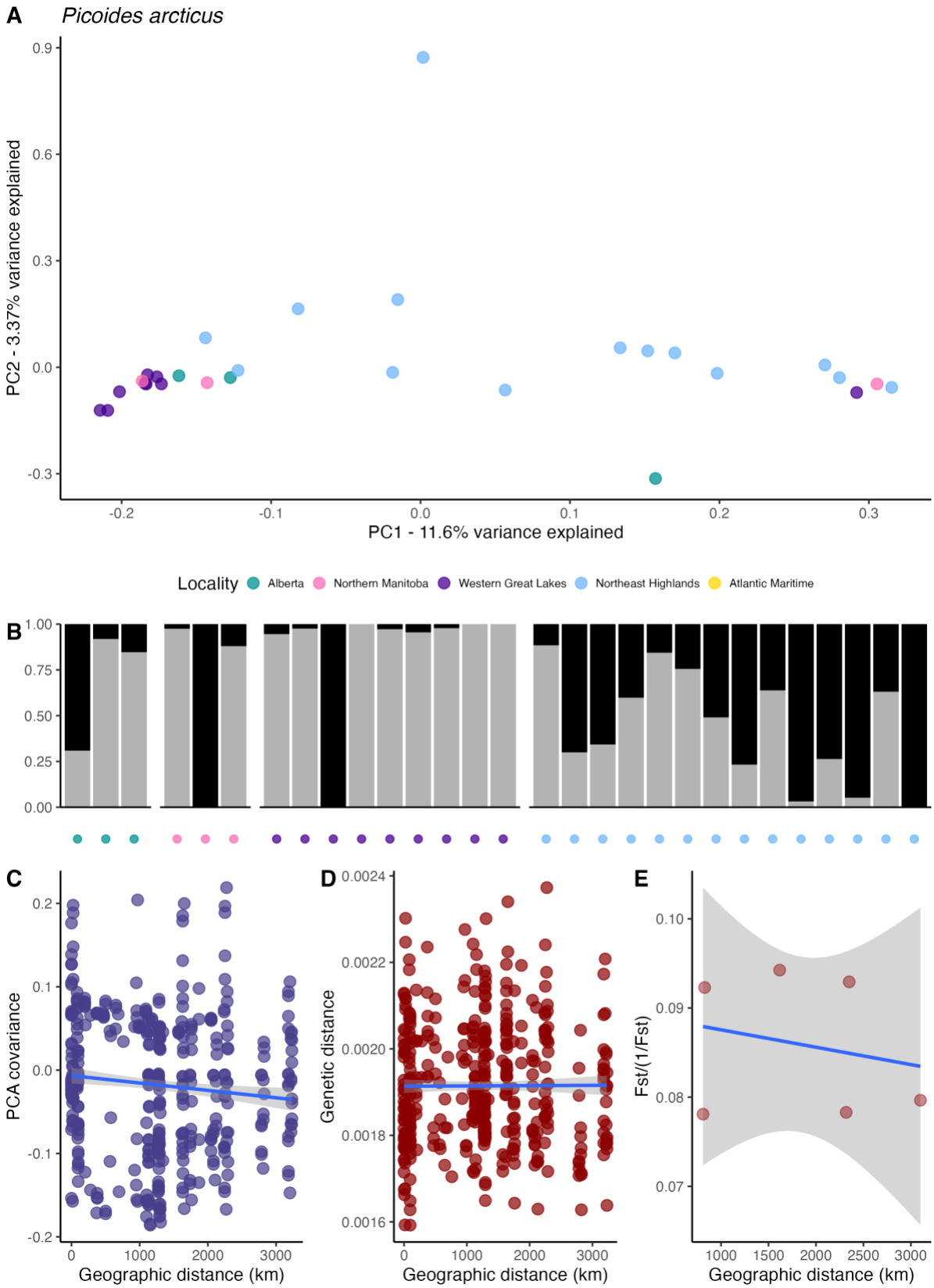

Appendix Figure B.3-3. Spatial genetic patterns for *Picoides arcticus*.

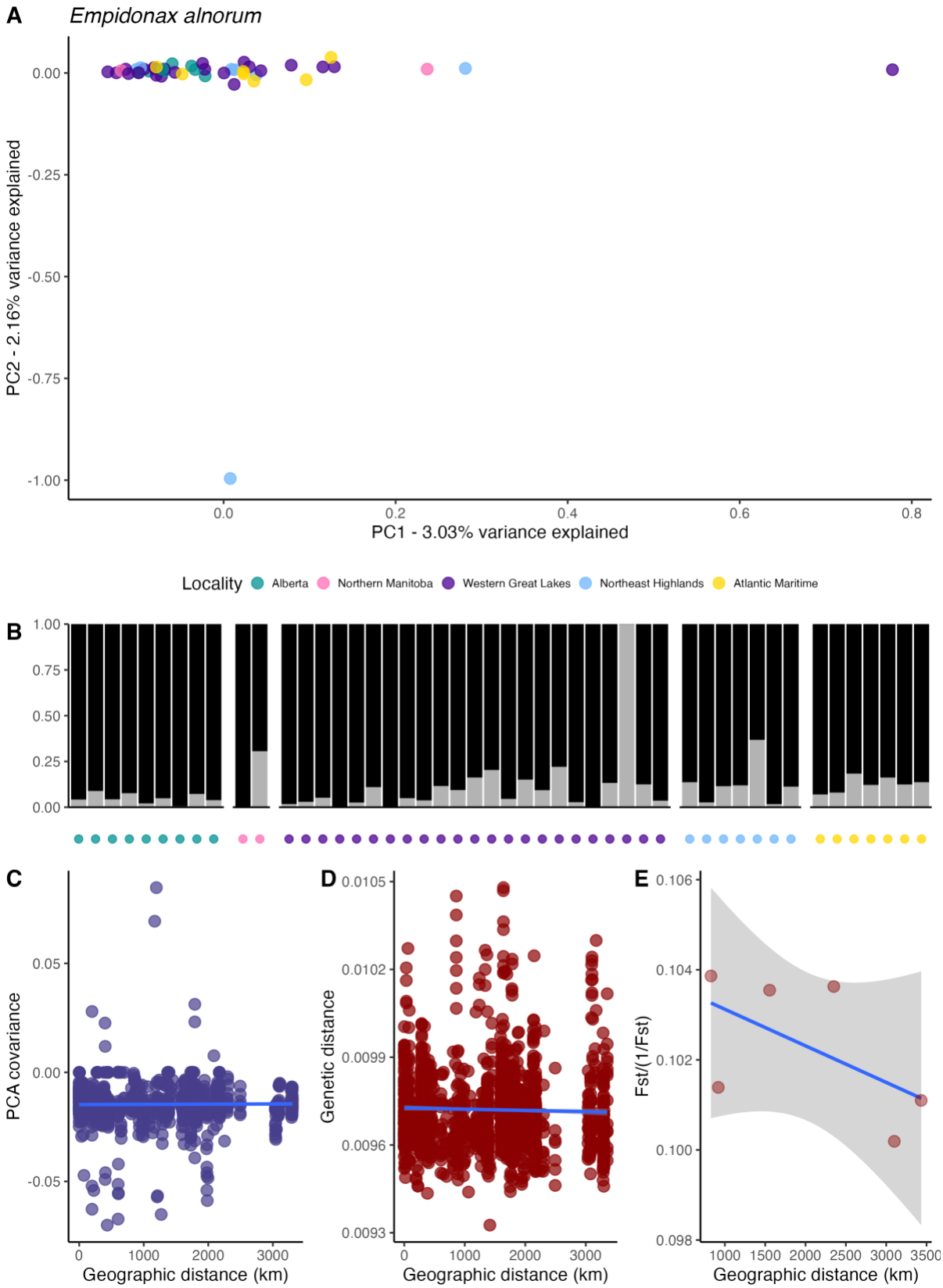

Appendix Figure B.3-4. Spatial genetic patterns for *Empidonax alnorum*.

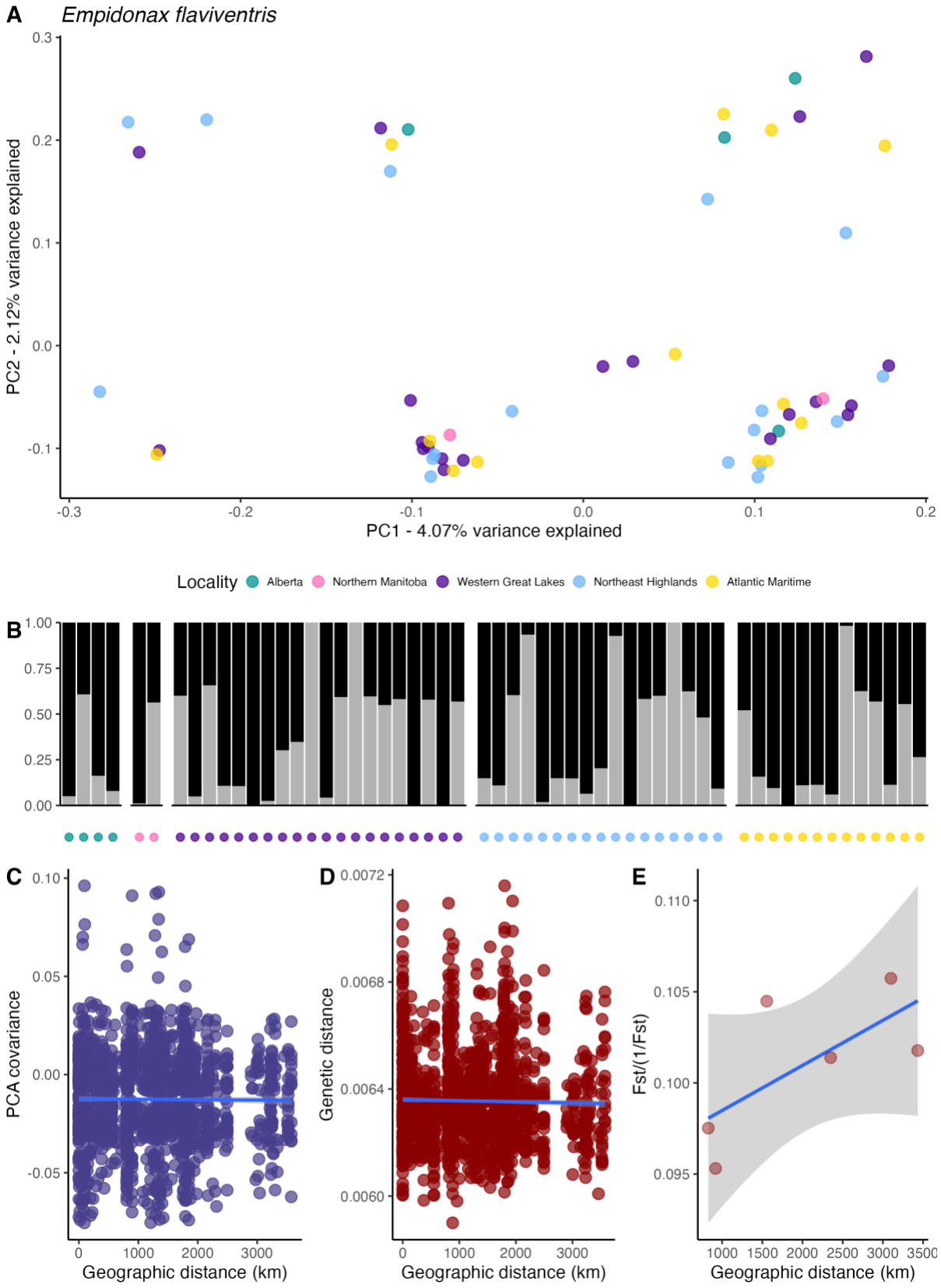

Appendix Figure B.3-5. Spatial genetic patterns for *Empidonax flaviventris*.

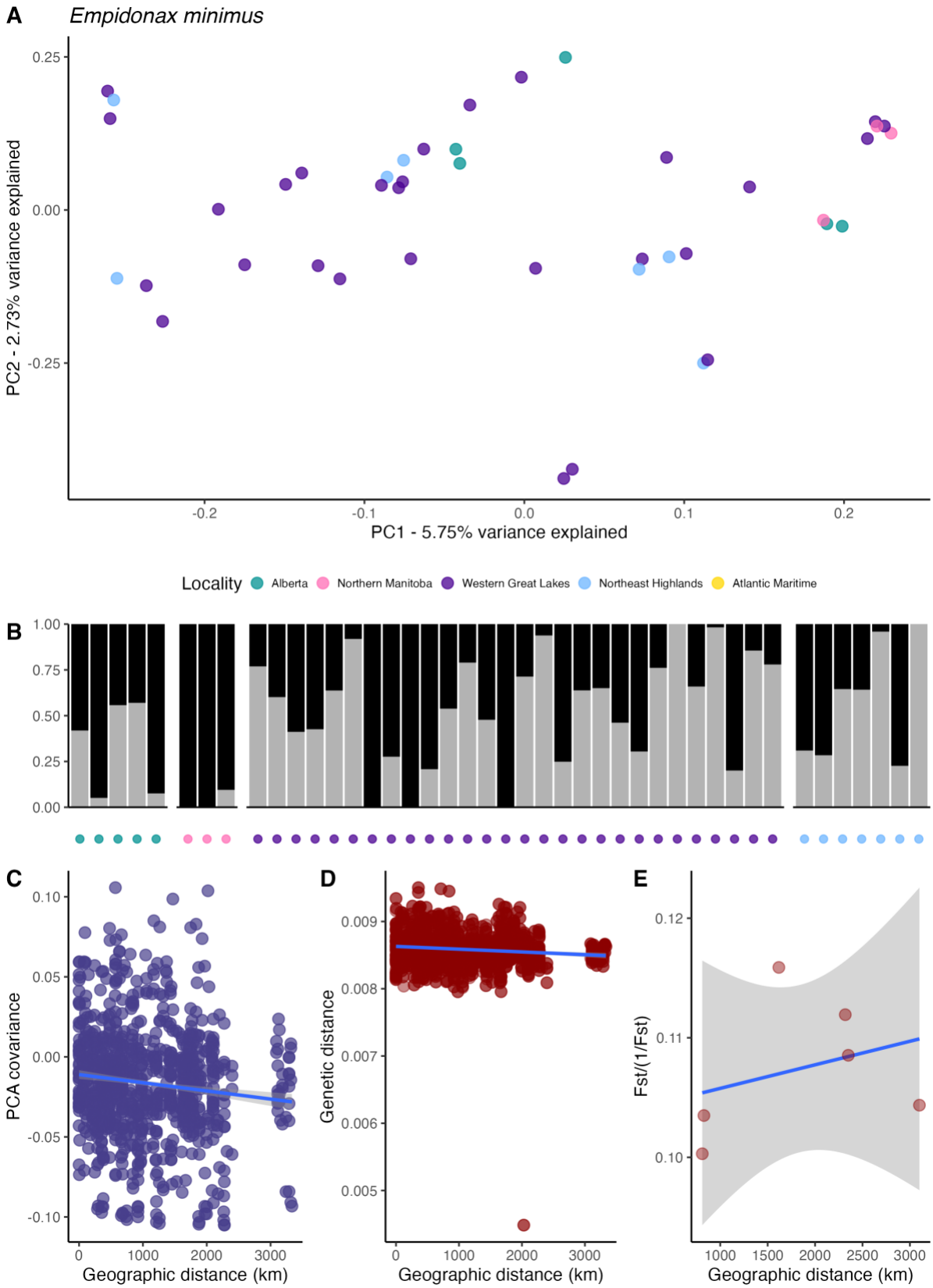

Appendix Figure B.3-6. Spatial genetic patterns for *Empidonax minimus*.

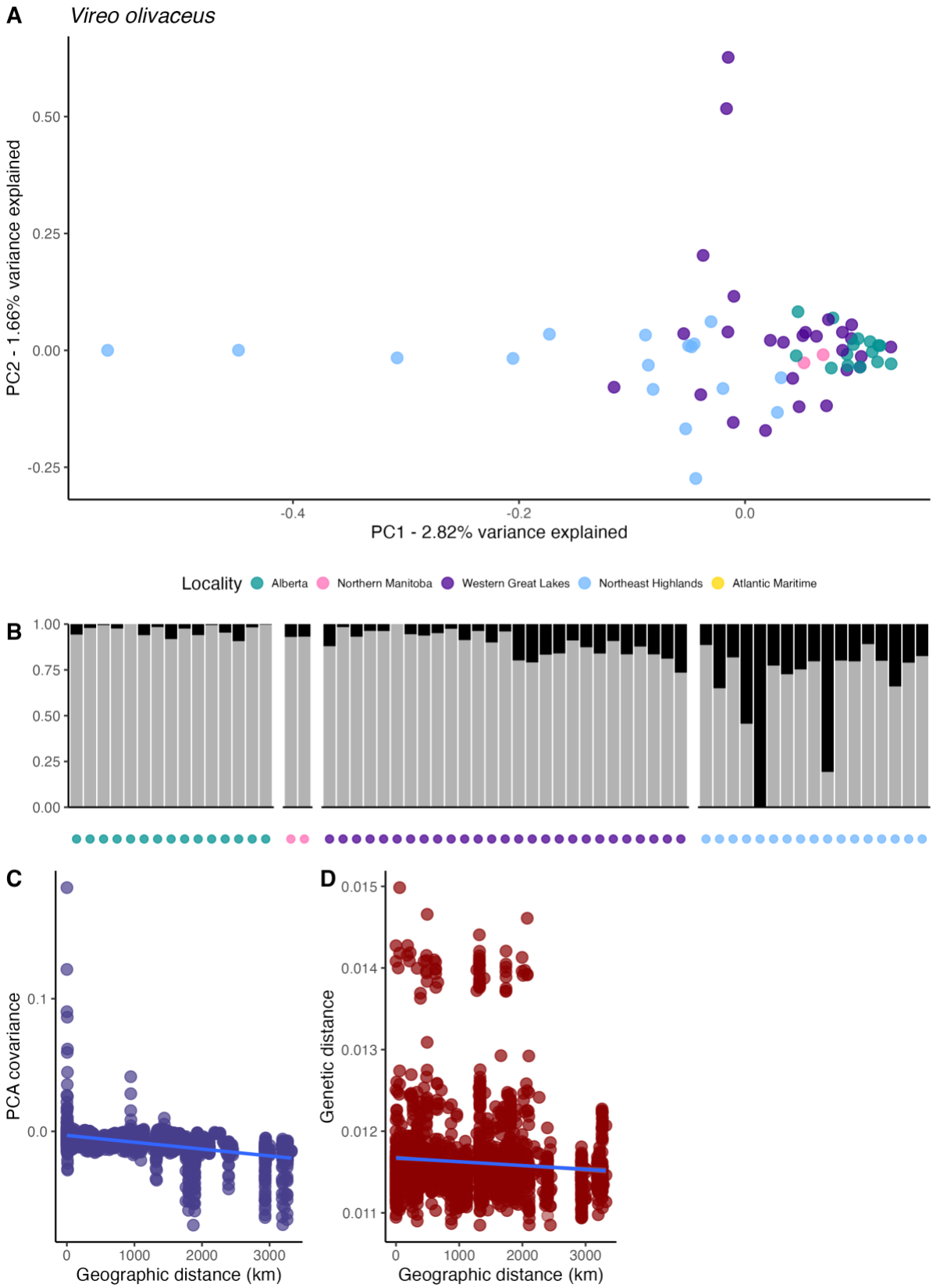

Appendix Figure B.3-7. Spatial genetic patterns for *Vireo olivaceus*.

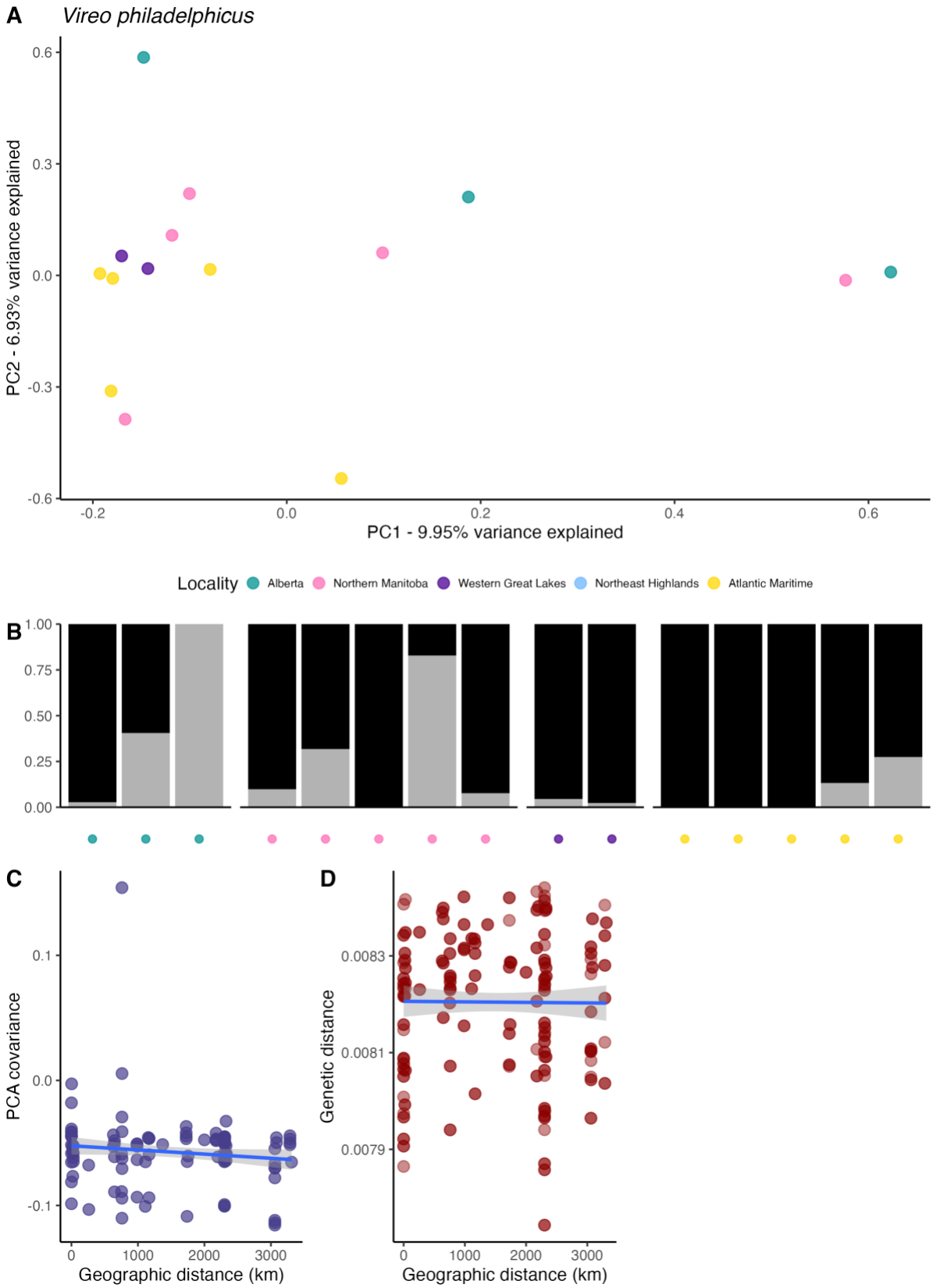

Appendix Figure B.3-8. Spatial genetic patterns for *Vireo philadelphicus*.

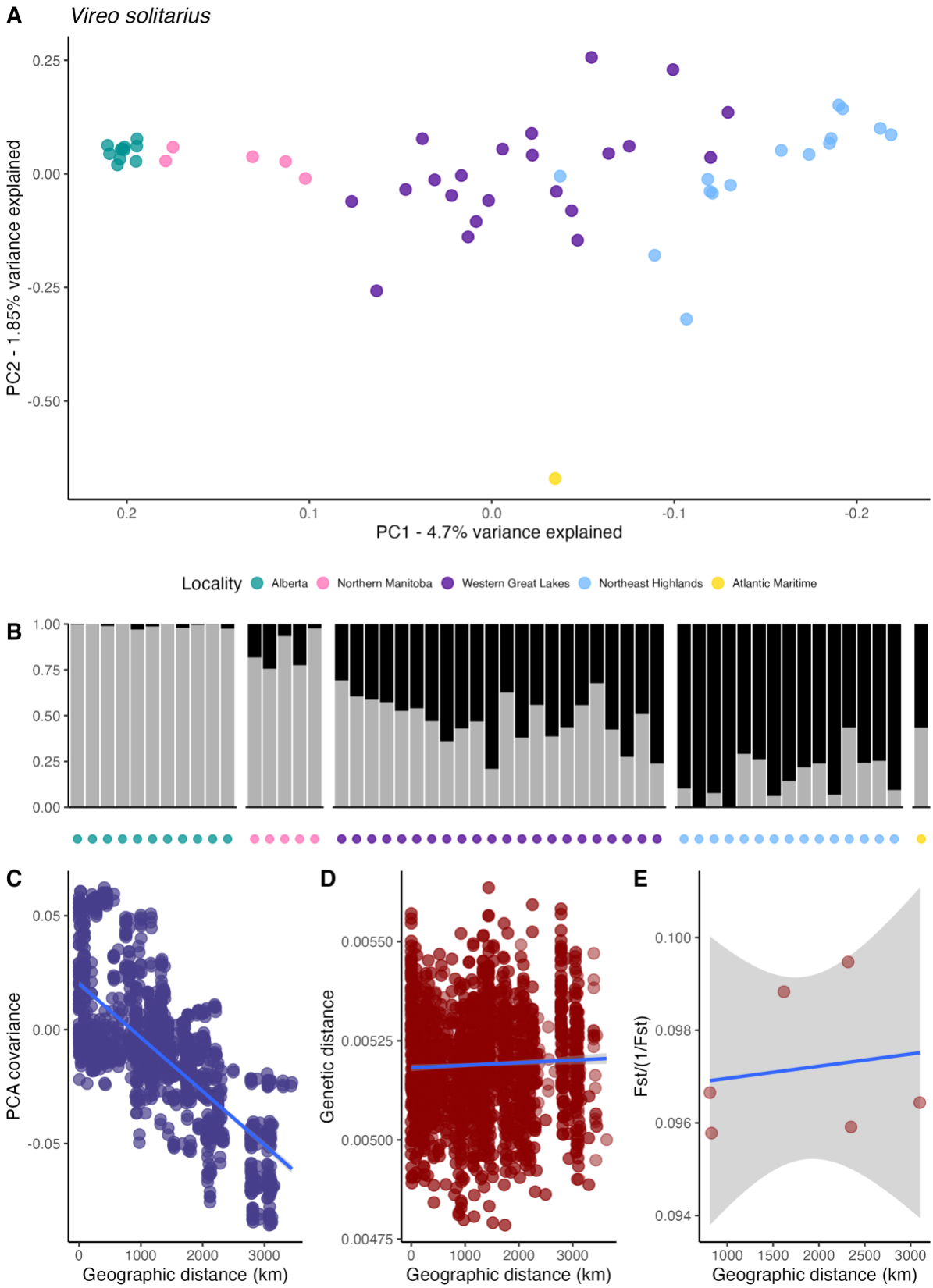

Appendix Figure B.3-9. Spatial genetic patterns for *Vireo solitarius*.

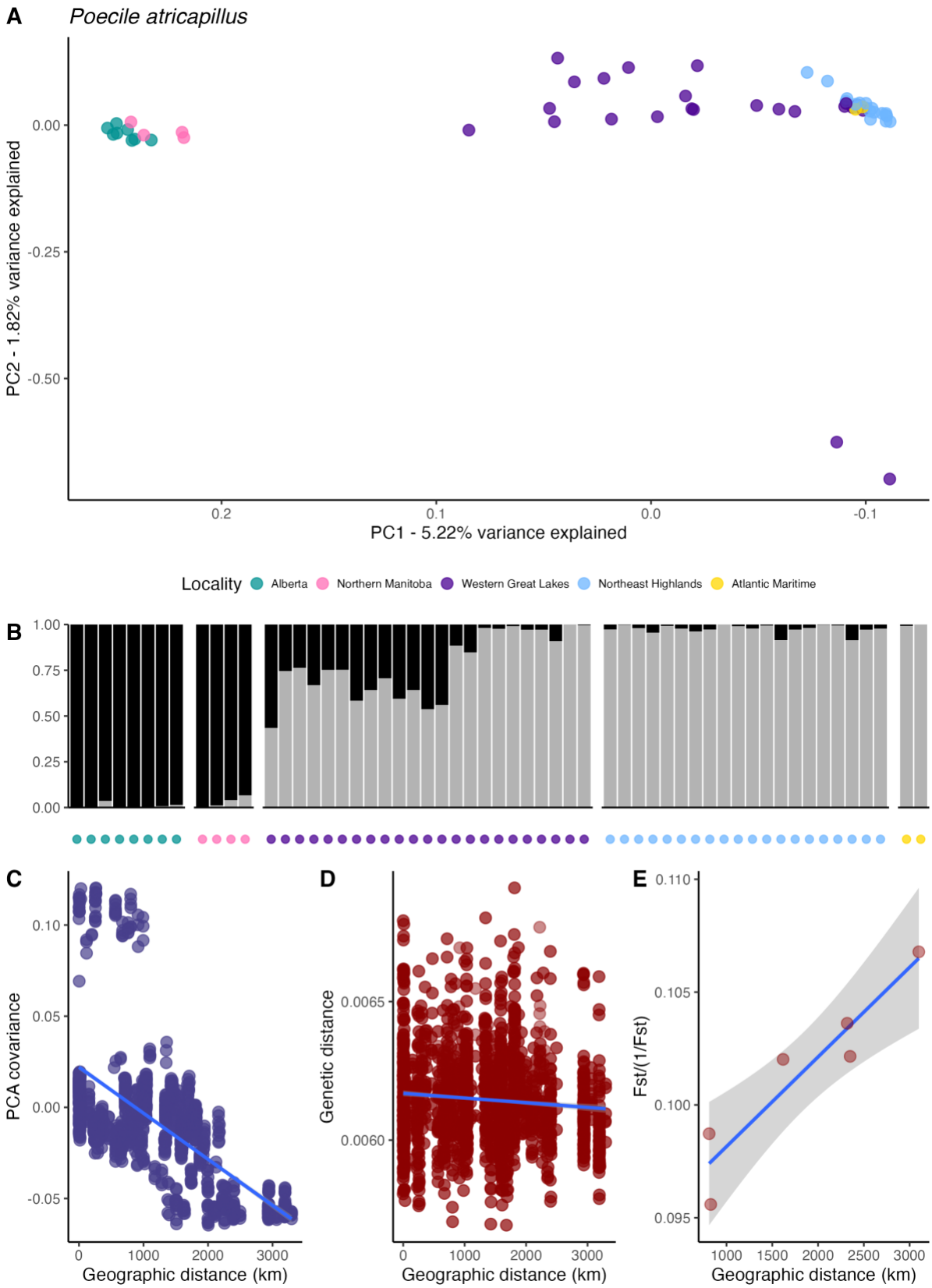

Appendix Figure B.3-10. Spatial genetic patterns for *Poecile atricapillus*.

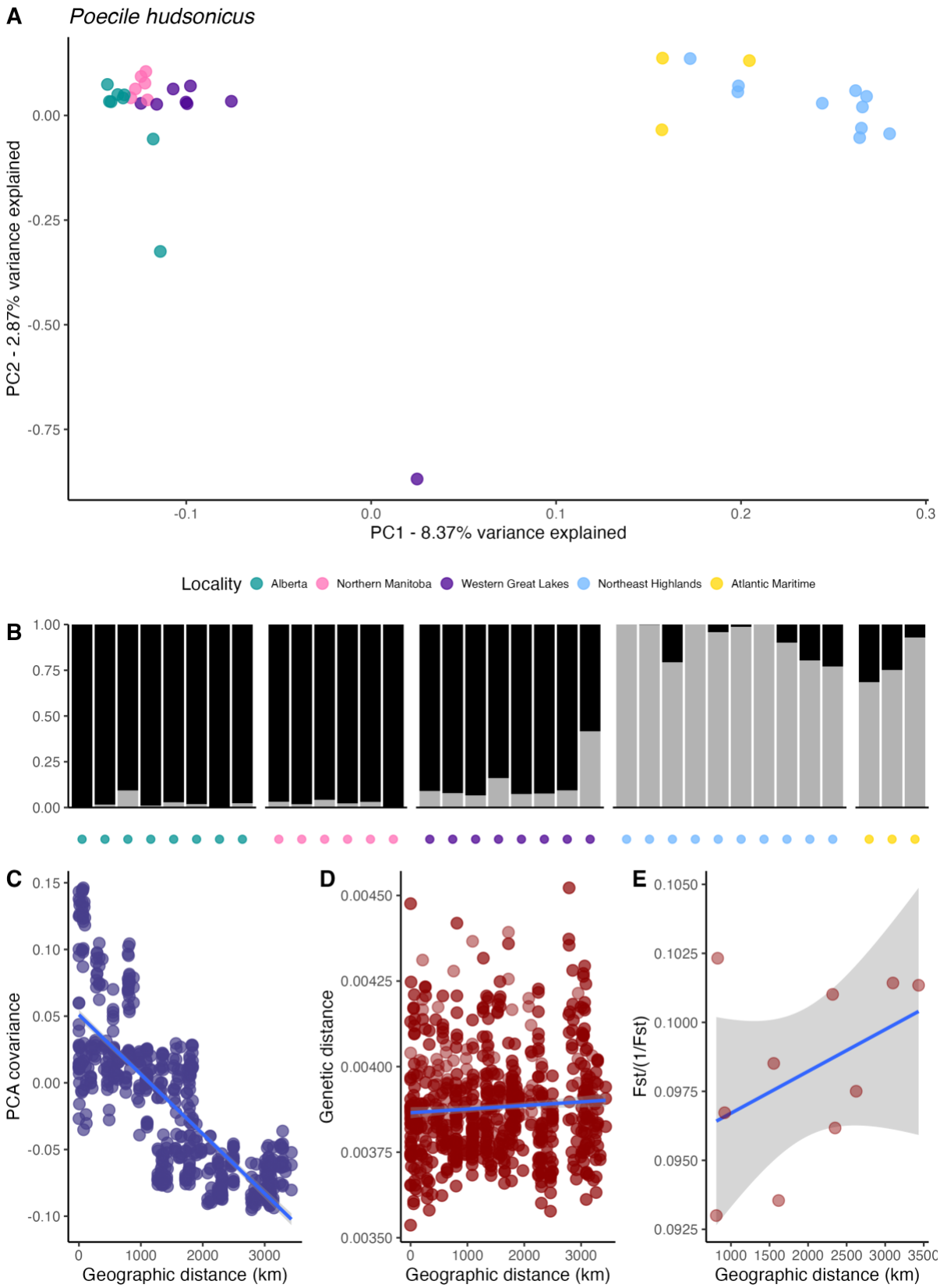

Appendix Figure B.3-11. Spatial genetic patterns for *Poecile hudsonicus*.

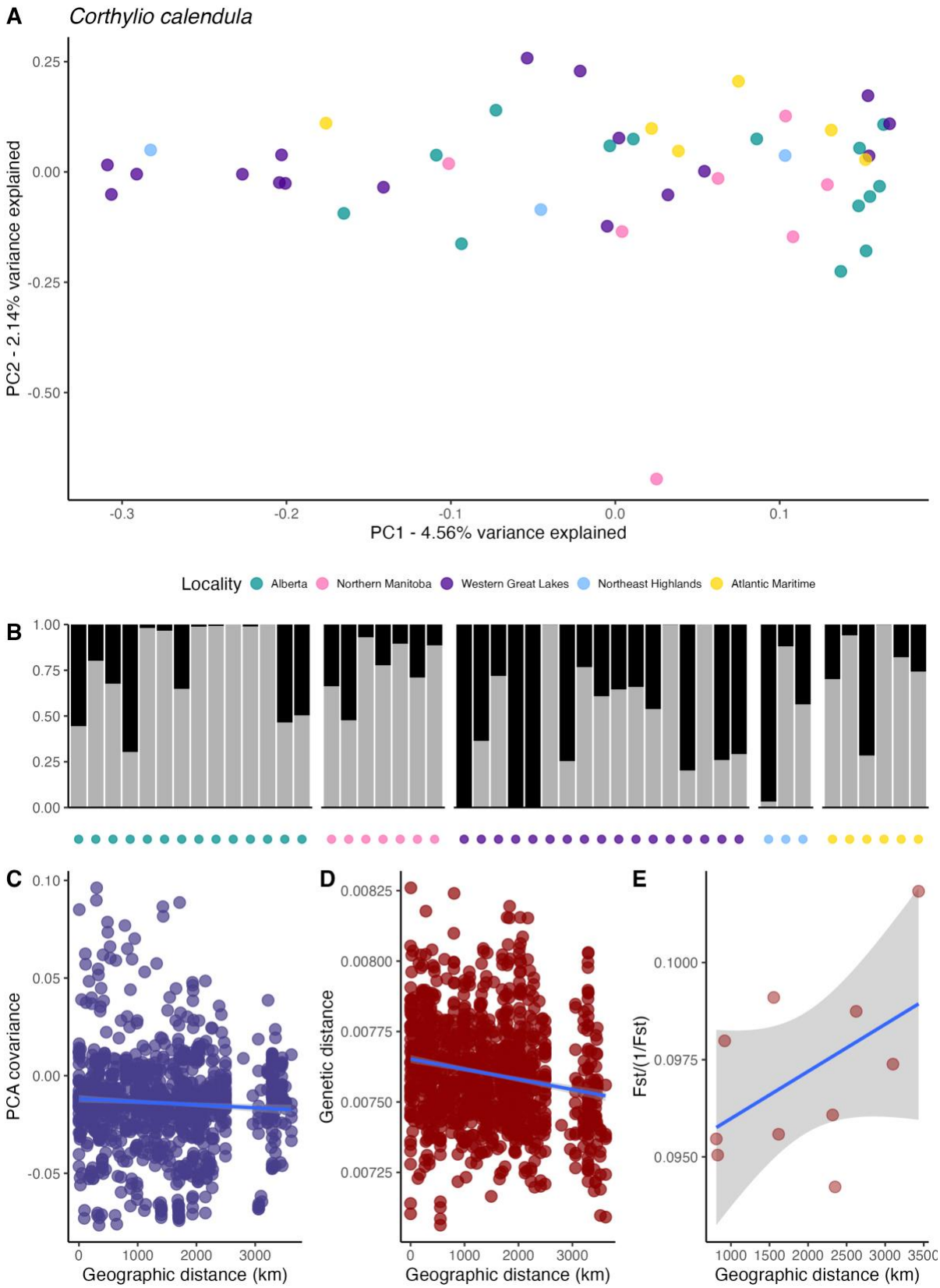

Appendix Figure B.3-12. Spatial genetic patterns for *Corthylio calendula*.

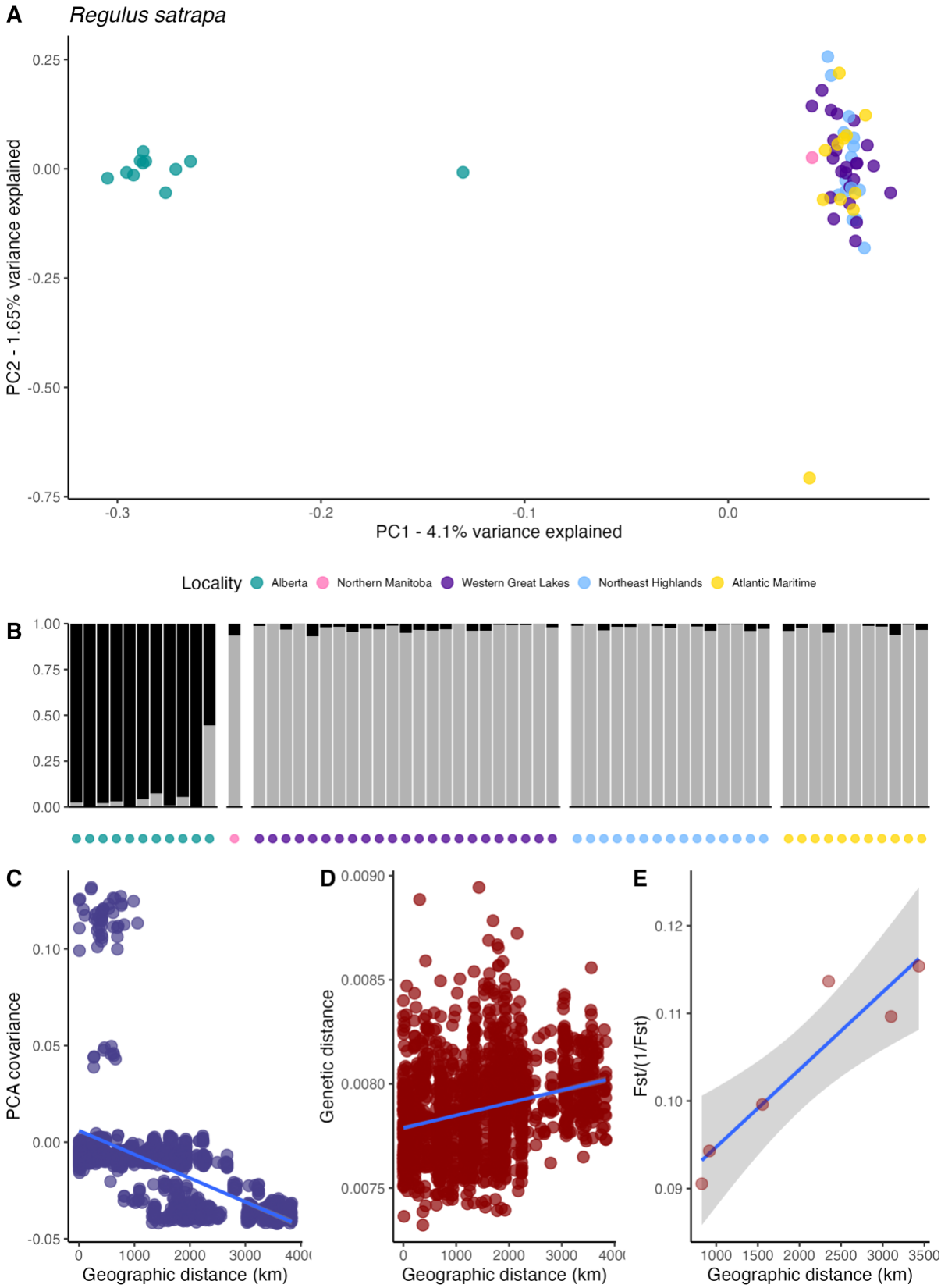

Appendix Figure B.3-13. Spatial genetic patterns for *Regulus satrapa*.

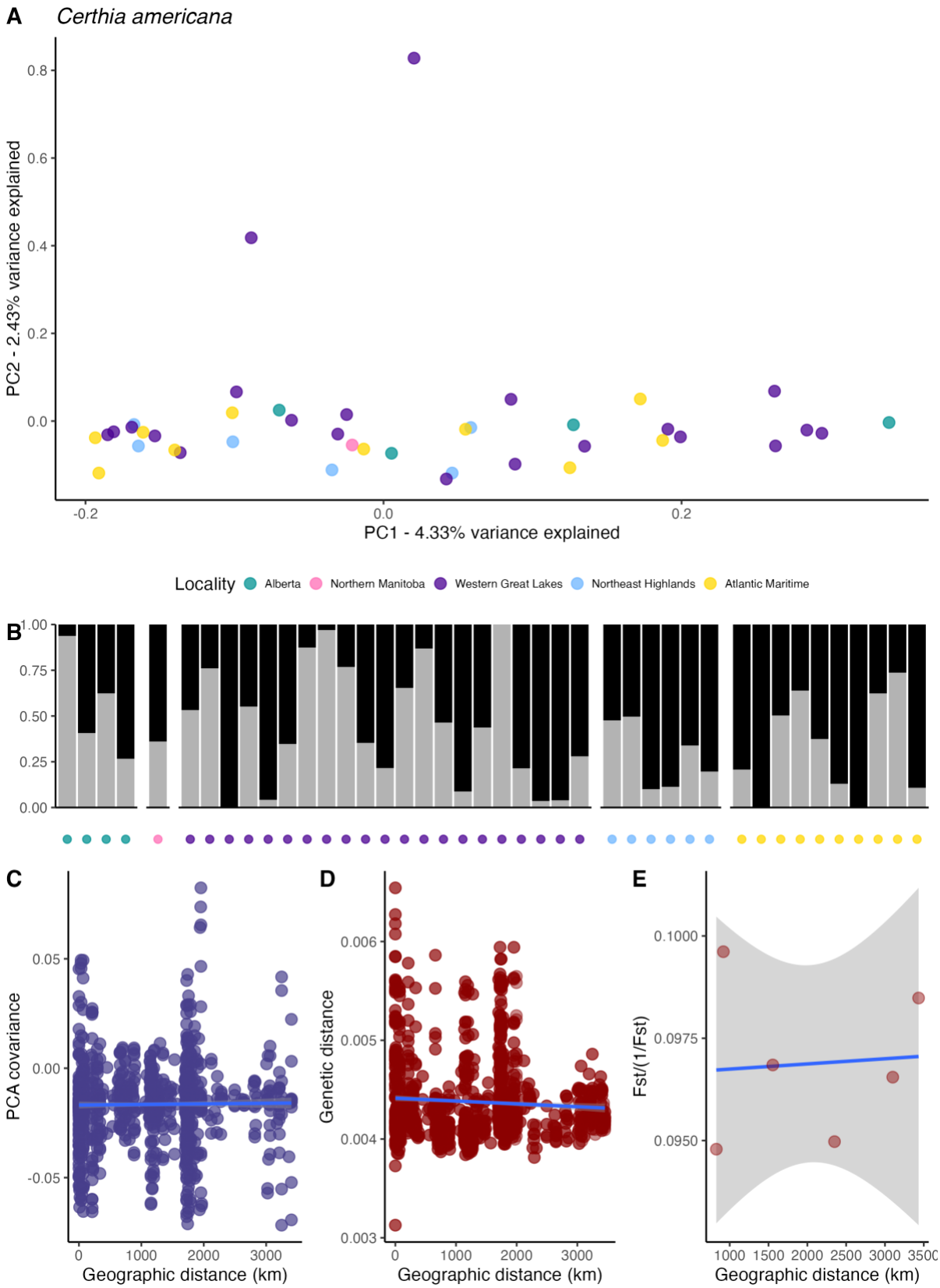

Appendix Figure B.3-14. Spatial genetic patterns for *Certhia americana*.

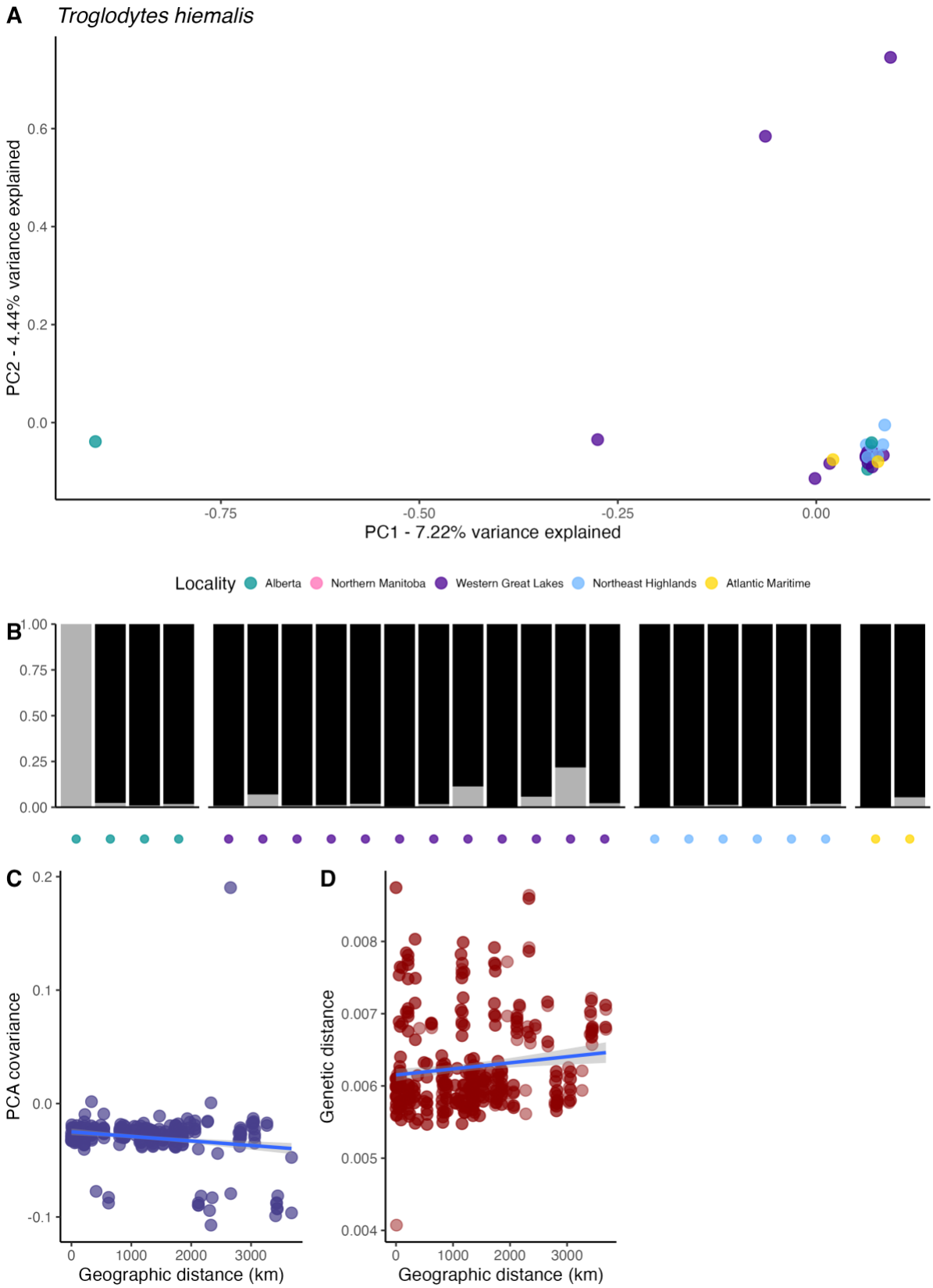

Appendix Figure B.3-15. Spatial genetic patterns for *Troglodytes hiemalis*.

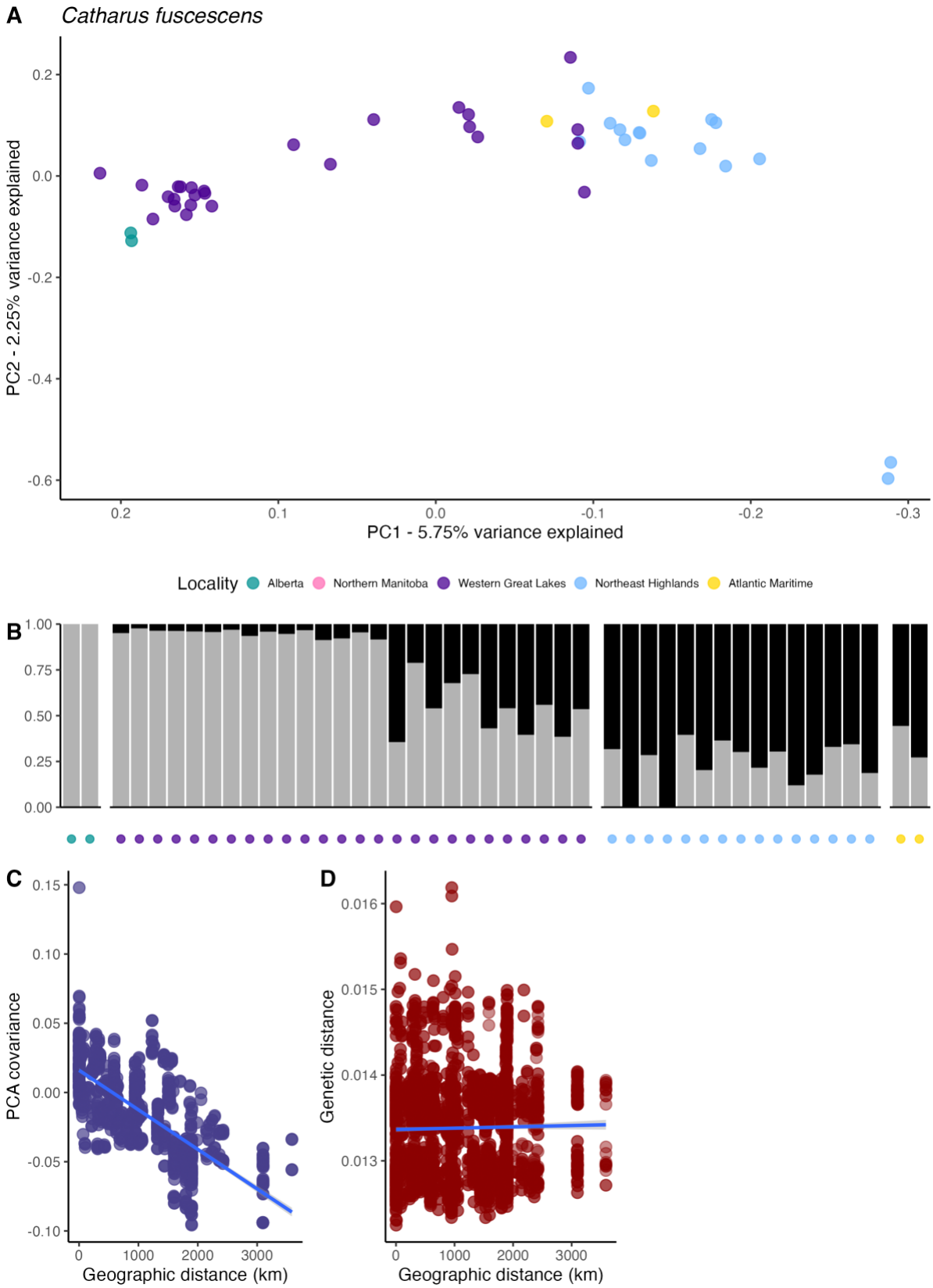

Appendix Figure B.3-16. Spatial genetic patterns for *Catharus fuscescens*.

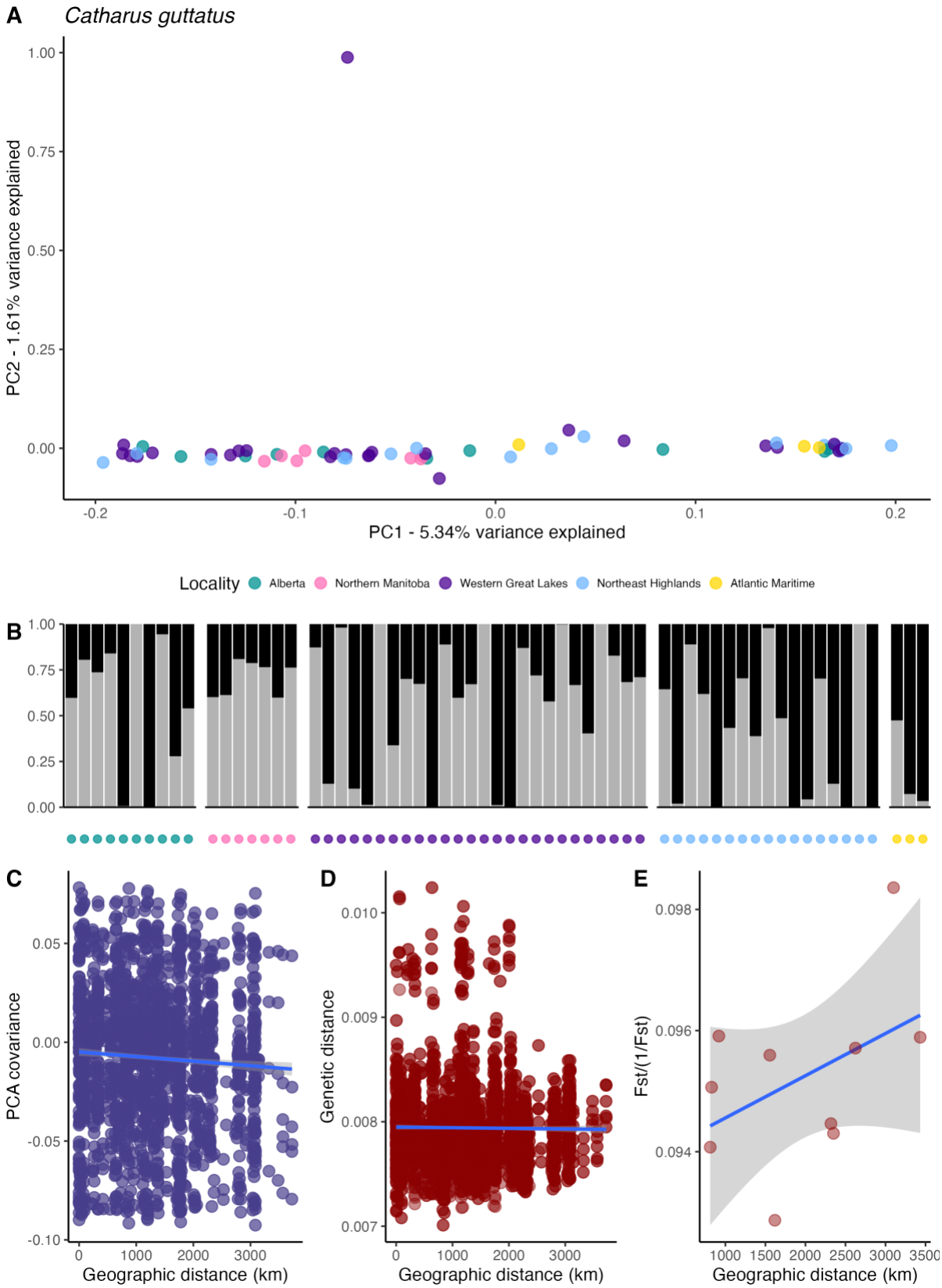

Appendix Figure B.3-17. Spatial genetic patterns for *Catharus guttatus*.

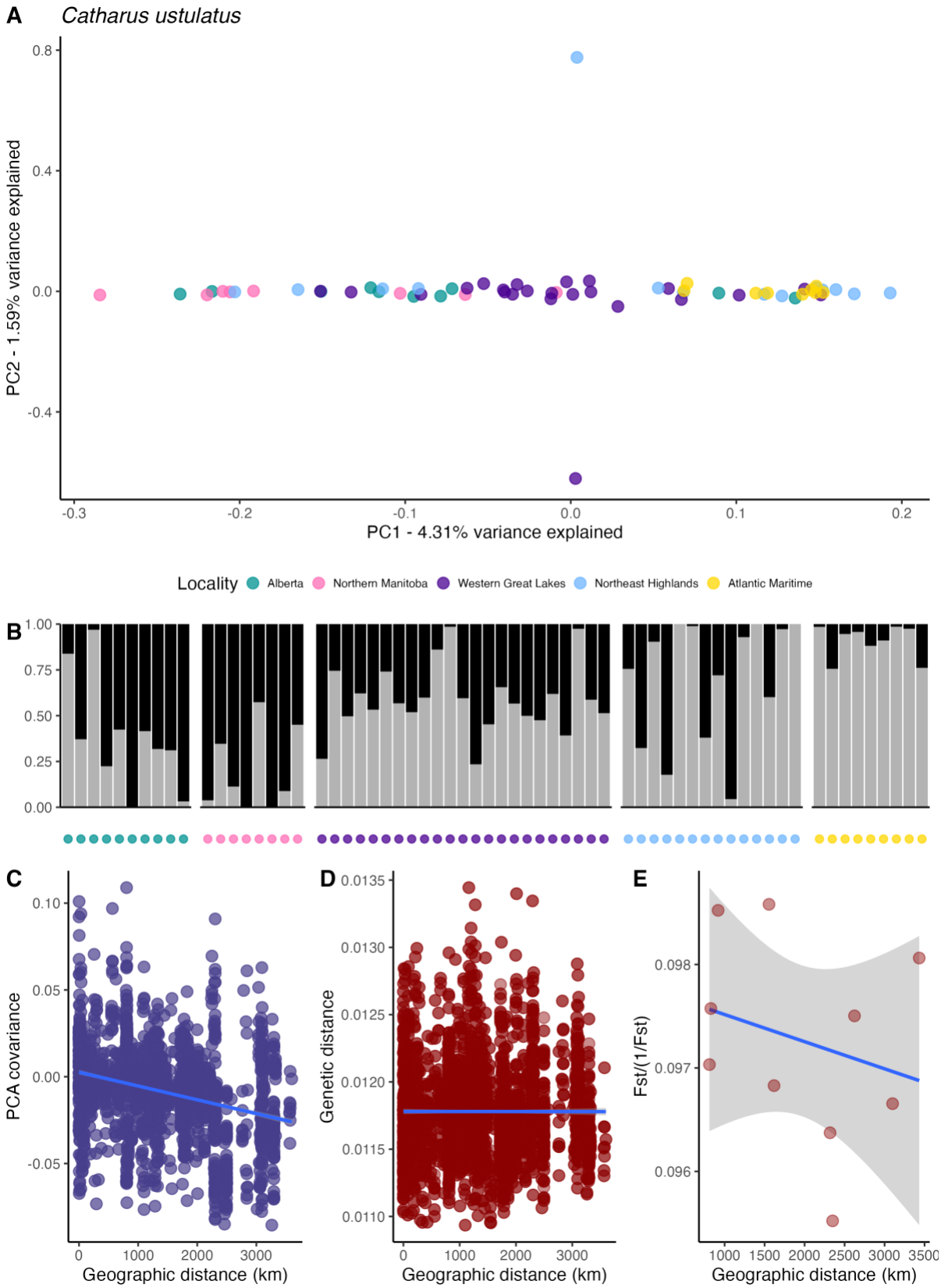

Appendix Figure B.3-18. Spatial genetic patterns for *Catharus ustulatus*.

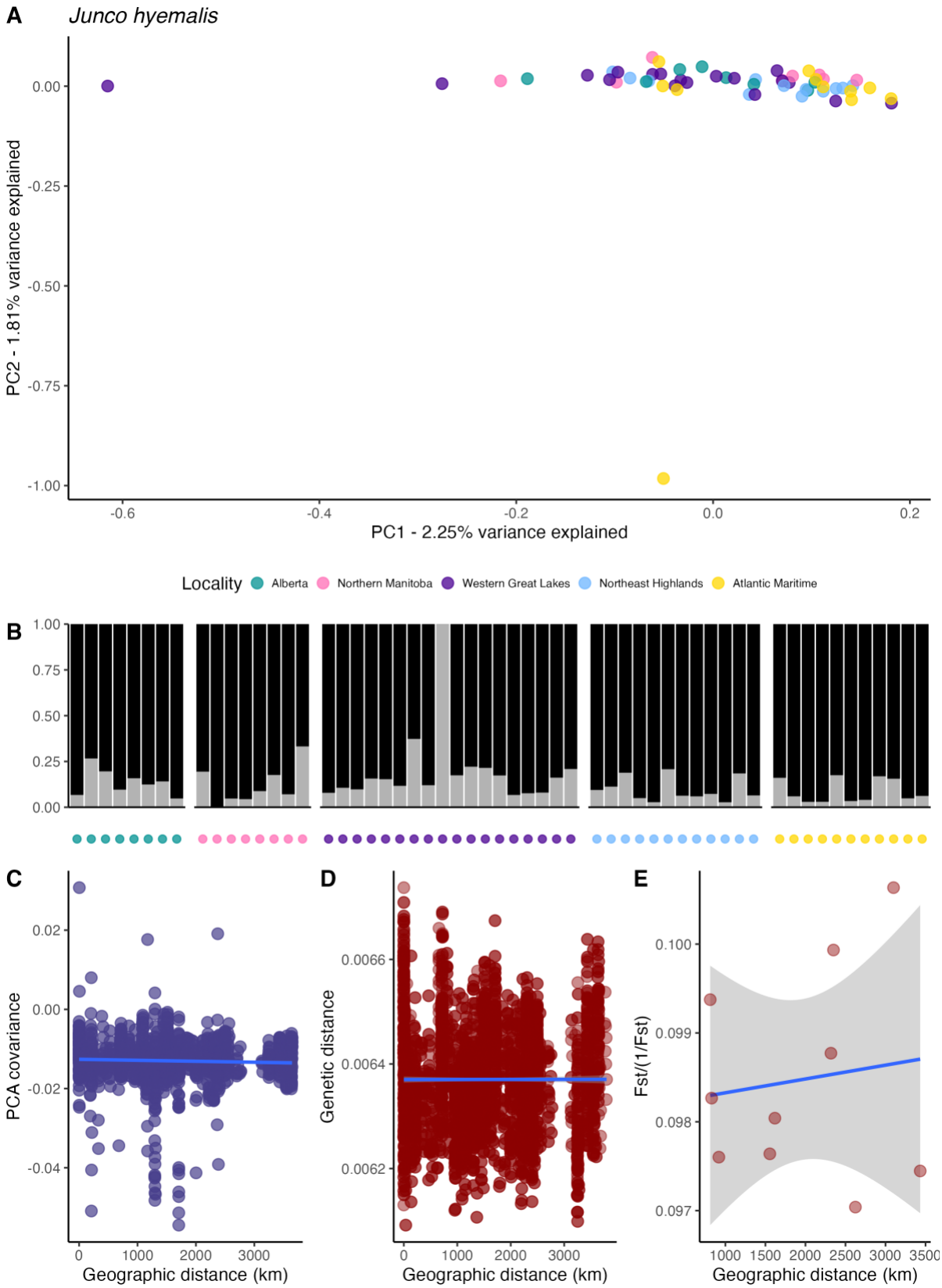

Appendix Figure B.3-19. Spatial genetic patterns for *Junco hyemalis*.

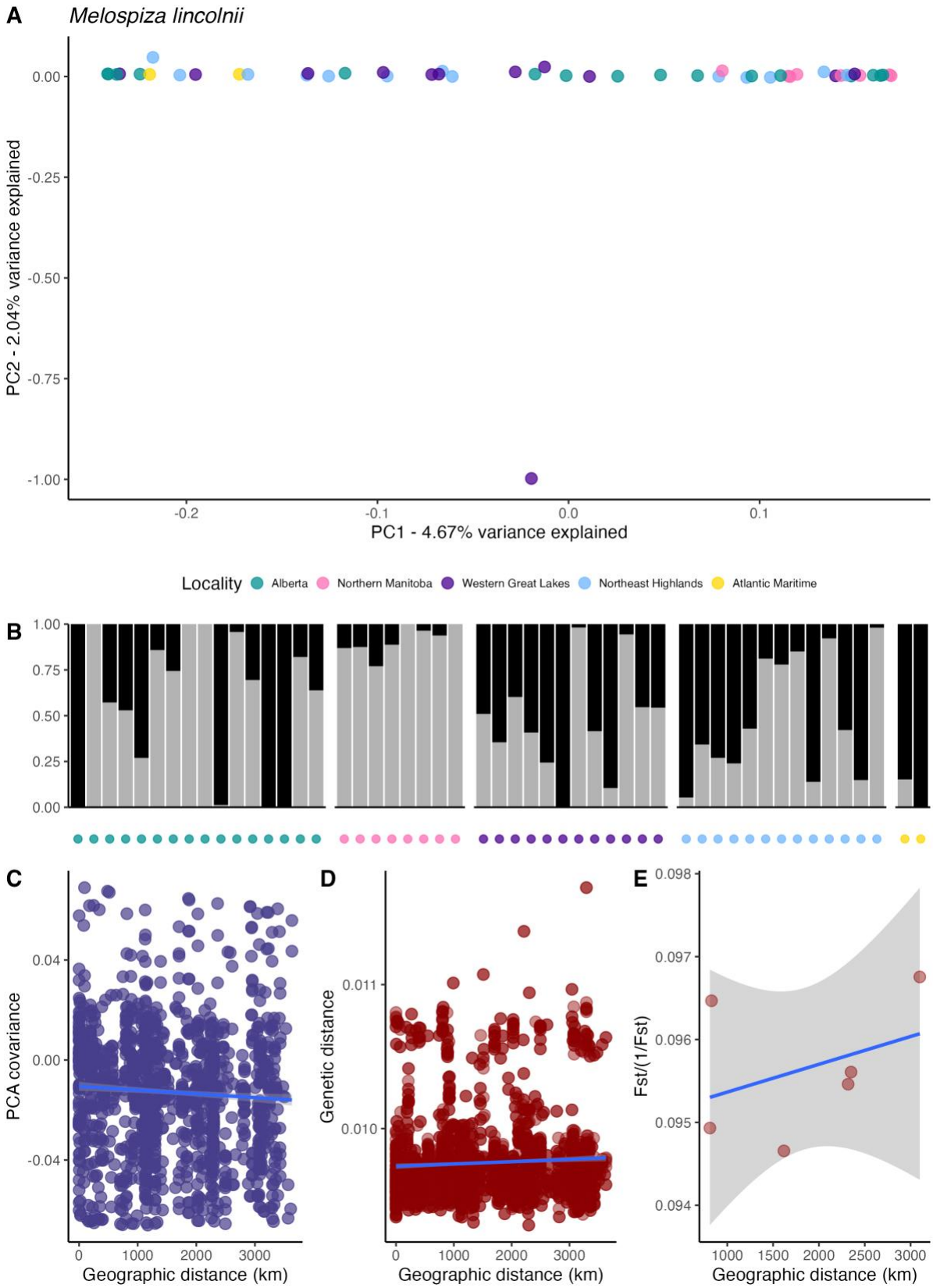

Appendix Figure B.3-20. Spatial genetic patterns for *Melospiza lincolnii*.

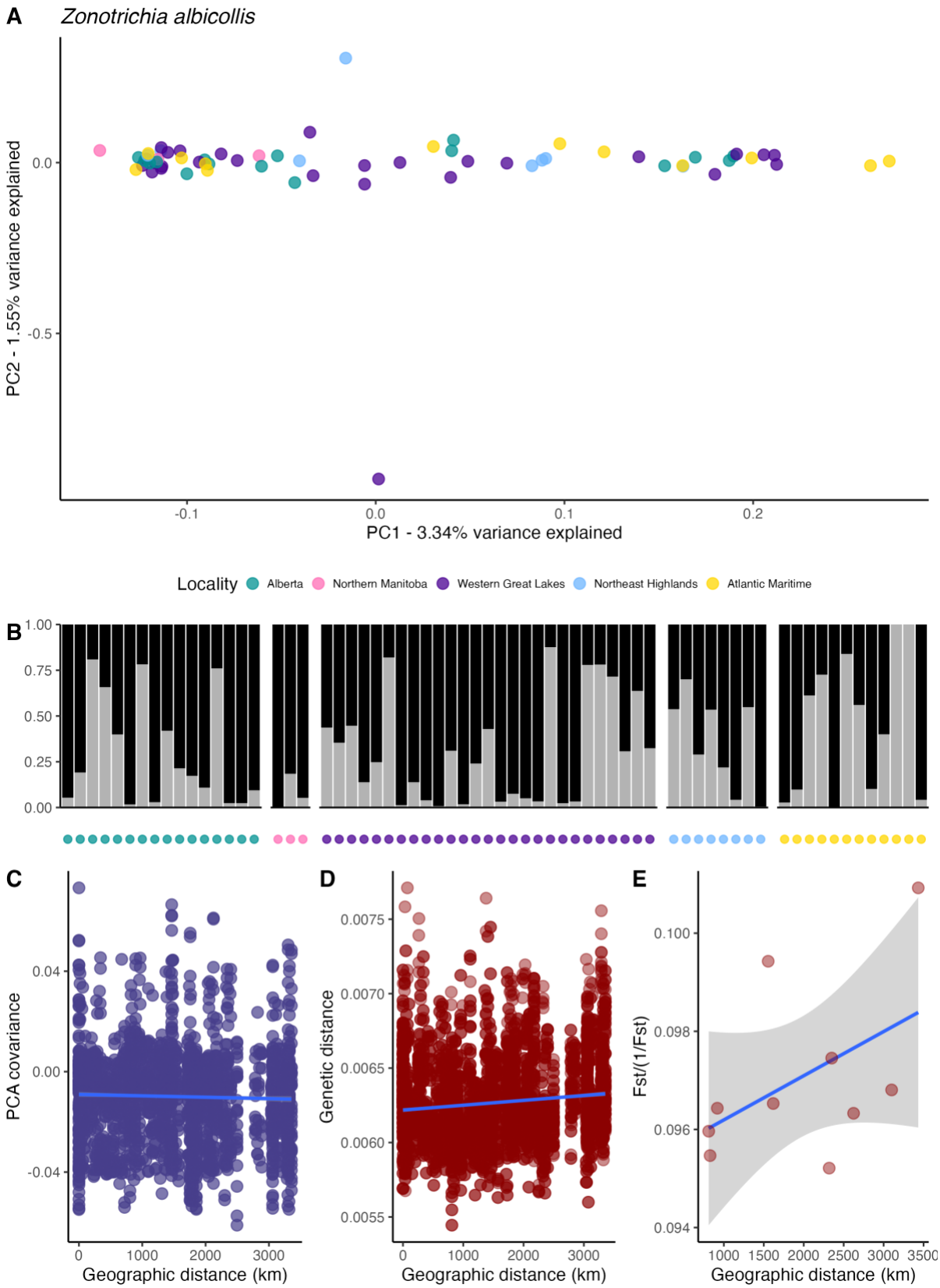

Appendix Figure B.3-21. Spatial genetic patterns for *Zonotrichia albicollis*.

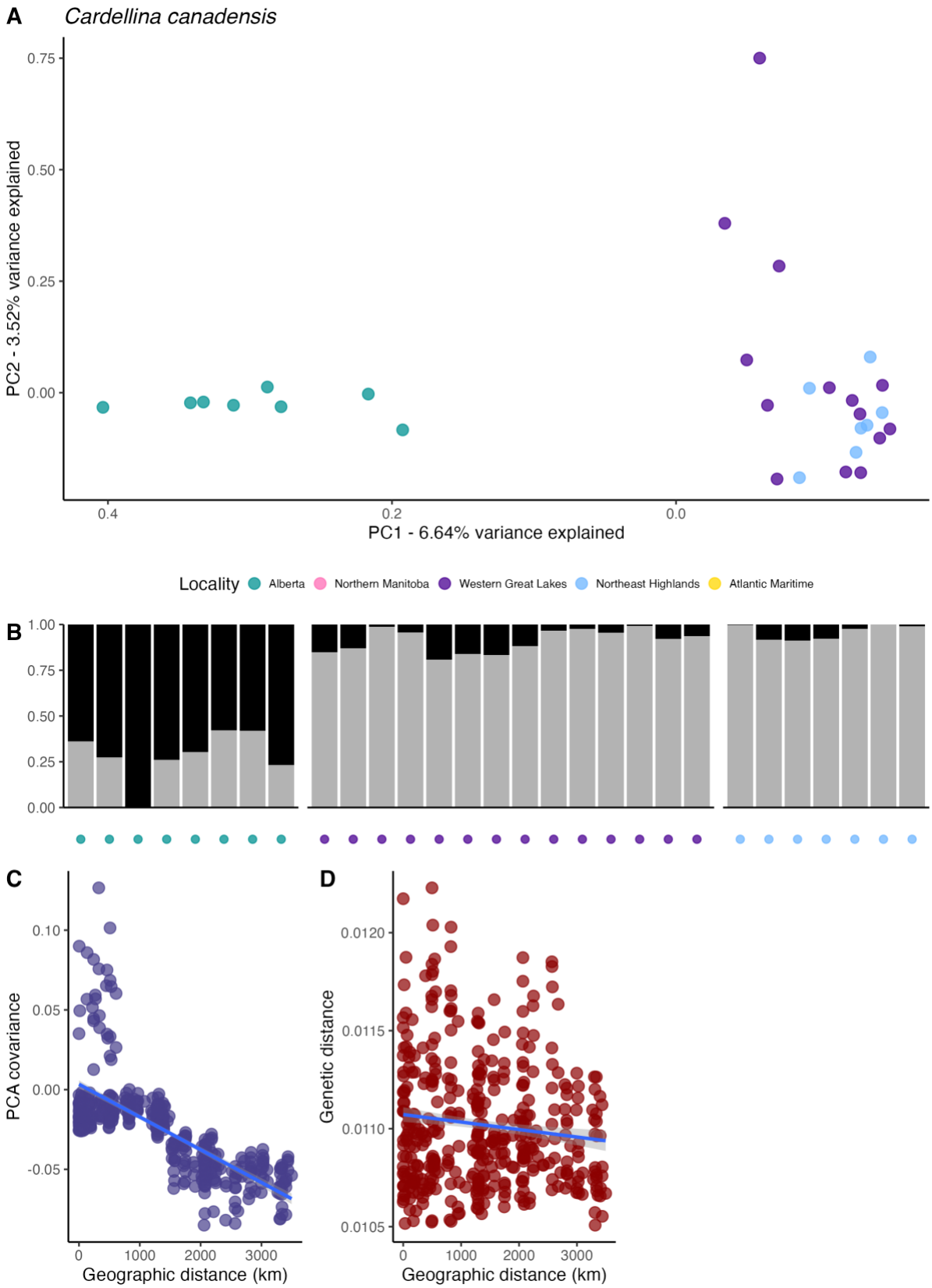

Appendix Figure B.3-22. Spatial genetic patterns for *Cardellina canadensis*.

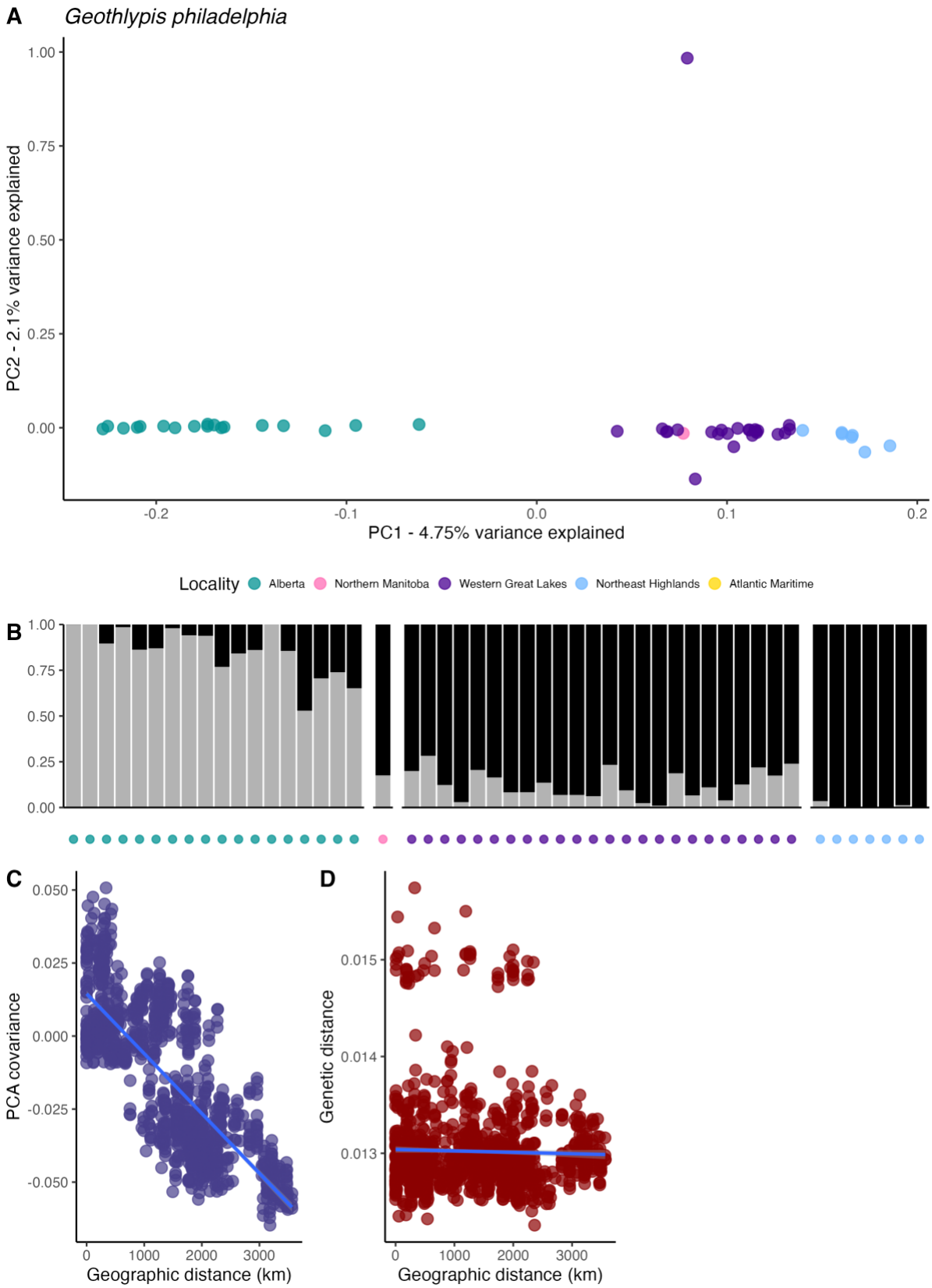

Appendix Figure B.3-23. Spatial genetic patterns for *Geothlypis philadelphia*.

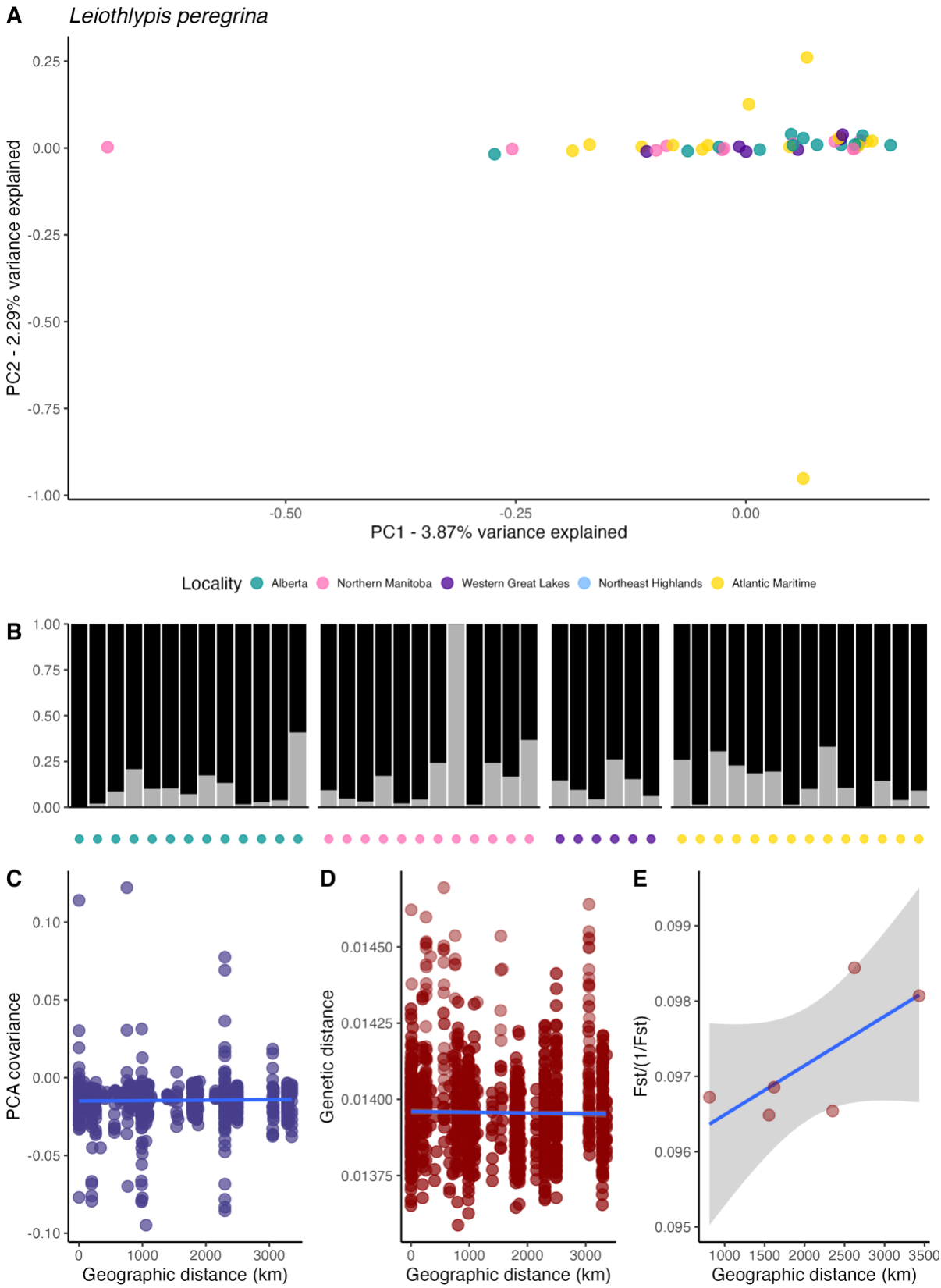

Appendix Figure B.3-24. Spatial genetic patterns for *Leiothlypis peregrina*.

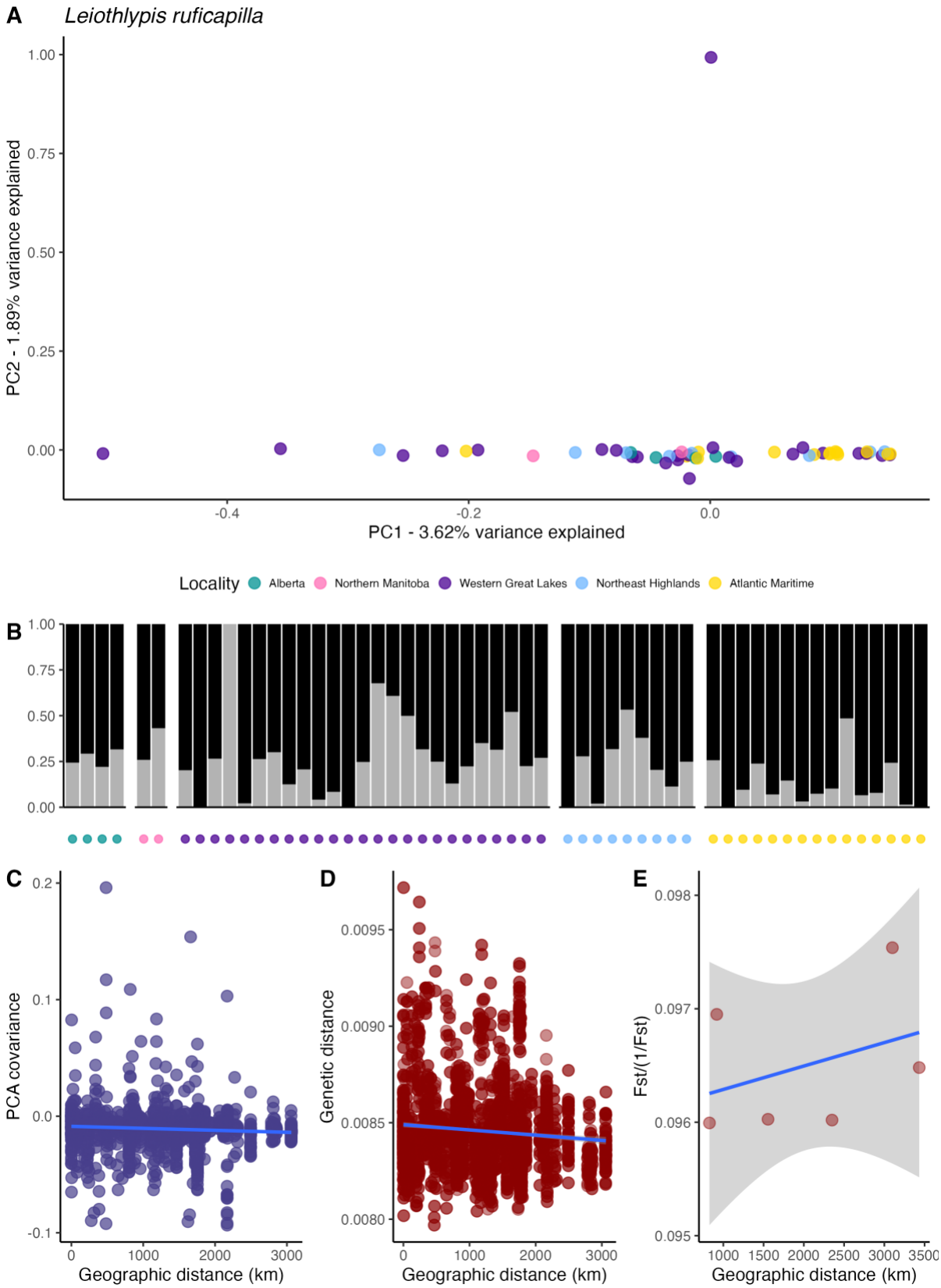

Appendix Figure B.3-25. Spatial genetic patterns for *Leiothlypis ruficapilla*.

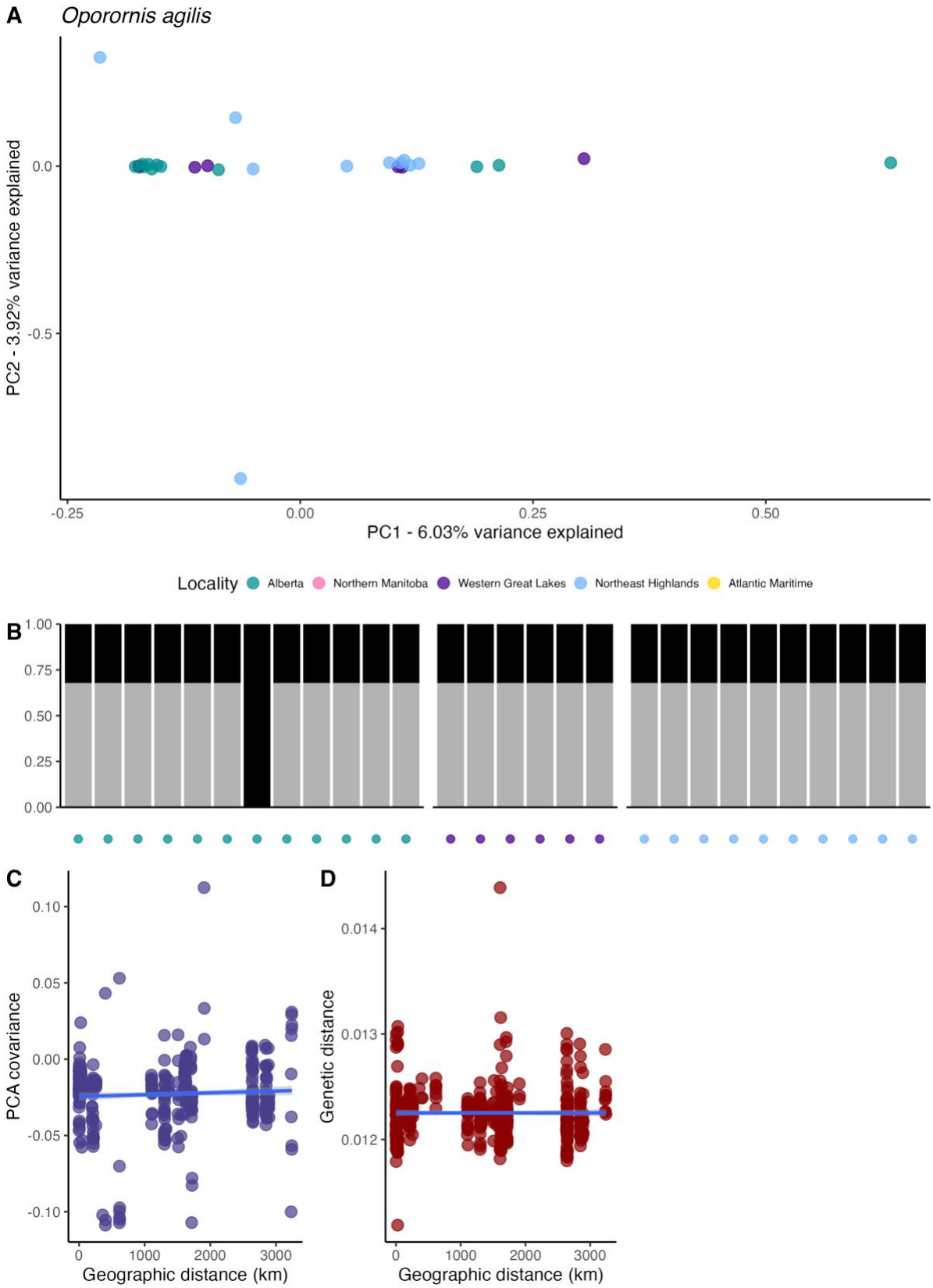

Appendix Figure B.3-26. Spatial genetic patterns for *Oporornis agilis*.

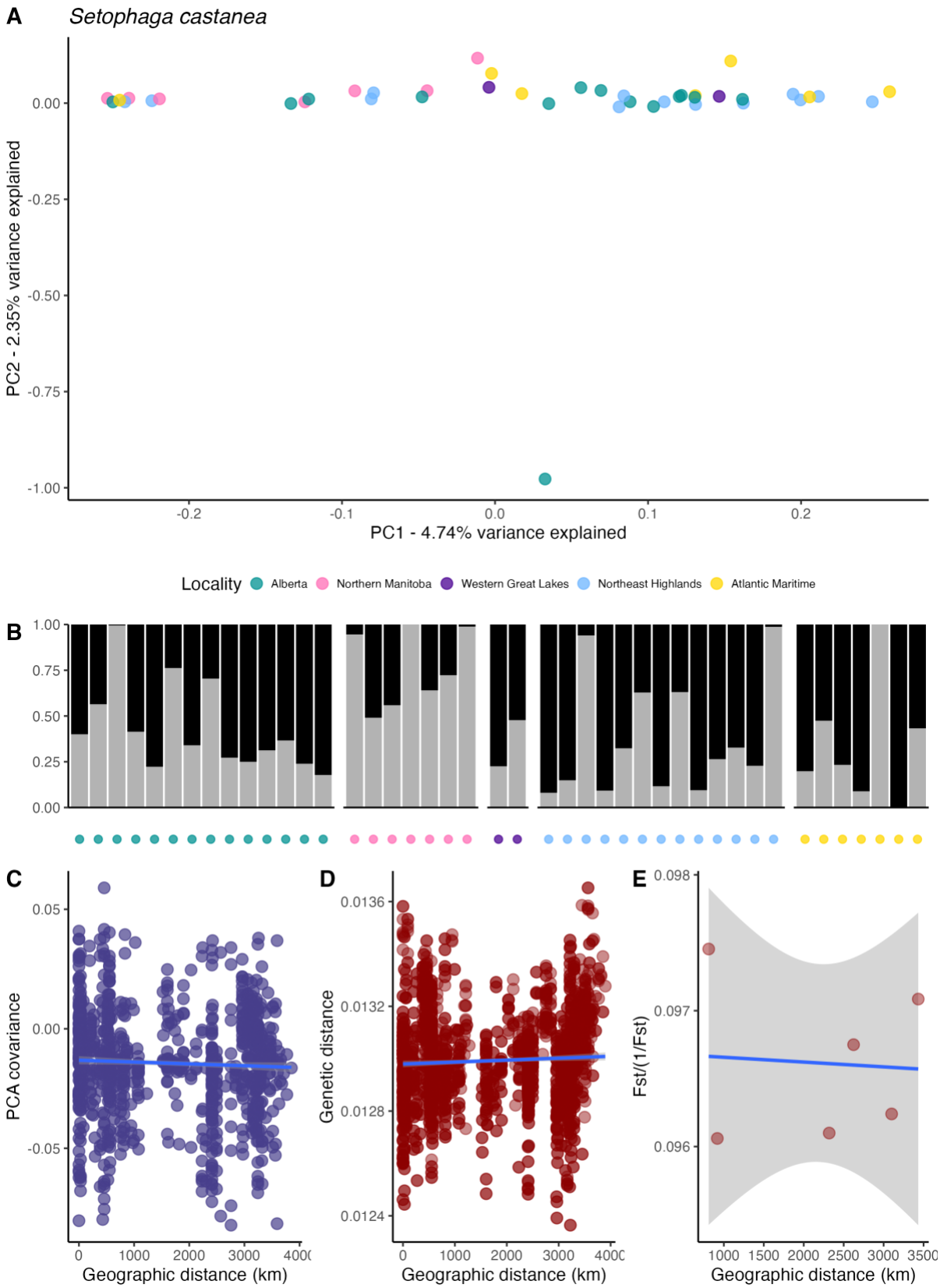

Appendix Figure B.3-27. Spatial genetic patterns for *Setophaga castanea*.

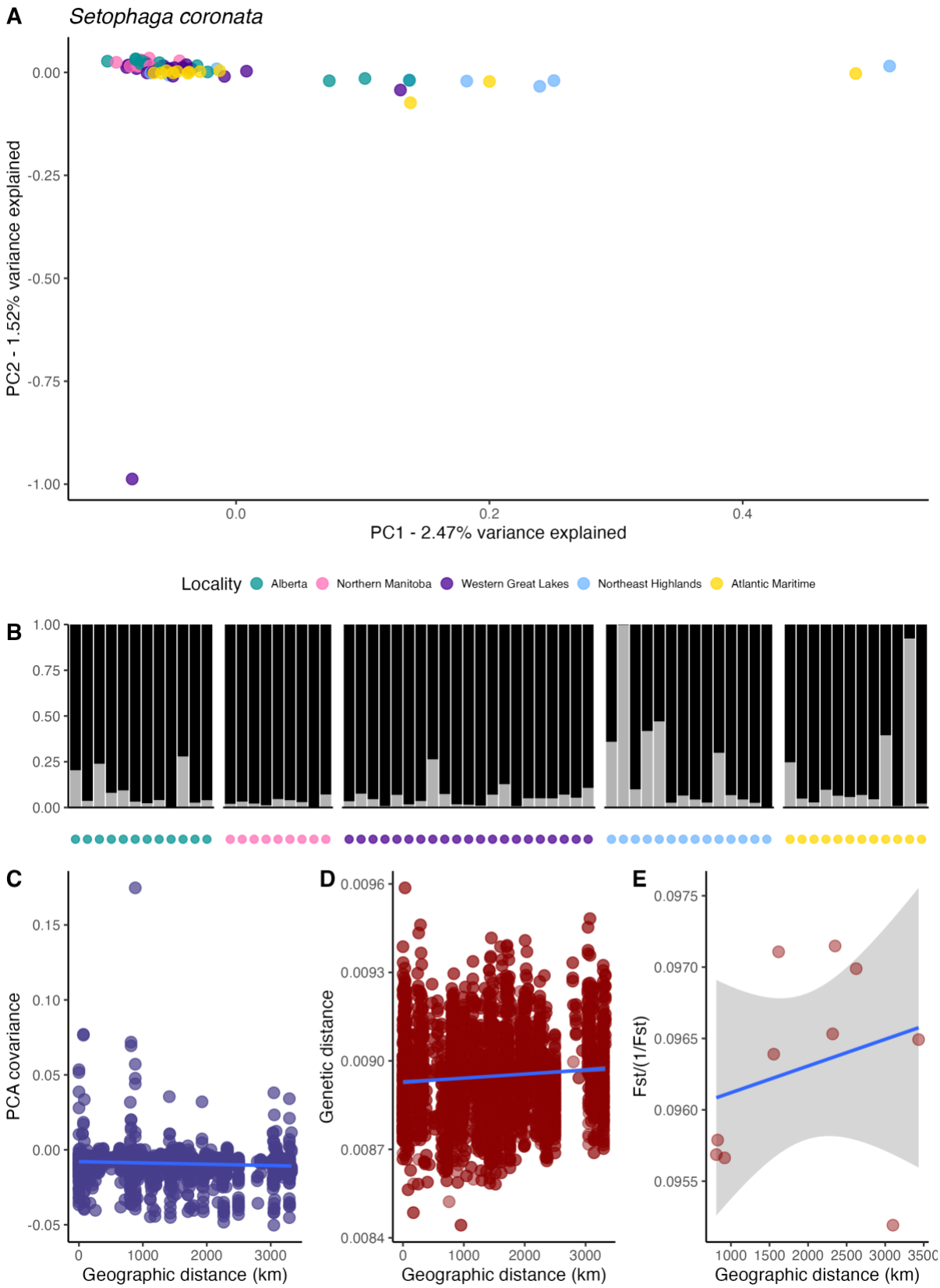

Appendix Figure B.3-28. Spatial genetic patterns for *Setophaga coronata*.

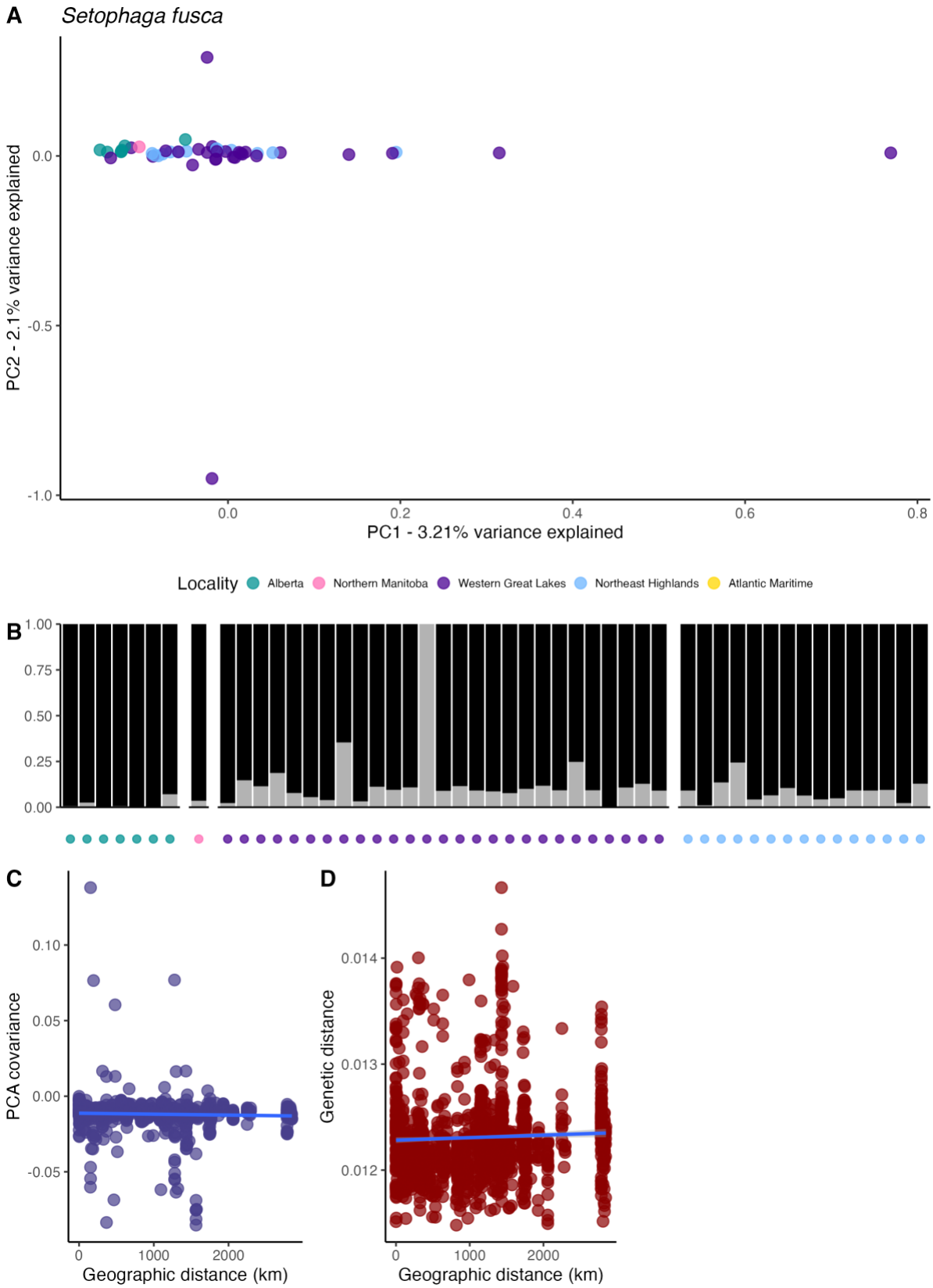

Appendix Figure B.3-29. Spatial genetic patterns for *Setophaga fusca*.

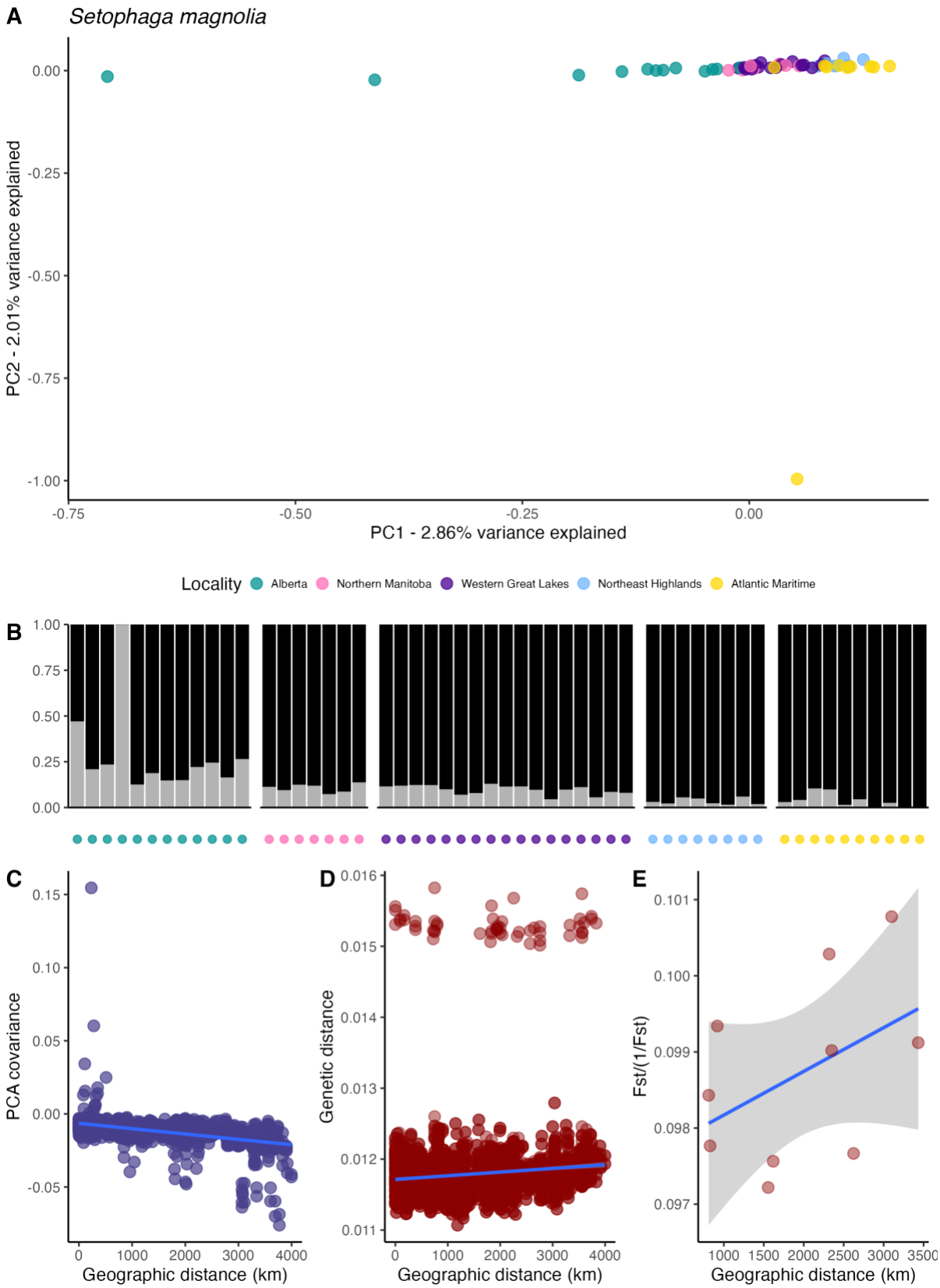

Appendix Figure B.3-30. Spatial genetic patterns for *Setophaga magnolia*.

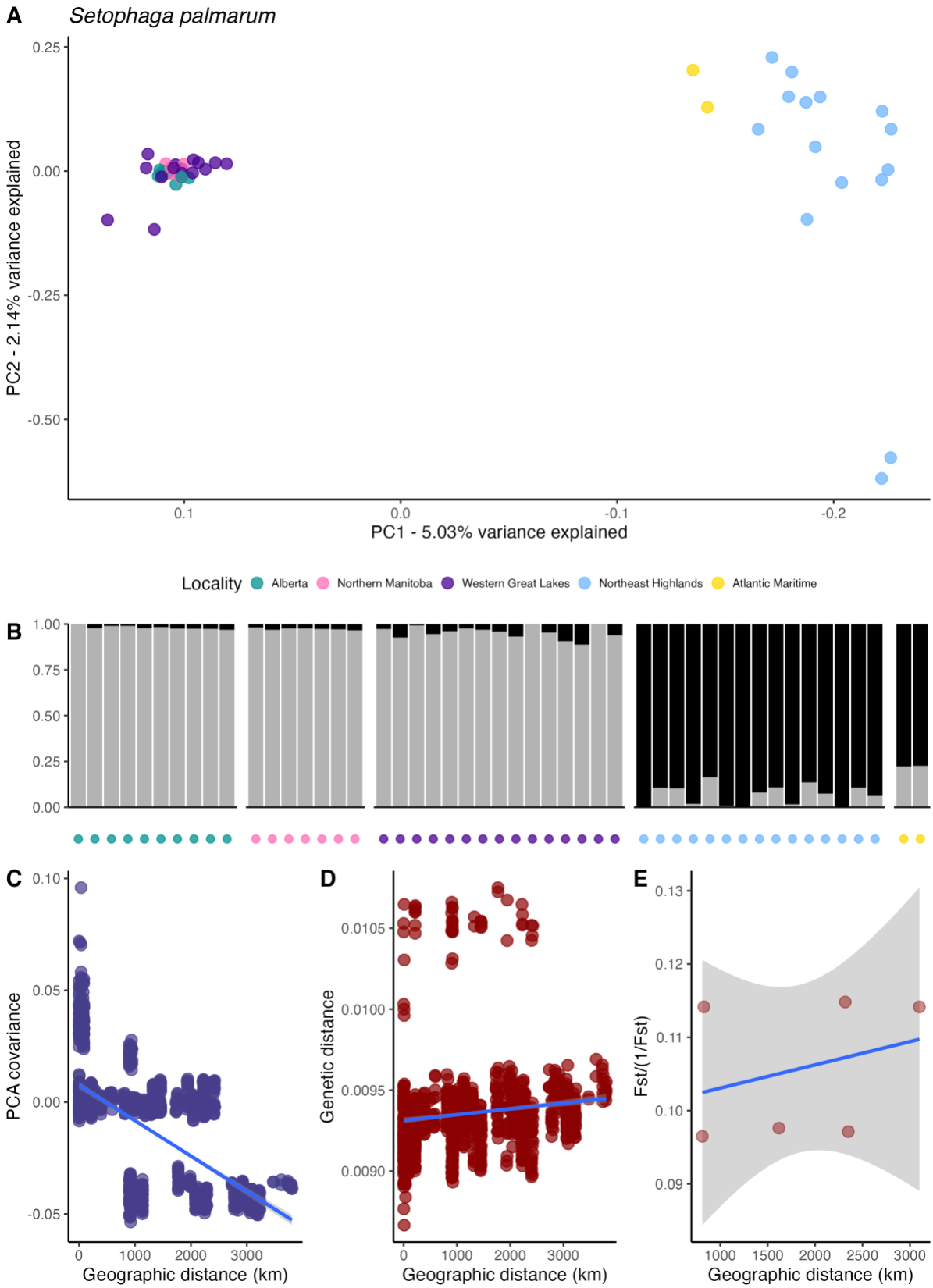

Appendix Figure B.3-31. Spatial genetic patterns for *Setophaga palmarum*.

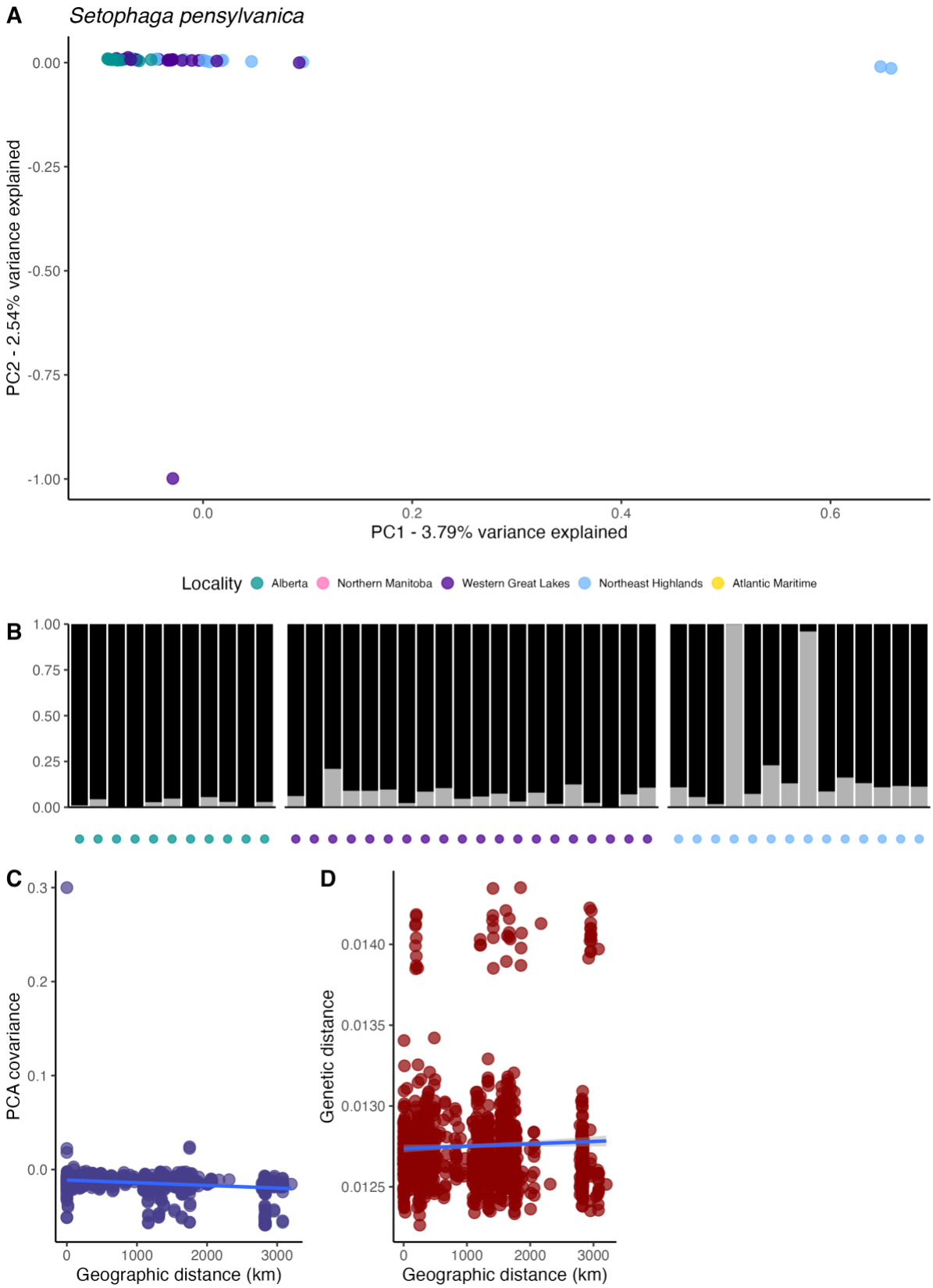

Appendix Figure B.3-32. Spatial genetic patterns for *Setophaga pensylvanica*.

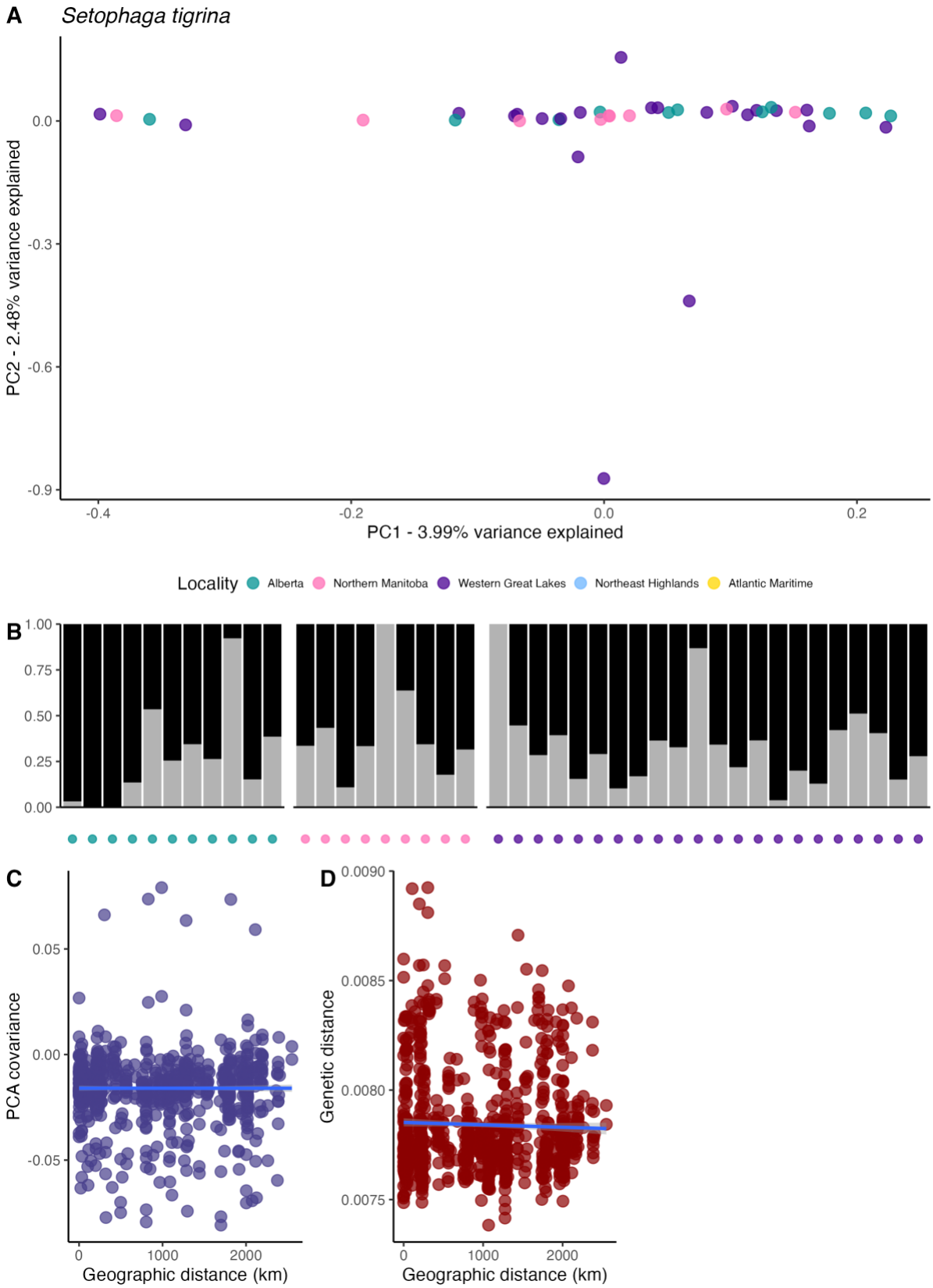

Appendix Figure B.3-33. Spatial genetic patterns for *Setophaga tigrina*.

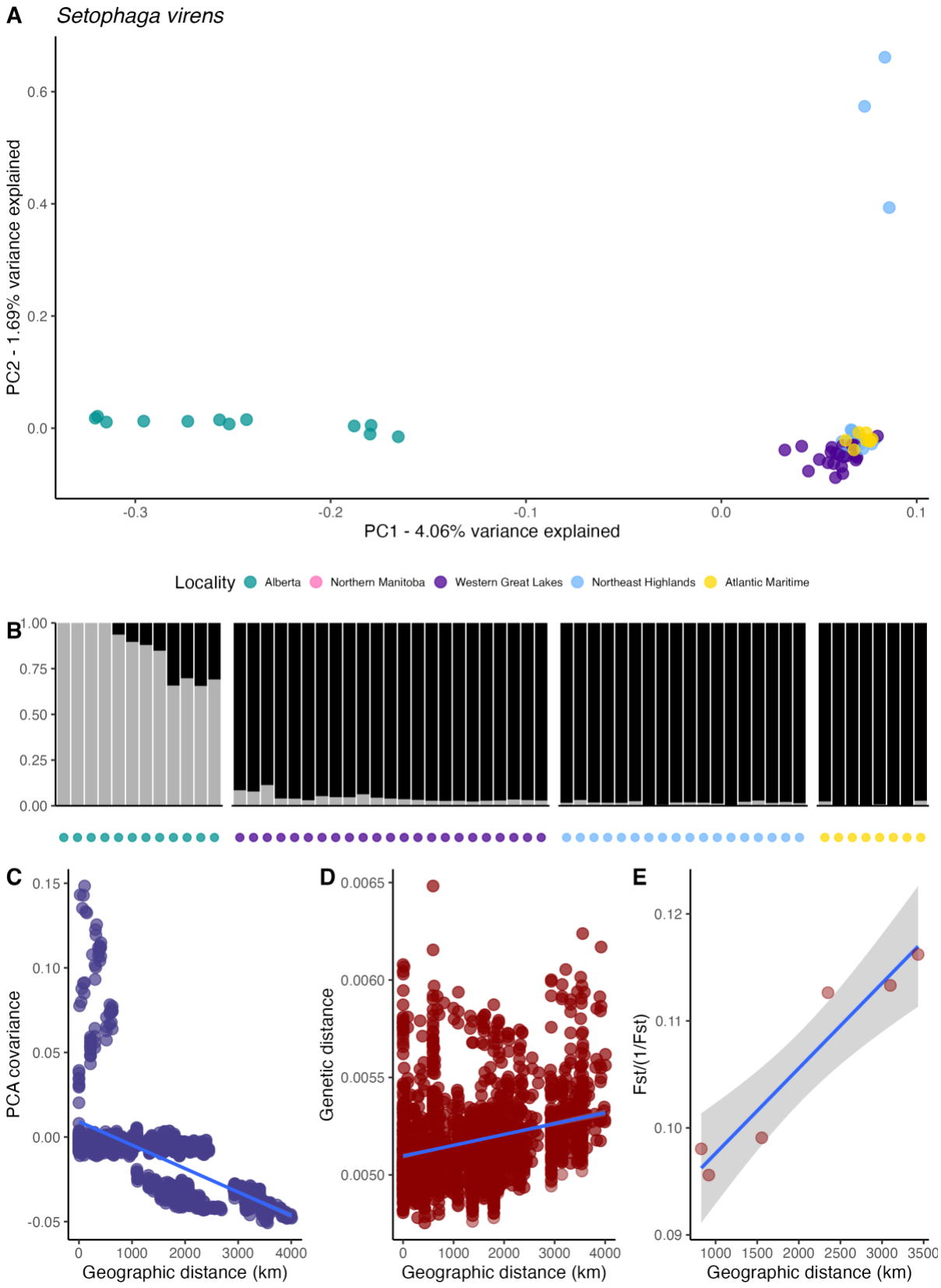

Appendix Figure B.3-34. Spatial genetic patterns for *Setophaga virens*.

B.4 Results of modeling with PGLS

Appendix Table B.4-1. Phylogenetic generalized least squares model selection results for sets of models predicting each version of IBD. These PGLS models used a phylogenetic covariance matrix based on a Brownian motion model. Response variables (the different versions of IBD) are indicated in bold above their respective model sets. The "type" column describes which set of predictors were included in each model. Model coefficients are listed with their standard error in parentheses within the column corresponding to each predictor. Model comparison with AICc indicates that the θ predictor improves model fit over the null model in the model predicting F_{st} IBD.

Type	Migration Status: migratory	Migration Distance	θ_π	logLik	AICc	∂AICc	Weight	Sample size
PCA covariance IBD								
null				98.19	-192.0	0.00	0.686	34
θ_π			-0.00052 (0.0024)	98.21	-189.6	2.36	0.211	34
migration	0.011 (0.013)	-0.00062 (0.0027)		98.56	-187.7	4.25	0.082	34
migration + θ_π	0.011 (0.014)	-0.000088 (0.0036)	-0.00074 (0.0032)	98.59	-185.0	6.95	0.021	34
Genetic distance IBD								
null				-50.86	106.1	0.00	0.662	34
θ_π			0.018 (0.019)	-50.67	108.1	2.04	0.238	34
migration	-0.13 (0.11)	0.00089 (0.022)		-50.49	110.3	4.25	0.079	34
migration + θ_π	-0.12 (0.11)	-0.025 (0.028)	0.036 (0.025)	-50.44	113.0	6.93	0.021	34
Fst IBD								
θ_π			-0.0023 (0.0011)	85.74	-164.2	0.00	0.636	23
null				83.62	-162.6	1.58	0.288	23
migration + θ_π	0.0035 (0.0060)	0.00062 (0.0020)	-0.0028 (0.0016)	86.10	-158.7	5.56	0.040	23
migration	0.0041 (0.0063)	-0.0018 (0.0016)		84.35	-158.5	5.75	0.036	23

B.5 F_{st} between sampling regions

Appendix Table B.5-1. Pairwise F_{st} values between sampling regions are presented for each species. F_{st} values are the "weighted" output from ANGSD using the Reynolds 1983 estimator. Each sampling region (shown in Reg1 and Reg2 columns) is represented by 3 samples.
Sampling region abbreviations:
AB=Alberta
NMB=Northern Manitoba
WGL=Western Great Lakes
NEH=Northeastern Highlands
AM=Atlantic Maritime

Species	Reg1	Reg2	Lat1	Lat2	Lon1	Lon2	Geo distance Km	Fst
Picoides arcticus	AB	NEH	55.2724	44.2239	-114.7801	-74.4641	3100	0.075
Picoides arcticus	AB	NMB	55.2724	55.4859	-114.7801	-101.9826	810	0.074
Picoides arcticus	AB	WGL	55.2724	45.8222	-114.7801	-84.729	2350	0.098
Picoides arcticus	NEH	NMB	44.2239	55.4859	-74.4641	-101.9826	2318	0.083
Picoides arcticus	NEH	WGL	44.2239	45.8222	-74.4641	-84.729	828	0.088
Picoides arcticus	NMB	WGL	55.4859	45.8222	-101.9826	-84.729	1618	0.101
Dryobates villosus	AB	NEH	55.2724	44.2239	-114.7801	-74.4641	3100	0.095
Dryobates villosus	AB	WGL	55.2724	45.8222	-114.7801	-84.729	2350	0.089
Dryobates villosus	NEH	WGL	44.2239	45.8222	-74.4641	-84.729	828	0.086
Sphyrapicus varius	AB	NEH	55.2724	44.2239	-114.7801	-74.4641	3100	0.090
Sphyrapicus varius	AB	NMB	55.2724	55.4859	-114.7801	-101.9826	810	0.089
Sphyrapicus varius	AB	WGL	55.2724	45.8222	-114.7801	-84.729	2350	0.084
Sphyrapicus varius	NEH	NMB	44.2239	55.4859	-74.4641	-101.9826	2318	0.092
Sphyrapicus varius	NEH	WGL	44.2239	45.8222	-74.4641	-84.729	828	0.090
Sphyrapicus varius	NMB	WGL	55.4859	45.8222	-101.9826	-84.729	1618	0.089
Empidonax alnorum	AB	AM	55.2724	48.9131	-114.7801	-64.5836	3433	0.092
Empidonax alnorum	AB	NEH	55.2724	44.2239	-114.7801	-74.4641	3100	0.094
Empidonax alnorum	AB	WGL	55.2724	45.8222	-114.7801	-84.729	2350	0.093
Empidonax alnorum	AM	NEH	48.9131	44.2239	-64.5836	-74.4641	918	0.096
Empidonax alnorum	AM	WGL	48.9131	45.8222	-64.5836	-84.729	1555	0.098
Empidonax alnorum	NEH	WGL	44.2239	45.8222	-74.4641	-84.729	828	0.096
Empidonax flaviventris	AB	AM	55.2724	48.9131	-114.7801	-64.5836	3433	0.088
Empidonax flaviventris	AB	NEH	55.2724	44.2239	-114.7801	-74.4641	3100	0.091
Empidonax flaviventris	AB	WGL	55.2724	45.8222	-114.7801	-84.729	2350	0.091

Empidonax flaviventris	AM	NEH	48.9131	44.2239	-64.5836	-74.4641	918	0.092
Empidonax flaviventris	AM	WGL	48.9131	45.8222	-64.5836	-84.729	1555	0.091
Empidonax flaviventris	NEH	WGL	44.2239	45.8222	-74.4641	-84.729	828	0.086
Empidonax minimus	AB	NEH	55.2724	44.2239	-114.7801	-74.4641	3100	0.096
Empidonax minimus	AB	NMB	55.2724	55.4859	-114.7801	-101.9826	810	0.095
Empidonax minimus	AB	WGL	55.2724	45.8222	-114.7801	-84.729	2350	0.095
Empidonax minimus	NEH	NMB	44.2239	55.4859	-74.4641	-101.9826	2318	0.102
Empidonax minimus	NEH	WGL	44.2239	45.8222	-74.4641	-84.729	828	0.096
Empidonax minimus	NMB	WGL	55.4859	45.8222	-101.9826	-84.729	1618	0.105
Vireo olivaceus	AB	NEH	55.2724	44.2239	-114.7801	-74.4641	3100	0.085
Vireo olivaceus	AB	WGL	55.2724	45.8222	-114.7801	-84.729	2350	0.097
Vireo olivaceus	NEH	WGL	44.2239	45.8222	-74.4641	-84.729	828	0.096
Vireo philadelphicus	AB	AM	55.2724	48.9131	-114.7801	-64.5836	3433	0.091
Vireo philadelphicus	AB	NMB	55.2724	55.4859	-114.7801	-101.9826	810	0.088
Vireo philadelphicus	AM	NMB	48.9131	55.4859	-64.5836	-101.9826	2624	0.089
Vireo solitarius	AB	NEH	55.2724	44.2239	-114.7801	-74.4641	3100	0.092
Vireo solitarius	AB	NMB	55.2724	55.4859	-114.7801	-101.9826	810	0.092
Vireo solitarius	AB	WGL	55.2724	45.8222	-114.7801	-84.729	2350	0.087
Vireo solitarius	NEH	NMB	44.2239	55.4859	-74.4641	-101.9826	2318	0.091
Vireo solitarius	NEH	WGL	44.2239	45.8222	-74.4641	-84.729	828	0.091
Vireo solitarius	NMB	WGL	55.4859	45.8222	-101.9826	-84.729	1618	0.081
Poecile atricapillus	AB	NEH	55.2724	44.2239	-114.7801	-74.4641	3100	0.099
Poecile atricapillus	AB	NMB	55.2724	55.4859	-114.7801	-101.9826	810	0.089
Poecile atricapillus	AB	WGL	55.2724	45.8222	-114.7801	-84.729	2350	0.097
Poecile atricapillus	NEH	NMB	44.2239	55.4859	-74.4641	-101.9826	2318	0.097
Poecile atricapillus	NEH	WGL	44.2239	45.8222	-74.4641	-84.729	828	0.094
Poecile atricapillus	NMB	WGL	55.4859	45.8222	-101.9826	-84.729	1618	0.091
Poecile hudsonicus	AB	AM	55.2724	48.9131	-114.7801	-64.5836	3433	0.089
Poecile hudsonicus	AB	NEH	55.2724	44.2239	-114.7801	-74.4641	3100	0.097
Poecile hudsonicus	AB	NMB	55.2724	55.4859	-114.7801	-101.9826	810	0.081
Poecile hudsonicus	AB	WGL	55.2724	45.8222	-114.7801	-84.729	2350	0.087
Poecile hudsonicus	AM	NEH	48.9131	44.2239	-64.5836	-74.4641	918	0.087
Poecile hudsonicus	AM	NMB	48.9131	55.4859	-64.5836	-101.9826	2624	0.083
Poecile hudsonicus	AM	WGL	48.9131	45.8222	-64.5836	-84.729	1555	0.093

Poecile hudsonicus	NEH	NMB	44.2239	55.4859	-74.4641	-101.9826	2318	0.094
Poecile hudsonicus	NEH	WGL	44.2239	45.8222	-74.4641	-84.729	828	0.099
Poecile hudsonicus	NMB	WGL	55.4859	45.8222	-101.9826	-84.729	1618	0.089
Corthylio calendula	AB	AM	55.2724	48.9131	-114.7801	-64.5836	3433	0.083
Corthylio calendula	AB	NEH	55.2724	44.2239	-114.7801	-74.4641	3100	0.086
Corthylio calendula	AB	NMB	55.2724	55.4859	-114.7801	-101.9826	810	0.078
Corthylio calendula	AB	WGL	55.2724	45.8222	-114.7801	-84.729	2350	0.079
Corthylio calendula	AM	NEH	48.9131	44.2239	-64.5836	-74.4641	918	0.082
Corthylio calendula	AM	NMB	48.9131	55.4859	-64.5836	-101.9826	2624	0.083
Corthylio calendula	AM	WGL	48.9131	45.8222	-64.5836	-84.729	1555	0.083
Corthylio calendula	NEH	NMB	44.2239	55.4859	-74.4641	-101.9826	2318	0.081
Corthylio calendula	NEH	WGL	44.2239	45.8222	-74.4641	-84.729	828	0.086
Corthylio calendula	NMB	WGL	55.4859	45.8222	-101.9826	-84.729	1618	0.085
Regulus satrapa	AB	AM	55.2724	48.9131	-114.7801	-64.5836	3433	0.101
Regulus satrapa	AB	NEH	55.2724	44.2239	-114.7801	-74.4641	3100	0.095
Regulus satrapa	AB	WGL	55.2724	45.8222	-114.7801	-84.729	2350	0.103
Regulus satrapa	AM	NEH	48.9131	44.2239	-64.5836	-74.4641	918	0.092
Regulus satrapa	AM	WGL	48.9131	45.8222	-64.5836	-84.729	1555	0.090
Regulus satrapa	NEH	WGL	44.2239	45.8222	-74.4641	-84.729	828	0.084
Certhia americana	AB	AM	55.2724	48.9131	-114.7801	-64.5836	3433	0.088
Certhia americana	AB	NEH	55.2724	44.2239	-114.7801	-74.4641	3100	0.088
Certhia americana	AB	WGL	55.2724	45.8222	-114.7801	-84.729	2350	0.088
Certhia americana	AM	NEH	48.9131	44.2239	-64.5836	-74.4641	918	0.090
Certhia americana	AM	WGL	48.9131	45.8222	-64.5836	-84.729	1555	0.089
Certhia americana	NEH	WGL	44.2239	45.8222	-74.4641	-84.729	828	0.092
Troglodytes hiemalis	AB	NEH	55.2724	44.2239	-114.7801	-74.4641	3100	0.088
Troglodytes hiemalis	AB	WGL	55.2724	45.8222	-114.7801	-84.729	2350	0.088
Troglodytes hiemalis	NEH	WGL	44.2239	45.8222	-74.4641	-84.729	828	0.091
Catharus fuscescens	NEH	WGL	44.2239	45.8222	-74.4641	-84.729	828	0.091
Catharus guttatus	AB	AM	55.2724	48.9131	-114.7801	-64.5836	3433	0.087
Catharus guttatus	AB	NEH	55.2724	44.2239	-114.7801	-74.4641	3100	0.092
Catharus guttatus	AB	NMB	55.2724	55.4859	-114.7801	-101.9826	810	0.084
Catharus guttatus	AB	WGL	55.2724	45.8222	-114.7801	-84.729	2350	0.087
Catharus guttatus	AM	NEH	48.9131	44.2239	-64.5836	-74.4641	918	0.086
Catharus guttatus	AM	NMB	48.9131	55.4859	-64.5836	-101.9826	2624	0.087
Catharus guttatus	AM	WGL	48.9131	45.8222	-64.5836	-84.729	1555	0.087

Catharus guttatus	NEH	NMB	44.2239	55.4859	-74.4641	-101.9826	2318	0.089
Catharus guttatus	NEH	WGL	44.2239	45.8222	-74.4641	-84.729	828	0.087
Catharus guttatus	NMB	WGL	55.4859	45.8222	-101.9826	-84.729	1618	0.083
Catharus ustulatus	AB	AM	55.2724	48.9131	-114.7801	-64.5836	3433	0.085
Catharus ustulatus	AB	NEH	55.2724	44.2239	-114.7801	-74.4641	3100	0.082
Catharus ustulatus	AB	NMB	55.2724	55.4859	-114.7801	-101.9826	810	0.080
Catharus ustulatus	AB	WGL	55.2724	45.8222	-114.7801	-84.729	2350	0.085
Catharus ustulatus	AM	NEH	48.9131	44.2239	-64.5836	-74.4641	918	0.084
Catharus ustulatus	AM	NMB	48.9131	55.4859	-64.5836	-101.9826	2624	0.081
Catharus ustulatus	AM	WGL	48.9131	45.8222	-64.5836	-84.729	1555	0.088
Catharus ustulatus	NEH	NMB	44.2239	55.4859	-74.4641	-101.9826	2318	0.083
Catharus ustulatus	NEH	WGL	44.2239	45.8222	-74.4641	-84.729	828	0.083
Catharus ustulatus	NMB	WGL	55.4859	45.8222	-101.9826	-84.729	1618	0.082
Junco hyemalis	AB	AM	55.2724	48.9131	-114.7801	-64.5836	3433	0.092
Junco hyemalis	AB	NEH	55.2724	44.2239	-114.7801	-74.4641	3100	0.091
Junco hyemalis	AB	NMB	55.2724	55.4859	-114.7801	-101.9826	810	0.090
Junco hyemalis	AB	WGL	55.2724	45.8222	-114.7801	-84.729	2350	0.090
Junco hyemalis	AM	NEH	48.9131	44.2239	-64.5836	-74.4641	918	0.093
Junco hyemalis	AM	NMB	48.9131	55.4859	-64.5836	-101.9826	2624	0.088
Junco hyemalis	AM	WGL	48.9131	45.8222	-64.5836	-84.729	1555	0.090
Junco hyemalis	NEH	NMB	44.2239	55.4859	-74.4641	-101.9826	2318	0.092
Junco hyemalis	NEH	WGL	44.2239	45.8222	-74.4641	-84.729	828	0.089
Junco hyemalis	NMB	WGL	55.4859	45.8222	-101.9826	-84.729	1618	0.087
Melospiza lincolnii	AB	NEH	55.2724	44.2239	-114.7801	-74.4641	3100	0.085
Melospiza lincolnii	AB	NMB	55.2724	55.4859	-114.7801	-101.9826	810	0.086
Melospiza lincolnii	AB	WGL	55.2724	45.8222	-114.7801	-84.729	2350	0.085
Melospiza lincolnii	NEH	NMB	44.2239	55.4859	-74.4641	-101.9826	2318	0.089
Melospiza lincolnii	NEH	WGL	44.2239	45.8222	-74.4641	-84.729	828	0.085
Melospiza lincolnii	NMB	WGL	55.4859	45.8222	-101.9826	-84.729	1618	0.084
Zonotrichia albicollis	AB	AM	55.2724	48.9131	-114.7801	-64.5836	3433	0.094
Zonotrichia albicollis	AB	NEH	55.2724	44.2239	-114.7801	-74.4641	3100	0.088
Zonotrichia albicollis	AB	NMB	55.2724	55.4859	-114.7801	-101.9826	810	0.087
Zonotrichia albicollis	AB	WGL	55.2724	45.8222	-114.7801	-84.729	2350	0.089
Zonotrichia albicollis	AM	NEH	48.9131	44.2239	-64.5836	-74.4641	918	0.088

Zonotrichia albicollis	AM	NMB	48.9131	55.4859	-64.5836	-101.9826	2624	0.089
Zonotrichia albicollis	AM	WGL	48.9131	45.8222	-64.5836	-84.729	1555	0.089
Zonotrichia albicollis	NEH	NMB	44.2239	55.4859	-74.4641	-101.9826	2318	0.084
Zonotrichia albicollis	NEH	WGL	44.2239	45.8222	-74.4641	-84.729	828	0.084
Zonotrichia albicollis	NMB	WGL	55.4859	45.8222	-101.9826	-84.729	1618	0.089
Cardellina canadensis	AB	NEH	55.2724	44.2239	-114.7801	-74.4641	3100	0.084
Cardellina canadensis	AB	WGL	55.2724	45.8222	-114.7801	-84.729	2350	0.089
Cardellina canadensis	NEH	WGL	44.2239	45.8222	-74.4641	-84.729	828	0.083
Geothlypis philadelphia	AB	NEH	55.2724	44.2239	-114.7801	-74.4641	3100	0.090
Geothlypis philadelphia	AB	WGL	55.2724	45.8222	-114.7801	-84.729	2350	0.088
Geothlypis philadelphia	NEH	WGL	44.2239	45.8222	-74.4641	-84.729	828	0.089
Leiothlypis peregrina	AB	AM	55.2724	48.9131	-114.7801	-64.5836	3433	0.088
Leiothlypis peregrina	AB	NMB	55.2724	55.4859	-114.7801	-101.9826	810	0.088
Leiothlypis peregrina	AB	WGL	55.2724	45.8222	-114.7801	-84.729	2350	0.088
Leiothlypis peregrina	AM	NMB	48.9131	55.4859	-64.5836	-101.9826	2624	0.089
Leiothlypis peregrina	AM	WGL	48.9131	45.8222	-64.5836	-84.729	1555	0.087
Leiothlypis peregrina	NMB	WGL	55.4859	45.8222	-101.9826	-84.729	1618	0.092
Leiothlypis ruficapilla	AB	AM	55.2724	48.9131	-114.7801	-64.5836	3433	0.091
Leiothlypis ruficapilla	AB	NEH	55.2724	44.2239	-114.7801	-74.4641	3100	0.092
Leiothlypis ruficapilla	AB	WGL	55.2724	45.8222	-114.7801	-84.729	2350	0.089
Leiothlypis ruficapilla	AM	NEH	48.9131	44.2239	-64.5836	-74.4641	918	0.092
Leiothlypis ruficapilla	AM	WGL	48.9131	45.8222	-64.5836	-84.729	1555	0.093
Leiothlypis ruficapilla	NEH	WGL	44.2239	45.8222	-74.4641	-84.729	828	0.091

Oporornis agilis	AB	NEH	55.2724	44.2239	-114.7801	-74.4641	3100	0.085
Oporornis agilis	AB	WGL	55.2724	45.8222	-114.7801	-84.729	2350	0.088
Oporornis agilis	NEH	WGL	44.2239	45.8222	-74.4641	-84.729	828	0.091
Setophaga castanea	AB	AM	55.2724	48.9131	-114.7801	-64.5836	3433	0.088
Setophaga castanea	AB	NEH	55.2724	44.2239	-114.7801	-74.4641	3100	0.088
Setophaga castanea	AB	NMB	55.2724	55.4859	-114.7801	-101.9826	810	0.085
Setophaga castanea	AM	NEH	48.9131	44.2239	-64.5836	-74.4641	918	0.088
Setophaga castanea	AM	NMB	48.9131	55.4859	-64.5836	-101.9826	2624	0.088
Setophaga castanea	NEH	NMB	44.2239	55.4859	-74.4641	-101.9826	2318	0.088
Setophaga coronata	AB	AM	55.2724	48.9131	-114.7801	-64.5836	3433	0.088
Setophaga coronata	AB	NEH	55.2724	44.2239	-114.7801	-74.4641	3100	0.088
Setophaga coronata	AB	NMB	55.2724	55.4859	-114.7801	-101.9826	810	0.089
Setophaga coronata	AB	WGL	55.2724	45.8222	-114.7801	-84.729	2350	0.093
Setophaga coronata	AM	NEH	48.9131	44.2239	-64.5836	-74.4641	918	0.087
Setophaga coronata	AM	NMB	48.9131	55.4859	-64.5836	-101.9826	2624	0.087
Setophaga coronata	AM	WGL	48.9131	45.8222	-64.5836	-84.729	1555	0.090
Setophaga coronata	NEH	NMB	44.2239	55.4859	-74.4641	-101.9826	2318	0.087
Setophaga coronata	NEH	WGL	44.2239	45.8222	-74.4641	-84.729	828	0.093
Setophaga coronata	NMB	WGL	55.4859	45.8222	-101.9826	-84.729	1618	0.090
Setophaga fusca	AB	NEH	55.2724	44.2239	-114.7801	-74.4641	3100	0.087
Setophaga fusca	AB	WGL	55.2724	45.8222	-114.7801	-84.729	2350	0.090
Setophaga fusca	NEH	WGL	44.2239	45.8222	-74.4641	-84.729	828	0.085
Setophaga magnolia	AB	AM	55.2724	48.9131	-114.7801	-64.5836	3433	0.091
Setophaga magnolia	AB	NEH	55.2724	44.2239	-114.7801	-74.4641	3100	0.095
Setophaga magnolia	AB	NMB	55.2724	55.4859	-114.7801	-101.9826	810	0.090
Setophaga magnolia	AB	WGL	55.2724	45.8222	-114.7801	-84.729	2350	0.090
Setophaga magnolia	AM	NEH	48.9131	44.2239	-64.5836	-74.4641	918	0.090
Setophaga magnolia	AM	NMB	48.9131	55.4859	-64.5836	-101.9826	2624	0.089
Setophaga magnolia	AM	WGL	48.9131	45.8222	-64.5836	-84.729	1555	0.089
Setophaga magnolia	NEH	NMB	44.2239	55.4859	-74.4641	-101.9826	2318	0.091
Setophaga magnolia	NEH	WGL	44.2239	45.8222	-74.4641	-84.729	828	0.088
Setophaga magnolia	NMB	WGL	55.4859	45.8222	-101.9826	-84.729	1618	0.088
Setophaga palmarum	AB	NEH	55.2724	44.2239	-114.7801	-74.4641	3100	0.104
Setophaga palmarum	AB	NMB	55.2724	55.4859	-114.7801	-101.9826	810	0.089
Setophaga palmarum	AB	WGL	55.2724	45.8222	-114.7801	-84.729	2350	0.089

Setophaga palmarum	NEH	NMB	44.2239	55.4859	-74.4641	-101.9826	2318	0.100
Setophaga palmarum	NEH	WGL	44.2239	45.8222	-74.4641	-84.729	828	0.101
Setophaga palmarum	NMB	WGL	55.4859	45.8222	-101.9826	-84.729	1618	0.091
Setophaga pensylvanica	AB	NEH	55.2724	44.2239	-114.7801	-74.4641	3100	0.088
Setophaga pensylvanica	AB	WGL	55.2724	45.8222	-114.7801	-84.729	2350	0.090
Setophaga pensylvanica	NEH	WGL	44.2239	45.8222	-74.4641	-84.729	828	0.087
Setophaga tigrina	AB	NMB	55.2724	55.4859	-114.7801	-101.9826	810	0.080
Setophaga tigrina	AB	WGL	55.2724	45.8222	-114.7801	-84.729	2350	0.083
Setophaga tigrina	NMB	WGL	55.4859	45.8222	-101.9826	-84.729	1618	0.081
Setophaga virens	AB	AM	55.2724	48.9131	-114.7801	-64.5836	3433	0.108
Setophaga virens	AB	NEH	55.2724	44.2239	-114.7801	-74.4641	3100	0.099
Setophaga virens	AB	WGL	55.2724	45.8222	-114.7801	-84.729	2350	0.105
Setophaga virens	AM	NEH	48.9131	44.2239	-64.5836	-74.4641	918	0.087
Setophaga virens	AM	WGL	48.9131	45.8222	-64.5836	-84.729	1555	0.094
Setophaga virens	NEH	WGL	44.2239	45.8222	-74.4641	-84.729	828	0.086

Appendix C Supplemental Material for Chapter 4

C.1 Supplemental figure for chapter 4

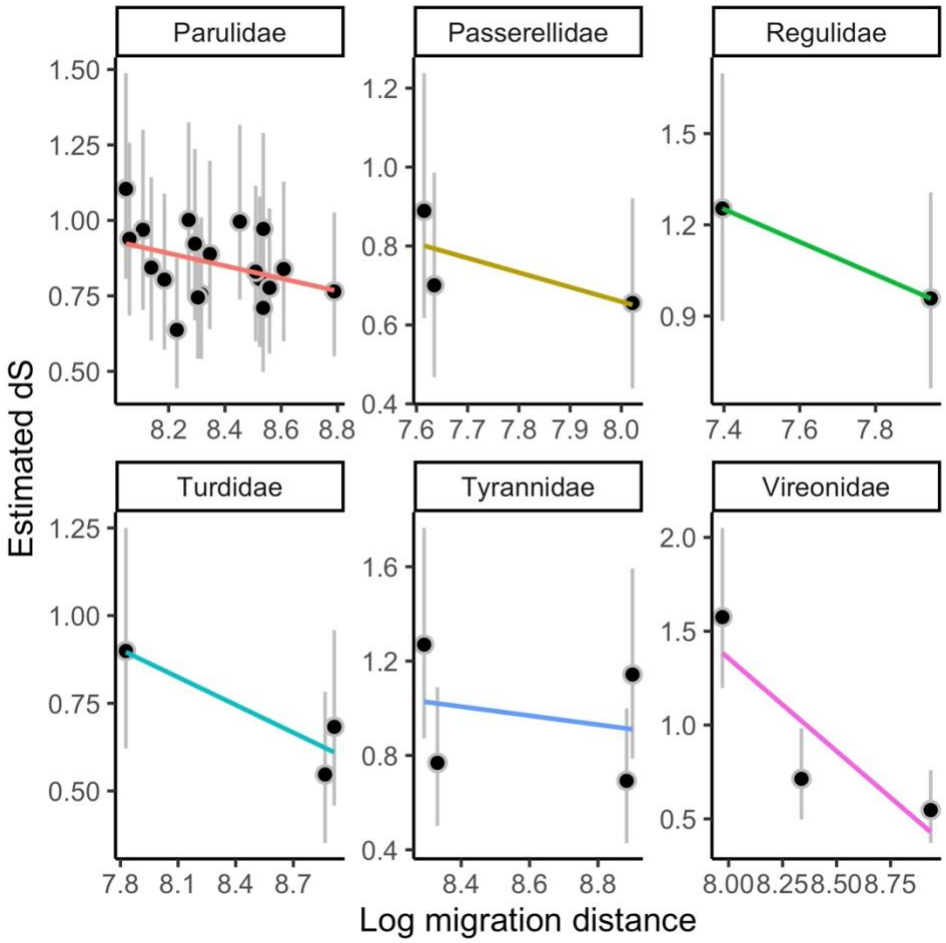

Appendix Figure C.1-1. The relationship between dS and migration distance within each family represented in our study by more than one species. Posterior mean tip estimates of dS (black dots) from Coevol are shown compared to migration distance (left), and mass (right) from models using our full species set. Gray vertical bars indicate 95% credible intervals for each estimate. Plotted lines use linear models to visualize the relationship between estimated tip dS and a given covariate within each family, demonstrating a consistently negative relationship between dS and migration distance within and among major clades in our system.

C.2 Table of species used in chapter 4

Appendix Table C.2-1. Species used in this study with information about previously-published GenBank sequences used during sample processing for each species (seed sequence provided to NOVOPlasty and mitochondrial coding sequences used for annotation with Geneious); data used in this study (mass and migration distance from sources described in the methods, θ as calculated in this study); the number of samples used to calculate population genetic summary statistics; posterior mean estimates of dS and dN/dS with upper and lower 95% credible intervals; and πN/πS estimates. Estimates of dS and dN/dS (and credible intervals) each come from one replicate of a Coevol model using the entire 39-species dataset and serve as representative estimates.

Species	Family	NOVOPlasty Seed Sequence	Geneious Annotation Dataset	Mass	Migration distance	θ	Population dataset size	dS	dS uci	dS lci	dN/dS	dN/dS uci	dN/dS lci	piN/piS
Cardellina canadensis	Parulidae	GU932128.1	NC_051027.1	10.42	5480	0.009827	27	0.838826	0.599611	1.12846	0.0203241	0.00837705	0.0365099	0.20921844
Catharus fuscescens	Turdidae	KY995091.1	MN356183.1	31.2	7429	0.010966	32	0.68279	0.457971	0.958956	0.0242271	0.00820784	0.0461707	0.14530011
Catharus guttatus	Turdidae	KY994761.1	MN356183.1	31	2511	0.006751	49	0.899237	0.621058	1.24995	0.0284658	0.010279	0.0516291	0.14435146
Catharus ustulatus	Turdidae	MG182754.1	MN356183.1	30.8	7082	0.018641	42	0.546945	0.351318	0.782981	0.0149716	0.00401427	0.030701	0.12266583
Empidonax alnorum	Tyrannidae	MG722574.1	NC_051025.1	12.79	7338	0.010982	22	1.14291	0.786774	1.59264	0.0474294	0.0216193	0.0788241	0.23075273
Empidonax flaviventris	Tyrannidae	MG722570.1	NC_051025.1	11.6	4148	0.015973	25	0.76852	0.501808	1.08921	0.0145421	0.00396384	0.0299008	0.15525913
Empidonax minimus	Tyrannidae	MG722577.1	NC_051025.1	10.3	3990	0.015729	23	1.26976	0.873056	1.76434	0.0406846	0.0178575	0.0694158	0.14712985
Geothlypis philadelphia	Parulidae	GU932107.1	NC_051027.1	12.61	5094	0.018803	31	0.710057	0.497549	0.967853	0.0135311	0.00477487	0.0259945	0.12439347
Junco hyemalis	Passerellidae	AF407044.1	NC_053110.1	19.89	2028	0.004623	44	0.889067	0.617124	1.23796	0.0305062	0.0125049	0.0538149	0.09974895
Leiothlypis peregrina	Parulidae	GU932133.1	NC_051027.1	10.02	4961	0.019542	31	0.830234	0.599365	1.1152	0.019793	0.00814448	0.0352215	0.1637438
Leiothlypis ruficapilla	Parulidae	MG686779.1	NC_051027.1	8.73	3423	0.027332	29	0.843644	0.601744	1.14293	0.0177523	0.00782966	0.0328033	0.08360634
Melospiza lincolnii	Passerellidae	DQ459535.1	NC_053110.1	17.4	3047	0.009129	43	0.655533	0.439407	0.920908	0.0370244	0.0115798	0.0686476	0.12078491
Oporornis agilis	Parulidae	GU932105.1	NC_051027.1	15.2	6559	0.004542	12	0.76465	0.549688	1.02677	0.0240992	0.0101664	0.0420661	0.25299145
Corthylio calendula	Regulidae	AY329435.1	NC_024866.1	6.68	2823	0.003458	31	0.958002	0.662535	1.30668	0.0435983	0.0177666	0.0726624	0.27098214
Regulus satrapa	Regulidae	AY136591.1	NC_024866.1	6.23	1629	0.019596	34	1.25354	0.884229	1.69857	0.0321083	0.0109379	0.0579177	0.06537048
Setophaga castanea	Parulidae	GU932076.1	NC_051027.1	12.59	5032	0.008056	26	0.80621	0.580767	1.07929	0.0170637	0.00669956	0.0320218	0.05966523
Setophaga coronata	Parulidae	GU932078.1	NC_051027.1	12.51	3127	0.015953	46	1.10434	0.805801	1.48785	0.0243574	0.0108242	0.0431281	0.04449572
Setophaga fusca	Parulidae	GU932086.1	NC_051027.1	9.7	5097	0.016563	39	0.9719	0.71744	1.28968	0.0240719	0.0112687	0.0414567	0.10701754
Setophaga magnolia	Parulidae	GU932089.1	NC_051027.1	8.72	4088	0.018339	42	0.754591	0.541051	1.00986	0.0203356	0.00752289	0.0373887	0.11847543
Setophaga palmarum	Parulidae	JN568655.1	NC_051027.1	10.3	3323	0.009104	43	0.968871	0.703293	1.30027	0.0213028	0.00900333	0.0383997	0.08351444
Setophaga pensylvanica	Parulidae	GU932093.1	NC_051027.1	9.64	3997	0.022577	36	0.922695	0.669312	1.23686	0.0157531	0.00655591	0.028837	0.08358069
Setophaga tigrina	Parulidae	JN568673.1	NC_051027.1	11	4688	0.011655	32	0.99595	0.738093	1.31621	0.0249487	0.011603	0.0428572	0.04954187
Setophaga virens	Parulidae	GU932102.1	NC_051027.1	8.8	3909	0.011991	39	1.00145	0.738681	1.32506	0.0279462	0.013107	0.04764	0.10294564
Sphyrapicus varius	Picidae	JF909891.1	KT119343.1	50.3	2893	0.009355	32	0.672255	0.39035	0.973128	0.0221766	0.00171547	0.0556067	0.13854167
Vireo olivaceus	Vireonidae	KM115367.1	NC_024869.1	16.7	7600	0.038373	46	0.546764	0.370849	0.759125	0.01526	0.00418827	0.0310671	0.06066081
Vireo solitarius	Vireonidae	KM115394.1	NC_024869.1	16.6	2896	0.016101	34	1.57508	1.19741	2.05021	0.0883793	0.0601106	0.121365	0.116431
Zonotrichia albicollis	Passerellidae	KJ455699.1	NC_053110.1	25.9	2069	0.019106	48	0.700496	0.467802	0.986183	0.0214357	0.00676031	0.0417646	0.10504545

C.3 Full model results

Appendix Table C.3-1 Full output from Coevol models with dS and dN as independent variables. Four models are summarized: two replicate models with the full dataset of 39 species, and two replicate models with the subset of 27 species with available estimates of θ. Each row contains a flattened pairwise matrix for each pair of variables (dS, dN, mass, migration distance, and θ), showing covariance, correlation coefficients, posterior probabilities of correlation coefficients, precisions, partial correlation coefficients, and posterior probabilities of partial correlation coefficients. Posterior probabilities near 0 indicate strong support for a negative relationship while posterior probabilities near 1 indicate strong support for a positive relationship. Values obtained from replicate models are highly similar.

Dataset	Independent variables	Rep	Parameter	dS-dS	dS-dN	dS-Mass	dS-MigDist	dS-Theta	dN-dN	dN-Mass	dN-MigDist	dN-Theta	Mass-Mass	Mass-MigDist	Mass-Theta	MigDist-MigDist	Migdist-Theta	Theta-Theta
Full 39 spp	dS and dN	1	Covariance	0.24	0.32	-0.11	-0.143	NA	2.49	-0.38	0.0915	NA	0.66	0.0138	NA	0.559	NA	NA
Full 39 spp	dS and dN	1	Correlation Coefficient	1	0.41	-0.28	-0.392	NA	1	-0.29	0.0679	NA	1	0.0252	NA	1	NA	NA
Full 39 spp	dS and dN	1	Cor. Coeff. Posterior Prob	NA	0.96	0.065	0.017	NA	NA	0.15	0.61	NA	NA	0.56	NA	NA	NA	NA
Full 39 spp	dS and dN	1	Precision	9.41	-1.4	0.845	2.6	NA	0.824	0.239	-0.452	NA	2.21	0.132	NA	2.99	NA	NA
Full 39 spp	dS and dN	1	Partial Correlation Coefficient	-1	0.46	-0.18	-0.474	NA	-1	-0.17	0.264	NA	-1	-0.049	NA	-1	NA	NA
Full 39 spp	dS and dN	1	Part. Cor. Coeff. Posterior Prob	NA	0.97	0.19	0.0089	NA	NA	0.28	0.82	NA	NA	0.39	NA	NA	NA	NA
Full 39 spp	dS and dN	2	Covariance	0.24	0.32	-0.11	-0.141	NA	2.49	-0.38	0.0969	NA	0.65	0.0121	NA	0.557	NA	NA
Full 39 spp	dS and dN	2	Correlation Coefficient	1	0.41	-0.28	-0.387	NA	1	-0.29	0.073	NA	1	0.023	NA	1	NA	NA
Full 39 spp	dS and dN	2	Cor. Coeff. Posterior Prob	NA	0.97	0.065	0.019	NA	NA	0.15	0.62	NA	NA	0.56	NA	NA	NA	NA
Full 39 spp	dS and dN	2	Precision	9.42	-1.4	0.84	2.6	NA	0.823	0.234	-0.459	NA	2.21	0.131	NA	2.99	NA	NA
Full 39 spp	dS and dN	2	Partial Correlation Coefficient	-1	0.46	-0.18	-0.472	NA	-1	-0.17	0.268	NA	-1	-0.049	NA	-1	NA	NA
Full 39 spp	dS and dN	2	Part. Cor. Coeff. Posterior Prob	NA	0.97	0.2	0.0091	NA	NA	0.28	0.82	NA	NA	0.39	NA	NA	NA	NA
Subset 27 spp	dS and dN	1	Covariance	0.13	0.21	-0.06	-0.0968	-0.122	1.87	0.099	-0.264	-1.3	0.35	0.0417	-0.16	0.567	0.0694	1.82
Subset 27 spp	dS and dN	1	Correlation Coefficient	1	0.4	-0.3	-0.359	-0.25	1	0.121	-0.246	-0.7	1	0.0947	-0.19	1	0.0646	1
Subset 27 spp	dS and dN	1	Cor. Coeff. Posterior Prob	NA	0.89	0.1	0.065	0.17	NA	0.66	0.22	0.007	NA	0.68	0.2	NA	0.61	NA
Subset 27 spp	dS and dN	1	Precision	23.6	-2.8	4.79	2.44	-0.028	3.21	-0.66	0.745	1.88	5.15	0.115	0.318	3.33	0.522	2.12
Subset 27 spp	dS and dN	1	Partial Correlation Coefficient	-1	0.31	-0.4	-0.264	-0.015	-1	0.137	-0.197	-0.66	-1	-0.02	-0.11	-1	-0.176	-1
Subset 27 spp	dS and dN	1	Part. Cor. Coeff. Posterior Prob	NA	0.82	0.039	0.16	0.47	NA	0.68	0.28	0.013	NA	0.46	0.3	NA	0.23	NA
Subset 27 spp	dS and dN	2	Covariance	0.13	0.21	-0.06	-0.0965	-0.119	1.86	0.1	-0.264	-1.31	0.35	0.0412	-0.16	0.571	0.0729	1.83
Subset 27 spp	dS and dN	2	Correlation Coefficient	1	0.39	-0.3	-0.356	-0.243	1	0.124	-0.248	-0.71	1	0.0934	-0.19	1	0.0674	1
Subset 27 spp	dS and dN	2	Cor. Coeff. Posterior Prob	NA	0.88	0.1	0.068	0.18	NA	0.67	0.22	0.006	NA	0.68	0.2	NA	0.61	NA
Subset 27 spp	dS and dN	2	Precision	22.9	-2.7	4.67	2.4	-0.044	3.26	-0.63	0.786	1.92	5.13	0.108	0.315	3.34	0.538	2.15
Subset 27 spp	dS and dN	2	Partial Correlation Coefficient	-1	0.3	-0.4	-0.262	-0.015	-1	0.133	-0.203	-0.66	-1	-0.018	-0.11	-1	-0.179	-1
Subset 27 spp	dS and dN	2	Part. Cor. Coeff. Posterior Prob	NA	0.81	0.039	0.16	0.47	NA	0.68	0.27	0.013	NA	0.47	0.31	NA	0.22	NA

Appendix Table C.3-2. Full output from Coevol models with dS and dN/dS as independent variables. Four models are summarized: two replicate models with the full dataset of 39 species, and two replicate models with the subset of 27 species with available estimates of θ. Each row contains a flattened pairwise matrix for each pair of variables (dS, dN/dS, mass, migration distance, and θ), showing covariance, correlation coefficients, posterior probabilities of correlation coefficients, precisions, partial correlation coefficients, and posterior probabilities of partial correlation coefficients. Posterior probabilities near 0 indicate strong support for a negative relationship while posterior probabilities near 1 indicate strong support for a positive relationship. Values obtained from replicate models are highly similar.

Dataset	Independent variables	Rep	Parameter	dS-dS	dS-dN/dS	dS-Mass	dS-MigDist	dS-Theta	dN/dS-dN/dS	dN/dS-Mass	dN/dS-MigDist	dN/dS-Theta	Mass-Mass	Mass-MigDist	Mass-Theta	MigDist-MigDist	Migdist-Theta	Theta-Theta
Full 39 spp	dS and dN/dS	1	Covariance	0.27	0.328	-0.2	-0.112	NA	2.02	-0.305	0.106	NA	0.637	0.0183	NA	0.508	NA	NA
Full 39 spp	dS and dN/dS	1	Correlation Coefficient	1	0.435	-0.4	-0.304	NA	1	-0.254	0.0964	NA	1	0.0339	NA	1	NA	NA
Full 39 spp	dS and dN/dS	1	Cor. Coeff. Posterior Prob	NA	0.95	0.03	0.07	NA	NA	0.19	0.63	NA	NA	0.58	NA	NA	NA	NA
Full 39 spp	dS and dN/dS	1	Precision	8.18	-1.35	1.46	2.02	NA	1.03	0.105	-0.487	NA	2.42	0.195	NA	3.02	NA	NA
Full 39 spp	dS and dN/dS	1	Partial Correlation Coefficient	-1	0.434	-0.3	-0.395	NA	-1	-0.074	0.26	NA	-1	-0.0686	NA	-1	NA	NA
Full 39 spp	dS and dN/dS	1	Part. Cor. Coeff. Posterior Prob	NA	0.95	0.05	0.016	NA	NA	0.4	0.82	NA	NA	0.34	NA	NA	NA	NA
Full 39 spp	dS and dN/dS	2	Covariance	0.27	0.326	-0.2	-0.11	NA	1.99	-0.299	0.105	NA	0.629	0.0158	NA	0.501	NA	NA
Full 39 spp	dS and dN/dS	2	Correlation Coefficient	1	0.437	-0.4	-0.302	NA	1	-0.252	0.0954	NA	1	0.0307	NA	1	NA	NA
Full 39 spp	dS and dN/dS	2	Cor. Coeff. Posterior Prob	NA	0.95	0.03	0.071	NA	NA	0.19	0.63	NA	NA	0.58	NA	NA	NA	NA
Full 39 spp	dS and dN/dS	2	Precision	8.25	-1.37	1.47	2.04	NA	1.05	0.099	-0.491	NA	2.45	0.204	NA	3.06	NA	NA
Full 39 spp	dS and dN/dS	2	Partial Correlation Coefficient	-1	0.437	-0.3	-0.394	NA	-1	-0.07	0.258	NA	-1	-0.0707	NA	-1	NA	NA
Full 39 spp	dS and dN/dS	2	Part. Cor. Coeff. Posterior Prob	NA	0.96	0.05	0.017	NA	NA	0.41	0.82	NA	NA	0.34	NA	NA	NA	NA
Subset 27 spp	dS and dN/dS	1	Covariance	0.15	0.142	-0.1	-0.101	-0.16	1.57	0.195	-0.173	-1.3	0.354	0.0379	-0.19	0.565	0.0841	1.93
Subset 27 spp	dS and dN/dS	1	Correlation Coefficient	1	0.282	-0.3	-0.352	-0.3	1	0.255	-0.177	-0.742	1	0.0883	-0.22	1	0.0764	1
Subset 27 spp	dS and dN/dS	1	Cor. Coeff. Posterior Prob	NA	0.81	0.13	0.069	0.13	NA	0.8	0.3	0.007	NA	0.67	0.18	NA	0.62	NA
Subset 27 spp	dS and dN/dS	1	Precision	19.1	-1.15	4.29	2.59	1.07	5.18	-1.46	0.768	3.05	5.52	0.00057	-0.06	3.33	0.526	2.87
Subset 27 spp	dS and dN/dS	1	Partial Correlation Coefficient	-1	0.119	-0.4	-0.309	-0.17	-1	0.234	-0.168	-0.686	-1	0.00251	-0.04	-1	-0.161	-1
Subset 27 spp	dS and dN/dS	1	Part. Cor. Coeff. Posterior Prob	NA	0.64	0.04	0.11	0.27	NA	0.79	0.31	0.013	NA	0.51	0.42	NA	0.26	NA
Subset 27 spp	dS and dN/dS	2	Covariance	0.15	0.132	-0.1	-0.101	-0.15	1.59	0.197	-0.163	-1.3	0.358	0.0403	-0.19	0.567	0.077	1.93
Subset 27 spp	dS and dN/dS	2	Correlation Coefficient	1	0.262	-0.3	-0.353	-0.28	1	0.254	-0.165	-0.737	1	0.0919	-0.22	1	0.0696	1
Subset 27 spp	dS and dN/dS	2	Cor. Coeff. Posterior Prob	NA	0.79	0.12	0.067	0.14	NA	0.8	0.32	0.007	NA	0.67	0.18	NA	0.61	NA
Subset 27 spp	dS and dN/dS	2	Precision	18.7	-0.972	4.19	2.58	1.06	5.12	-1.38	0.723	3.01	5.45	0.00606	-0.03	3.28	0.497	2.81
Subset 27 spp	dS and dN/dS	2	Partial Correlation Coefficient	-1	0.108	-0.4	-0.315	-0.17	-1	0.227	-0.161	-0.685	-1	0.00131	-0.04	-1	-0.153	-1
Subset 27 spp	dS and dN/dS	2	Part. Cor. Coeff. Posterior Prob	NA	0.63	0.05	0.1	0.27	NA	0.78	0.32	0.012	NA	0.5	0.41	NA	0.27	NA

Appendix Table C.3-3. Full model selection results for models predicting πN/πS.

Model formula	**logLik**	**AICc**	**deltaAICc**	**weight**
πN/πS ~ θ + migration distance	44.40	-79.0	0	0.55
πN/πS ~ θ	41.90	-76.7	2.23	0.18
πN/πS ~ θ + mass + migration distance	44.71	-76.6	2.40	0.17
πN/πS ~ θ + mass	41.97	-74.1	4.86	0.049
πN/πS ~ 1 (null)	38.53	-72.6	6.42	0.022
πN/πS ~ migration distance	39.43	-71.8	7.15	0.016
πN/πS ~ mass	38.53	-70.0	8.96	0.006
πN/πS ~ mass + migration distance	39.44	-69.1	9.91	0.004

Appendix Table C.3-4. Full model selection results for models predicting θ.

Model formula	**logLik**	**AICc**	**deltaAICc**	**weight**
θ ~ 1 (null model)	93.95	-183.4	0	0.47
θ ~ migration distance	94.58	-182.1	1.29	0.25
θ ~ mass	94.26	-181.5	1.93	0.18
θ ~ mass + migration distance	95.03	-180.2	3.17	0.10